

**Isolierung des Paprika *Bs3*-Resistenzgens und Interaktionsanalyse  
zwischen TAL-Effektoren und pflanzlichen Promotoren**

DISSERTATION

zur Erlangung des akademischen Grades  
doctor rerum naturalium (Dr. rer. nat.)

vorgelegt der  
NATURWISSENSCHAFTLICHEN FAKULTÄT I  
BIOWISSENSCHAFTEN

DER MARTIN-LUTHER-UNIVERSITÄT HALLE-WITTENBERG

von Patrick Römer

geboren am 18.04.1979 in der Lutherstadt Wittenberg

Gutachter /in:

1. Prof. Dr. Ulla Bonas
2. Prof. Dr. Christiane Gatz
3. Prof. Dr. Christoph Peterhänsel

Halle (Saale), 18.06.2010

## Zusammenfassung

Das Resistenz (*R*)-Gen *Bs3* aus dem Paprika (*Capsicum annuum*) Kultivar ECW-30R vermittelt Resistenz gegenüber *Xanthomonas campestris* pv. *vesicatoria* (*Xcv*)-Stämmen, die das Typ-III-Effektorprotein AvrBs3 translozieren. Im Rahmen dieser Arbeit wurde das *Bs3*-Gen mittels kartengestützter Klonierung isoliert. Es kodiert für ein 342 Aminosäuren langes Protein, welches Homologie zu Flavin-abhängigen Monooxygenasen aufweist. Die Expression des *Bs3*-Transkripts wird durch Infektion mit *Xcv*-Stämmen, die AvrBs3 translozieren induziert. Die Aktivierung des Promotors ist abhängig von der  $UPT_{AvrBs3}$ -Box (*upregulated by transcription activator like effectors*), einem Sequenzmotiv des *Bs3*- und anderer AvrBs3-induzierbarer Wirtspromotoren. AvrBs3 bindet spezifisch an die  $UPT_{AvrBs3}$ -Box und vermittelt die transkriptionelle Aktivierung des *Bs3*-Gens. Das *Bs3-E*-Allel aus der Paprikalinie ECW enthält eine 13-Bp Insertion in der  $UPT_{AvrBs3}$ -Box, die bedingt, dass AvrBs3 nur mit geringer Affinität bindet und folglich dahinterliegende Gene nicht aktiviert. Die 13-Bp Insertion im *Bs3-E*-Promotor bedingt jedoch, dass das AvrBs3-Derivat AvrBs3 $\Delta$ rep16 diesen Promotor binden und aktivieren kann. Da der 13-Bp Insertion-/Deletionspolymorphismus diagnostisch für die AvrBs3-vermittelte HR-Induktion ist, konnte ein diagnostischer DNA-basierter Marker ("PR-*Bs3*") abgeleitet werden, der zwischen *Bs3*-resistenten und -suszeptiblen Pflanzen in einer kodominanten Weise diskriminieren kann. Durch Substitutionsmutagenese des *Bs3*- und des *Bs3-E*-Promotors wurden die exakten Längen der  $UPT_{AvrBs3}$ - und der  $UPT_{AvrBs3\Delta rep16}$ -BOX bestimmt. Die Verschiebung der  $UPT_{AvrBs3}$ -Box an verschiedene Positionen im *Bs3*-Promotor zeigte, dass dieses Sequenzmodul den Transkriptionsstart (*transcriptional start site*; TSS) definiert. Der Abstand zwischen der  $UPT_{AvrBs3}$ -Box und dem TSS variiert zwischen 41 Bp und 46 Bp. Analysen des *R*-Gens *Xa27* aus Reis, das durch das AvrBs3-ähnliche AvrXa27-Protein aus dem Reispathogen *Xanthomonas oryzae* pv. *oryzae* transkriptionell induziert wird zeigten, dass dieses eine zu AvrXa27 korrespondierende  $UPT_{AvrXa27}$ -Box im Promotor enthält. Weiterhin konnte gezeigt werden, dass für die durch *transcription activator like* (TAL)-Effektoren induzierten Suszeptibilitätsgene *Os8N3*, *Os11N3* und *OsTFX1* aus Reis die spezifische Promotorbindung die Grundlage für die Aktivierung der dahinterliegenden Gene ist. Somit funktionieren diese durch TAL-Effektoren induzierten Gene nach einem vergleichbaren molekularen Mechanismus wie die *R*-Gene *Bs3* und *Xa27*. Außerdem konnte im Rahmen dieser Arbeit gezeigt werden, dass drei funktionell unterschiedliche  $UPT$ -Boxen in einem komplexen Promotor kombiniert werden können, wobei die Spezifität und Funktionalität der einzelnen Boxen erhalten bleibt. Dieser Ansatz könnte die Grundlage sein um Breitspektrum- und dauerhafte Resistenz zu erzeugen.

## Summary

The resistance (*R*) gene *Bs3* derived from the pepper (*Capsicum annuum*) cultivar ECW-30R confers resistance to *Xanthomonas campestris* pv. *vesicatoria* (*Xcv*), which deliver the type-III-effector protein AvrBs3. In these studies the *Bs3* gene was isolated by map based cloning. *Bs3* encodes a 342 aminoacid protein, which shows homology to flavin dependent monooxygenases. The expression of *Bs3* transcript is induced by the infection of *Xcv* strains that deliver AvrBs3. The activation of the *Bs3* promoter depends on the  $UPT_{AvrBs3}$  box, a sequence motif, which is common in the *Bs3* and other AvrBs3 inducible host promoters. AvrBs3 binds in a specific form to the  $UPT_{AvrBs3}$  box and mediates the transcriptional activation of *Bs3*. The *Bs3-E* allele from the pepper cultivar ECW contains a 13-bp insertion in the  $UPT_{AvrBs3}$  box and as a result AvrBs3 binds with much lower affinity to this motif and that is why it could not activate genes behind it. As a result of the 13-bp insertion in the *Bs3-E* promoter the AvrBs3 deletion derivative AvrBs3 $\Delta$ rep16 binds and activates this promoter. For the reason that the 13-bp insertion/deletion (InDel) polymorphism is diagnostic for the AvrBs3 dependent HR induction it was possible to generate the DNA based marker “PR-Bs3“, which discriminates between *Bs3* resistant and susceptible plants in a co-dominant manner. Caused by the substitution mutagenesis of the *Bs3* and the *Bs3-E* promoter we determined the exact boundaries of the  $UPT_{AvrBs3}$  and the  $UPT_{AvrBs3\Delta rep16}$  boxes. The displacement of the  $UPT_{AvrBs3}$  box to various positions in the *Bs3* promoter showed, that this sequence motif defines the transcriptional start site (TSS). The distance between the  $UPT_{AvrBs3}$  and the TSS varies between 41 and 46 nucleotides.

Analysis of the *R* gene *Xa27* from rice which is induced by the AvrBs3 like protein AvrXa27 from the rice pathogen *Xanthomonas oryzae* pv. *oryzae* showed that the *Xa27* promoter contains an  $UPT_{AvrXa27}$  box. Furthermore it was possible to point out that for the susceptibility genes *Os8N3*, *Os11N3* and *OsTFX1* from rice the specific binding of the promoter by the corresponding transcription-activator like (TAL) effector is the basis for the gene activation. Therefore these TAL effector induced genes function in a comparable way like the *R* genes *Bs3* and *Xa27*.

It could also be shown in this work, that three functionally different *UPT* boxes can be combined in a complex promoter, keeping their specificity and their functionality. This could be the basis for the generation of broad spectrum and durable disease resistance.

## Inhaltsverzeichnis

<b>Zusammenfassung .....</b>	<b>I</b>
<b>Summary .....</b>	<b>II</b>
<b>Inhaltsverzeichnis .....</b>	<b>III</b>
<b>Abbildungsverzeichnis .....</b>	<b>V</b>
<b>Tabellenverzeichnis .....</b>	<b>V</b>
<b>Abkürzungsverzeichnis .....</b>	<b>VI</b>
<b>1 Einleitung .....</b>	<b>1</b>
1.1 Pflanzliche Abwehrmechanismen .....	1
1.2 Das Typ-III-Sekretionssystem .....	2
1.3 Modelle der <i>R</i> -Gen vermittelten Resistenz .....	3
1.4 <i>R</i> -Genprodukte weisen strukturelle Homologien auf .....	4
1.5 Signalwegkomponenten der R-Protein vermittelten Resistenz .....	7
1.6 Die Bakteriengattung <i>Xanthomonas</i> .....	8
1.6.1 <i>Xanthomonas campestris</i> pv. <i>vesicatoria</i> , der Erreger der bakteriellen Fleckenkrankheit auf Paprika und Tomate .....	8
1.6.2 <i>Xanthomonas oryzae</i> pv. <i>oryzae</i> , der Erreger der bakteriellen Weissblättrigkeit .	10
1.7 Die TAL-Effektoren aus <i>Xanthomonas</i> , Struktur und Funktion .....	10
1.7.1 <i>UPA</i> -Gene werden durch den TAL-Effektor AvrBs3 induziert .....	12
1.7.2 Suszeptibilitätsgene aus Reis werden durch TAL-Effektoren induziert .....	12
1.7.3 <i>R</i> -Gene, die Resistenz gegen TAL-Effektoren vermitteln, sind strukturell divers	13
1.8 Das <i>R</i> -Gen <i>Bs3</i> und mögliche Allele in den verschiedenen <i>Capsicum</i> -Arten .....	16
1.9 Vorarbeiten und Zielstellung der Arbeit .....	17
<b>2 Ergebnisse .....</b>	<b>18</b>
2.1 Übersicht der Publikationen .....	18
2.2 Isolierung und Charakterisierung des Paprika <i>Bs3</i> -Resistenzgens .....	21
2.2.1 Publikation 1 .....	21
2.2.2 Anlagen zur Publikation 1 .....	25
2.2.3 Zusätzliche Ergebnisse .....	43
2.2.3.1 Die <i>Bs3</i> -vermittelte HR wird von der Signalwegkomponente <i>SGT1</i> beeinflußt .....	43
2.2.3.2 Das <i>Bs3</i> -Protein ist im Zytoplasma und Zellkern lokalisiert .....	44
2.2.3.3 <i>Bs3</i> -Homologe aus <i>C. pubescens</i> vermitteln nicht die Erkennung von AvrBs4, jedoch die Erkennung von AvrBs3 $\Delta$ rep16 .....	46
2.2.4 Zusammenfassung der Ergebnisse .....	48

---

2.3	Mutationsbasierte Analyse des <i>Bs3</i> - und des <i>Bs3-E</i> -Promotors.....	49
2.3.1	Publikation 2.....	49
2.3.2	Anlagen zur Publikation 2.....	65
2.3.3	Zusammenfassung der Ergebnisse.....	70
2.4	Etablierung eines diagnostischen <i>Bs3</i> -Markers.....	71
2.4.1	Publikation 3.....	71
2.4.2	Zusammenfassung der Ergebnisse.....	75
2.5	Erstellung eines komplexen Promotors.....	76
2.5.1	Publikation 4.....	76
2.5.2	Anlagen zur Publikation 4.....	82
2.5.3	Zusammenfassung der Ergebnisse.....	90
2.6	Promotoren von Reissuszeptibilitätsgenen werden von korrespondierenden TAL-Effektoren gebunden und aktiviert.....	91
2.6.1	Publikation 5.....	91
2.6.2	Anlagen zur Publikation 5.....	101
2.6.3	Zusammenfassung der Ergebnisse.....	106
<b>3</b>	<b>Diskussion.....</b>	<b>107</b>
3.1	<i>Bs3</i> kodiert für ein neuartiges R-Protein.....	107
3.2	Kernlokalisierung von <i>Bs3</i> ist für das Auslösen der Resistenzreaktion nötig.....	109
3.3	<i>Bs3</i> -vermittelte Resistenz: Ein Beispiel für das <i>Decoy</i> -Modell.....	110
3.4	Die Funktion von <i>Bs3</i> ist nur die Generierung von Resistenz gegen <i>Xcv</i> .....	111
3.5	Spezifische Promotorbindung ist die Grundlage für TAL-Effektor vermittelte Promotoraktivierung.....	112
3.6	Funktionell austauschbare TAL-Effektoren.....	113
3.7	Der “CODE“ erklärt Einiges in der Promotor-TAL-Effektorinteraktion.....	116
3.8	Die Interaktion von <i>UPT</i> -Boxen mit TAL-Effektoren.....	120
3.9	TAL-Effektoren interagieren vermutlich als Monomere mit der DNA.....	122
3.10	Nutzung der TAL-Effektor-Technologie und mögliche Probleme.....	123
<b>4</b>	<b>Literaturverzeichnis.....</b>	<b>126</b>
<b>5</b>	<b>Anhang.....</b>	<b>139</b>
	<b>Danksagung.....</b>	<b>145</b>
	<b>Lebenslauf.....</b>	<b>146</b>
	<b>Veröffentlichungen.....</b>	<b>147</b>
	<b>Erklärung.....</b>	<b>149</b>

## Abbildungsverzeichnis

Abbildung 1: Zickzack-Modell der Koevolution von Pflanzen und Pathogenen.....	2
Abbildung 2: Modelle der Avr-R-Protein Interaktionen .....	4
Abbildung 3: Modulare Struktur von R-Proteinen.....	6
Abbildung 4: Durch <i>Xanthomonas</i> spp. ausgelöste Krankheitssymptome auf bedeutenden Kulturpflanzen.....	9
Abbildung 5: Aufbau von AvrBs3 und Sequenzvergleich der einzelnen <i>Repeat</i> -Einheiten.....	11
Abbildung 6: Struktur von AvrBs3-ähnlichen Proteinen und ihre Erkennung .....	17
Abbildung 7: Lokalisation von Bs3::GFP .....	45
Abbildung 8: Ausschnitt aus dem Sequenzvergleich der <i>Bs3</i> -Homologen von <i>C. pubescens</i> und <i>C. annuum</i> .....	46
Abbildung 9: Die <i>Bs3</i> -Allele aus <i>C. pubescens</i> vermitteln Erkennung von AvrBs3 $\Delta$ rep16.....	47
Abbildung 10: Struktur und möglicher Reaktionszyklus der FMOs.....	108
Abbildung 11: Vergleich der RVDs der TAL-Effektoren AvrBs3 und AvrHah1 .....	113
Abbildung 12: Vergleich der RVDs der TAL-Effektoren AvrBs3 und AvrBs3 $\Delta$ rep16 .....	114
Abbildung 13: Modell der Wirkungsweise von TAL-Effektoren mit ähnlicher <i>Repeat</i> -Struktur.....	115
Abbildung 14: Einige Positionen in den $UPT_{AvrBs3}$ -Boxen sind nicht durch den “CODE“ erklärbar.....	119
Abbildung 15: Modell der Bindung von AvrBs3 an die <i>UPT</i> -Box.....	121
Abbildung 16: Möglichkeiten der Resistenzgenerierung durch Kombination von <i>UPT</i> -Boxen.....	125
Abbildung 17: Sequenzvergleich der <i>Bs3</i> -Homologen von <i>C. pubescens</i> und <i>C. annuum</i> ....	141
Abbildung 18: Proteinsequenzvergleich der <i>Bs3</i> -Allele aus <i>C. pubescens</i> und <i>C. annuum</i> ...	142

## Tabellenverzeichnis

Tabelle 1: R-Gene und ihre korrespondierenden TAL-Effektoren.....	15
Tabelle 2: SGT1 ist notwendig für die Bs3-vermittelte HR.....	43
Tabelle 3: Der “CODE“ der TAL-Effektoren .....	117
Tabelle 4: Analyse der F <sub>2</sub> - <i>C. pubescens</i> -Pflanzen, die für den Kopplungstest verwendet wurden .....	143
Tabelle 5: Bestimmte Nukleotide im oberen Strang der DNA werden präferentiell von bestimmten RVDs gebunden.....	144

**Abkürzungsverzeichnis**

A	Adenin(nukleotid)
AD	Aktivierungsdomäne ( <i>acidic activation domain</i> )
AS	Aminosäuren
<i>avr</i> , Avr	Avirulenz
BAC	<i>bacterial artificial chromosome</i>
Bp	Basenpaare
Bs	<i>bacterial spot</i>
bspw.	beispielsweise
bzw.	beziehungsweise
C	Cytosin(nukleotid)
CC	coiled-coiled Domäne
cDNA	<i>complementary DNA</i>
cv.	Kultivar
d.h.	das heisst
DNA	Desoxiribonukleinsäure
et al.	Et alii (und andere)
ECW	„Early Californian Wonder“ Kultivar von <i>Capsicum annuum</i>
EMSA	<i>Electrophoretic mobility shift assay</i>
FAD	Flavinadenindinukleotid
FMO	Flavin-abhängige Monooxygenase
G	Guanin(nukleotid)
GFP	grün fluoreszierendes Protein ( <i>green fluorescent protein</i> )
GTF	genereller Transkriptionsfaktor
GUS	$\beta$ -Glucuronidase
h	Stunden ( <i>hour</i> )
<i>hax</i> , Hax	Homolog von AvrBs3 in <i>Xanthomonas</i>
HR	hypersensitive Reaktion ( <i>hypersensitive reaction</i> )
hrp	hypersensitive Reaktion und Pathogenität
Kb	Kilobasenpaare (1000 Bp)
kda	Kilodalton
LRR	Leucin-reiche Wiederholung ( <i>leucine rich repeat</i> )
LSM	konfokales Laser-Scanning Mikroskop
NADPH	Nicotinamidadenindinukleotidphosphat

---

NB	Nukleotidbindestelle
NLS	Kernlokalisierungssignal ( <i>nuclear localisation signal</i> )
PCR	Polymerase-Ketten-Reaktion ( <i>polymerase chain reaction</i> )
PR-Bs3	Patrick Römers <i>Bs3</i> -Marker
pv.	Pathovar
qRT-PCR	quantitative Reverse Transkription und PCR ( <i>reverse transcribed PCR</i> )
R, R	Resistenz
RNA	Ribonukleinsäure ( <i>ribonucleic acid</i> )
RLK	Rezeptor ähnliche Kinase ( <i>receptor like kinase</i> )
RLP	Rezeptor ähnliches Protein ( <i>receptor like protein</i> )
RT-PCR	reverse Transkription und PCR ( <i>reverse transcribed PCR</i> )
RVD	<i>repeat variable diresidue</i>
spp.	Subspezies
sus	Suszeptibilität
T	Thymin(nukleotid)
T3SS	Typ-III-Sekretionssystem
TAL	<i>transcription activator like</i>
TBP	TATA-Box bindendes Protein
TFIIA	Transkriptionsfaktor zwei A
TIR	TOLL und Interleukin-1 homologe Region
TSS	Transkriptionsstart ( <i>transcriptional start site</i> )
u.a.	unter anderem
<i>UPA</i>	<i>upregulated by AvrBs3</i>
<i>UPT</i>	<i>upregulated by TALE</i>
<i>Xaa</i>	<i>Xanthomonas axonopodis</i> pv. <i>allii</i>
<i>Xac</i>	<i>Xanthomonas axonopodis</i> pv. <i>citri</i>
<i>Xca</i>	<i>Xanthomonas campestris</i> pv. <i>armoraciae</i>
<i>Xcm</i>	<i>Xanthomonas campestris</i> pv. <i>malvacearum</i>
<i>Xcv</i>	<i>Xanthomonas campestris</i> pv. <i>vesicatoria</i>
<i>Xg</i>	<i>Xanthomonas gardneri</i>
<i>Xoc</i>	<i>Xanthomonas oryzae</i> pv. <i>oryzicola</i>
<i>Xoo</i>	<i>Xanthomonas oryzae</i> pv. <i>oryzae</i>
z.B.	zum Beispiel



# 1 Einleitung

## 1.1 Pflanzliche Abwehrmechanismen

Pflanzen haben in der Evolution ein vielschichtiges Immunsystem entwickelt, um sich vor Befall durch phytopathogene Bakterien, Oomyceten, Pilzen, Nematoden, Viren und Insekten zu schützen. Die passive Resistenz von Pflanzen gegen potentiell pathogene Mikroorganismen erfolgt durch anatomisch-morphologische Merkmale, wie z.B. Dornen, Haare oder Zellwandverdickungen. Membranständige Immunrezeptoren, so genannte *pattern recognition receptors* (PRRs), vermitteln eine weitere Ebene der basalen Resistenz. Sie detektieren typische pathogenassoziierte molekulare Strukturen (*microbe/pathogen-associated molecular patterns*, MAMPs/PAMPs), wie z.B. Lipopolysaccharide, Peptide des bakteriellen Flagellins (flg22) oder des Elongationsfaktors EF-Tu (elf18) und lösen ein Abwehrprogramm aus (Gómez-Gómez und Boller, 2002; Zipfel und Felix, 2005; Chinchilla et al., 2006; Nürnberger und Kemmerling, 2006; Chinchilla et al., 2007; Schwessinger und Zipfel, 2008; Nürnberger und Kemmerling, 2009; Zipfel, 2009). Diese Stufe der Resistenz wird auch als PAMP-induzierte Resistenz (*PAMP-triggered immunity*, PTI) bezeichnet (Jones und Dangl, 2006).

Im Laufe der Koevolution von Wirt und Parasit haben Mikroben Effektorproteine entwickelt, um die Aktivierung der PTI zu vermeiden bzw. diese Form der Resistenz zu unterdrücken (Abramovitch et al., 2006; He et al., 2007; Zhou und Chai, 2008). Dies wird als Effektorbedingte Suszeptibilität (*effector triggered susceptibility*, ETS) bezeichnet (Jones und Dangl, 2006). Als Anpassung an mikrobielle Effektorproteine haben einige Pflanzen Resistenzgene (*R-Gene*) entwickelt, welche die Erkennung von Effektoren vermitteln. Diese Form der Resistenz bezeichnet man auch als Effektor induzierte Immunität (*effector-triggered immunity*, ETI) (Jones und Dangl, 2006). Häufig korreliert die ETI mit einem schnellen lokalen Zelltod des infizierten Gewebes, welcher als hypersensitive Reaktion (*hypersensitive response*, HR) bezeichnet wird (Greenberg und Yao, 2004). Einige Pathogene sind in der Lage, die ETI zu unterdrücken bzw. zu vermeiden, indem sie Effektorgene mutieren oder neue Effektorgene evolvieren (Jones und Dangl, 2006; Zhou und Chai, 2008). Durch Selektionsdruck bedingt, gibt es für diese immunsuppressiven Effektoren wiederum korrespondierende *R-Gene*, welche die ETI auslösen. So kommt es zu einem permanenten Wettlauf zwischen Pathogen und Wirt, was im sogenannten Zick-Zack-Modell dargestellt ist (Jones und Dangl, 2006; Abbildung 1).

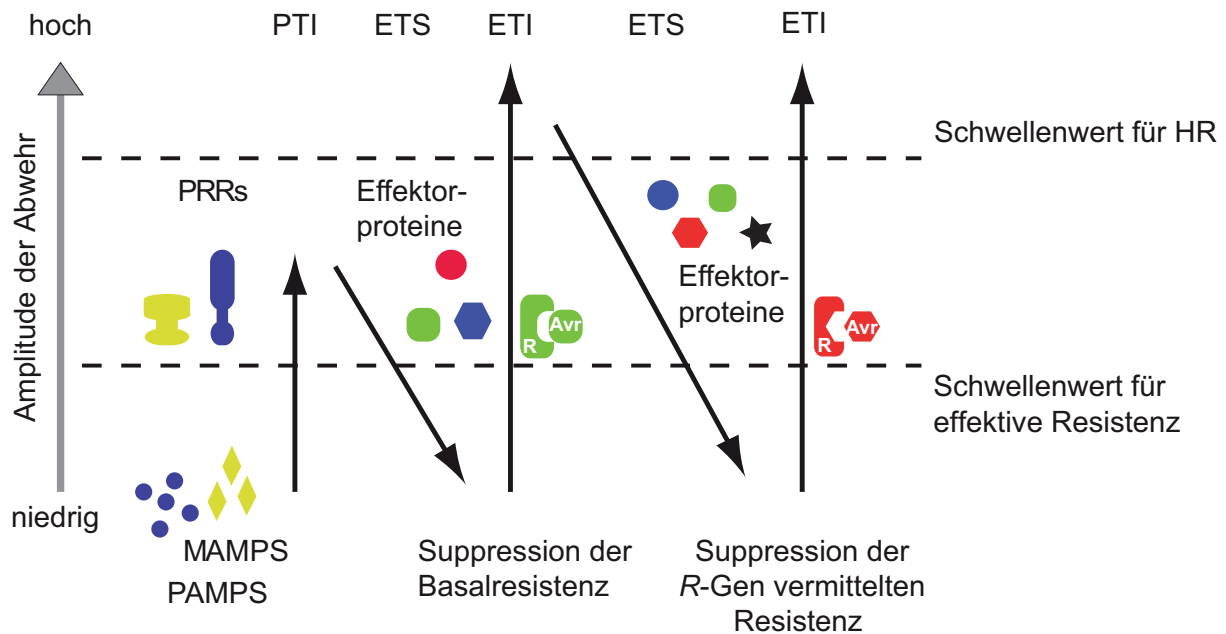


**Abbildung 1: Zickzack-Modell der Koevolution von Pflanzen und Pathogenen**

Bei der ersten Stufe erfolgt die Rezeptor (PRR) vermittelte Erkennung von PAMPs bzw. MAMPs und die Induktion der Basalabwehr (PAMP-induzierte Immunität, PTI). Dadurch wird das Wachstum und die Verbreitung des Pathogens innerhalb der Wirtspflanze eingeschränkt. In der zweiten Stufe translozieren einige Pathogene Effektorproteine in die pflanzliche Zelle, wodurch die Basalabwehr unterdrückt werden kann (Effektor-induzierte Suszeptibilität, ETS). Durch die dritte Stufe, die R-Gen vermittelte Erkennung von Effektoren (Avirulenz (Avr)-Proteinen) wird eine stärkere Abwehrreaktion (Effektor induzierte Immunität, ETI) induziert, welche oft mit der Auslösung einer HR einhergeht. Im vierten Schritt ermöglicht der Verlust oder die Modifikation bzw. der Neuerwerb von Effektoren dem Pathogen die Suppression der R-Gen vermittelten Abwehr und damit die erneute Kolonisierung der Pflanze. Durch die Entwicklung neuer R-Gene ist die Pflanze wiederum in der Lage, neuerworbene Effektoren der Pathogene zu erkennen und eine Abwehrreaktion zu initiieren. Die Abbildung wurde verändert nach Jones und Dangl, 2006.

## 1.2 Das Typ-III-Sekretionssystem

Ein zentraler Pathogenitätsfaktor vieler Gram-negativer Pflanzen- und Tierpathogene ist das Typ-III-Sekretionssystem (T3SS) (Ghosh, 2004). Die T3SS-abhängige Translokation von Proteinen in das Zytoplasma der eukaryotischen Wirtszelle wurde als Erstes bei dem Tierpathogen *Yersinia enterocolitica* nachgewiesen (Michiels et al., 1991). Kodiert wird das T3SS in pflanzenpathogenen Bakterien vom *hrp*-Gen-Cluster (*hypersensitive response and pathogenicity*). Mutationen in diesem Gencluster bedingen ein reduziertes Bakterienwachstum, abgeschwächte Krankheitssymptome in anfälligen Pflanzen und einen Verlust der Gen-für-Gen Immunantwort in resistenten Pflanzen (Lindgren et al., 1986). Mit Hilfe des T3SS werden eine Vielzahl strukturell und funktionell diverser Effektorproteine in die Pflanzenzelle transloziert (Roden et al., 2004; Thieme et al., 2005; Furutani et al., 2009). Die T3SS-Effektoren aus *Xanthomonas* spp. können in ca. 40 verschiedene Gruppen eingeteilt werden (White et al., 2009). Aber bisher konnte nur für wenige eine Funktion als Virulenzfaktor gezeigt werden. Beispiele hierfür sind AvrBs2 und die *transcription activator-*

*like* (TAL)-Effektoren AvrXa7, PthA und PthXo1 (Swarup et al., 1991; Bai et al., 2000; Yang und White, 2004; Gürlebeck et al., 2006; Yang et al., 2006; Al-Saadi et al., 2007).

### 1.3 Modelle der R-Gen vermittelten Resistenz

Harald Flor, der die Interaktion zwischen Flachs (*Linum usitatissimum*) und Flachsrost (*Melampsora lini*) untersuchte, stellte die Gen-für-Gen-Hypothese auf. Diese postuliert, dass jedes R-Gen in der Pflanze spezifisch mit einem korrespondierenden Avirulenz (*avr*)-Gen des Pathogens genetisch interagiert (Flor, 1942, 1971). Wenn eine Pflanze, die ein R-Gen trägt, von einem Pathogen befallen wird, welches das korrespondierende *avr*-Gen exprimiert, kommt es zu einer inkompatiblen Interaktion. Ist eine der beiden „komplementären“ genetischen Komponenten nicht funktional oder abwesend, ist die Pflanze anfällig und das Pathogen kann sich vermehren (kompatible Interaktion). Durch die Isolierung und die molekulare Analyse zahlreicher Avr-Proteine und der korrespondierenden R-Proteine konnte die Gültigkeit der Gen-Für-Gen-Hypothese bestätigt werden (Ronald et al., 1992; Martin et al., 1993; Tai et al., 1999; Schornack et al., 2004; Rafiqi et al., 2009). Aktuell gibt es drei Modelle, in denen versucht wird, die bekannten *avr*- und R-Gen-Interaktionen auf molekularer Ebene mechanistisch zu erklären (Gabriel und Rolfe, 1990; Van der Biezen und Jones, 1998a; Van der Hoorn und Kamoun, 2008). Die einfachste Interpretation der Gen-für-Gen-Hypothese ist das Rezeptor-Liganden-Modell, das eine direkte Interaktion zwischen Avr- und R-Protein als Auslöser der Resistenzreaktion postuliert (Gabriel und Rolfe, 1990; Keen, 1990; Abbildung 2). Zur Zeit gibt es fünf experimentell nachgewiesene Avr-R-Interaktionen, die diesem Modell folgen (Jia et al., 2000; Deslandes et al., 2003; Dodds et al., 2006; Ueda et al., 2006; Catanzariti et al., 2010).

Das *Guard*-Modell ist eine alternative biochemische Interpretation der Gen-für-Gen-Hypothese. Dieses Modell wurde entwickelt, weil für zahlreiche Avr-R-Paare keine direkte Interaktion nachgewiesen werden konnte. Das *Guard*-Modell postuliert für das R-Protein die Rolle des *Guards* (Wächters), der über das Zielprotein (*Guardee*) oder vielmehr über dessen Funktion wacht. Das Zielprotein interagiert vermutlich direkt mit dem Avr-Protein und ist somit ein mögliches Virulenzziel (*pathogenicity target*) des Avr-Proteins (Van der Biezen und Jones, 1998a; Dangl und Jones, 2001; Abbildung 2B). Ein klassisches Beispiel für ein Pathogenitätsziel im Kontext des *Guard*-Modells ist RIN4 (*RPM1 interactor 4*), das von den beiden *P. syringae*-Effektoren AvrB und AvrRpm1 phosphoryliert wird und dessen Modifikation eine Resistenzreaktion auslöst (Mackey et al., 2002; DeYoung und Innes, 2006). Das *Guard*-Modell gibt unter anderem an, dass die Interaktion des Avr-Proteins mit dem

Pathogenitätsziel (Virulenztarget) die Pathogenität des Pathogens begünstigt. Häufig bedingen Avr-induzierte Modifizierungen des Pathogenitätstargets jedoch keine erhöhte Pathogenität. Aufgrund dieser Erkenntnis wurde ein neues Modell, das sogenannte *Decoy*-Modell postuliert (Van der Hoorn und Kamoun, 2008). Dabei stellt der *Decoy* (die Falle) eine strukturelle Kopie des Pathogenitätsziels dar. In resistenten Pflanzen löst die Interaktion zwischen *Decoy* und Avr-Protein die Immunantwort aus. In suszeptiblen Pflanzen dagegen führt das *Decoy* zu keinem Vorteil für die Virulenz des Pathogens (Abbildung 2C).

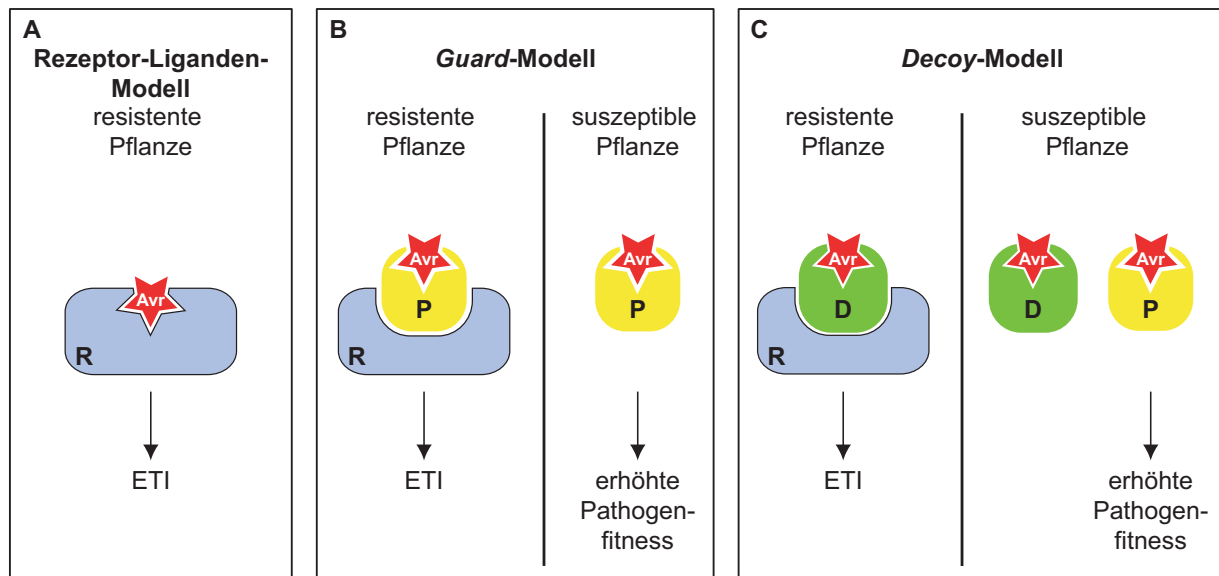


**Abbildung 2: Modelle der Avr-R-Protein Interaktionen**

A) Rezeptor-Liganden-Modell: Eine direkte Interaktion zwischen Avr- (Effektor)- und R-Protein (R) löst die Resistenzreaktion (*Effector triggered immunity*, ETI) aus. B) *Guard*-Modell: Das Pathogenitätstarget (P) vermittelt die indirekte Interaktion zwischen Avr- und R-Protein. In resistenten Pflanzen wird die strukturelle und/oder funktionale Integrität des Pathogenitätstargets (*Guardee*) durch ein R-Protein, das als Wächter (*Guard*) fungiert, überwacht und ggf. eine ETI ausgelöst. In suszeptiblen Pflanzen resultiert die Avr-Protein induzierte Modifikation des Pathogenitätstargets in einer gesteigerten Pathogenität des Pathogens. C) *Decoy*-Modell: In resistenten Pflanzen wird vom *Decoy* die Auslösung der Immunantwort vermittelt bzw. es wird von einem R-Protein überwacht, das die Resistenz initiiert. In suszeptiblen Pflanzen werden vom Avr-Protein mehrere Pathogenitätstargets modifiziert. Unter diesen befindet sich auch das *Decoy*, welches allerdings nicht zur Virulenz beiträgt.

#### 1.4 R-Genprodukte weisen strukturelle Homologien auf

In den letzten Jahren wurden über 80 dominante Resistenz (R)-Gene aus verschiedenen Pflanzenspezies isoliert (Sacco und Moffett, 2009). Diese R-Gene verleihen Resistenz gegenüber phylogenetisch diversen Pathogenen wie Viren, Bakterien, Pilze, Oomyzeten, Nematoden und Insekten. Ein prozentual kleiner Anteil der R-Gene kodiert Genprodukte, die strukturell einmalig sind. Die Mehrzahl der R-Proteine sind jedoch strukturell ähnlich und lassen sich in wenige Protein-Klassen einteilen (Gómez-Gómez, 2004; Liu et al., 2007; van Ooijen et al., 2007; Sacco und Moffett, 2009).

Die meisten *R*-Gene kodieren für NB-LRR-Proteine. Namensgebend ist die Nukleotid-Bindestelle (NB) im zentralen Bereich des Polypeptides und eine C-terminale *leucine-rich-repeat* (LRR)-Domäne (Sacco und Moffett, 2009). Auf Basis ihrer N-terminalen Domänen werden NB-LRR-Proteine in TIR- (Toll und Interleukin-1 Rezeptor) und Nicht-TIR-NB-LRRs unterteilt (Sacco und Moffett, 2009; Abbildung 3). Die größte Variabilität zwischen den NB-Proteinen ist in der LRR-Domäne vorhanden. Experimente, bei denen diese Domäne von nahverwandten Proteinen ausgetauscht wurden zeigten, dass die LRR-Domäne die Erkennungsspezifität determiniert (Ellis et al., 2000; Shen et al., 2003; Dodds et al., 2006; Qu et al., 2006; Rairdan und Moffett, 2006). Zwischen der NB- und der LRR-Domäne weisen die NB-LRR-Proteine die sogenannte ARC- (APAF-1, plant R and CED-4 proteins) Domäne auf (Van der Biezen und Jones, 1998b). Diese Domäne kann auf Grund der funktionellen Unterschiede in die ARC1- und ARC2-Domäne unterteilt werden (Albrecht und Takken, 2006; McHale et al., 2006; Rairdan und Moffett, 2006). Für die NB-LRR-Proteine wird angenommen, dass die Pathogenerkennung mit einer Änderung der intramolekularen Interaktionen einhergeht, wobei die ARC-Domäne von entscheidender Bedeutung ist (Moffett et al., 2002; Rairdan und Moffett, 2006; Rairdan et al., 2008).

Eine weitere Klasse von R-Proteinen bilden Cf-2, Cf-4, Cf-5 und Cf-9 aus Tomate, welche Resistenz gegen den Pilz *Cladosporium fulvum* vermitteln. Diese weisen eine extrazelluläre LRR-Domäne auf, die sich strukturell von der LRR-Domäne der NB-LRR-Proteine unterscheidet (Jones und Jones, 1997; Kajava, 1998) und über eine hydrophile Domäne in der Membran verankert ist. Außerdem weisen Cf-Proteine eine kurze C-terminale zytoplasmatische Region auf (Hammond-Kosack et al., 1994; Dixon et al., 1996; Dixon et al., 1998). Da für die LRR-Domäne oft eine Funktion als Liganden-bindende Domäne postuliert wurde, werden die Proteine auch als RLPs (*receptor-like proteins*) bezeichnet (Sacco und Moffett, 2009). In Übereinstimmung mit dieser Hypothese zeigten Domänen austauschexperimente zwischen verschiedenen Cf-Proteinen, dass die LRR-Domäne wie bei den NB-LRR-Proteinen die Erkennungsspezifität bestimmt (Parniske et al., 1997; Wulff et al., 2001).

Den RLPs strukturell sehr ähnlich ist das R-Protein Xa3/Xa26. Dieses Protein weist eine zytoplasmatische Kinase-Domäne auf (Sun et al., 2004). Proteine mit dieser Domänenstruktur werden deshalb auch als RLKs (*receptor-like kinases*) bezeichnet (Xiang et al., 2006). Interessanterweise sind die PAMP-Rezeptoren Xa21, FLS2 und EFR1, ebenfalls RLK Proteine (Gómez-Gómez und Boller, 2000; Zipfel et al., 2006; Lee et al., 2009).

Eine Kinase-Domäne enthalten auch R-Proteine wie Pto. Pto ist eine Serin/Threonin Kinase, die ein Myristoylierungsmotiv am N-Terminus aufweist (Pedley und Martin, 2003).

Neben den mitgliederreichen R-Proteinklassen gibt es auch R-Proteine, welche bestimmte Domänen dieser Klassen enthalten, aber im Gegensatz zu den Hauptklassen nicht alle charakteristische Domänen aufweisen, jedoch andere zusätzliche Domänen besitzen. Beispiele hierfür sind Pi-d2, RFO1, RPG1, RPW8 und RLM3 (Xiao et al., 2001; Brueggeman et al., 2002; Diener und Ausubel, 2005; Chen et al., 2006; Staal et al., 2008; Abbildung 3). Desweiteren gibt es R-Proteine, welche neue Strukturmodule beinhalten und keine Homologie zu den genannten R-Protein-Klassen aufweisen. Dazu gehören unter anderem das Mais Hm1-Protein und die Reis Xa27-, xa5- und xa13-Proteine (Johal und Briggs, 1992; Meeley et al., 1992; Iyer und McCouch, 2004; Gu et al., 2005; Chu et al., 2006; Abbildung 3).

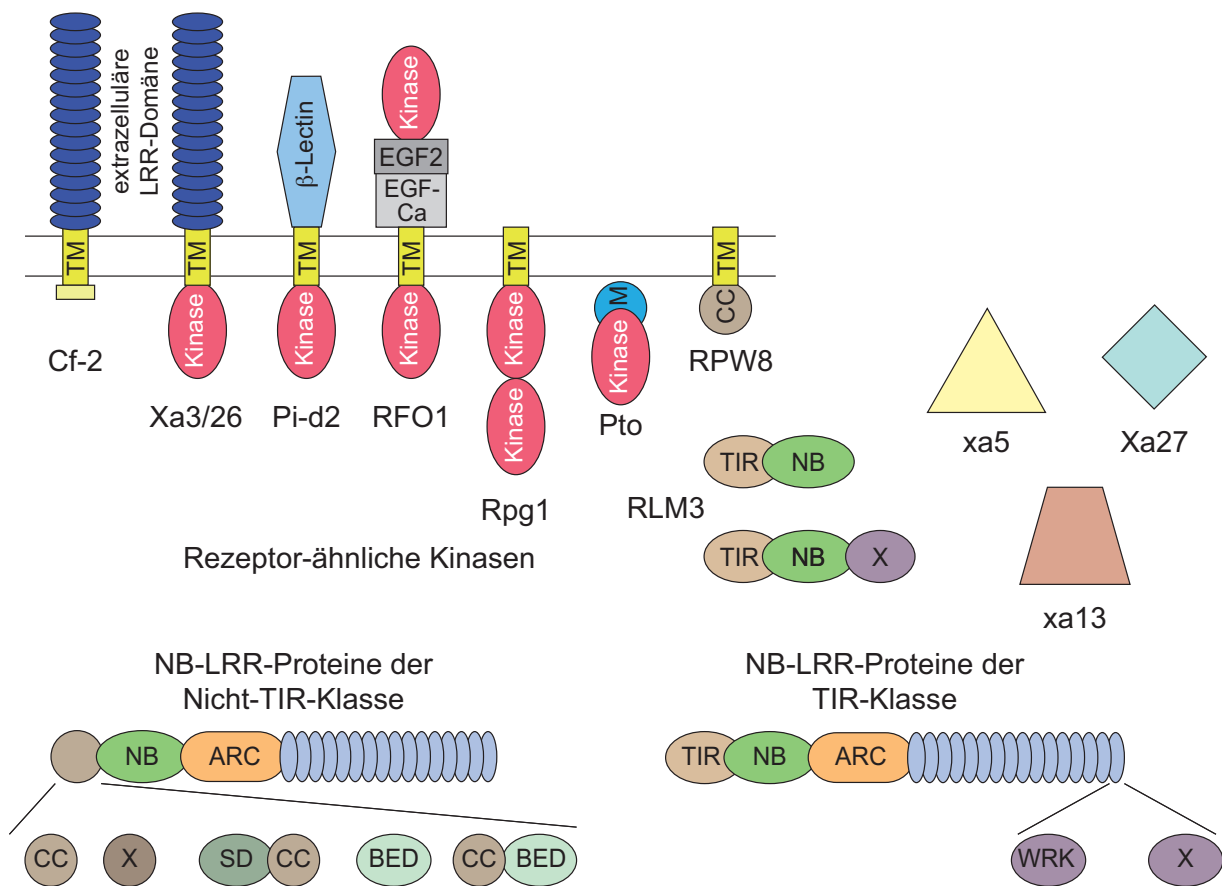


**Abbildung 3: Modulare Struktur von R-Proteinen**

Dargestellt sind repräsentative Beispiele der Rezeptor-ähnlichen Proteine (RLPs) und der Rezeptor-ähnlichen Kinasen (RLKs). Diese sind durch die Transmembrandomäne in der Membran verankert und weisen verschiedene intra- und extrazelluläre Domänen auf. Das R-Protein Pto, das auch eine Kinasedomäne besitzt, weist am N-Terminus ein Myristoylierungsmotiv (M) auf. Weitere Besonderheiten sind die beiden Proteinvarianten von RLM3, welche von den unterschiedlichen Spleißvarianten des *RLM3*-Gens kodiert werden. Die zwei großen Klassen der R-Proteine sind schematisch dargestellt, wobei die NB-, die ARC- und die LRR-Domänen gezeigt wurden. Die Proteine der Nicht-TIR-Klasse weisen eine hohe Variabilität am N-Terminus auf. Dort befindet sich bei diesen Proteinen die CC-, die BED-, die SD-Domäne oder eine Domäne unbekannter Struktur (X). Bei den Proteinen der TIR-Klasse wurde bei einigen eine zusätzliche Domäne am C-Terminus identifiziert, welche Homologien zu den WRKY-Transkriptionsfaktoren aufweisen oder aus großen Domänen mit unbekannter Struktur bestehen (X). Strukturelle Ausnahmen stellen die R-Proteine xa5, xa13 und Xa27 dar, da sie keine Homologien bzw. Gemeinsamkeiten zu anderen bekannten R-Proteinen aufweisen. Die Abbildung wurde verändert nach Sacco und Moffett, 2009.

## 1.5 Signalwegkomponenten der R-Protein vermittelten Resistenz

Die Signaltransduktion in der pflanzlichen Pathogenantwort wurde in der Vergangenheit vorwiegend durch genetische Ansätze analysiert. Die Ergebnisse von Mutantensichtungen, bei denen auf Verminderung oder Verlust der R-Gen vermittelten Resistenz selektiert wurde, deuten darauf hin, dass es bereits sehr früh nach der Pathogenerkennung zu einer Verzweigung der Signalwege kommt (Parker, 2000).

Zu den am besten untersuchten Komponenten der Signalweiterleitung gehören die pflanzen-spezifischen Proteine EDS1 (*enhanced disease susceptibility 1*), PAD4 (*phytoalexin deficient 4*) und NDR1 (*nonrace-specific disease resistance 1*), die aus *Arabidopsis thaliana* isoliert wurden. EDS1 und PAD4 sind Lipase-ähnliche Proteine, die bei der Signaltransduktion von TIR-NB-LRR-Proteinen notwendig sind (Falk et al., 1999; Jirage et al., 1999). NDR1 ist ein Plasmamembran-lokalisiertes Protein, das für die Funktion der meisten Nicht-TIR-NB-LRR-Proteine erforderlich ist (Century et al., 1995; Century et al., 1997; Coppinger et al., 2004). Weitere intensiv untersuchte Signalwegproteine sind Rar1 (*required for Mla-dependent resistance 1*) und SGT1 (*suppressor of G-two allele of SKP 1*). SGT1 ist ein Knotenpunkt in der Signalweiterleitung, da es sowohl für die Funktion von TIR- als auch Nicht-TIR-NB-LRR-Proteinen und R-Proteine, die extrazelluläre Domänen besitzen, notwendig ist (Azevedo et al., 2002; Liu et al., 2002; Peart et al., 2002b; Schornack et al., 2004; Zhang et al., 2004; Hein et al., 2005; Leister et al., 2005).

Neben den Signalwegkomponenten, die durch die Reduktion oder den Verlust der R-Gen vermittelten Resistenz identifiziert wurden, konnte in *A. thaliana* auch eine Komponente identifiziert werden, deren Überexpression in einer erhöhten Basalresistenz resultiert. Bei dieser Komponente handelt es sich um die Flavin-abhängige Monooxygenase FMO1 (Koch et al., 2006). Neben *Arabidopsis* wurden auch in Tomate, Kartoffel, Petunie, Reis, Pappel, Wein, Zitrus und in zahlreichen Kreuzblütengewächsen FMOs identifiziert (Exposito-Rodriguez et al., 2007; Hansen et al., 2007; Li et al., 2008). FMOs haben in Pflanzen eine Funktion in der Auxinbiosynthese und in der Pathogenabwehr (Zhao et al., 2001; Bartsch et al., 2006; Cheng et al., 2006; Koch et al., 2006; Mishina und Zeier, 2006; Yamamoto et al., 2007). Die tierischen FMOs dienen als Hauptdetoxifikationsenzyme, die für den Abbau von vielen Xenobiotika und zahlreichen Arzneimitteln verantwortlich sind (Krueger und Williams, 2005; Cashman und Zhang, 2006; Phillips und Shephard, 2008; Palfey und McDonald, 2010). In Säugern gibt es fünf funktionelle FMOs, wovon drei (FMO1, FMO2 und FMO3) genetische Polymorphismen aufweisen (Lawton et al., 1994; Krueger und Williams, 2005). In *A. thaliana*

wurden dagegen 29 FMO-ähnliche Gene annotiert, was darauf schließen lässt, dass diese ein weniger breites Substratspektrum als die tierischen FMOs haben (Schlauch, 2007).

## 1.6 Die Bakteriengattung *Xanthomonas*

Die Gattung *Xanthomonas* umfasst pflanzenpathogene Bakterien, die zur Untergruppe der  $\gamma$ -Proteobakterien gehören (Cutino-Jimenez et al., 2010). Xanthomonaden sind stäbchenförmige, polar begeißelte, obligat aerobe Bakterien, die eine optimale Wachstumstemperatur von 25-30°C haben (Bradbury, 1984). Die Kolonien von *Xanthomonas*-Bakterien haben eine gelbliche Färbung, was auf das Vorhandensein des membrangebundenen Pigments Xanthomonadin zurückzuführen ist, welches den Bakterien möglicherweise als Lichtschutzpigment dient (Starr und Stephens, 1964; Jenkins und Starr, 1982; Rajagopal et al., 1997). Für Mitglieder der Gattung *Xanthomonas* wurden 124 monokotyledone und 268 dikotyledone Wirtspflanzen beschrieben. Wirtschaftliche Bedeutung hat der Erreger vor allem in tropischen Gebieten mit feucht-warmen Klima (Leys et al., 1984; Chan und Goodwin, 1999; Büttner und Bonas, 2010). Zu den Wirtspflanzen gehören u.a. die ökonomisch relevanten Spezies Reis, Tomate, Paprika, Zwiebel, Kohl, Zitrus, Banane, Maniok und Soja. Der Befall dieser Pflanzen mit *Xanthomonas* spp. führt oft zu erheblichen Ernteaussfällen und damit zu hohen finanziellen Verlusten.

### 1.6.1 *Xanthomonas campestris* pv. *vesicatoria*, der Erreger der bakteriellen Fleckenkrankheit auf Paprika und Tomate

*Xanthomonas campestris* pv. *vesicatoria* (Doidge) Dye (*Xcv*), auch als *Xanthomonas axonopodis* pv. *vesicatoria* bzw. als *Xanthomonas euvesicatoria* bezeichnet, ist der Erreger der bakteriellen Fleckenkrankheit auf Paprika (*Capsicum* spp.) und Tomate (*Solanum lycopersicon* und *Lycopersicon* spp.) (Vauterin et al., 1995; Jones et al., 2004). *Xcv* infiziert das Wirtsgewebe über natürliche Öffnungen wie z. B. Stomata oder Verwundungen und vermehrt sich lokal im Interzellularraum (Apoplasten) des Blattes. Im Gegensatz zu vielen anderen *Xanthomonas*-Gattungen verbreitet sich *Xcv* nicht systemisch. Die Verbreitung des Erregers erfolgt über Regen- und Spritzwasser. Bei einer kompatiblen Interaktion von *Xcv* mit der Pflanze kommt es zur Ausbildung von Krankheitssymptomen, den sogenannten wässrigen Läsionen, welche später nekrotisch werden (Abbildung 4). Aufgrund ihrer Wirtsspezifität wurden *Xcv*-Stämme in elf verschiedene Rassen eingeteilt (Jones et al., 1998; Stall et al., 2009).



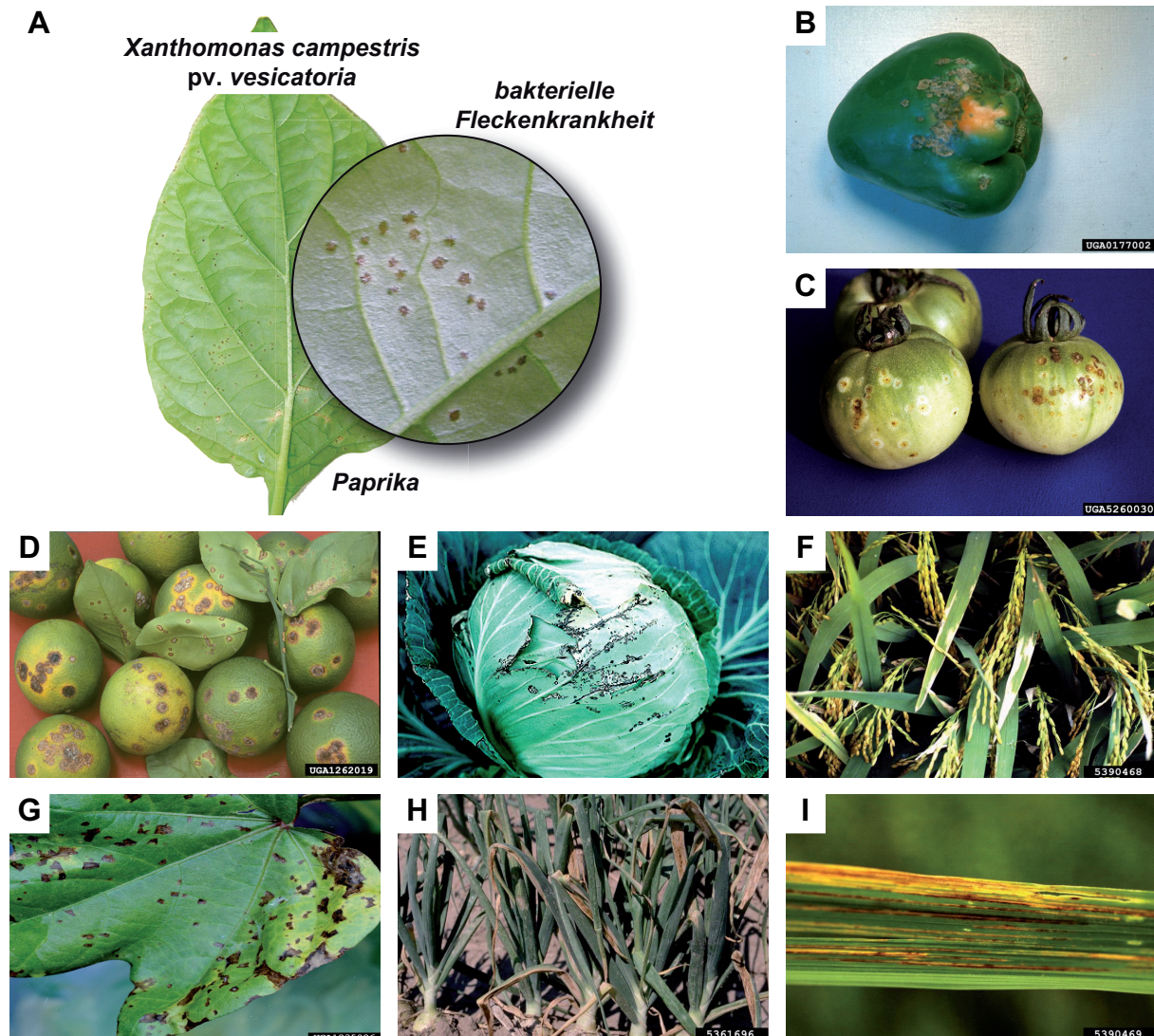


**Abbildung 4: Durch *Xanthomonas* spp. ausgelöste Krankheitssymptome auf bedeutenden Kulturpflanzen**

**A-C)** *Xanthomonas campestris* pv. *vesicatoria* (*Xcv*) ist der Erreger der bakteriellen Fleckenkrankheit auf Paprika und Tomate und verursacht zunächst die typischen Flecken (*bacterial spots*) auf den Paprikablättern. Die Flecken, die durch *Xcv* ausgelöst werden, erscheinen später nekrotisch, was auf den Paprika- und Tomatenfrüchten zu erkennen ist. **D)** *Xanthomonas axonopodis* pv. *citri* (*Xac*) ist der Erreger des Zitruskrebs, der Läsionen auf Früchten, Blättern und Stängeln auslöst. Diese erscheinen zunächst als Pusteln und werden später zu korkartigen braunen Tumoren. **E)** *Xanthomonas campestris* pv. *armoraciae* (*Xca*) ist der Auslöser der Blattfleckenkrankheit auf Kohl. *Xca* verursacht wässrige Läsionen, die später nekrotisch werden und miteinander verschmelzen. Durch *Xca* entstehen entlang der Blattadern nekrotische Streifen. **F)** Die Weissblättrigkeit von Reis wird durch *Xanthomonas oryzae* pv. *oryzae* (*Xoo*) ausgelöst. Dies ist eine vaskuläre Krankheit, welche sich in grauen bis weissen Läsionen entlang der Blattadern äußert (Mew et al., 1993). **G)** *Xanthomonas campestris* pv. *malvacearum* (*Xcm*) verursacht die eckige Blattfleckenkrankheit auf Baumwolle. Symptomatisch für diese Krankheit sind eckige rotbraune Blattflecken, welche durch die Blattadern begrenzt sind. **H)** Auf Zwiebeln ausgelöste Symptome durch *Xanthomonas axonopodis* pv. *allii* (*Xaa*). *Xaa* induziert wässrige Läsionen, die später chlorotisch werden und den Gewebekollaps bedingen (Roumagnac et al., 2004). **I)** Auf Reisblättern ausgelöste Symptome durch *Xanthomonas oryzae* pv. *oryzicola* (*Xoc*), den Erreger der bakteriellen Blattstreifenkrankheit. Symptomatisch sind gelbe Streifen, die später nekrotisch werden. Die Läsionen, die *Xoc* verursacht, sind wesentlich dünner und in der Farbe gelber, als die durch *Xoo* verursachten und daher gut voneinander zu unterscheiden (Niño-Liu et al., 2006). (Bildquellen: [A] S. Schornack, MLU Halle-Wittenberg; [B] Volcani Center Archive, Agricultural Research Organization, Bugwood.org; [C] Division of Plant Industry Archive, Florida Department of Agriculture and Consumer Services, Bugwood.org; [D] Timothy Schubert, Florida Department of Agriculture and Consumer Services, Bugwood.org; [E] AVRDC International Cooperators Fact Sheet: Crucifer diseases, *Xanthomonas* leaf spot; <http://www.avrdc.org/LC/cabbage/xant.html#1>; [F] Donald Groth, LSU AgCenter, Bugwood.org; [G] Clemson University- USDA Cooperative Extension Slide Series, Bugwood.org [H] Howard F. Schwartz, Colorado State University, Bugwood.org; [I] Donald Groth, LSU AgCenter, Bugwood.org).

### 1.6.2 *Xanthomonas oryzae* pv. *oryzae*, der Erreger der bakteriellen Weissblättrigkeit

*Xanthomonas oryzae* pv. *oryzae* (*Xoo*) ist der Erreger der bakteriellen Weissblättrigkeit von Reis und verursacht Ertragseinbußen im asiatischen und afrikanischen Raum. *Xoo* wurde aber auch schon in Australien, Lateinamerika und der Karibik identifiziert (Mew et al., 1993). *Xoo* dringt über die Hydathoden an der Blattspitze bzw. am Blattrand in die Reisblätter ein (Ou, 1985). Die Bakterien vermehren sich im Interzellularraum und dringen dann in das Xylem ein, von wo aus sich *Xoo* in der Pflanze systemisch ausbreitet (Noda und Hisatoshi, 1999). Die Weissblättrigkeit beginnt als wässrige Läsionen an den Blattspreiten und breitet sich dann entlang des gesamten Blattes aus. Dadurch verfärben sich die Blätter grau-weiss und es kommt schließlich zum Austrocknen des gesamten Blattes.

### 1.7 Die TAL-Effektoren aus *Xanthomonas*, Struktur und Funktion

TAL-Effektoren (*transcription activator like*) werden nach dem ersten sequenzierten Mitglied dieser Proteinfamilie, AvrBs3 aus *Xcv*, auch als AvrBs3-ähnliche Proteine bezeichnet (Bonas et al., 1989). Gene, die für Proteine dieser Familie kodieren, wurden bis jetzt nur in Xanthomonaden und *Ralstonia solanacearum* nachgewiesen (Salanoubat et al., 2002; Cunnac et al., 2004). In späteren Arbeiten zu *Xoo* wurden AvrBs3-ähnliche Proteine auf Grund ihrer postulierten Funktion als Transkriptionsfaktoren auch als TAL-Effektoren bezeichnet (Yang et al., 2006). TAL-Effektoren weisen im N-terminalen Bereich ein Typ-III-Sekretions- und Translokationssignal auf, das determiniert, dass diese bakteriellen Effektorproteine über das T3SS in die eukaryotische Wirtszelle injiziert werden. Ein charakteristisches Merkmal der TAL-Effektoren ist die zentral gelegene *Repeat*-Region (Abbildung 5). Diese setzt sich aus einer variablen Anzahl (1,5 bis 33,5) hintereinander geschalteter sogenannter *Repeat*-Einheiten zusammen (Lee et al., 2005; Wu et al., 2007). Eine *Repeat*-Einheit besteht in den meisten Fällen aus 34 Aminosäuren (AS). Es wurden aber auch TAL-Effektoren beschrieben, welche vereinzelt 33 AS *Repeat*-Einheiten aufweisen. Beispiele hierfür sind einige *Repeat*-Einheiten aus PthXo1, PthXo6, PthXo7, AvrXa27 und AvrXa7 (Yang und White, 2004; White et al., 2009). Einige TAL-Effektoren aus *Xanthomonas* weisen auch 35 AS lange *Repeat*-Einheiten auf. Beispiele hierfür sind AvrHah1 aus *Xanthomonas gardneri* und Hax2 aus *Xca* (Kay et al., 2005; Schornack et al., 2008). Im Gegensatz dazu sind die *Repeat*-Einheiten aus allen bisher bekannten *Ralstonia* TAL-Effektoren ausschließlich aus 35 AS aufgebaut (Cunnac et al., 2004; Mukaihara et al., 2004; Heuer et al., 2007).

Die *Repeat*-Einheiten sind zueinander nahezu sequenzidentisch, zeigen jedoch in den AS 12 und 13, den sogenannten hypervariablen AS, welche in neueren Publikationen als *repeat variable-diresidue* (RVD) bezeichnet wurden eine hohe Variabilität auf (Abbildung 5; Moscou und Bogdanove, 2009). Strukturvorhersagen haben ergeben, dass die RVDs Lösungsmittel exponiert sind (Schornack et al., 2006). Folglich stellen diese AS mögliche DNA Interaktionsstellen dar.

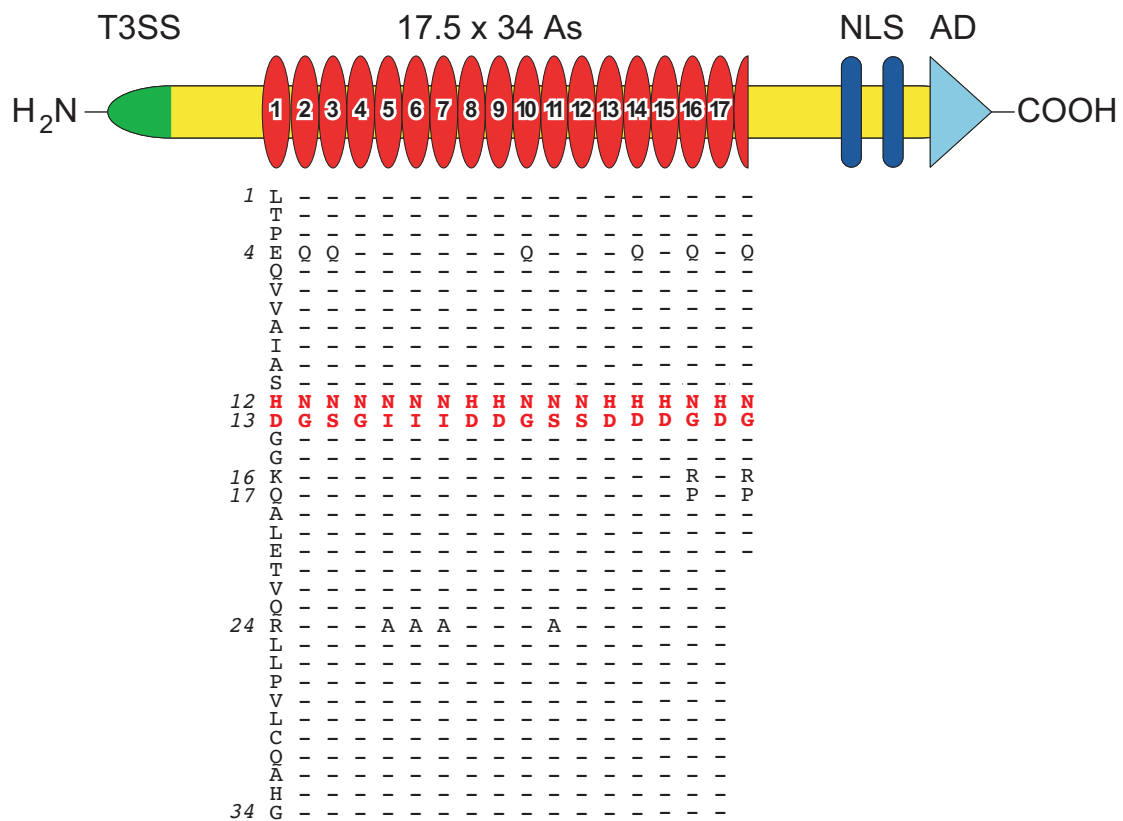


**Abbildung 5: Aufbau von AvrBs3 und Sequenzvergleich der einzelnen *Repeat*-Einheiten**

Schematische Darstellung des TAL-Effektors AvrBs3. Im N-terminalen Bereich befindet sich das Typ-3-Sekretions- und Translokationssignal (T3SS). Die zentrale Region besteht aus 17,5 nahezu identischen *Repeat*-Einheiten. Aminosäuren, die identisch zu *Repeat*-Einheit 1 sind, sind als Striche dargestellt. Unterschiede zwischen *Repeat*-Einheiten befinden sich nur an den AS-Positionen 4, 12, 13, 16, 17 und 24 (Zahlen in Kursivdruck). Im C-terminalen Bereich befinden sich die Kernlokalisierungssignale (NLS) und die saure Aktivierungsdomäne (AD), die typischen Strukturmerkmale eukaryotischer Transkriptionsfaktoren.

Im C-terminalen Bereich von TAL-Effektoren befinden sich typische Merkmale eukaryotischer Transkriptionsfaktoren, wie Kernlokalisierungssignale (*nuclear localisation signals*, NLS) und eine saure Aktivierungsdomäne (*acidic activation domän*, AD) (Abbildung 5). Die NLS vermitteln über die Interaktion mit Importin- $\alpha$  den Kernimport (Szurek et al., 2001). Die AD vermittelt vermutlich die Interaktion mit Komponenten der eukaryotischen Transkriptionsmaschinerie. Funktionelle NLS und AD sind für die meisten bisher untersuchten Virulenzfunktionen und Avirulenzfunktion von TAL-Effektoren in Pflanzen essentiell (Van den Ackerveken et al., 1996; Gabriel, 1997; Zhu et al., 1998; Yang et al., 2000;

Szurek et al., 2001; Marois et al., 2002; Kay et al., 2007; Athinuwat et al., 2009). Für AvrBs3 wurde bspw. gezeigt, dass die NLS und die AD sowohl für die Ausbildung der Hypertrophie in suszeptiblen, als auch für die Induktion der HR in resistenten Paprikapflanzen notwendig sind (Van den Ackerveken et al., 1996; Szurek et al., 2001; Marois et al., 2002).

### 1.7.1 *UPA*-Gene werden durch den TAL-Effektor AvrBs3 induziert

Für AvrBs3 konnten mittels differentieller Transkriptanalyse Zielgene aus dem suszeptiblen Paprika Kultivar ECW isoliert werden. Da diese Gene durch AvrBs3 transkriptionell aktiviert werden, wurden sie als *UPA*-Gene (*upregulated by AvrBs3*) definiert (Marois et al., 2002; Kay et al., 2007; Kay et al., 2009). In einer parallel zu der hier vorliegenden Arbeit angefertigten Dissertation konnte auf Basis von Sequenzvergleichen zwischen verschiedenen AvrBs3 induzierten *UPA*-Promotoren ein gemeinsames Sequenzmotiv identifiziert werden, welches als *UPA*-Box definiert wurde (Kay et al., 2007). Für das *UPA*-Gen *UPA20* konnte gezeigt werden, dass es für einen *basic helix-loop-helix* (bHLH)-Transkriptionsfaktor kodiert, der hinreichend und notwendig für die Ausbildung der durch AvrBs3 bedingten Hypertrophie ist (Marois et al., 2002; Kay et al., 2007). Die Bindung von AvrBs3 an die *UPA*-Box des *UPA20*-Promotors erfolgt über die *Repeat*-Einheiten von AvrBs3 (Kay et al., 2007). Da vermutet wird, dass auch weitere TAL-Effektoren an Promotorbereiche TAL-Effektor-induzierter Wirtsgene binden, erfolgt die Einführung des Begriffes *upregulated by TALes* (*UPT*)-Box. Dabei wird der TAL-Effektor, der eine spezifische *UPT*-Box ansteuert, mit tief gestellter Schrift vermerkt (z.B. *UPT<sub>AvrBs3</sub>*-Box für die *UPT*-Box, welche von AvrBs3 angesteuert wird (Römer et al., 2009a; Römer et al., 2010)).

### 1.7.2 Suszeptibilitätsgene aus Reis werden durch TAL-Effektoren induziert

Für AvrBs3 konnte gezeigt werden, dass es in *C. annuum* ECW Wirtsgene aktiviert, die möglicherweise das Wachstum im Blattgewebe begünstigen (Marois et al., 2002; Kay et al., 2007). Auch für TAL-Effektoren des Reispathogens *Xoo* konnten Suszeptibilitätsgene isoliert und charakterisiert werden. Beispiele für solche Suszeptibilitätsgene aus Reis sind *Os8N3* und *Os11N3* (Chu et al., 2006; Yang et al., 2006; Antony et al., 2009), welche durch die TAL-Effektoren PthXo1 bzw. AvrXa7 aktiviert werden und Homologien zur *MtN3*-Familie aufweisen. Zur *MtN3*-Familie gehören frühe Nodulingene aus *Medicago truncatula* und *NEC1* aus Petunie (Gamas et al., 1996). Für *NEC1* konnte gezeigt werden, dass es im Zusammenhang mit der Phloementwicklung und der Staubbeutelreifung steht (Ge et al., 2000;

Ge et al., 2001). Vertreter der *MtN3*-Familie werden aber nicht nur durch TAL-Effektoren, sondern auch durch zahlreiche andere Stimulie wie z. B. Chemikalien ( $\text{NH}_4^+$ ) und Nematoden induziert (Jammes et al., 2005; Lopes und Araus, 2008). Neben *Os8N3* und *Os11N3* wurden *OsTFX1*, *OsTFIIA $\gamma$ 1* und *OsHen1* als weitere TAL-Effektor-induzierte und potentielle Suszeptibilitätsgene aus Reis identifiziert. *OsTFX1*, *OsTFIIA $\gamma$ 1* werden durch die *Xoo* TAL-Effektoren PthXo6 bzw. PthXo7 und *OsHen1* durch PthXo8 induziert. Ob die TAL-Effektor vermittelte Induktion dieser Wirtsgene durch direkte Promotorbindung erfolgt, ist jedoch bisher nicht geklärt (Sugio et al., 2007; Ryan et al., 2009).

### 1.7.3 R-Gene, die Resistenz gegen TAL-Effektoren vermitteln, sind strukturell divers

Für einige TAL-Effektoren konnte eine Virulenzfunktion demonstriert werden (siehe 1.7.2). Bis jetzt ist aber nur für wenige der bekannten TAL-Effektoren ein korrespondierender *R*-Gen-Lokus in den verschiedenen Pflanzenspezies bekannt. Zu Beginn der hier vorliegenden Arbeit waren fünf *R*-Gene, die von TAL-Effektoren angesteuert werden (*Bs4*, *xa5*, *xa13*, *Xa27* und *Xa3/Xa26*) isoliert und charakterisiert (Iyer und McCouch, 2004; Schornack et al., 2004; Sun et al., 2004; Gu et al., 2005; Chu et al., 2006; Xiang et al., 2006; Yang et al., 2006).

Das *R*-Gen *Bs4* aus Tomate kodiert für ein TIR-NB-LRR Protein und gehört damit zu der größten Klasse von R-Proteinen (Schornack et al., 2004). *Bs4* vermittelt Resistenz gegen *AvrBs4* exprimierende *Xcv*-Stämme. Eine Besonderheit dabei ist, dass auch NLS- und AD-Deletionskonstrukte von *AvrBs4* die *Bs4*-bedingte HR auslösen. Auch ein *AvrBs4*-Deletionskonstrukt, welches nur aus 3,5 der 17,5 *Repeat*-Einheiten besteht, ist in der Lage eine *Bs4*-vermittelte HR auszulösen (Bonas et al., 1993; Ballvora et al., 2001a; Schornack et al., 2004). Neben der Erkennung von *AvrBs4* vermittelt *Bs4* auch die Erkennung der TAL-Effektoren *Hax3* und *Hax4* aus *Xca* (Kay et al., 2005; Schornack et al., 2005). Eine weitere Besonderheit von *Bs4* ist, dass es die Erkennung aller bisher getesteten TAL-Effektoren vermittelt, die aus 34 AS *Repeat*-Einheiten bestehen, wenn die korrespondierenden TAL-Effektor Gene unter der Kontrolle des starken, konstitutiven Cauliflower Mosaik Virus 35S-Promotors in der Pflanzenzelle exprimiert werden (Schornack et al., 2005; S. Schornack, P. Römer und T. Lahaye, unveröffentlicht).

Das TAL-Effektor *R*-Gen *xa5* aus Reis kodiert für eine allelische Variante der  $\gamma$ -Untereinheit des generellen Transkriptionsfaktors TFIIA. Generelle Transkriptionsfaktoren (GTFs) wie TFIIA bilden einen Komplex mit der RNA-Polymerase II und sind essentielle Komponenten der Transkription. Neuere Daten weisen jedoch darauf hin, dass TFIIA kein essentieller GTF ist, jedoch als Koaktivator fungiert (Høiby et al., 2007; Sikorski und Buratowski, 2009). Reis

hat zwei Homologe Gene, die für die  $\gamma$ -Untereinheit kodieren und auf Chromosom 1 (*OsTFIIA $\gamma$ 1*) und auf Chromosom 5 (*OsTFIIA $\gamma$ 5*; *Xa5*) lokalisiert sind (Iyer und McCouch, 2004; Jiang et al., 2006; Sugio et al., 2007; Iyer-Pascuzzi et al., 2008). Sowohl für *Xa5* als auch für das rezessive *R*-Gen *xa5* konnte gezeigt werden, dass sie zu ähnlichen Mengen in Blättern von Reispflanzen exprimiert werden (Iyer und McCouch, 2004; Jiang et al., 2006). Des Weiteren konnte ermittelt werden, dass die beiden *Xa5/xa5*-Allele auch im Stängel und der Wurzel konstitutiv exprimiert werden (Jiang et al., 2006). Der exakte Wirkmechanismus der *xa5*-vermittelten Resistenz konnte bis jetzt nicht aufgeklärt werden. Es ist jedoch naheliegend, dass TAL-Effektoren aus *Xoo* über eine Interaktion mit *Xa5* das Wirtstranskriptom zu Gunsten von *Xoo* modifizieren (Schornack et al., 2006). Die vom *xa5*-Allel kodierte TFIIA $\gamma$ -Variante weist einen AS-Polymorphismus auf, der möglicherweise bedingt, dass TAL-Effektoren nicht mehr bzw. mit einer geringeren Affinität mit dieser Variante interagieren können. Dass *xa5* einen Einfluss auf die transkriptionelle Aktivierung durch TAL-Effektoren hat, konnte unlängst in Reis gezeigt werden. Dort war es möglich zu zeigen, dass in *xa5*-Pflanzen, die durch *AvrXa27* induzierte transkriptionelle Aktivierung des *Xa27*-Gens drastisch reduziert wird (Gu et al., 2009).

Das rezessive *R*-Gen *xa13* ist eine allelische Variante von *Os8N3* (*Xa13*) und kodiert für ein Protein der MtN3-Familie (siehe 1.7.2). Die Induktion von *Os8N3* durch *PthXo1* ist notwendig, um *Xoo*-Stämmen, welche *PthXo1* exprimieren das Wachstum und die Verbreitung in Reis zu ermöglichen (Yang et al., 2006). Neben der Funktion als Suszeptibilitätsprotein hat *Os8N3* auch eine Funktion in der Pollenentwicklung. In resistenten Pflanzen bedingen wahrscheinlich Sequenzunterschiede im Promotor, dass *xa13* nicht mehr durch *PthXo1* induziert werden kann, was eine reduzierte *Xoo* Virulenz bedingt (Chu et al., 2006; Yang et al., 2006; Yuan et al., 2009).

Das dominant vererbte Reis *R*-Gen *Xa27* kodiert für ein Protein ohne Homologien zu anderen bekannten *R*-Proteinen (Gu et al., 2005). Analysen mit *Xoo*-Stämmen, die den TAL-Effektor *AvrXa27* exprimieren ergaben, dass es nur in resistenten *Xa27*-Pflanzen, nicht jedoch in suszeptiblen *xa27*-Pflanzen zu einer *AvrXa27*-vermittelten Genaktivierung kommt. Die beiden *Xa27*-Allele unterscheiden sich nur in der Sequenz der Promotoren, jedoch nicht in der kodierenden Sequenz. Folglich ist anzunehmen, dass Polymorphismen im Promotor für die unterschiedliche Induzierbarkeit der beiden Allele verantwortlich sind (Gu et al., 2005). *Xa27* konnte im Apoplasten lokalisiert werden und es wurde festgestellt, dass diese Lokalisation für das Auslösen der Resistenzreaktion notwendig ist (Wu et al., 2008).

Xa3/Xa26 kodiert für ein RLK-Protein, welches Resistenz gegen die *Xoo* TAL-Effektoren Avr/Pth3 und AvrXa3 vermittelt (Sun et al., 2004). Xa3/Xa26 wird konstitutiv exprimiert, wobei die höchsten Expressionslevel in den Blättern von jungen Pflanzen detektiert wurden (Sun et al., 2004; Xiang et al., 2006). Wie die Erkennung der TAL-Effektoren durch ein RLK-Protein erfolgt, ist bis jetzt noch nicht geklärt (Zhao, 2009).

**Tabelle 1: R-Gene und ihre korrespondierenden TAL-Effektoren**

R-Gen	Referenzen <sup>a</sup>	Avr-Protein	Repeat Anzahl und Aufbau	Pathogen	Referenzen <sup>b</sup>
<b>Baumwolle</b>					
<i>B1, b6</i>	(Gabriel et al., 1986; De Feyter et al., 1993)	AvrB6	13,5 x 34 AS	<i>Xcm</i>	(De Feyter et al., 1993)
<b>Paprika</b>					
<i>Bs3</i>	(Pierre et al., 2000)	AvrBs3	17,5 x 34 AS	<i>Xcv</i>	(Bonas et al., 1989)
<i>Bs3</i>	(Pierre et al., 2000)	AvrHah1	13,5 x 34/35 AS	<i>X. gardneri</i>	(Schornack et al., 2008)
<b>Tomate</b>					
<i>Bs4</i>	(Ballvora et al., 2001b; Schornack et al., 2004) <sup>#</sup>	AvrBs4	17,5 x 34 AS	<i>Xcv</i>	(Bonas et al., 1993)
<i>Bs4</i>	(Ballvora et al., 2001b; Schornack et al., 2004) <sup>#</sup>	Hax3	11,5 x 34 AS	<i>Xca</i>	(Kay et al., 2005)
<i>Bs4</i>	(Ballvora et al., 2001b; Schornack et al., 2004) <sup>#</sup>	Hax4	14,5 x 34 AS	<i>Xca</i>	(Kay et al., 2005)
<b>Reis</b>					
<i>Xa3/Xa26</i>	(Ezuka et al., 1975; Ogawa et al., 1986; Sun et al., 2004 <sup>#</sup> ; Xiang et al., 2006 <sup>#</sup> ; Cao et al., 2007)	Avr/Pth3	1,5 x 34 AS	<i>Xoo</i>	(Wu et al., 2007)
<i>Xa3/Xa26</i>	(Ezuka et al., 1975; Ogawa et al., 1986; Sun et al., 2004 <sup>#</sup> ; Xiang et al., 2006 <sup>#</sup> ; Cao et al., 2007)	AvrXa3	8,5 x 34 AS*	<i>Xoo</i>	(Li et al., 2004)
<i>xa5</i>	(Blair et al., 2003; Zhong et al., 2003; Iyer und McCouch, 2004) <sup>#</sup>	Avrxa5	5,5 x 34 AS	<i>Xoo</i>	(Hopkins et al., 1992; Bai et al., 2000)
<i>Xa7</i>	(Sidhu et al., 1978; Porter et al., 2003; Chen et al., 2008)	AvrXa7	25,5 x 34 AS* <sup>1</sup>	<i>Xoo</i>	(Hopkins et al., 1992; Vera Cruz et al., 2000)
<i>Xa10</i>	(Yoshimura et al., 1983; Xinghua et al., 1996; Gu et al., 2008)	AvrXa10	15,5 x 34 AS	<i>Xoo</i>	(Hopkins et al., 1992; Zhu et al., 1998)
<i>xa13</i>	(Chu et al., 2006 <sup>#</sup> ; Yang et al., 2006) <sup>#</sup>	PthXo1 (Avrxa13)	23,5 x 34 AS*	<i>Xoo</i>	(Yang und White, 2004)
<i>Xa27</i>	(Gu et al., 2005) <sup>#</sup>	AvrXa27	16,5 x 34 AS*	<i>Xoo</i>	(Gu et al., 2005)

a) Referenzen, die die genetische Kartierung und die Isolierung (#) beschreiben

b) Referenzen, welche die Isolierung und Charakterisierung der korrespondierenden *avr*-Gene beschreiben

\* einzelne *Repeat*-Einheiten bestehen nur aus 33 AS, I: Insertion von 6 AS in der 13 *Repeat*-Einheit;

## 1.8 Das *R*-Gen *Bs3* und mögliche Allele in den verschiedenen *Capsicum*-Arten

In Paprika (*Capsicum* spp.) wurden die drei *R*-Gene *Bs1*, *Bs2* und *Bs3* genetisch definiert, welche eine spezifische Resistenz gegenüber *Xcv*-Stämmen verleihen, die die *avr*-Gene *avrBs1*, *avrBs2* bzw. *avrBs3* exprimieren. Die Vererbung dieser *R*-Gene erfolgt monogen und dominant (Hibberd et al., 1987). Ursprünglich wurden *Bs1* und *Bs3* in den *C. annuum* Linien PI 271322 und PI 163192 identifiziert, das *Bs2*-Gen stammt aus *C. chacoense* PI 260435 (Cook und Stall, 1963; Cook und Guevara, 1984; Kim und Hartmann, 1985). Alle drei *Bs*-Gene wurden in die suszeptible *C. annuum* Linie ECW eingekreuzt, woraus die fast isogenen Linien ECW-10R, ECW-20R und ECW-30R hervorgingen (Stall et al., 2009). Wie die Erkennung von AvrBs3 durch *Bs3* auf molekularer Ebene abläuft, konnte bis jetzt nicht geklärt werden, da das *Bs3*-Gen erst im Verlauf dieser Arbeit isoliert und charakterisiert wurde. Neben AvrBs3 gibt es noch weitere TAL-Effektoren, die eine HR in Paprika auslösen. Die Erkennung dieser Effektoren ist, wie die von AvrBs3, NLS- und AD-abhängig. So konnte bspw. gezeigt werden, dass das AvrBs3-Deletionsderivat AvrBs3 $\Delta$ rep16, bei dem die *Repeat*-Einheiten 11-14 deletiert sind, in der Lage ist eine NLS- und AD-abhängige HR in der Paprikalinie *C. annuum* ECW zu induzieren, nicht jedoch in der Paprikalinie ECW-30R, die das *R*-Gen *Bs3* trägt (Herbers et al., 1992). Daraus wurde geschlussfolgert, dass die Anzahl und die Abfolge der *Repeat*-Einheiten die Spezifität zu den korrespondierenden *R*-Genen vermittelt (Herbers et al., 1992). Auch AvrBs4, welches in Tomate (*Solanum lycopersicon*) eine NLS- und AD-unabhängige HR auslöst (Ballvora et al., 2001a), ist in der Lage in der *C. pubescens* Akzession PI 235047, jedoch nicht in der Akzession PI 585270 eine NLS- und AD-abhängige HR zu induzieren (Minsavage et al., 1999; D. Gürlebeck und U. Bonas, unveröffentlicht). Diese Befunde legten die Vermutung nahe, dass es sich bei den Genen, welche die Erkennung der AvrBs3-ähnlichen Proteine vermitteln auch um *Bs3*-Orthologe handelt. Um die *R*-Gene im weiteren Verlauf der Arbeit klar von einander unterscheiden zu können, erfolgte die Zuordnung einer Genbezeichnung. Das *R*-Gen aus der Linie *C. annuum* ECW wurde in früheren Arbeiten als *bs3* bezeichnet (Herbers et al., 1992; Pierre et al., 2000). Die Bezeichnung *bs3* resultierte aus dem Befund, dass in *C. annuum* ECW Pflanzen AvrBs3 keine HR induziert und daher das *bs3*-Allel in diesen Pflanzen ein nicht funktionales Allel in der Interaktion darstellt. In der vorliegenden Arbeit wird *bs3* als *Bs3-E* definiert, da es sich hierbei höchstwahrscheinlich um das *Bs3*-Allel aus der Linie ECW handelt. Die analysierten *R*-Gene aus Paprika und Tomate sowie deren Erkennung sind in der Abbildung 6 zusammengefasst.



Effektorproteine	Struktur	HR-Induktion				
		<i>C. annuum</i>		<i>C. pubescens</i>	<i>L. esculentum</i>	
		ECW 30R Bs3	ECW Bs3-E	PI 235047	PI 585270	Bs4
AvrBs3		+	-	-	-	-
AvrBs3ΔAD		-	-	-	-	-
AvrBs3ΔNLS		-	-	-	-	-
AvrBs3Δrep16		-	+	-	-	-
AvrBs3Δrep16ΔAD		-	-	-	-	-
AvrBs3Δrep16ΔNLS		-	-	-	-	-
AvrBs4		-	-	+	-	+
AvrBs4ΔAD		-	-	-	-	+
AvrBs4ΔNLS		-	-	-	-	+

**Abbildung 6: Struktur von AvrBs3-ähnlichen Proteinen und ihre Erkennung**

Dargestellt sind AvrBs3 und AvrBs4 und die dazugehörigen AD- und NLS-Deletionsderivate. Ein “+“ zeigt an, dass der TAL-Effektor in der Pflanze von dem korrespondierenden *R*-Gen erkannt wird und es zur Induktion der HR kommt. Ein “-“ symbolisiert, dass keine HR induziert wird. Angegeben sind die *R*-Gen-Spezifitäten von *Xcv*-translozierten TAL-Effektoren.

## 1.9 Vorarbeiten und Zielstellung der Arbeit

In Vorarbeiten konnte das genetische Zielintervall des *R*-Gens *Bs3*, das Resistenz gegen *Xcv*-Stämme vermittelt, die AvrBs3 exprimieren, mittels eines kartengestützten Ansatzes genetisch eingegrenzt werden. Es wurden BAC-Klone isoliert, die den *Bs3*-Lokus physikalisch überspannen (Jordan et al., 2006).

Ziel der vorliegenden Arbeit war die molekulare Isolierung und Charakterisierung des *Bs3*-Gens aus ECW-30R, sowie des Allels *Bs3-E* aus ECW. Außerdem sollten *Bs3*-Allele in anderen *Capsicum*-Arten auf Erkennung von AvrBs3 sowie AvrBs3-ähnlicher Proteine getestet werden.

Weiterhin sollte in der hier vorliegenden Arbeit analysiert werden, ob andere Gene, die von TAL-Effektoren angesteuert werden nach dem gleichen Mechanismus funktionieren wie *Bs3* und ob mehrere *UPT*-Boxen in einem komplexen Promotor kombiniert werden können.

## 2 Ergebnisse

### 2.1 Übersicht der Publikationen

**Römer, P.,** Hahn, S., Jordan, T., Strauß, T., Bonas, U. and Lahaye, T. (2007)

Plant pathogen recognition mediated by promoter activation of the pepper *Bs3* resistance gene  
Science **318**: 645-648

Eigenanteil: Isolierung und Komplementationsanalysen von *Bs3* und *Bs3-E*, Erstellung aller Konstrukte für die Paprika *Bs3*- und *Bs3-E*-Allele, Planung, Durchführung und Auswertung der Experimente mit Ausnahme der EMSA und Chromatin-IP-Analysen und der dazugehörigen Abbildungsunterschrift, Erstellung der Abbildungen 1A, 1B, 2 und 3 sowie der *Supporting-Figures* S3 bis S8 und S10, Anfertigung von Material und Methoden sowie der Abbildungsunterschriften.

**Römer, P.,** Strauß, T., Hahn, S., Scholze, H., Morbitzer, R., Grau, J., Bonas, U. and Lahaye, T. (2009)

Recognition of AvrBs3-like proteins is mediated by specific binding to promoters of matching pepper *Bs3* alleles  
Plant Physiology **150**: 1697-1712

Eigenanteil: Erstellung von 59 der 69 Konstrukte für die Einzelnukleotidaustausche im Paprika *Bs3*-Promotor, sowie Erstellung aller weiteren Konstrukte mit Mutationen im Paprika *Bs3*- oder *Bs3-E*-Promotor. Planung, Durchführung und Auswertung der Experimente mit Ausnahme der EMSA-Studien (Abbildung 8), der Sequenzierung, der funktionellen Analyse der *Bs3*-Allele (Tabelle 1) und der Erstellung der *Supporting-Figures* S1A, S1B und S2. Manuskriptentwurf, Anfertigung von Material und Methoden sowie der Abbildungsunterschriften ausser die EMSA-Analysen.

**Römer, P.,** Recht, S. and Lahaye, T. (2009)

A single plant resistance gene promoter engineered to recognize multiple TAL effectors from disparate pathogens  
Proceedings of the National Academy of Sciences USA **106**: 20526-20531

Eigenanteil: Erstellung aller Konstrukte für den *Xa27*-Promotor und die Kombination der verschiedenen *UPT*-Boxen, Planung, Durchführung und Auswertung der Experimente mit Ausnahme der EMSA-Analysen. Anfertigung des Manuskripts.

**Römer, P.**, Jordan, T. and Lahaye, T. (2010)

Identification and application of a DNA-based marker that is diagnostic for the pepper (*Capsicum annuum*) bacterial spot resistance gene *Bs3*  
Plant Breeding (DOI: 10.1111/j.1439-0523.2009.01750.x *in press*)

Eigenanteil: Planung, Durchführung und Auswertung der Experimente, sowie Erstellung des Manuskriptentwurfs.

**Römer, P.**, Recht, S., Strauß, T., Elsaesser, J., Schornack, S., Boch, J., Wang, S. and Lahaye, T. (2010)

Promoter elements of rice susceptibility genes are bound and activated by specific TAL effectors from the bacterial blight pathogen, *Xanthomonas oryzae* pv. *oryzae*  
New Phytologist (DOI: 10.1111/j.1469-8137.2010.03217.x *in press*)

Eigenanteil: Erstellung der Konstrukte für die Kombination der verschiedenen *UPT*-Boxen zur Analyse im GUS-Assay, Planung, Durchführung und Auswertung der Experimente mit Ausnahme der EMSA-Analysen. Anfertigung des Manuskriptentwurfs.

nicht in diese Arbeit eingegangene Publikationen:

Jordan, T., **Römer, P.**, Meyer, A., Szczesny, R., Pierre, M., Piffanelli, P., Bendahmane, A., Bonas, U. and Lahaye, T. (2006).

Physical delimitation of the pepper *Bs3* resistance gene specifying recognition of the AvrBs3 protein from *Xanthomonas campestris* pv. *vesicatoria*  
Theor. Appl. Genet. **113**: 895-905

Eigenanteil: Isolierung von BAC103 und BAC104. Isolierung und Anordnung der Enden von den BAC-Klonen 128, 103 und 104 und Erstellung einer Karte, die den *Bs3*-Lokus überspannt.

Übersichtsartikel:

Schornack, S., Meyer, A., **Römer, P.**, Jordan, T., and Lahaye, T. (2006).

Gene-for-gene-mediated recognition of nuclear-targeted AvrBs3-like bacterial effector proteins.

Journal of Plant Physiology **163**: 256-272.

Patent:

Titel des Patents	"Bs3 Resistance Genes and Methods of Use"
Int. Application No	PCT/US2008/077639
Int. Filing Date	25.09.2008
Inventors	Thomas Lahaye, Ulla Bonas, Patrick Römer

## 2.2 Isolierung und Charakterisierung des Paprika *Bs3*-Resistenzgens

### 2.2.1 Publikation 1

---

# Plant Pathogen Recognition Mediated by Promoter Activation of the Pepper *Bs3* Resistance Gene

Patrick Römer, Simone Hahn, Tina Jordan,\* Tina Strauß, Ulla Bonas, Thomas Lahaye†

Plant disease resistance (R) proteins recognize matching pathogen avirulence proteins. Alleles of the pepper R gene *Bs3* mediate recognition of the *Xanthomonas campestris* pv. *vesicatoria* (*Xcv*) type III effector protein AvrBs3 and its deletion derivative AvrBs3Δrep16. Pepper *Bs3* and its allelic variant *Bs3-E* encode flavin monooxygenases with a previously unknown structure and are transcriptionally activated by the *Xcv* effector proteins AvrBs3 and AvrBs3Δrep16, respectively. We found that recognition specificity resides in the *Bs3* and *Bs3-E* promoters and is determined by binding of AvrBs3 or AvrBs3Δrep16 to a defined promoter region. Our data suggest a recognition mechanism in which the Avr protein binds and activates the promoter of the cognate R gene.

Resistance (R) proteins, a class of plant immune receptors that mediate recognition of pathogen-derived avirulence (Avr) proteins, are a well-studied facet of the plant defense system (1). The bacterial plant pathogen

*Xanthomonas campestris* pv. *vesicatoria* (*Xcv*) uses a type III secretion (T3S) system to inject an arsenal of about 20 effector proteins into the host cytoplasm that collectively promote virulence (2). R protein-mediated defense in response to *Xcv* effector proteins is typically accompanied by a programmed cell death response referred to as the hypersensitive response (HR).

One Avr protein that R proteins recognize is AvrBs3, a member of a *Xanthomonas* family of highly conserved proteins (3). The central region of AvrBs3 consists of 17.5 tandem near-perfect

Institute of Biology, Department of Genetics, Martin-Luther-University Halle-Wittenberg, D-06099 Halle (Saale), Germany.

\*Present address: Institute of Plant Biology, University of Zürich, Zollikerstrasse 107, 8008 Zürich, Switzerland.

†To whom correspondence should be addressed. E-mail: lahaye@genetik.uni-halle.de

REPORTS

34-amino acid repeat units that determine avirulence specificity (4). AvrBs3 also contains nuclear localization signals (NLSs) and an acidic transcriptional activation domain (AD) (5, 6), similar to eukaryotic transcription factors, and induces host gene transcription (7). Mutations in the NLS or AD of AvrBs3 abolish pathogen recognition by the matching pepper R gene *Bs3* (5, 8), which suggests that recognition involves the transcriptional activation of host genes.

Previously we identified bacterial artificial chromosome (BAC) clones derived from the pep-

per (*Capsicum annuum*) cultivar Early California Wonder 30R (ECW-30R) that cover the *Bs3* gene (9). For complementation-based identification, fragments of a *Bs3*-containing BAC (9) were cloned into a plant transformation vector and were delivered into *Nicotiana benthamiana* leaves via *Agrobacterium tumefaciens*-mediated transient transformation. Two nonidentical clones carrying the same coding sequence triggered an HR in *N. benthamiana* when cotransformed with *avrBs3*. A genomic DNA fragment containing only the predicted coding sequence and ~1 kb

of sequence upstream of the ATG mediated AvrBs3 recognition, confirming that this gene is *Bs3* (Fig. 1A).

AvrBs3 mutants lacking the AD (AvrBs3ΔAD) or repeat units 11 to 14 (AvrBs3Δrep16) did not trigger HR in pepper *Bs3* plants (4, 5) and also failed to trigger HR in *N. benthamiana* when coexpressed with the cloned *Bs3* gene (Fig. 1A). AvrBs4, which is 97% identical to AvrBs3 but is not recognized by pepper *Bs3* genotypes (10), also did not trigger HR in *N. benthamiana* when coexpressed with *Bs3* (Fig. 1A). Therefore, *Bs3* mediates specific recognition of wild-type AvrBs3 in both pepper and *N. benthamiana*, but not when AvrBs3 lacks the AD or repeat units 11 to 14; nor does *Bs3* mediate recognition of the AvrBs3-like AvrBs4 protein (Fig. 1C).

The *Bs3* gene has three exons and two introns (Fig. 1D), is 342 amino acids long (fig. S1), and is homologous to flavin-dependent mono-

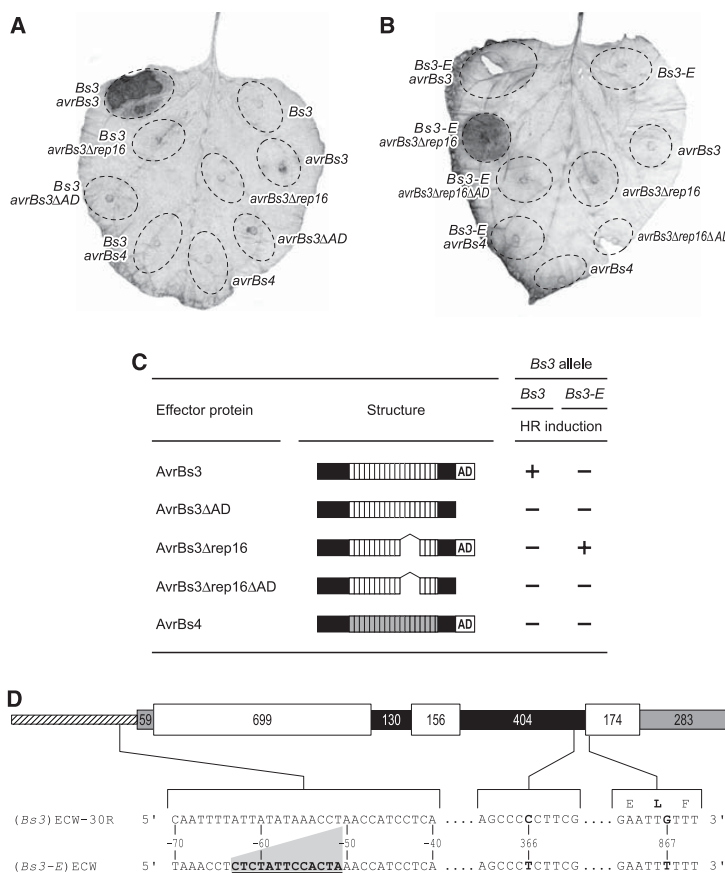


**Fig. 1.** (A) Recognition specificity of the *Bs3* allele from ECW-30R. The *Bs3* gene and/or *avr* genes were expressed transiently in *N. benthamiana* leaves via *A. tumefaciens* (OD<sub>600</sub> = 0.8). Dashed lines mark the inoculated areas. Four days after infiltration, the leaves were cleared to visualize the HR (dark areas). (B) *Bs3-E* and/or *avr* genes were transiently expressed in *N. benthamiana* leaves. (C) The relationship between domain structure and activity of AvrBs3, AvrBs3 derivatives, and AvrBs4. Plus and minus signs indicate presence or absence of the HR in *N. benthamiana* upon coexpression of the pepper *Bs3* or *Bs3-E* allele, respectively. For details, see Fig. 1A. White- and gray-boxed areas in the central part of the protein represent the repeat region of AvrBs3 and AvrBs4, respectively. AD refers to the C-terminal acidic transcriptional activation domain. (D) Gene structure of the ECW-30R *Bs3* and the ECW *Bs3-E* alleles. Exons, introns, untranslated regions, and promoter regions are displayed to scale as white, black, gray, and hatched boxes, respectively. The length of these elements (in base pairs) is indicated within the boxes. Differences between the *Bs3* alleles are marked in boldface. A 13-bp insertion in the *Bs3-E* promoter relative to the *Bs3* promoter is underlined. Nucleotide positions of the promoter and exon 3 polymorphisms are relative to the transcriptional and translational start sites, respectively. Amino acids encoded by the polymorphic region in exon 3 (E, Glu; L, Leu; F, Phe) are depicted above and below the nucleotide sequences.

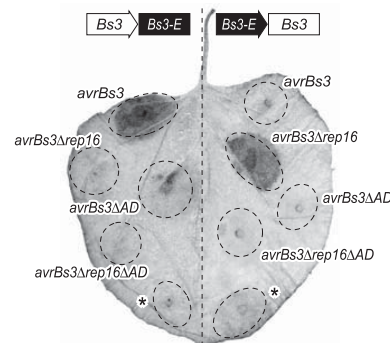


**Fig. 2.** Chimeras containing the promoter (arrow) of the *Bs3* allele (white) and the coding region (box) of the *Bs3-E* allele (black) or the reciprocal combination (right side of the leaf) were expressed together with *avrBs3*, *avrBs3Δrep16*, and derivatives as indicated. Asterisks mark areas in which only *A. tumefaciens* delivering the chimeric constructs was infiltrated. Dashed lines mark the inoculated areas. Four days after inoculation, leaves were cleared to visualize the HR (dark areas).

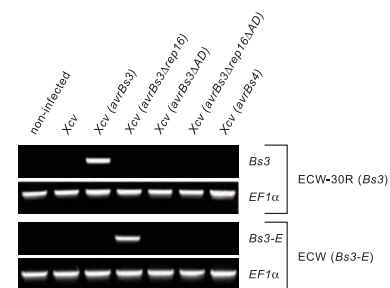


**Fig. 3.** Semiquantitative RT-PCR on cDNA of non-infected and *Xcv*-infected pepper ECW-30R (*Bs3*) and ECW (*Bs3-E*) leaves 24 hours after infection. The *avrBs3*-like genes that are expressed in the given *Xcv* strains are indicated in parentheses. Elongation factor 1α (EF1α) was amplified as a control.

oxygenases (FMOs) (fig. S2) (11). Bs3 is most closely related to FMOs of the *Arabidopsis* YUCCA family (fig. S3) but lacks a stretch of ~70 amino acids present in all related FMOs (fig. S4).

The AvrBs3 derivative AvrBs3Δrep16, which lacks repeat units 11 to 14, triggers HR in the pepper cultivar ECW but not in the near-isogenic Bs3-resistant cultivar ECW-30R (4). We transformed *N. benthamiana* with the ECW Bs3 allele (termed Bs3-E) including ~1 kb of the promoter and showed that it mediated recognition of AvrBs3Δrep16 but not AvrBs3 (Fig. 1B). Furthermore, AvrBs3Δrep16 lacking the C-terminal AD did not trigger HR when coexpressed with Bs3-E (Fig. 1B), and Bs3-E did not mediate recognition of AvrBs4. Thus, Bs3 and

Bs3-E represent functional alleles with distinct recognition specificities (Fig. 1C). The coding sequences of the two Bs3 alleles differ by a single nucleotide conferring a nonsynonymous change in exon 3, resulting in a leucine-phenylalanine difference (Fig. 1D and fig. S1). The promoter regions also differed by a 13-bp insertion in Bs3-E compared to Bs3, at position -50 relative to the transcription start site.

We fused the Bs3 promoter to the Bs3-E coding sequence and vice versa, then cotransformed *N. benthamiana* with these chimeras in combination with *avrBs3*, *avrBs3Δrep16*, or the corresponding AD mutant derivatives. The Bs3 promoter fused to the Bs3-E coding sequence mediated exclusively AvrBs3 recognition, whereas the reciprocal chimera (Bs3-E promoter fused to

the Bs3 coding sequence) mediated exclusively recognition of AvrBs3Δrep16 (Fig. 2). Thus, the promoter and not the coding region determines recognition specificity of the pepper Bs3 alleles.

Semiquantitative reverse transcription polymerase chain reaction (RT-PCR) revealed strongly increased Bs3 transcript levels in pepper ECW-30R Bs3 plants upon infection with *avrBs3*-expressing, but not *avrBs3Δrep16*- or *avrBs4*-expressing, *Xcv* strains (Fig. 3). Likewise, Bs3-E levels in ECW Bs3-E plants increased upon infection with *avrBs3Δrep16*-expressing *Xcv* strains, but not when infected with *avrBs3*- or *avrBs4*-expressing *Xcv* strains. AD-mutant derivatives of *avrBs3* and *avrBs3Δrep16* did not induce accumulation of Bs3 or Bs3-E mRNA. Expression patterns were unaltered in the presence of the translation inhibitor cycloheximide (fig. S5), which indicates that accumulation of the Bs3 and Bs3-E transcripts was independent of de novo protein synthesis.

*Agrobacterium*-mediated transient coexpression of *avrBs3* and a Bs3-GFP (green fluorescent protein) fusion construct under the control of the Bs3 promoter caused GFP emission, whereas delivery of Bs3-GFP on its own did not result in GFP emission (fig. S6). Together these data indicate that AvrBs3 and AvrBs3Δrep16 induce transcription of the respective R genes Bs3 and Bs3-E, and that the subsequent accumulation of these R proteins triggers HR. In agreement with this result, constitutive expression of Bs3 or Bs3-E under the cauliflower mosaic virus 35S promoter triggered an *avr*-independent HR (fig. S7). We identified Bs3 mutants with single amino acid replacements that were not compromised in protein stability but no longer triggered HR when expressed in *N. benthamiana* (fig. S8), indicating that the enzymatic activity of Bs3 is crucial to its function as a cell death inducer.

Electrophoretic mobility shift assays (EMSA) with GST-AvrBs3 fusion protein and biotin-labeled Bs3 and Bs3-E promoter fragments (Fig. 4A) showed that AvrBs3 bound to both Bs3- and Bs3-E-derived promoter fragments containing the polymorphism, although affinity appeared higher for the Bs3-derived fragment (Fig. 4B). Competition assays with labeled Bs3- and Bs3-E-derived promoter fragments, and vice versa, confirmed that AvrBs3 binds with high affinity to the Bs3 promoter fragment and with low affinity to the Bs3-E promoter fragment (Fig. 4C). In contrast, AvrBs3 did not bind to a DNA fragment from a nonpolymorphic region of the Bs3 promoter (Fig. 4B). Furthermore, EMSA studies showed that both AvrBs3 and AvrBs3Δrep16 have a higher affinity for the Bs3 promoter than for the Bs3-E promoter (Fig. 4 and fig. S9). Therefore, promoter binding per se of AvrBs3 or AvrBs3Δrep16 is not the basis for promoter activation specificity.

We performed chromatin immunoprecipitation assays by infiltrating pepper ECW-30R (Bs3) and ECW (Bs3-E) leaves either with *avrBs3*-expressing *Xcv* wild-type strains or with an iso-

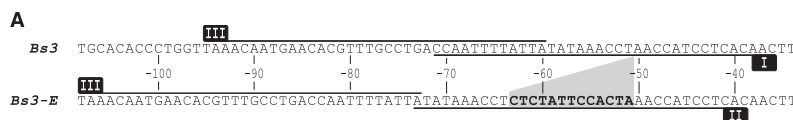
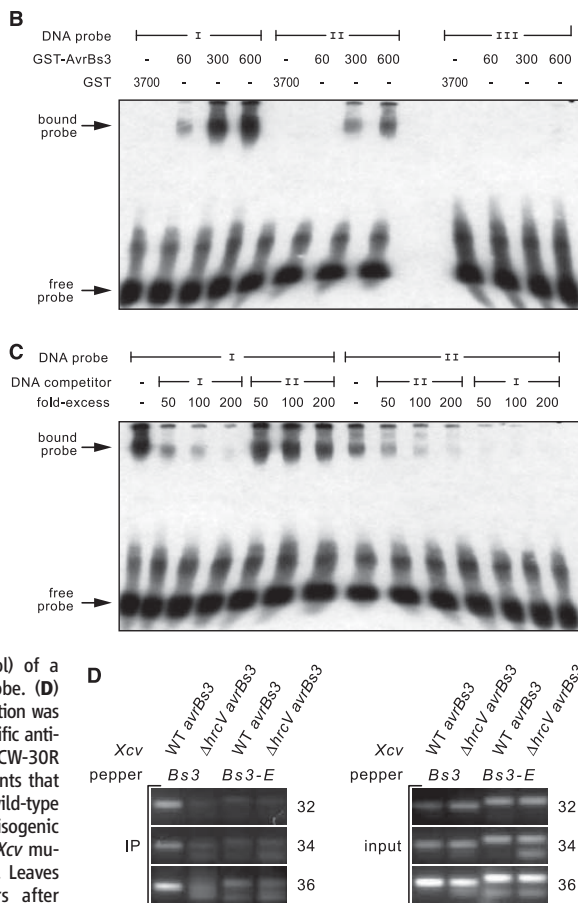


**Fig. 4.** (A) Probes derived from Bs3 and Bs3-E promoter sequences used in EMSAs. Numbering is relative to the transcriptional start site. The 13-bp insertion in the Bs3-E promoter is indicated in boldface. Positions of biotin-labeled DNA fragments are indicated by lines above and below the promoter sequences. Probes I and II correspond to Bs3 and Bs3-E promoters, respectively, whereas probe III corresponds to an identical region in both promoters. (B) EMSA with AvrBs3 and Bs3- or Bs3-E-derived probes in a 6% non-denaturing polyacrylamide gel. Protein amounts are in fmol. Positions of the bound and free probe are indicated on the left. (C) EMSA competition experiment between AvrBs3 and different amounts (in fmol) of a nonlabeled competitor probe. (D) Chromatin immunoprecipitation was conducted with AvrBs3-specific antibodies on extracts from ECW-30R (Bs3) and ECW (Bs3-E) plants that were infected with *Xcv* wild-type (WT *avrBs3*) strains or an isogenic type III secretion-deficient *Xcv* mutant strain ( $\Delta$ *hrcV* *avrBs3*). Leaves were harvested 12 hours after inoculation. Semiquantitative PCR with 32, 34, and 36 cycles was conducted before immunoprecipitation (input) or on immunoprecipitated material (IP). ECW-30R (Bs3) and ECW (Bs3-E) derived PCR products differ in size because of a 13-bp insertion in the Bs3-E promoter.



## REPORTS

genic *hrcV* mutant strain. HrcV is a conserved protein of the core T3S system with mutants incapable of delivering T3S effector proteins (12). After immunoprecipitation with an antibody to AvrBs3 (13), enrichment of the *Bs3* but not the *Bs3-E* promoter region was detected by semi-quantitative PCR (Fig. 4D). This demonstrates that *Xcv*-delivered AvrBs3 binds to the *Bs3* promoter in vivo with higher affinity than to the *Bs3-E* promoter. Given that *Bs3* promoter enrichment was detected in leaf material inoculated with the wild type but not with the *hrcV* mutant strain, we conclude that the *Bs3* promoter is bound before cell lysis.

We also infected the pepper cultivar ECW-123R containing the *R* genes *Bs1*, *Bs2*, and *Bs3* with xanthomonads delivering either the structurally unrelated AvrBs1, AvrBs2, or AvrBs3 protein or none of these Avr proteins. RT-PCR showed that the *Bs3*-derived transcripts were detectable only upon infection with *avrBs3*-expressing *Xcv* strains (fig. S10). Therefore, *Bs3* is not transcriptionally activated in the course of the *Bs1*- or *Bs2*-mediated HR.

Isolation of the pepper *Bs3* gene uncovered a mechanistically novel type of recognition mechanism and a structurally novel type of R protein that shares homology to FMOs. Recently, FMO1, an *Arabidopsis* protein that is sequence-related to Bs3 (fig. S2), was shown to be involved in pathogen defense (14–16). Thus, FMO1 and Bs3 may have similar functions. However, FMO1 is transcriptionally induced by a variety of stimuli including virulent and avirulent microbial pathogens (14, 16, 17). In contrast, *Bs3* was not induced by virulent *Xcv* strains (Fig. 3), nor by resistance reactions mediated by the pepper *R* genes *Bs1* and *Bs2* (fig. S10). Moreover, 35S-driven *Bs3* alleles triggered an HR reaction (fig. S7), whereas a 35S-driven FMO1 gene mediates broad-spectrum resistance but not HR (14, 15). Thus, *Arabidopsis* FMO1 and pepper *Bs3* differ with respect to their transcriptional regulation and function.

Our results show that the bacterial effector protein AvrBs3 binds to and activates the promoter of the matching pepper *R* gene *Bs3*. Analysis of host genes that are up-regulated by AvrBs3 (“*upa*” genes) in a compatible *Xcv*-pepper interaction (7, 18) led to the identification of the *upa*-box (TATATAAACCN<sub>2-3</sub>CC), a conserved DNA element that was shown to be bound by AvrBs3 and that is also present in the *Bs3* promoter (Fig. 1D) (18). This suggests that binding of AvrBs3 to the *upa*-box is crucial for activation of corresponding promoters. However, binding of an AvrBs3-like protein does not necessarily result in promoter activation, because AvrBs3Δrep16 bound with higher affinity to the *Bs3* than to the *Bs3-E* promoter (fig. S9) but only activated the *Bs3-E* and not the *Bs3* promoter (Fig. 3). Because AvrBs3Δrep16 and AvrBs3 differ in their structure, we postulate that upon DNA binding, their functional domains (e.g., AD) are exposed at different promoter locations, which may define whether

AvrBs3Δrep16 and AvrBs3 are able to activate a given promoter. Additionally, given that the *Bs3* promoter determines recognition specificity, the *Bs3* promoter might be coevolving to maintain compatibility with rapidly changing AvrBs3-like proteins, similar to that seen in the NB-LRR proteins (19, 20).

We consider it likely that not only AvrBs3 but also other AvrBs3 homologs bind to and activate promoters of matching *R* genes. The recently isolated rice *R* gene *Xa27*, which mediates recognition of the AvrBs3-like AvrXa27 protein from *Xanthomonas oryzae* pv. *oryzae* (21), is transcriptionally induced by AvrXa27, and thus it is tempting to speculate that the *Xa27* promoter is a direct target of AvrXa27. However, whether AvrXa27 acts directly at the *Xa27* promoter remains to be clarified.

## References and Notes

1. J. D. Jones, J. L. Dangl, *Nature* **444**, 323 (2006).
2. F. Thieme et al., *J. Bacteriol.* **187**, 7254 (2005).
3. S. Schornack, A. Meyer, P. Römer, T. Jordan, T. Lahaye, *J. Plant Physiol.* **163**, 256 (2006).
4. K. Herbers, J. Conrads-Strauch, U. Bonas, *Nature* **356**, 172 (1992).
5. B. Szurek, E. Marois, U. Bonas, G. Van den Ackerveken, *Plant J.* **26**, 523 (2001).
6. B. Szurek, O. Rossier, G. Hause, U. Bonas, *Mol. Microbiol.* **46**, 13 (2002).
7. E. Marois, G. Van den Ackerveken, U. Bonas, *Mol. Plant Microbe Interact.* **15**, 637 (2002).
8. G. Van den Ackerveken, E. Marois, U. Bonas, *Cell* **87**, 1307 (1996).
9. T. Jordan et al., *Theor. Appl. Genet.* **113**, 895 (2006).
10. U. Bonas, J. Conrads-Strauch, I. Balbo, *Mol. Gen. Genet.* **238**, 261 (1993).
11. N. L. Schlaich, *Trends Plant Sci.* **12**, 412 (2007).
12. O. Rossier, K. Wengelnik, K. Hahn, U. Bonas, *Proc. Natl. Acad. Sci. U.S.A.* **96**, 9368 (1999).
13. V. Knoop, B. Staskawicz, U. Bonas, *J. Bacteriol.* **173**, 7142 (1991).
14. M. Bartsch et al., *Plant Cell* **18**, 1038 (2006).
15. M. Koch et al., *Plant J.* **47**, 629 (2006).
16. T. E. Mishina, J. Zeier, *Plant Physiol.* **141**, 1666 (2006).
17. B. Olszak et al., *Plant Sci.* **170**, 614 (2006).
18. S. Kay, S. Hahn, E. Marois, G. Hause, U. Bonas, *Science* **318**, 648 (2007).
19. J. M. McDowell, S. A. Simon, *Mol. Plant Pathol.* **7**, 437 (2006).
20. J. G. Ellis, P. N. Dodds, G. J. Lawrence, *Annu. Rev. Phytopathol.* **45**, 289 (2007).
21. K. Gu et al., *Nature* **435**, 1122 (2005).
22. We thank N. Collins, L. Rose, J. Parker, M. Dow, S. Peterhänzel, E. Marois, N. Schlaich, C. Pabst, S. Schornack, A. Strauß, and S. Kay for helpful comments and suggestions on the manuscript, and H. Scholze, B. Rosinsky, and C. Kretschmer for excellent technical assistance. T. Nakagawa provided the pGWB vector series. Supported by funds from the Deutsche Forschungsgemeinschaft to T.L. (LA 1338/2-2) and U.B. (SFB 648). *Bs3* and *Bs3-E* sequences have been deposited in GenBank with accession numbers EU078684 and EU078683, respectively.

## Supporting Online Material

www.sciencemag.org/cgi/content/full/318/5850/645/DC1  
Materials and Methods  
Figs. S1 to S10  
References

10 May 2007; accepted 21 September 2007  
10.1126/science.1144958



### 2.2.2 Anlagen zur Publikation 1

Das folgende „*Supporting Online Material*“ (SOM) (veröffentlicht unter: [www.sciencemag.org/cgi/content/full/318/5850/645/DC1](http://www.sciencemag.org/cgi/content/full/318/5850/645/DC1)) enthält Zusatzinformationen zu Kapitel 2.2.1: Material und Methoden, Abbildungen S1 bis S10 und Referenzen. Das SOM wurde so verändert, dass sich jede Legende unter bzw. hinter der jeweiligen Abbildung befindet.

## Material and Methods

### *Plant material and infiltrations*

Pepper (*Capsicum annuum*) plants of cultivar Early California Wonder (ECW) and the near-isogenic line ECW-30R containing the resistance gene *Bs3* and *N. benthamiana* plants were grown in the greenhouse under standard conditions (day and night temperatures of 24 and 19°C, respectively), with 16 h of light and 60 to 40% humidity. Pepper cultivar ECW and the near-isogenic line ECW-30R seeds were provided by R. E. Stall (University of Florida, Gainesville). Six-week-old pepper plants were inoculated with *Xanthomonas* with  $5 \times 10^8$  colony forming units/ml with a needleless syringe. For cycloheximide treatment, leaf tissue was inoculated with a bacterial suspension as above, containing 50 µM cycloheximide.

### *Complementation with BAC sub-clones*

BAC clone 128, which spans the *Bs3* locus (*S1*), was partially digested with *Hind*III (Fermentas, St. Leon-Rot, Germany). Restriction fragments of  $\geq 10$  kb were ligated into the binary-vector pVB61 (*S2*), which contains no promoter in its T-DNA region, and transformed into *A. tumefaciens* strain GV3101 (*S3*). Transformants ( $OD_{600} = 0.8$ ) were mixed 1:1 with an *A. tumefaciens* strain that delivers a T-DNA containing 35S-driven *avrBs3*. The mixture was injected into the lower side of fully expanded leaves of *C. annuum* cultivar ECW or *N. benthamiana* with a blunt syringe. *A. tumefaciens* strains that delivered the *Bs3* gene induced an HR 3-4 days after inoculation.

### *Generation of expression clones containing the Bs3 or the Bs3-E gene*

The *Bs3* coding sequence and 1 kb sequence 5' of the ATG were PCR-amplified from genomic DNA of pepper cultivar ECW-30R. The amplification was carried out with Phusion high-fidelity DNA polymerase (New England Biolabs, Frankfurt, Germany) and the primers A1-fwd-PR (CTACGGAATAGCAGCATTAAAGGCACATCAG) and final-entry-02-rev (CATTT-GTTCTTTCCAAATTTTGGCAATATC). The PCR fragment was cloned into pENTR-D

(Invitrogen, Karlsruhe, Germany), sequenced and transferred into the binary-vector pGWB1 (provided by Tsuyoshi Nakagawa, Shimane University, Japan) with Gateway recombination (Invitrogen). pGWB1-derivatives were transformed into *A. tumefaciens* GV3101 (S3) for transient expression assays. The *Bs3-E* allele was cloned in the same way using genomic DNA from the pepper cultivar ECW as template.

#### *Generation of chimeric constructs*

Chimerical gene constructs were generated by splicing using overlap extension (SOE) PCR (S4). *Bs3* and *Bs3-E* promoters were amplified from genomic DNA of ECW and ECW-30R pepper cultivars, respectively, with the Phusion-polymerase and A1-fwd-PR (CTACGGAATAGCAGCATTAAAGGCACATCAG) and B5-rev-PR (CATACGGAACACTGTATTGCTTAAGG) primers. The coding regions were amplified with final-entry-02-fwd (ATGATGAATCAGAATTGCTTTAATTCTTG-TTC) and final-entry-02-rev (CATTTGT-TCTTTCCAAATTTTGGCAATATC) primers. PCR-products of the coding and promoter region were mixed in a 1:1 ratio and PCR amplified using A1-fwd-PR and final-entry-02-rev primers. The PCR-product was cloned into pENTR-D and, after sequencing, recombined into the T-DNA vector pGWB1.

#### *Generation and analysis of Bs3 mutants*

The *Bs3* cDNA was amplified from *Capsicum annuum* cv. ECW-30R using Phusion high-fidelity DNA polymerase (New England Biolabs) and the primers final-entry-01-fwd 5'CACCATGATGAATCAGAATTGCTTTAATTCTTGTTTC3' and final-entry-02-rev 5'CATTTGTTCTTTCCAAATTTTGGCAATATCTTGTGCAAC3'. The PCR product was cloned into pENTR-D (Invitrogen) and checked for fidelity by sequence analysis. Mutagenesis of *Bs3* was done by error-prone PCR by using M13fwd 5'GTAAAA-CGACGGCCAGT3' and M13rev 5'GGAAACAGCTATGACCATG3' oligos and *Bs3*-ENTRY as template DNA. The PCR-product was recombined by LR-recombination in the pGWB5 (provided by Tsuyoshi Nakagawa) using Gateway recombination (Invitrogen). In the pGWB5 T-DNA vector the *Bs3* cDNA is translationally fused to a C-terminal GFP epitope and is under transcriptional control of the Cauliflower mosaic virus 35S promoter. The T-DNA constructs were transformed into *Agrobacterium* (GV3101) and infiltrated into *N. benthamiana* for functional analysis. The clones that did not trigger HR were sequenced. The stability of the corresponding proteins was analysed by immunoblot with the GFP antibody (Invitrogen). Protein extracts from leaf tissue were prepared by grinding six leaf discs (5 mm diameter) in liquid nitrogen and adding 120 µl 4

x Laemmli buffer (S5). The resuspended material was boiled for 5 minutes and centrifuged for 5 minutes at 14000 rpm. 20 µl of the supernatants were loaded on a 10% sodium dodecyl sulfate (SDS) polyacrylamide gel and subjected to immunoblot analysis.

#### *RT-PCR analysis of Xcv infected leaves*

The abaxial leaf surface of ECW and ECW-30R pepper plants was inoculated with *Xcv* strain 85-10 ( $OD_{600} = 0.4$ ) with a blunt syringe. Inoculations were carried out with isogenic *Xcv* strains expressing *avrBs3* (pDS300F) (S6), *avrBs3ΔAD* (pDSF341) (S7), *avrBs4* (pDSF200) (S2), *avrBs3Δrep16* (pDSF316) (S8) or *avrBs3Δrep16ΔAD* (pDSF317). Four leaf discs (5-mm diameter) were harvested 24 hours after inoculation and were used for each RNA-extraction with the Qiagen RNeasy Plant Miniprep kit (Qiagen, Hilden, Germany). RNA concentrations were determined with a ND-1000 spectrophotometer (NanoDrop Technologies, Rockland, DE, USA) and adjusted prior to cDNA synthesis. cDNA was synthesized by reverse transcription with an oligo dT-primer and the Revert Aid First Strand Synthesis Kit (Fermentas). For RT-PCR of *Bs3* the Cand-7-01-fwd (ATGAATCAGAATTGCTTTAATTCTTGTTCA) and Cand-7-01-rev (TGATTCTTGTGCTACATTTGTTCTTTCC) primers were used. To amplify *EF1α* (used for RT-PCR normalization) primers RS-EFrt-F1 (AGTCAACTACCACTGGTCAC) and RS-EFrt-R1 (GTGCAGTAGTACTTAGTGGTC) were used. The 5' and 3' ends of the *Bs3* and *Bs3-E* cDNAs were isolated by rapid amplification of cDNA ends (RACE) with the SMART RACE Kit (Clontech, Heidelberg, Germany).

#### *Sequences and alignments*

Proteins with sequence similarity to pepper *Bs3* were identified by BLAST searching of databases at the National Center for Biotechnology Information ([www.ncbi.nlm.nih.gov/BLAST/](http://www.ncbi.nlm.nih.gov/BLAST/)) and the SOL Genomics Network (<http://www.sgn.cornell.edu/tools/blast/>). FMO-like sequences from *Arabidopsis* were retrieved from TAIR ([www.arabidopsis.org](http://www.arabidopsis.org)).

#### *Chromatin immunoprecipitation (ChIP)*

For ChIP, 3 g pepper ECW or ECW-30R leaf material was harvested 12 hpi with *X. campestris* pv. *vesicatoria* strains 82-8 and 82-8Δ*hrcV*, respectively. ChIP was performed as described (S9) with the following modifications: All buffers were supplemented with DTT instead of β-mercaptoethanol. 1x complete (Roche, Mannheim, Germany) was used as proteinase inhibitor. The chromatin was sonicated 6x 20 sec with a Branson sonifier G250 (output control 3) and diluted 1:8.5 with ChIP dilution buffer. 100 µl pre-cleared chromatin solution was saved as

input control, the rest was subjected to immunoprecipitation with 15  $\mu$ l of affinity-purified and depleted AvrBs3-specific antibody Sta7 (10). The recovered DNA was analyzed by semiquantitative PCR with input DNA as loading control. Different PCR cycle numbers were tested for both input and co-precipitated DNA.

#### *Electrophoretic mobility shift assay (EMSA)*

For DNA binding studies, GST fusion proteins were purified from *E. coli* BL21 with Glutathione Sepharose 4B (GE Healthcare Bio-Sciences AB, Uppsala) and the protein concentration was determined by Bradford protein assay (BioRad, Hercules, CA, U.S.A.). Complementary pairs of nonlabeled or 5'-biotin-labeled oligonucleotides were annealed. EMSA was performed with the Light Shift® Chemiluminescent EMSA Kit (Pierce, Rockford, IL, U.S.A.) according to the manufacturer's protocol. The following parameters were used: Binding reactions contained 12 mM Tris-HCl (pH 7.5), 60 mM KCl, 1 mM DTT, 2.5% Glycerol, 5 mM MgCl<sub>2</sub>, 50 ng/ $\mu$ l poly(dI•dC), 0.05% NP-40, 0.2 mM EDTA, 50 fmol biotin-labeled DNA, 0-10 pmol unlabeled DNA, 60-600 fmol GST fusion protein. The binding reactions were kept on ice for 10 min before biotin-labeled DNA was added. Gel electrophoresis was performed on a 6% native polyacrylamide gel. After blotting to a positively charged nylon membrane (Roche) the DNA was linked by baking at 100°C for 1 h.

## Supplementary figures

## Figure S1

GTTCTTGTACCCGCTAAATCTATCAAAACACAAGTAGTCTTAGTTGCACATATATTTTC

M M N Q N C F N S C S P L T V D A L E P 20  
ATGATGAATCAGAATTGCTTTAATTCTTGTTACCTCTAACTGTTGATGCACTTGAACCA 60

K K S S C A A K C I Q V N G P L I V **G A** 40  
AAAAATCCTCTTGTGCTGCTAAATGCATACAAAGTAAATGGTCTCTTATTGTTGGAGCT 120

**G P S G** L A T A A V L K Q Y S V P Y V I 60  
GGCCCTTCAGGCCTGGCTACTGCTGCCGTCTTAAGCAATACAGTGTTCGGTATGTAATC 180

I E R A D C I A S L W Q H K T Y D R L R 80  
ATTGAACGCGCGGACTGCATTGCTTCTCTGTGGCAACACAAGACCTACGATCGGCTTAGG 240

L N V P R Q Y C E L P G L P F P P D F P 100  
CTTAACGTGCCACGACAACTACTGCGAATTGCCTGGCTTGCCATTTCCACCAGACTTTCCA 300

E Y P T K N Q F I S Y L V S Y A K H F E 120  
GAGTATCCAACCAAAAACCAATTTCATCAGCTACCTCGTATCTTATGCAAAGCATTTCGAG 360

I K P Q L N E S V N L A G Y D E T C G L 140  
ATCAAACCACAACTCAACGAGTCAGTAACTTAGCTGGATATGATGAGACATGTGGTTTA 420

W K V K T V S E I N G S T S E Y M C K W 160  
TGGAAGGTGAAAACAGTTTCTGAAATCAATGGTTCAACCTCTGAATACATGTGTAAGTGG 480

L I V A T G E N A E M I V P E F E G L Q 180  
CTTATTGTGGCCACAGGAGAGAATGCTGAGATGATAGTGCCCGAATTCGAAGGATTGCAA 540

D **F G G Q V I H A C E Y** K T G E Y Y T G 200  
GATTTTGGTGGCCAGGTTATTCATGCTTGTGAGTACAAGACTGGGGAATACTATACTGGA 600

E N V L A V **G C G N S G** I D I S L D L S 220  
GAAAATGTGCTGGCGGTTGGCTGTGGCAATTCGGGATCGATATCTCACTTGATCTTTCC 660

Q H N A N P F M V V R S S V Q G R N F P 240  
CAACATAATGCAAATCCATTCATGGTAGTTGCAAGCTCGGTACAGGGTTCGTAATTTCCCT 720

E E I N I V P A I K K F T Q G K V E F V 260  
GAGGAAATAAACATAGTTCCAGCAATCAAGAAATTTACTCAAGGAAAAGTAGAATTTGTT 780

N G Q I L E I D S V I **L A T G Y** T S N V 280  
AATGGACAAATTCATAGAGATCGACTCTGTTATCTTGCCAACCTGGTTATACCAGCAATGTA 840

T S W L M E S E L F S R E G C P K S P F 300  
ACTTCTTGGTTAATGGAGAGTGAATTTGTTTTCAAGGGAGGGATGTCCAAAAAGCCCATTC 900

P N G W K G E D G L Y A V G F T G I G L 320  
CCAAATGGTTGGAAGGGGGAGGATGGTCTCTATGCAGTTGGATTTACAGGAATAGGACTG 960

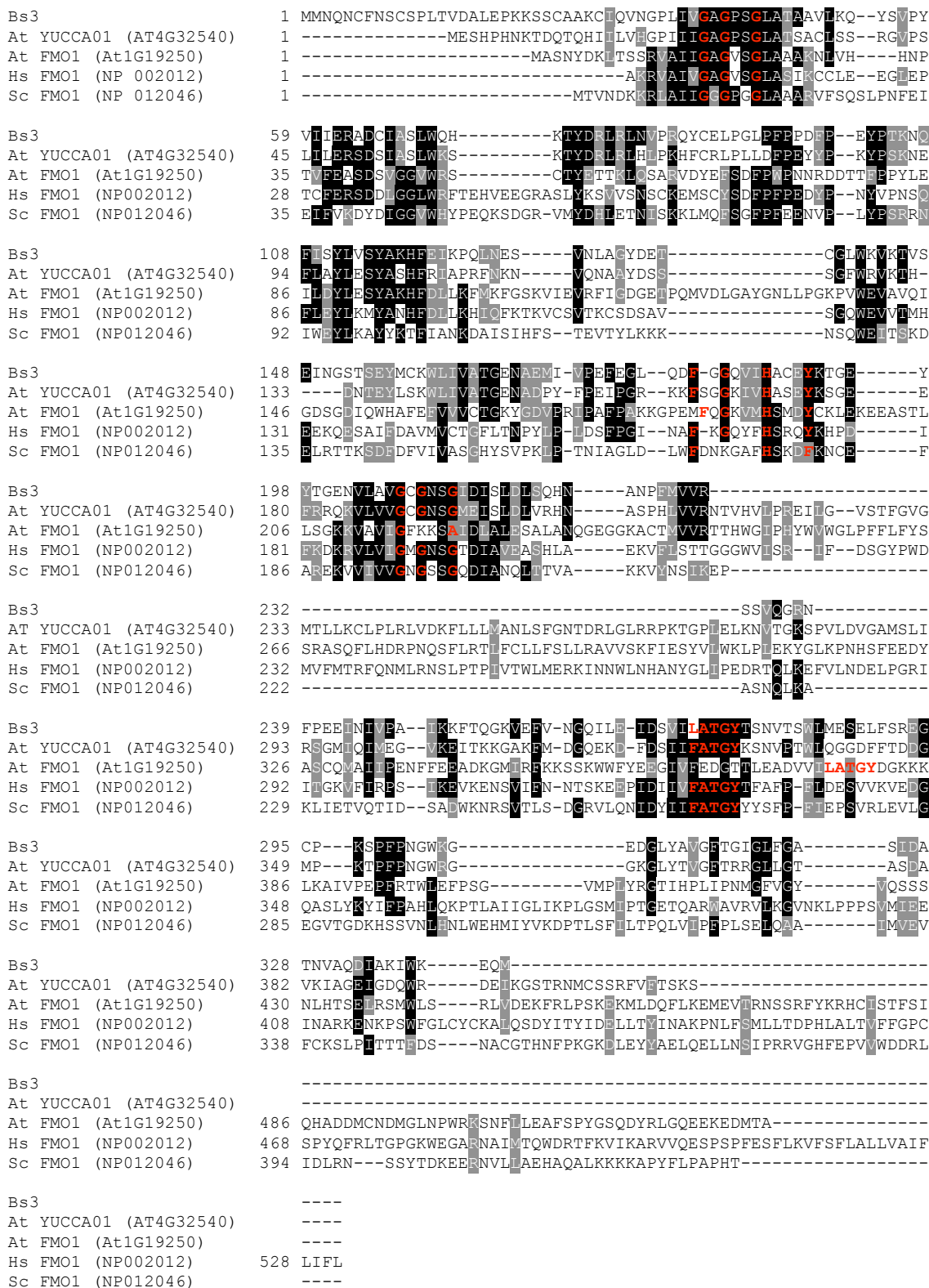
F G A S I D A T N V A Q D I A K I W K E 340  
TTTGGTGCTTCTATAGATGCCACTAATGTTGCACAAGATATTGCCAAAATTTGGAAAGAA 1020

Q M \* 342  
CAAATGTAGCACAGAATCATAATCAATCTGTTGGATGCATGCCATGGAGAAGAAGCAAG 1080

TTACTTTTCTCATGTCAAGAAAATAAGATTTTTTTTTTTTCTT

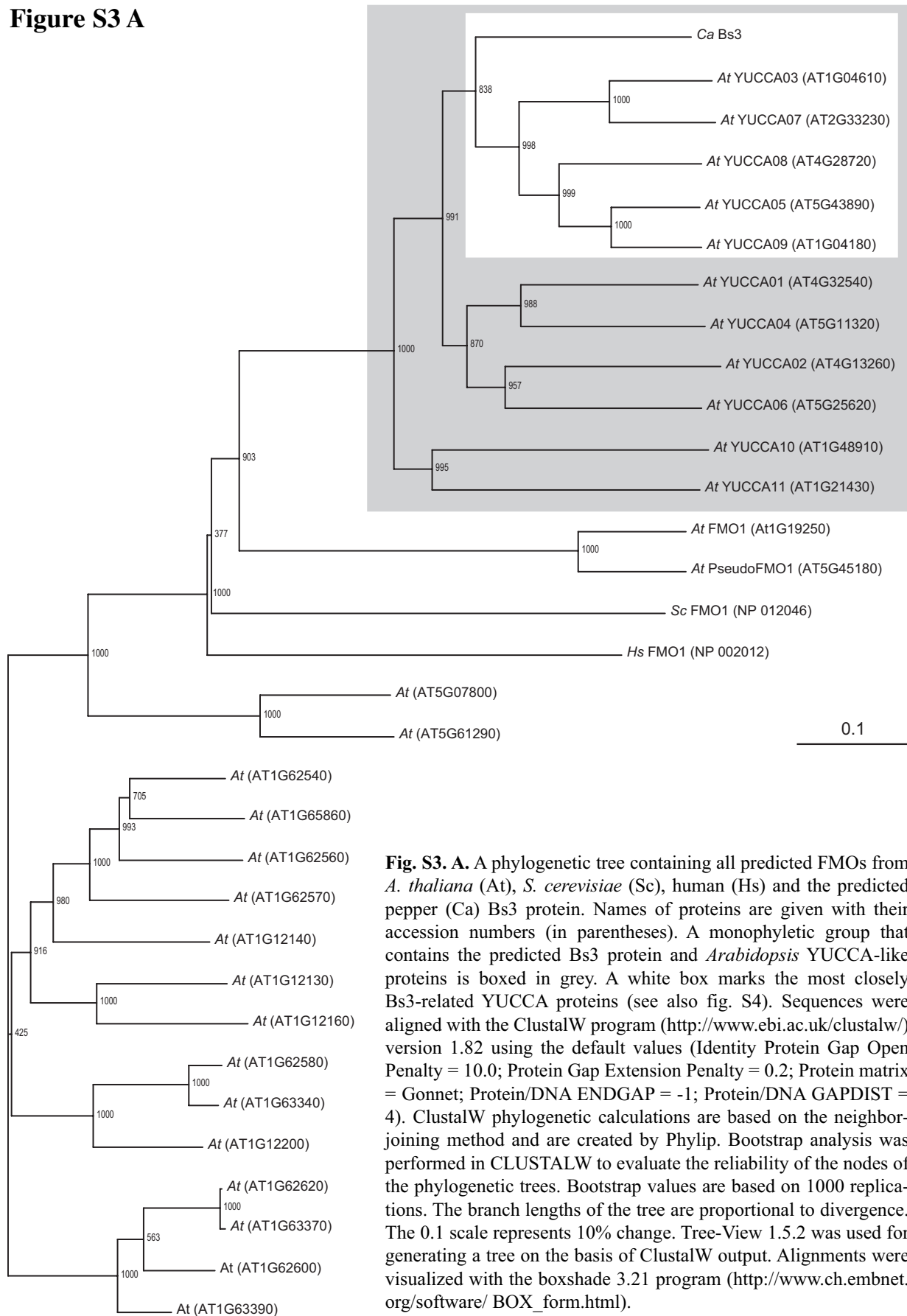
**Fig. S1.** Nucleotide and predicted amino acid sequences of the pepper *Bs3* cDNA. Nucleotide sequence was obtained by RT-PCR and RACE (rapid amplification of cDNA ends) performed on RNA from pepper cultivar ECW-30R. RNA was isolated from leaves that were inoculated with *avrBs3*-expressing *Xcv*. The translational stop codon is marked by an asterisk (\*). Positions of introns identified by comparison with the genomic sequence are indicated by triangles. A guanine nucleotide present in cultivar ECW-30R that is replaced by thymidine in cultivar ECW (underlined) causes a leucine to phenylalanine change in the predicted ECW protein. Sequence motifs that are characteristic of Flavin monooxygenases (FMOs) are boxed in gray. Conserved residues in these motifs are shown in bold type. I, FAD binding motif (GXGXXG); II, FMO identifying sequence motif (FXGXXXHXXX[Y/F]); III, NADPH-binding domain (GXGXX[G/A]) and IV, "FATGY" domain ([F/L]ATGY).

Figure S2



**Fig. S2.** Alignment of the predicted pepper Bs3 protein to representative FMOs. Conserved residues of the FAD-binding domain (GXGXXG), the FMO-identifying sequence motif (FXGXXXHXXX[Y/F]), the NADPH-binding domain (GXGXX[G/A]) and the conserved FATGY motif ([L/F]ATGY) are marked in red. Names of proteins from *A. thaliana* (At) *Homo sapiens* (Hs) and *Saccharomyces cerevisiae* (Sc) are given along with their accession numbers (in parentheses). Alignments were constructed with ClustalW. Identical amino acids (white text on black background) and similar amino acids present in  $\geq 50\%$  of sequences (on grey background) were shaded using Boxshade. Dashes (-) indicate gaps.

Figure S3 A



**Fig. S3. A.** A phylogenetic tree containing all predicted FMOs from *A. thaliana* (*At*), *S. cerevisiae* (*Sc*), human (*Hs*) and the predicted pepper (*Ca*) Bs3 protein. Names of proteins are given with their accession numbers (in parentheses). A monophyletic group that contains the predicted Bs3 protein and *Arabidopsis* YUCCA-like proteins is boxed in grey. A white box marks the most closely Bs3-related YUCCA proteins (see also fig. S4). Sequences were aligned with the ClustalW program (<http://www.ebi.ac.uk/clustalw/>) version 1.82 using the default values (Identity Protein Gap Open Penalty = 10.0; Protein Gap Extension Penalty = 0.2; Protein matrix = Gonnet; Protein/DNA ENDGAP = -1; Protein/DNA GAPDIST = 4). ClustalW phylogenetic calculations are based on the neighbor-joining method and are created by Phylip. Bootstrap analysis was performed in CLUSTALW to evaluate the reliability of the nodes of the phylogenetic trees. Bootstrap values are based on 1000 replications. The branch lengths of the tree are proportional to divergence. The 0.1 scale represents 10% change. Tree-View 1.5.2 was used for generating a tree on the basis of ClustalW output. Alignments were visualized with the boxshade 3.21 program ([http://www.ch.embnet.org/software/BOX\\_form.html](http://www.ch.embnet.org/software/BOX_form.html)).

Figure S3 B

AT1G62620	1	-----MAPALS---PTRSH	VAVIGAGPAGI	VAAARELRREG	---H			
AT1G63370	1	-----MAPALS---PTRSH	VAVIGAGPAGI	VAAARELRREG	---H			
AT1G62600	1	-----MAPSLS---PTRSH	VAVIGAGAAGI	VAAARELRREG	---H			
AT1G63390	1	-----MAPSLS---PTRSH	VAVIGAGAAGI	VAAARELRREG	---H			
AT1G62580	1	-----MVPAVNP--PTTSH	VAVIGAGAAGI	VAAARELRREG	---H			
AT1G63340	1	-----MVPAVNP--PTTSH	VAVIGAGAAGI	VAAARELRREG	---H			
AT1G12200	1	-----MATSHPD--PTTSR	VAVIGAGAAGI	VAAARELRREG	---H			
AT1G12130	1	-----MTPPPN---STSSRN	VAVIGAGAAGI	VAAARELRREG	---H			
AT1G12160	1	-----MTSVIT---SR-AR	VAVIGAGAAGI	VAAARELRREG	---H			
AT1G62540	1	-----MAPAQN---PTSSQ	VAVIGAGAAGI	VAAARELSREG	---H			
AT1G65860	1	-----MAPTQN---TICSK	VAVIGAGAAGI	VTAARELRREG	---H			
AT1G62560	1	-----MAPAQN---QITSK	VAVIGAGPAGI	LITSRELRREG	---H			
AT1G62570	1	-----MAPAPS---PTNSQ	VAVIGAGAAGI	VAAARELRREG	---H			
AT1G12140	1	-----MAPART---RVNSLN	VAVIGAGAAGI	VAAARELRREN	---H			
AT5G07800	1	-----MVTFTSEASRSRSK	VAVIGAGPAGI	VSAARELRKEG	---H			
AT5G61290	1	-----MVLVITEPIKSQSK	VAVIGAGPSGL	VSAARELRKEG	---H			
FM01 (At1G19250)	1	-----MASNYD---KITSS	VAVIGAGVSLAAAK	NLVH---	H			
PseudoFM01 (AT5G45180)	1	-----MHTSS	VAVIGAGVSLAAAK	NLVH---	H			
YUCCA03 (AT1G04610)	1	MYGNNNKKSINITSMFQNL	IPEGSDIFSRRCT	IWVNGPVI	VGAGPSGLAVAAGL	KREG--V		
YUCCA07 (AT2G33230)	1	MCNNTNTSCVNISSMLQ---	PE--DIFSRRCT	IWVNGPVI	VGAGPSGLAVAAGL	KRQE--V		
YUCCA05 (AT5G43890)	1	-----MENMFR-LMGSEDS	DRRRCI	IWVNGPVI	VGAGPSGLATAACL	LDQ--V		
YUCCA09 (AT1G04180)	1	-----MENMFR-LMASEEY	FSEERRC	IWVNGPVI	VGAGPSGLATAACL	LDQ--V		
YUCCA08 (AT4G28720)	1	-----MENMFR-LMDQD	DLTNNRC	IWVNGPVI	VGAGPSGLATAACL	HEQN--V		
Bs3	1	--MMNQNCFNCSPLTVDALE	PKKSCAAKCI	QVNGPLI	VGAGPSGLATAAVL	KQYS--V		
YUCCA01 (AT4G32540)	1	-----MESHPHNK--TDQT	QHIL	LVHGPII	IIGAGPSGLATSACL	SSRC--V		
YUCCA04 (AT5G11320)	1	-----MENMFR-LMGSEDS	DRRRCI	IWVNGPVI	VGAGPSGLATAACL	LDQ--V		
YUCCA02 (AT4G13260)	1	-----MEFVT--ETLGKRI	HDP--YVEETRC	LIPGPII	VGAGPSGLATAACL	KSRD--I		
YUCCA06 (AT5G25620)	1	-----MDFCWKREMEGKLAH	DHRGMTSPRRIC	VVTVGPVI	VGAGPSGLATAACL	KERG--I		
YUCCA10 (AT1G48910)	1	-----METVV	VIVGAGPAGLATS	VCLN	QHS--I			
YUCCA11 (AT1G21430)	1	-----MEKEIKILVLI	IIGAGPAGLATS	ACL	NRLN--I			
Hs FM01 (NP_002012)	1	-----AKRVA	IIGAGVSLAS	I	CCLE	EC--L		
Sc FM01 (NP_012046)	1	-----MTVNDK	KRIAIIGGPGGLAAAR	VFSQSL	LPNF			
AT1G62620	35	SVVVFERQKQVGGT	WLYTDEV	ESDPI	SVDPT----	RSVHSSVYRSLR	INGTRECTG	YR
AT1G63370	35	SVVVFERQKQVGGT	WLYTDEV	ESDPI	SVDPT----	RSVHSSVYRSLR	INGTRECTG	YR
AT1G62600	35	SVVVFERQKQVGGT	WLYTDHI	EPDPI	SVDPT----	RSVHSSVYRSLR	TNLPRECM	YR
AT1G63390	35	SVVVFERQKQVGGT	WLYTDHI	EPDPI	SVDPT----	RSVHSSVYRSLR	TNLPRECM	YR
AT1G62580	36	SVVVFERGNHIGG	WYATPNV	EPDPI	SIDPT----	RPVHSSLYSSLR	TIIIPQECM	GFT
AT1G63340	36	SVVVFERGNHIGG	WYATPNV	EPDPI	SIDPT----	RPVHSSLYSSLR	TIIIPRECM	GFT
AT1G12200	36	SVVVFERGSOIGG	WYATSNV	EPDPI	SLDPT----	RPVHSSLYRSLR	TNIPRECM	GFT
AT1G12130	35	TVTIFERQKQVGG	LWYCTPNV	EPDPI	SIDPD----	RTVHSSVYRSLR	TNLPRECM	YS
AT1G12160	34	TVIGFEREKHVG	LWYTDREV	ESDPI	SVDPD----	RTIVHSSVYRSLR	TNLPRECM	YS
AT1G62540	35	TVVVFEREKVGG	LWYSPKA	ESDPI	SLDPT----	RSIVHSSVYRSLR	TNLPRECM	GFT
AT1G65860	35	TVVVFEREKVGG	LWYSSKA	ESDPI	SLDPT----	RTIVHSSVYRSLR	TNLPRECM	GFT
AT1G62560	35	SVVVFEREKQVGG	LWYTPET	ESDPI	SLDPT----	RSKVVHSSVYRSLR	TNLPRECM	GVR
AT1G62570	35	TVVVFEREKQVGG	LWYTPET	ESDPI	GLDPT----	RPVHSSVYRSLR	TNLPRECM	GK
AT1G12140	35	TVVVFERDSKVG	LWYTPNS	EPDPI	SLDPN----	RTIVHSSVYRSLR	TNLPRECM	YR
AT5G07800	38	KVVVFERQNE	DVGGQWYQPNVE	EDDPI	GRSSGSINGEL	KVHSSVYRSLR	LTSPREIM	MGYS
AT5G61290	38	KVVVFERQNH	DVGGQWYQPNVE	EDDPI	GLGKTK----	TLKVHSSVYRSLR	LASPREVM	CF
FM01 (At1G19250)	33	NPTVFERASDS	VGGVWR	-----	-----	SCTYETTKL	Q SARVDYEF	S
PseudoFM01 (AT5G45180)	27	HPQVFERASDS	VGGVWR	-----	-----	KCTYETTKL	Q SVRVSYELS	S
YUCCA03 (AT1G04610)	59	PFVILERANCI	ASLWQ	-----	-----	NRTYDR	LKLHLPKQFC	QLP
YUCCA07 (AT2G33230)	54	PFVILERANCI	ASLWQ	-----	-----	NRTYDR	LKLHLPKQFC	QLP
YUCCA05 (AT5G43890)	47	PFVILERADCI	ASLWQ	-----	-----	KRTYDR	LKLHLPKKVC	QLP
YUCCA09 (AT1G04180)	47	PFVILERADCI	ASLWQ	-----	-----	KRTYDR	LKLHLPKKVC	QLP
YUCCA08 (AT4G28720)	47	PFVILERADCI	ASLWQ	-----	-----	KRTYDR	LKLHLPKQFC	QLP
Bs3	57	PYVILERADCI	ASLWQ	-----	-----	HKTYDR	LRLNVP	RYCELP
YUCCA01 (AT4G32540)	43	PSLILERSDSI	ASLWK	-----	-----	SKTYDR	LRLHLPKHF	CRLP
YUCCA04 (AT5G11320)	39	PSVILERTDC	ASLWQ	-----	-----	KRTYDR	LKLHLPKHF	CELP
YUCCA02 (AT4G13260)	50	PSLILERSTCI	ASLWQ	-----	-----	HKTYDR	LRLHLPK	DFCELP
YUCCA06 (AT5G25620)	54	TSVILERSNCI	ASLWQ	-----	-----	LKTYDR	LRLHLPKQ	FCCELP
YUCCA10 (AT1G48910)	27	PNVILEKEDI	YASLWK	-----	-----	KRAYDR	LKLHLAKE	FCQLP
YUCCA11 (AT1G2143)	31	PNVILERDVCS	ASLWK	-----	-----	RRSYDR	LKLHLAKQ	FCQLP
Hs FM01 (NP_002012)	26	EPTCFERSDD	LGGLWRTEHVE	EG	-----	RASLYK	SVVNSCK	EMSCYS
Sc FM01 (NP_012046)	33	EIEIFVKDYD	GGVWHYPEQK	-----	-----	SDGRVMY	DHLETN	ISKMLQFS



AT1G62620	90	DFPFVVRSGVS--RDPRRFPSPHGEVLAFLKDFAKEFGIEE---MVRFEETEVEVKVSP----
AT1G63370	90	DFPFVVRSGVS--RRRRRFPSPHGEVLAFLKDFAKEFGIEE---MVRFEETEVEVKVSP----
AT1G62600	90	DFPFVIRSDVSESRRDPRRFPSPHGEVLAFLQDFAKEFAIEE---MIRREDTAVVKVAP----
AT1G63390	90	DFPFVVRSGVSESRRDPRRFPSPHG-----
AT1G62580	91	DFPFSTRLENG-SRDPRRFPSPHGEVLAFLRDFVREFKIEE---MIRFEETEVEVVRVEQ----
AT1G63340	91	DFPFSTGPNK-SRDPRRFPSPHIEVLAFLKDFARKEFKIDE---MIRFEETEVEVRAEP----
AT1G12200	91	DFPFATRPHDG-SRDPRRFPSPHTEVLAFLRDFAKEFDIEE---MVRFEETEVEVKAEQ----
AT1G12130	90	DFPFVTRP-DDESRRDPRRFPSPHREVMRYLQDFAKEFKIEE---MIRFEETEVEVVRVEP----
AT1G12160	89	DFPFVTRS-SD--GDRRFPSPHREVMRYLQDFAKEFKIED---MIRFEETEVEVLRVEP----
AT1G62540	90	DFPFVPRF-DDESRRDPRRFPSPHMEVLAFLQDFAREFNLEE---MVRFEETEVEVVRVE----
AT1G65860	90	DFPFVPRF-DDESRRDPRRFPSPHREVMRYLQDFAREFKIEE---MVRFEETEVEVVRVE----
AT1G62560	90	DFPFLPRF-DDESRRDPRRFPSPHREVMRYLQDFAREFKIEE---MIRFEETEVEVVRVE----
AT1G62570	90	DFPFVPRG-DDPSRRDPRRFPSPHREVMRYLQDFATEFNIEE---MIRFEETEVEVVRVE----
AT1G12140	90	DFPFVPRPEDESRRDPRRFPSPHREVMRYLQDFAREFKLVE---MVRFKTEVVLVE----
AT5G07800	98	DFPFLAKK---GRDMRRFPSPHKEVWLYLQDFSEAFGLRE---MIRFNVRVEVFGV----
AT5G61290	93	DFPFIAKE---GRDSRRFPSPHHEVLLYLDQDFCQVFLRE---MIRFNVRVEVFGVMNE----
FMO1 (At1G19250)	68	DFPFPNN-----RDTTFEPDYLELLDYLESYAKHFDLLK---FMKFGSKVLRVFIGDG
PseudoFMO1 (AT5G45180)	62	DFLWPN-----RGESSEFPYVDVLLDYLEAYAKHFNLVK---FIKFNKSKVVELRFIGDG
YUCCA03 (AT1G04610)	94	NYFPDEF-----PEYPPKQFQCYLESYAANFDINP---KFNQTVQSAKYDETDF--
YUCCA07 (AT2G33230)	89	NLPPEDI-----PEYPPKYQFTEYLESYATHFDLRP---KFNQTVQSAKYDKRF--
YUCCA05 (AT5G43890)	82	KMPFPEDY-----PEYPPKQFTEYLESYANKFEITP---QFNQTVQSAKYDSETS--
YUCCA09 (AT1G04180)	82	KMPFPDHY-----PEYPPKQFTEYLESYANRFDIKP---EFNKSVE SARFDETS--
YUCCA08 (AT4G28720)	82	KMPFPEDF-----PEYPPKQFTEYLESYATREINP---KFNQTVQSAKYDSETS--
Bs3	92	GLPFPDF-----PEYPPKQFTEYLESYAKHFEIKP---QFNQTVQSAKYDSETS--
YUCCA01 (AT4G32540)	78	LLDFPEYY-----PKYPSKQFTEYLESYASHFRIP---RFNKNVQSAKYDSETS--
YUCCA04 (AT5G11320)	74	LMFPKPNF-----PKYPSKQFTEYLESYAAFNIPK---VFNQTVQSAKYDSETS--
YUCCA02 (AT4G13260)	85	LMFPSSY-----PTYPPKQFTEYLESYAEHFDLKP---VFNQTVQSAKYDSETS--
YUCCA06 (AT5G25620)	89	IIPFGDF-----PTYPPKQFTEYLESYARFDIKP---EFNQTVQSAKYDSETS--
YUCCA10 (AT1G48910)	62	FMPHGREV-----PTEFSPKELFNLYLDAYVAREFINP---RYNRTVKSSTFDES--
YUCCA11 (AT1G2143)	66	HMPFPSNT-----PTEVSKLGFNLYLDAYVAREFINP---RYNRTVKSSTFDES--
Hs FMO1 (NP_002012)	70	DFPFPEDY-----PNYVNSQFTEYLKMYANHFLLK---HIQFKTKVCSVTKCSDS
Sc FMO1 (NP_012046)	76	GFPFEENV-----PLYPSRRNWEYLKMYANHFLLK---HIQFKTKVCSVTKCSDS
AT1G62620	141	-AAEEGI-----GKWRISTEKE---KKVRRDEIDAVVVCNGHM--VEPRIAQ
AT1G63370	141	-AAEEGI-----GKWRISTEKE---KKVRRDEIDAVVVCNGHM--VEPRIAQ
AT1G62600	143	-AAEEGS-----GKWRISTEKE---KKVLRDEIDAVVVCNGHM--IEBRHAE
AT1G63390	113	-CSGGGR-----RKREMN-----
AT1G62580	143	-AGENPK-----KWRVSRNFG---D--ISDEIDAVVVCNGHM--TEBRHAL
AT1G63340	143	-AAENPK-----KWRVSRNSG---D--ISDEIDAVVVCNGHM--TEBRHAL
AT1G12200	143	-VAAESEE-----RGKWRVSRSSD---G--VVDEIDAVVVCNGHM--TEBRHAL
AT1G12130	142	-TAENSC-----KWRVQFRSSS---G-VSGEIDAVVVCNGHM--TEBRHAL
AT1G12160	139	-SPENNR-----KWRVQFKSSN---G-VSGEIDAVVVCNGHM--TEBRHAL
AT1G62540	141	--PVN-G-----KWRVSKTSG---G-VSHDEIDAVVVCNGHM--TEBRVAH
AT1G65860	141	--PVN-G-----KWSVRSKNSV---G-FAAHEIDAVVVCNGHM--TEBRVAH
AT1G62560	141	--PVDNG-----NWRVQSKNSG---G-FLEDEIDAVVVCNGHM--TEBRVAH
AT1G62570	141	--PVN-G-----KWRVSKTGG---G-FSNDEIDAVVVCNGHM--TEBRVAH
AT1G12140	142	--PED-K-----KWRVQSKNSD---G-ISKDEIDAVVVCNGHM--TEBRVAH
AT5G07800	146	-EKEEEDD-----VKRWIVRSREKF---SGKVMEEIDAVVVCNGHM--SHPRLES
AT5G61290	145	-DDDDDD-----VKKWMVKVKK---SGEVMEEIDAVVVCNGHM--SHPRLES
FMO1 (At1G19250)	119	ETPQMVDLGAYGNLLPGKPVVEAVQIGD---SGDIQWHAFFVVCNGHM--DVRPRLA
PseudoFMO1 (AT5G45180)	112	KTLQMGDLGAYGNLLPGKPVVEAVNTGD---GDIQWHAFFVVCNGHM--DVRPRLA
YUCCA03 (AT1G04610)	141	-----GLWRVKIISNMQLGSCFEFYICRWLVVAATGEN--AEKRVPE
YUCCA07 (AT2G33230)	136	-----GLWRVQLVLRSELLGYCFEYICRWLVVAATGEN--AEKRVPE
YUCCA05 (AT5G43890)	129	-----GLWRVKTSSS-SS-GSEMEYICRWLVVAATGEN--AEKRVPE
YUCCA09 (AT1G04180)	129	-----GLWRVRLTSD---GEEMEYICRWLVVAATGEN--AEKRVPE
YUCCA08 (AT4G28720)	129	-----GLWRVKIVSKSEST-QTEVEYICRWLVVAATGEN--AEKRVPE
Bs3	139	-----GLWKVKIVSEIN---GSTSEYICRWLVVAATGEN--AEKRVPE
YUCCA01 (AT4G32540)	125	-----GFWRV-----KTHDTEYISKWLVVAATGEN--AEKRVPE
YUCCA04 (AT5G11320)	121	-----GLWNV-----KTQDG-VYSTWLVVAATGEN--AEKRVPE
YUCCA02 (AT4G13260)	132	-----GLWRVRLTGG---KKDETMFYSRWLVVAATGEN--AEKRVPE
YUCCA06 (AT5G25620)	136	-----GMWRVTVG---EEGTTEYICRWLVVAATGEN--AEKRVPE
YUCCA10 (AT1G48910)	109	-----NKWRVVAENT---VTGETEVYWSEFLVVAATGEN--GEGNIPM
YUCCA11 (AT1G2143)	112	-----QWIVKVVNK---TTALIEVYSAKFMVAATGEN--GEGNIPM
Hs FMO1 (NP_002012)	119	-----AVSGQWEEVIMHEE-----KQESATFDVAVVVCNGHM--GEGNIPM
Sc FMO1 (NP_012046)	126	-----SQWETTSKDELK-----TTKSDDFVAVVVCNGHM--GEGNIPM

```

AT1G62620      184  IPG-----ISSWPGKEMHSHNYRIPEPFFDKVAVLIGNSSSAEDISRDILARVA
AT1G63370      184  IPG-----ISSWPGKEMHSHNYRIPEPFFDKVAVLIGNSSSAEDISRDILARVA
AT1G62600      186  IPG-----ISSWPGKEMHSHNYRIPEPFFDQVVVLIIGNSSASADDISRDILARVA
AT1G63390
AT1G62580      183  IPGNKINHFSFISGLGIDTWPGKQIHSNHYRVPEQVFDQVVVVIIGSSVSGVDISRDILANVT
AT1G63340      183  IPG-----GSSVSGVDISRDILANVT
AT1G12200      186  ITG-----IDSWPGKQIHSNHYRVDPQFNDQVVVVIIGSSASGVDIRDILAQVA
AT1G12130      183  IPG-----IESWPGKQIHSNHYRVSDPFKQGVVVIIGYQSSGSDISRDILAILA
AT1G12160      180  IPG-----IESWPGKQIHSNHYRIPDPFKDEVVVIIGSQASGNDISDILATIA
AT1G62540      180  IPG-----IKSWPGKQIHSNHYRVPGPFENEVVIIGNFASGADISRDILAKVA
AT1G65860      180  IPG-----IKSWPGKQIHSNHYRVPGPFENEVVIIGNYASGADISRDILAKVA
AT1G62560      181  IPG-----IKSWPGKQIHSNHYRVDPFENEVVIIGNFASGADISRDILAKVA
AT1G62570      180  IPG-----IESWPGKQIHSNHYRVDPFKDEVVVIIGNFASGADISRDILSKVA
AT1G12140      181  VPG-----IDSWPGKQIHSNHYRVDPQFNDQVVVVIIGNFASGADISRDILTGVA
AT5G07800      191  IKG-----MDSWKRKQIHSNHYRVDPFENEVVIIGNSMGSDISMEIIVEVA
AT5G61290      189  IKG-----MDLWKRKQIHSNHYRVPEPFCDEVVVIIGNSMGSDISMEIIVEVA
FM01 (At1G19250) 175  FPAKK-----GPEMCKVVMHSMQCKLEK-EEASTLISGKKVAVIGFKKSAIDLIA
PseudoFM01 (AT5G45180) 167  FPAKK-----GPEIICKKVLHSMQSKLQK-EKASQLLHGGKVVAVIGFKKSAIDLIA
YUCCA03 (AT1G04610) 181  FEGL-----DFG--GDVLAGADYRSGGRVQGGKVLVVGCGNSGMEVSLDILYNHG
YUCCA07 (AT2G33230) 176  FEGL-----DFG--GDVLAGADYRSGGRVQGGKVLVVGCGNSGMEVSLDILCNHD
YUCCA05 (AT5G43890) 167  IDGLTT-----EFE--GEVTHACEYRSGEKFRGKSVLIVVGCGNSGMEVSLDILANHN
YUCCA09 (AT1G04180) 164  INGLMT-----EFD--GEVTHACEYRSGEKFRGKSVLIVVGCGNSGMEVSLDILANHN
YUCCA08 (AT4G28720) 168  IDGLS-----EFS--GEVTHACDYRSGEKFRAGKVLVVGCGNSGMEVSLDILANHF
Bs3
YUCCA01 (AT4G32540) 157  IPGRK-----KFS--GKIIVHASEYRSGEEFRQKVLVVGCGNSGMEVSLDILCRYN
YUCCA04 (AT5G11320) 152  IPGLK-----KFT--G-PVVHTSAYRSGSARANKVIVVGCGNSGMEVSLDILCRYN
YUCCA02 (AT4G13260) 169  IDGIP-----DFG--GPIIHTSSYRSGEIPSEKKLIVVGCGNSGMEVCLDILCNFN
YUCCA06 (AT5G25620) 171  FEGMD-----KFAAGVVKHTCHYRTGGDFAGKRVIVVGCGNSGMEVCLDILCNFG
YUCCA10 (AT1G48910) 146  VEG-ID-----TFG--GEIIMHSEYRSGRDFDKNVLIVVGCGNSGMEVLSFDILCNFG
YUCCA11 (AT1G2143) 148  IPGLVE-----SFQ--CKYLSHSEYRNGEKFRAGKRVIVVGCGNSGMEVIAVDILSKCN
Hs FM01 (NP_002012) 159  FPG-----INAIRKQYTHSROYRHPDIFDKKRVIVIGMNSGTDIAVAASHLIA
Sc FM01 (NP_012046) 162  IAGLD-----LWFDNKGAFHSKDFRNCFEFAEKVVIVVGNGSSGODIANQLTTVA

```

```

AT1G62620      232  KEVHWACRSEN-PADTFIKQTG-YNNLWTHS-----
AT1G63370      232  KEVHWACRSEN-PADTFIKQTG-YNNLWTHS-----
AT1G62600      234  KEVHWACRSEN-AADTYIERPG-YSNLWMHS-----
AT1G63390
AT1G62580      243  KEVHSSRST-KPETYEKIPG-YDNLWLHS-----
AT1G63340      203  KEVHSSRST-KPETYEKISG-YDNLWLHS-----
AT1G12200      234  KEVHSSRST-SPDTYEKLTG-YENLWLHS-----
AT1G12130      231  KEVHTAAR----SDAYAKESSIYSNLHFHP-----
AT1G12160      228  KEVHTSSK----MVASDS-YGCYDNLRIHP-----
AT1G62540      228  KEVHTASRAS-EFDTYEKIPVPRNNLWTHS-----
AT1G65860      228  KEVHTASRAS-ESDTYQKLPVPQNNLWVHS-----
AT1G62560      229  KEVHTASRAR-EPHTYEKISVPQNNLWMHS-----
AT1G62570      228  KEVHTASRAS-KSNTFEKRPVNNLWMHS-----
AT1G12140      229  KEVHTASREN-PSKTYSKIPG-SNNLWLHS-----
AT5G07800      239  KEVHTSAKTLDISSGLSKVTSKHPNLLIHP-----
AT5G61290      237  KEVHTSTKSLDIPPGLSKVIKHNQLHLHP-----
FM01 (At1G19250) 225  LESALANQGGGKACTMVVTRTHWGIIPHYVWVGLPFF-----
PseudoFM01 (AT5G45180) 217  LESALANQGKGGKCTMVVTRPHWVLIIPHYW-----
YUCCA03 (AT1G04610) 229  ANPSVVRSVAVHVLPREIFGKSTFELGVTM-----
YUCCA07 (AT2G33230) 224  ASPSVVRSVHVLPREIVGKSTFELSVTM-----
YUCCA05 (AT5G43890) 216  ANASVVRSVHVLPREIIGKSSFELSMML-----
YUCCA09 (AT1G04180) 213  AITSVVRSVHVLPREIIGKSTFELSMVM-----
YUCCA08 (AT4G28720) 216  AKPSVVRSVHVLPREIVGKSTFELAMKM-----
Bs3
YUCCA01 (AT4G32540) 206  ASPHLVVRNIVHVLPREIIGVSTFGVGMTL-----
YUCCA04 (AT5G11320) 200  ALPHVVVRNSVHVLPREIDFFGLSTFGIAMTL-----
YUCCA02 (AT4G13260) 217  ALPSVVVRDSVHVLPQEMIGISTFGIISTSL-----
YUCCA06 (AT5G25620) 221  AQPSTVVVRDAVHVLPREIIGTSTFGISMFL-----
YUCCA10 (AT1G48910) 194  ANTTILIRIPRHVVTKEVVH----LGMTL-----
YUCCA11 (AT1G2143) 197  ANVSTVVRSQVHVLTRCIVR----IGMSL-----
Hs FM01 (NP_002012) 207  EKVFISTTGGGWVISRIFDSGYPWDVFMTRFQNMRLNSLPTPIVTLWLMERKINNWLNHA
Sc FM01 (NP_012046) 212  KKVYNSIREPASNLKAKIETVQTIIDSDAD-----

```

```

AT1G62620      260 -----MIESVHEDGSLVYQNGKTIISVDIIMH
AT1G63370      260 -----MIESVHEDGSLVYQNGKTIISVDIIMH
AT1G62600      262 -----MIESVHEDGSLVYQNGKTIISVDIIMH
AT1G63390
AT1G62580      271 -----NLETVREDGSLVFKNGKTVYADTIMH
AT1G63340      231 -----NLETVREDGSLVFKNGKTVYADTIMH
AT1G12200      262 -----TIQIAREDEGSLVFEENGKTIYADTIMH
AT1G12130      257 -----TIDRVYEDGSLVFDGKLIIFADIVH
AT1G12160      253 -----TIYRAREDEGSLVFRNGKVVFAIVH
AT1G62540      257 -----EIDTAYEDGSLVFKNGKVVYADSIIVY
AT1G65860      257 -----EIDFAHQDGSILFKNGKVVYADTIIVH
AT1G62560      258 -----EIDTTHEDEGSLVFKNGKVIIFADSIIVY
AT1G62570      257 -----EIDTAHEDGTLVFKNGKVVHADTIIVH
AT1G12140      257 -----MIESVHEDGTLVYQNGKVVQADTIIVH
AT5G07800      269 -----QIESLEDDGKLVIFVDGSLVVDITILY
AT5G61290      267 -----QIESLEEDGRVIFEDGSLVIVADITILY
FM01 (At1G19250) 262 -----LFYSSRASQFLHDRPNQSFRLRFLFCLLESLLEAVVSKFIES
PseudoFM01 (AT5G45180) 247 -----RATVSKFIES
YUCCA03 (AT1G04610) 259 -----MKYMPVWVADKTLFLIARILIGN
YUCCA07 (AT2G33230) 254 -----MKWMPVWVVDKTLFLVTRLLIGN
YUCCA05 (AT5G43890) 246 -----MKWFPLWVVDKILLIHLWLLIGN
YUCCA09 (AT1G04180) 243 -----MKWLPLWVVDKLLLSWLVLGS
YUCCA08 (AT4G28720) 246 -----LRWFPLWVVDKILLVLSWMLIGN
Bs3
YUCCA01 (AT4G32540) 236 -----LKCLPLRLVVDKFLLLMANLSFGN
YUCCA04 (AT5G11320) 230 -----LKWFPKLVVDKFLLLANSTLIGN
YUCCA02 (AT4G13260) 247 -----LKWFPVHVVDRFLLRMSRLVLGD
YUCCA06 (AT5G25620) 251 -----LKWLPPIRVDRFLLVVSRLFILGD
YUCCA10 (AT1G48910) 219 -----LKYAPVAVVDTLVTTMAKILYGD
YUCCA11 (AT1G2143) 222 -----LRFPPVKLVDRLCLELAE LRFRN
Hs FM01 (NP_002012) 267 NYGLIPEDRTQLKEFVLNDELPGRIITGKVFIRPSKEVKENSVEFNNTSKEEPTIIVF
Sc FM01 (NP_012046) 242 -----WKNRSVTISDGRVQLNIDYIIF

```

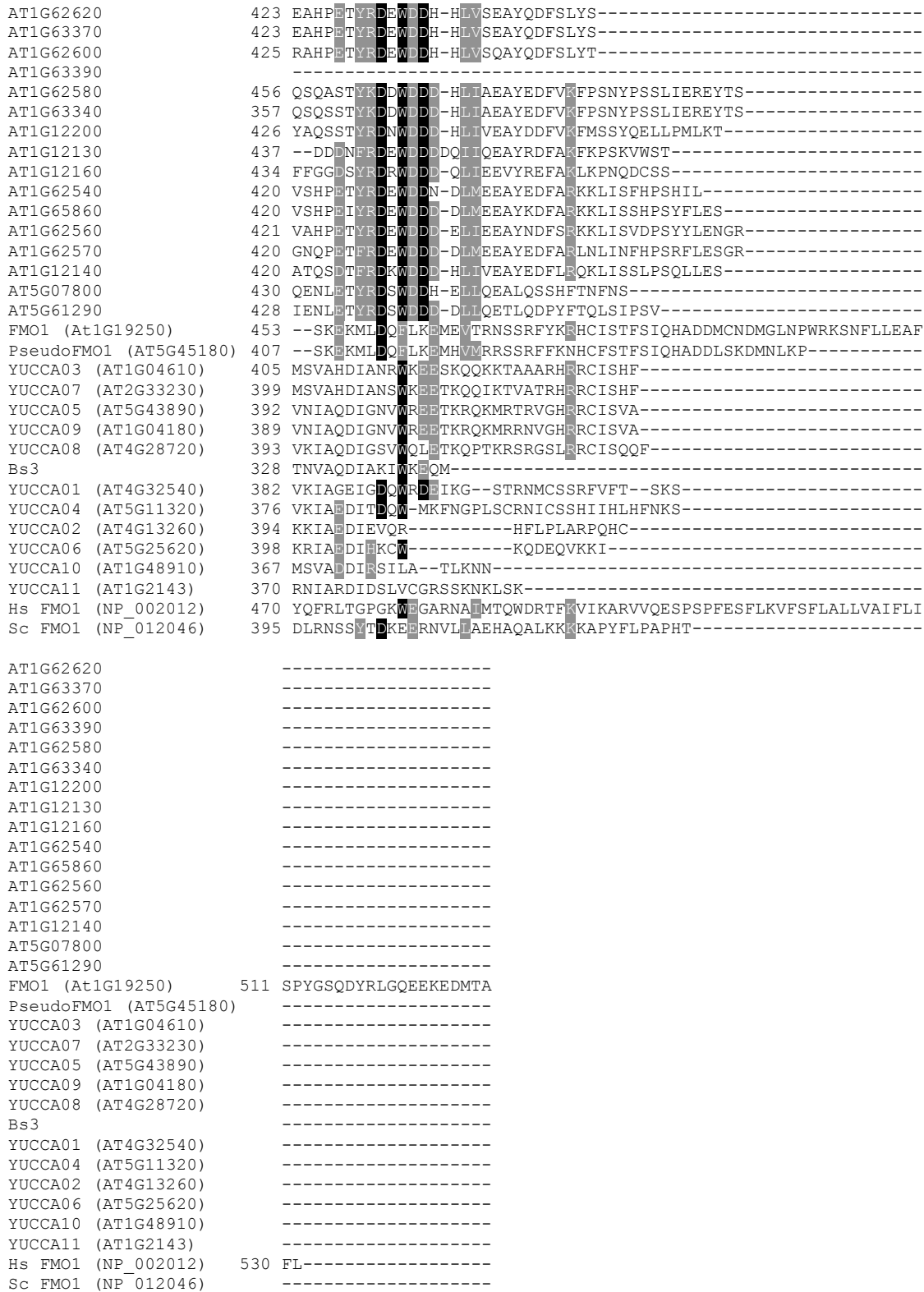
```

AT1G62620      286 CTGKYHFPFLDTNGIVTVDDN---RVGPLYKDVFPAPAPWLSFTIGLEWQ-----
AT1G63370      286 CTGKYHFPFLDTNGIVTVDDN---RVGPLYKDVFPAPAPWLSFTIGLEWQ-----
AT1G62600      288 CTGKYHFPFLETNGVTVDDN---RVGPLYKDVFPAPAPWLSFVGLIWK-----
AT1G63390
AT1G62580      297 CTGKYHFPFLDTKGEVTVDDN---RVGPLYKHVFPALSPGLSFTIGLEWQNMKILQTL
AT1G63340      257 CTGKYHFPFLDTKGEVTVDDN---RVGPLYKHVFPALSPGLSFTIGLEWQ-----
AT1G12200      288 CTGKYHFPFLDTKGEVTVDDN---RVGPLYKHVFPALAPSLSFTIGLEWQ-----
AT1G12130      283 CTGKYHFPFLETGKYVNVDDN---RVGPLYKHVFPALAPGLSFTIGLEWQ-----
AT1G12160      279 CTGKYHFPFLKTSGYVTVDDN---RVGPLYKHVFPALAPGLSFTIGLEWQ-----
AT1G62540      283 CTGKYHFPFLETNGYVNVDDN---RVEHLYKHVFPALSPGLSFTIGLEWQ-----
AT1G65860      283 CTGKYHFPFLETNGYVNVDDN---RVEHLYKHVFPALAPSLSFTIGLEWQ-----
AT1G62560      284 CTGKYHFPFLETNGYVNVDDN---RVEHLYKHVFPALAPGLSFTIGLEWQ-----
AT1G62570      283 CTGKYHFPFLETNNYMRVDDN---RVEHLYKHVFPALAPGLSFTIGLEWQ-----
AT1G12140      283 CTGKYHFPFLNTNGYVTVDDN---CVGPLYEHVFPALAPGLSFTIGLEWQ-----
AT5G07800      295 CTGYSYKFPFLESKGRVTVDDN---RVGPLYFEHFPPLSPSLSFTIGLEWQ-----
AT5G61290      293 CTGYSYKFPFLESKGRVTVDDN---RVGPLYFEHFPPLSPSLSFTIGLEWQ-----
FM01 (At1G19250) 303 YVLAKLPLEKYGLKPNHSEEDYASQMAIIPENFEEADKGMIRKRSKSKWVFEYEG--
PseudoFM01 (AT5G45180) 257 YVLAKLPLEKYGLKPDHAFSEEDYASQMALVPEKFEEDKGMIRKRTTNWVFDYDEG--
YUCCA03 (AT1G04610) 282 TDKYGLKREKIGPLELKNKSGKTPVLDIGALPKIRSGKIKIVPG-IKFGKPK-----
YUCCA07 (AT2G33230) 277 TDKYGLKREKIGPLELKNKTAGKTPVLDIGALSMIKSGKIKIVAG-IKFGPGK-----
YUCCA05 (AT5G43890) 269 LTKYGLKREKIGPMELKISGKTPVLDIGALEKIKSGEVEIVPG-IKRFRRSH-----
YUCCA09 (AT1G04180) 266 LSNYGLKREKIGPMELKISGKTPVLDIGALEKIKSGDVEIVPA-IKQFSRHH-----
YUCCA08 (AT4G28720) 269 IEKYGLKREKIGPMELKISGKTPVLDIGALEKIRLKGKINNVPG-IKRFNGNK-----
Bs3
236 ---GRNFP---EEINIVPA-IKKFTQK-----
YUCCA01 (AT4G32540) 259 TDRIGLRRPKTGPLELKNVTKGSPVLDVGAISLIRSGMIQIMEG-VKEITKKG-----
YUCCA04 (AT5G11320) 253 TDLLGLRRPKTGPIELKNVTKGTPVLDVGAISLIRSGQIKVTA-VKEITRNG-----
YUCCA02 (AT4G13260) 270 TDRIGLVRPKLGPLEKIKCGKTPVLDVGTAKIRSGHIKIVPE-LKRVMHYS-----
YUCCA06 (AT5G25620) 274 TLLGLNRPKLGPLELKNVSGKTPVLDVGTAKIKTGDIKVCSSG-IRRLKRHE-----
YUCCA10 (AT1G48910) 242 LSKYGLFRPKQGFATKLTGKAPVIDVGTVEKIRDGEIQVINGGIGSINGKT-----
YUCCA11 (AT1G2143) 245 TSRVGLVRPNNGPFLNKLITGRSATIDVGVGEIKSGKIQVVT-IKRIEGKT-----
Hs FM01 (NP_002012) 327 ATGYTFAFPFLDESIVKVEIQG---ASLYKYIFFAHLQKPTLAITGLIKPLG-----
Sc FM01 (NP_012046) 264 ATGYYSFPFLEPSVRLVLELGEV---VTGDKHSSVNLHNLWEHMLVVKDETL-----

```

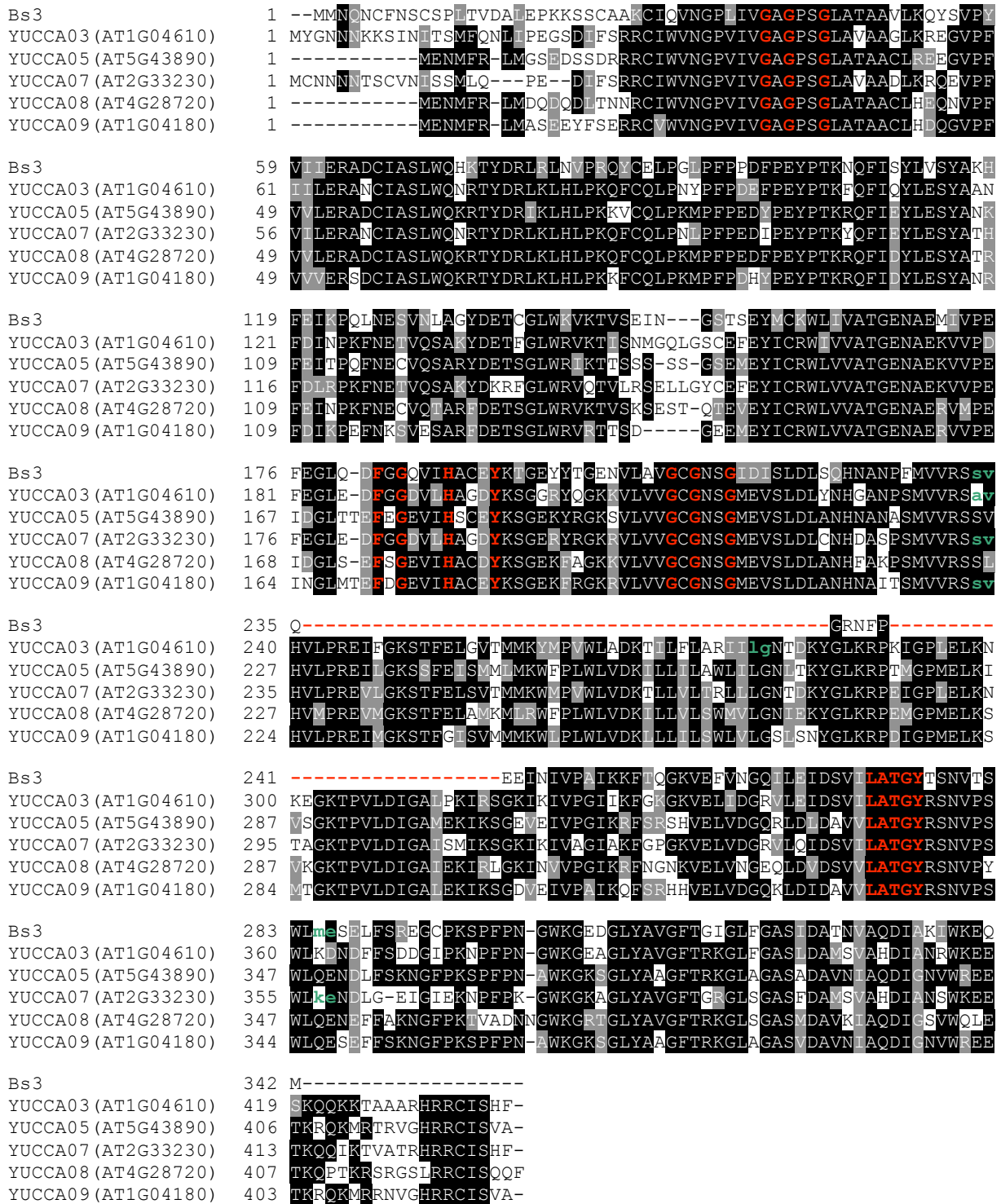
AT1G62620 334 -----VLPFPMFELQSKWVIAGVLSGRIPLPSKEDMMIEIKTFYSTLEVQGIIP  
 AT1G63370 334 -----VLPFPMFELQSKWVIAGVLSGRIPLPSKEDMMIEIKTFYSTLEVQGIIP  
 AT1G62600 336 -----VLPFPMFELQSKWVIAGVLSGRIPLPSKEDMMIEIKTLYSTLDAQGITA  
 AT1G63390 -----  
 AT1G62580 353 VNELIGQCFCGYLLVLPFPMFELQSKWVAAVLAGRVSLPSQ-EEEMETKMFYKLEASCIIP  
 AT1G63340 305 -----VLPFPMFELQSKWVAAVLAG-----  
 AT1G12200 336 -----ITPFPMFELQSKWVAAVLSGRVSLPSQDEMMIEITKAFYDKLEASGIIP  
 AT1G12130 332 -----IQFFMFELQSKRWVASVLSGRVKLPSEEQMMEDVIAFYAKLKSIGIIP  
 AT1G12160 328 -----IQFFMFELQSKRWVASVLSGRVKLPAEDKMMIEAVAFYKLELDIGIIP  
 AT1G62540 332 -----IQFVMEFELQSKWVAAVLSRRVTLPTEDKMMEDISAWYASLDAVGIIP  
 AT1G65860 332 -----IQFVMEFELQSKWVAAVLSGRVTLPSQDKMMEDIIIEWYATLDVIGIIP  
 AT1G62560 333 -----IVFVMEFELQSKWVAAVLSGRVTLPSQDKMMEDINAWYASLDALGIIP  
 AT1G62570 332 -----IQFYMFEFELQSKWVAAVLSGRVTLPSVDEMMDDIKLSYETQEALGIIP  
 AT1G12140 332 -----IQFFMFELQSKWVAAVLSGRVTLPSQDKMMEDVITAYYAKREAFGIIP  
 AT5G07800 344 -----IGFPPFEAQAKWIAQVLSGKSSLPSPDQMLQSVDEFYRSRDLAGVPI  
 AT5G61290 342 -----IGFPPFEAQAKWIAKLLSGKTSLPSSDQMMQSI SDFYLAREADGIIP  
 FMO1 (At1G19250) 361 -----IVFEDGTTLEADVVIATGYDGMKKLKAIVPEPFRYSLEFPWGIIP  
 PseudoFMO1 (AT5G45180) 315 -----IEFEDGTTLEADVVIATGYDGMKKLKAIVPEPFRYSLEFPWGIIP  
 YUCCA03 (AT1G04610) 334 -----VELIDGRVLEIDSVIATGYRSNVPYSLKNDIFFS-----DDGIIP  
 YUCCA07 (AT2G33230) 329 -----VELVDGRVQLIDSVIATGYRSNVPYSLKNDIG-----EIGIIP  
 YUCCA05 (AT5G43890) 321 -----VELVDGRVLDLDAVVIATGYRSNVPYSLKNDIFS-----KNGIIP  
 YUCCA09 (AT1G04180) 318 -----VELVDGQKLDIDAVVIATGYRSNVPYSLKNDIFS-----KNGIIP  
 YUCCA08 (AT4G28720) 321 -----VELVNGFQLDVSIVIATGYRSNVPYSLKNDIFFA-----KNGIIP  
 Bs3 257 -----VEFVNGQILEIDSVIATGYTSNVTYSLKNDIFS-----REGIIP  
 YUCCA01 (AT4G32540) 311 -----AKFMDGQEKDFDSIIIFATGYKSNVPYSLKNDIFFT-----DDGIIP  
 YUCCA04 (AT5G11320) 305 -----AKFNLNGKEIEFDSIIIFATGYKSNVPYSLKNDIFFT-----KEGIIP  
 YUCCA02 (AT4G13260) 322 -----AEFVDGRVDFDAIIFATGYKSNVPYSLKNDIFFS-----KNGIIP  
 YUCCA06 (AT5G25620) 326 -----VEFDNGKTERFDAIIFATGYKSNVPYSLKNDIFFS-----KNGIIP  
 YUCCA10 (AT1G48910) 295 -----LTFENGHKQDFDAIVFATGYKSNVSNWLEDEYVMK-----KNGIIP  
 YUCCA11 (AT1G2143) 297 -----VEFIDGNTKNVDSIVFATGYKSNVSNWLEDEYVMK-----KNGIIP  
 Hs FMO1 (NP\_002012) 376 -----SMIPTGTTQARWAVRVLKGVNKLPPPSVMIETINARKENKPSWFGIIP  
 Sc FMO1 (NP\_012046) 314 -----FILTPQLVIPPFLSEIQAAIMVEVFCKSLPITTTTFDSNACGTHNFIIP

AT1G62620 381 KRYTHRMGN-----TQFEYYNWLASQCGCSETEEWRKEMCLNGVRK  
 AT1G63370 381 KRYTHRMGN-----TQFEYDNWLASQCGCSETEEWRKEMCLNGVRK  
 AT1G62600 383 KRYTHQMGII-----SQFEYNSWLASQCGCSETEEWRKEMYFAIGVKK  
 AT1G63390 -----  
 AT1G62580 412 KRYTHLMAEL-----DSQFVYNNWLASQCGCSETEEWRKEMCLNGVRK  
 AT1G63340 325 -----RFVYDNNWLASQCGCSETEEWRKEMCLNGVRK  
 AT1G12200 383 KRYTHLMPD-----DSQFEYDNWLASQCGCSETEEWRKEMCLNGVRK  
 AT1G12130 378 KRFTHTFLTPQWTPMFEKLPHEAVLISQSEYFNWIAEQCGCSSETRWRREQYNTI IKK-  
 AT1G12160 374 KRYTHFLTPDPRGNPMLGTFTKPEDAVVISQSDYFNWIAKQCGCTSI ERWRERLYNV I IKKV  
 AT1G62540 378 KRYTHKLGK-----IQSEYLNWVAEECGCPLVEHWRNQIVR YQRL  
 AT1G65860 378 KRHTHKLGR-----ISCEYLNWVAEECHCSPVENWRHQEVEVERFQRM  
 AT1G62560 379 KRHTHTIGR-----IQSEYLNWVAEESGCELVLEHWRNQIIVR YQRL  
 AT1G62570 378 KRYTHKLGK-----SQCEYLDWIADLCGFPHVHWRDQEVTR YQRL  
 AT1G12140 378 KRYTHRLGG-----GQVDYLNWVAEIQGAPPGQWRVQIIN GCGYRL  
 AT5G07800 390 KHNTHDIAD-----FTYCDKYADYVGFPHLEWRKLLCLSLNNS  
 AT5G61290 388 KRNTHDIAD-----FNYSDKYADYVGFPHLEWRKLVCLSLNNS  
 FMO1 (At1G19250) 407 LYRGTIHLPLIPN-----MGFVGYVQSSSNLHTSELRSMLSLRVLDEKFRLP  
 PseudoFMO1 (AT5G45180) 361 LYRGTIHLPLIPN-----MGFVGYVQSSSNLKSSELHSRWSQLD KFTLP  
 YUCCA03 (AT1G04610) 374 KN-----PFPN-GWKGEAGLYAVGFTRKGLFGASLDA  
 YUCCA07 (AT2G33230) 368 KN-----PFPN-GWKGKAGLYAVGFTRGRLSASFDA  
 YUCCA05 (AT5G43890) 361 KS-----PFPN-AWKGKSGLYAAGFTRKGLAGASADA  
 YUCCA09 (AT1G04180) 358 KS-----PFPN-AWKGKSGLYAAGFTRKGLAGASVDA  
 YUCCA08 (AT4G28720) 361 KT-----VADNNGWKGRTGLYAVGFTRKGLSASMDA  
 Bs3 297 KS-----PFPN-GWKGEDGLYAVGFTRGILFGASIDA  
 YUCCA01 (AT4G32540) 351 KT-----PFPN-GWRGGKGLYTVGFTRRGLLGTASDA  
 YUCCA04 (AT5G11320) 345 KT-----PFPN-GWKGEKGLYTVGFTRRGLSCTAYDA  
 YUCCA02 (AT4G13260) 363 HK-----PFPN-GWKGESGLYAVGFTKLGLLGAIDA  
 YUCCA06 (AT5G25620) 367 IQ-----EPE-GWRGECGLYAVGFTRKGLSASMDA  
 YUCCA10 (AT1G48910) 336 KA-----PMPK-HWKGEKNLYCAGFSRKG IAGCAEDA  
 YUCCA11 (AT1G2143) 339 KR-----EFPD-HWKGNGLYAVGFTRKGLSASMDA  
 Hs FMO1 (NP\_002012) 422 CYCKALQSDYIT-----YIDELLYINAKPNLFSMLLTDPHLALTVFFPCPCSP  
 Sc FMO1 (NP\_012046) 360 KDKD-----LEYAELQELLNSIPRVRGHEFEPVVDWDRLLI



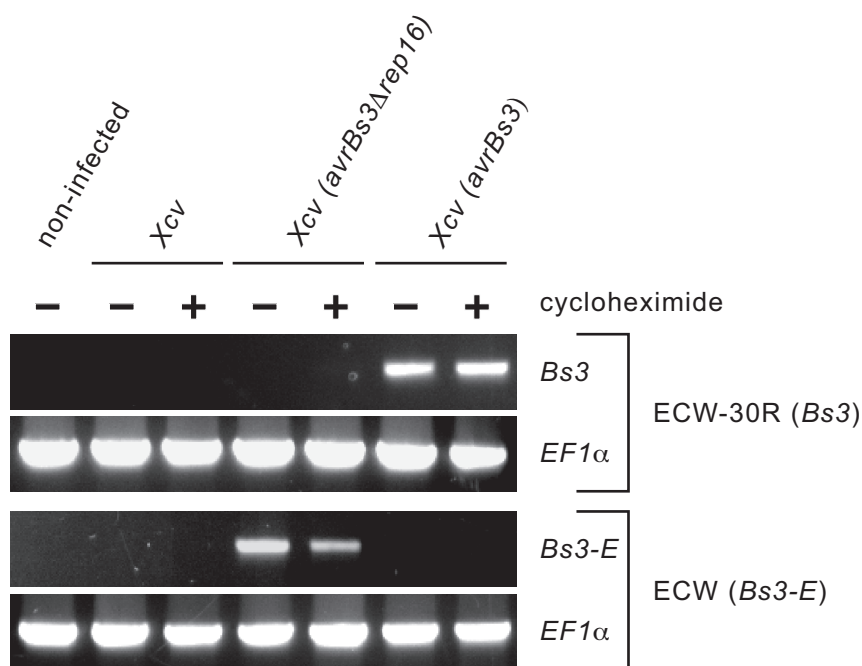
**Fig. S3. B.** Alignment corresponding to the phylogenetic tree displayed in fig. S3 A. Identical amino acids (white text on black background) and similar amino acids present in  $\geq 50\%$  of sequences (on grey background) were shaded using Boxshade. Dashes (-) indicate gaps.

Figure S4



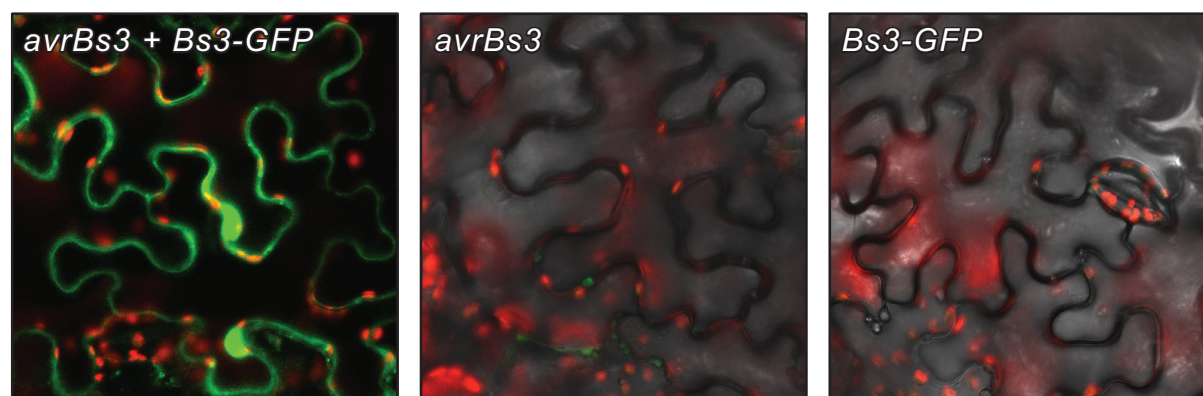
**Fig. S4.** The predicted Bs3 protein and YUCCA-like proteins from *Arabidopsis* are structurally diverse. Alignment of YUCCA-like proteins from *Arabidopsis* that are closely related to the predicted Bs3 protein. A stretch of 72 residues is conserved in YUCCA-like *Arabidopsis* proteins, but is absent from the predicted Bs3 protein (labeled with red dashes). Conserved residues of the FAD-binding domain (GXGXXG), the FMO-identifying sequence motif (FXGXXXHXXX[Y/F]), the NADPH-binding domain (GXGXX[G/A]) and the conserved FATGY motif ([L/F]ATGY) are marked in red. Amino acids that are located at the exon-exon junctions of the corresponding genes are marked in lowercase green. Names of proteins are given with their accession numbers (in parentheses). Alignments were constructed with ClustalW. Identical amino acids (white text on black background) and 50% similar amino acids (white on grey background) were shaded using Boxshade. A dash (-) indicates a gap.

## Figure S5



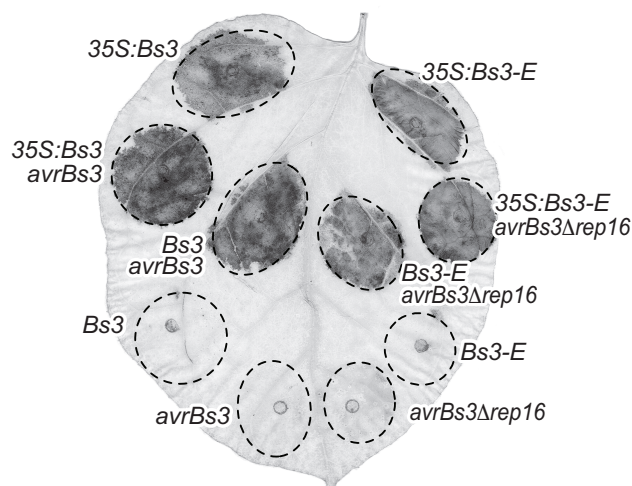
**Fig. S5.** Semi-quantitative reverse transcription-polymerase chain reaction was carried out on cDNA of non-infected and *Xcv*-infected pepper ECW-30R (*Bs3*) and ECW (*Bs3-E*) leaves 24 hours after infection. The *avrBs3*-like genes that are expressed in the given *Xcv* strains are indicated (in parentheses). Inoculations were carried out in the presence (+) or absence (-) of the eukaryotic protein synthesis inhibitor cycloheximide. Elongation factor 1 $\alpha$  (*EF1α*) was amplified as a control.

## Figure S6



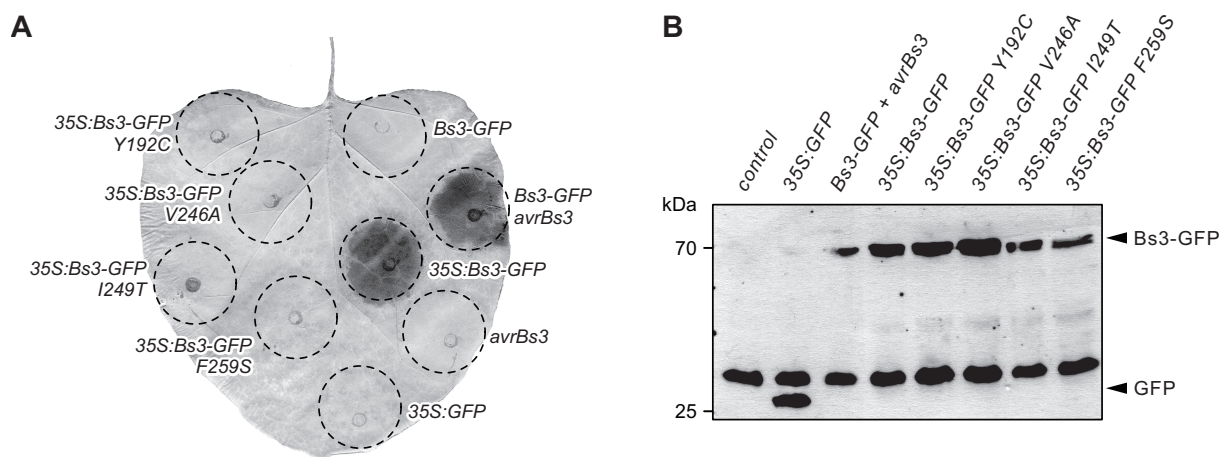
**Fig. S6.** Confocal imaging of GFP-tagged Bs3 was conducted two days after *A. tumefaciens* transient transformation of *N. benthamiana*. *Bs3-GFP* and *avrBs3* are under transcriptional control of the *Bs3* and the Cauliflower mosaic virus 35S promoter, respectively.

## Figure S7



**Fig. S7.** Constitutive expression of the *Bs3* and *Bs3-E* alleles triggers an Avr-independent HR. The coding regions of *Bs3* and *Bs3-E* were expressed under the control of their own promoter (*Bs3* and *Bs3-E*) or under control of the Cauliflower mosaic virus 35S promoter (*35S:Bs3* and *35S:Bs3-E*). The *Bs3* alleles were expressed alone or together with the depicted *avr* genes. The genes were delivered into *N. benthamiana* leaves via *A. tumefaciens* transient transformation ( $OD_{600} = 0.8$ ). Four days after infiltration the leaves were cleared to visualize the hypersensitive response (dark areas).

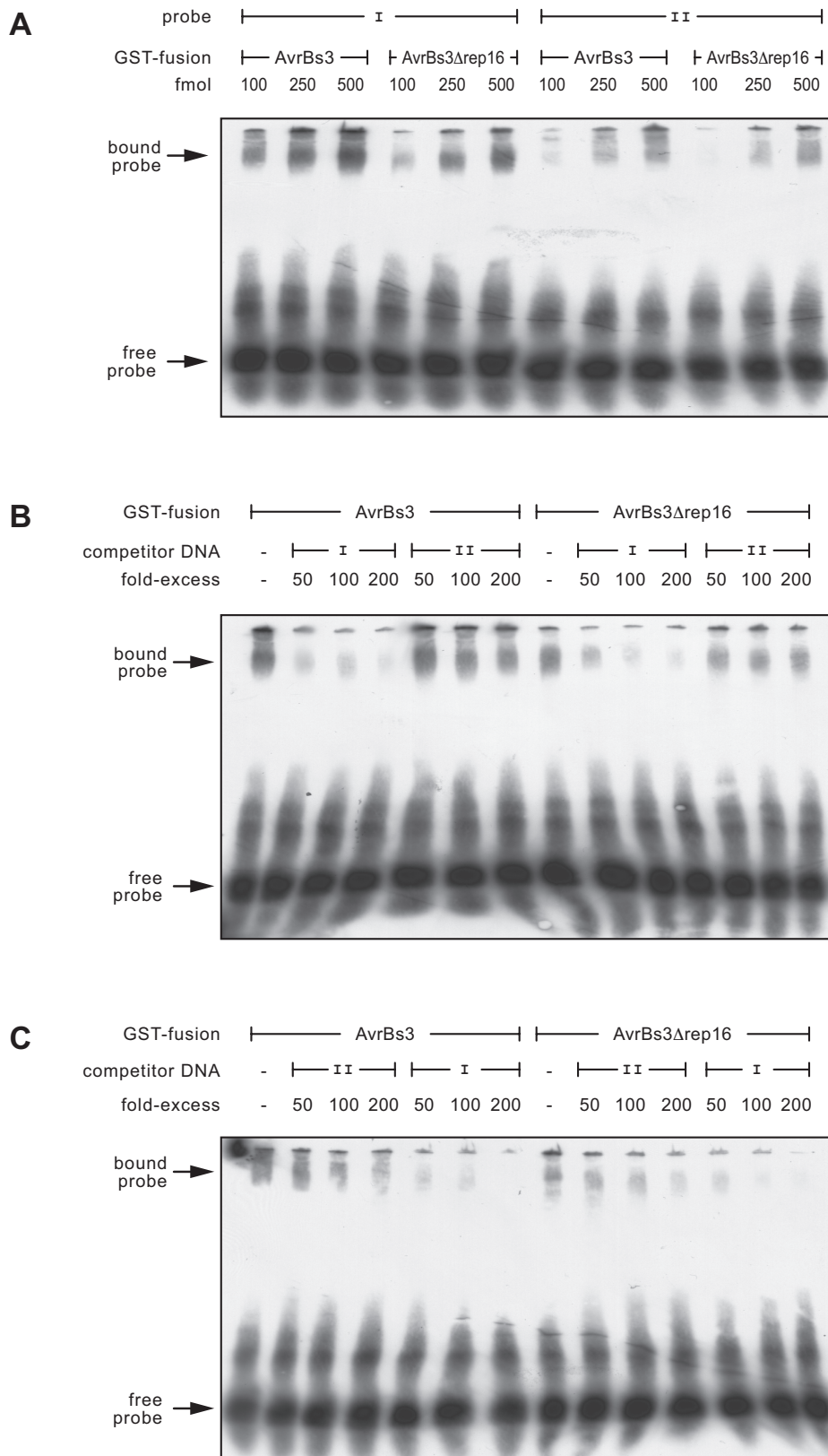
## Figure S8



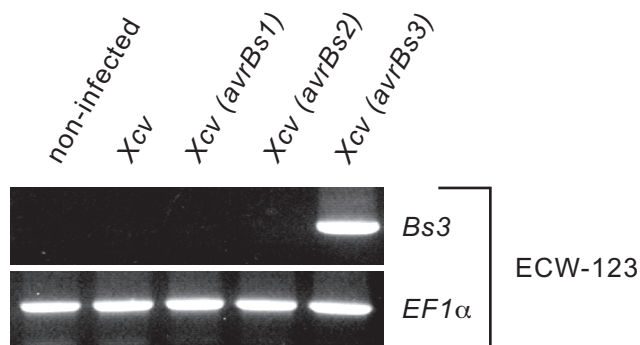
**Fig. S8. A.** *GFP*, *GFP*-fusion construct or an empty T-DNA (control) were transformed in *N. benthamiana* leaves by *A. tumefaciens*. *Bs3* and the depicted *Bs3* mutants are under transcriptional control of the *Bs3* promoter (*Bs3*) or the Cauliflower mosaic virus 35S promoter (*35S:Bs3*). *Bs3* was expressed either alone or together with *avrBs3* as indicated. Dashed lines mark the inoculated areas. Four days after infiltration the leaves were cleared to visualize the hypersensitive response (dark areas). **B.** Protein extracts from *N. benthamiana* leaves 40 hours after infiltration with the indicated *A. tumefaciens* strains. Proteins were separated by SDS-PAGE and analysed by immunoblot using a *GFP*-specific antibody. Molecular masses are given on the right in kilodalton (kDa). Arrowheads indicate the expected size of *GFP* and the *Bs3*-*GFP* fusion protein.



**Figure S9**



**Fig. S9.** **A.** Electrophoretic mobility shift assay (EMSA) with AvrBs3 and AvrBs3Δrep16. Protein amounts are given in fmol. The nucleotide sequences of DNA probe I and II are displayed in Fig. 4A. Positions of the bound and free probe are indicated by arrows on the left hand panel. **B.** EMSA competition assay with *Bs3*-derived probe DNA. **C.** Competition assay with *Bs3-E*-derived probe DNA.

**Figure S10**

**Fig. S10.** RT-PCR of non-inoculated and *Xcv*-inoculated leaves harvested 10 hours after *Xcv* infection of the pepper cultivar ECW-123R (contains the *R* genes *Bs1*, *Bs2* and *Bs3*). The *avr* genes that are expressed in the given *Xcv* strains are indicated. Elongation factor 1 $\alpha$  (*EF1 $\alpha$* ) expression was used to standardize the *Bs3* transcript levels in each sample.

**Supplementary References**

- S1. T. Jordan *et al.*, *Theor. Appl. Genet.* **113**, 895 (2006).
- S2. S. Schornack *et al.*, *Plant J.* **37**, 46 (2004).
- S3. M. Holsters *et al.*, *Plasmid* **3**, 212 (1980).
- S4. R. M. Horton, H. D. Hunt, S. N. Ho, J. K. Pullen, L. R. Pease, *Gene* **77**, 61(1989).
- S5. U. K. Laemmli, *Nature* **227**, 680 (1970).
- S6. G. Van den Ackerveken, E. Marois, U. Bonas, *Cell* **87**, 1307 (1996).
- S7. B. Szurek, E. Marois, U. Bonas, G. Van den Ackerveken, *Plant J.* **26**, 523 (2001).
- S8. K. Herbers, J. Conrads-Strauch, U. Bonas, *Nature* **356**, 172 (1992).
- S9. S. Offermann *et al.*, *Plant Physiol.* **141**, 1078 (2006).
- S10. V. Knoop, B. Staskawicz, U. Bonas, *J. Bacteriol.* **173**, 7142 (1991).

## 2.2.3 Zusätzliche Ergebnisse

### 2.2.3.1 Die Bs3-vermittelte HR wird von der Signalwegkomponente SGT1 beeinflusst

Da es sich bei *Bs3* nicht um ein *R*-Gen der NBS-LRR-Klasse handelt, sollte untersucht werden, von welchen Signalwegkomponenten die *Bs3*-vermittelte HR beeinflusst wird. Hierfür erfolgte das Tabakrattle-Virus (TRV)-basierte Virus-induziertes Gen-Silencing (VIGS) der Signalwegkomponenten EDS1, Rar1, SGT1, Hsp90 und NDR1 in *N. benthamiana* Pflanzen. GFP wurde als Kontrolle stillgelegt. Die Durchführung der *Silencing*-Experimente und die verwendeten Konstrukte sind in der Doktorarbeit von S. Schornack beschrieben (Schornack, 2006; Schornack et al., 2004). Um den Einfluß der Signalwegkomponenten hinsichtlich der *Bs3*-vermittelten HR zu analysieren, erfolgte drei Wochen nach TRV-Infektion die Kotransformation der Pflanzen mit *Bs3* und *avrBs3* mittels *A. tumefaciens* GV3101. Zusätzlich erfolgte die *A. tumefaciens* vermittelte Transformation der Pflanzen mit den *R*-Genen *Bs4* bzw. *Rx* in Kombination mit ihren korrespondierenden Effektoren und des Effektorgens *avrBsT*. Diese Konstrukte dienten als Kontrollen, da sie sich in ihrer Abhängigkeit von den einzelnen Signalwegkomponenten unterscheiden und ihre Abhängigkeit von diesen bereits bekannt ist (Peart et al., 2002a; Peart et al., 2002b; Schornack et al., 2004; R. Szczesny und U. Bonas, unveröffentlicht). Die Ergebnisse sind in Tabelle 2 zusammengefasst.

**Tabelle 2: SGT1 ist notwendig für die Bs3-vermittelte HR**

<i>Agrobacterium</i> vermittelte Transformation von	VIGS von					
	SGT1	Hsp90	Rar1	EDS1	NDR1	GFP
<i>35S:Bs3</i>	-	(+)	+	+	+	+
<i>Bs3+avrBs3</i>	-	(+)	+	+	+	+
<i>Bs4+avrBs4</i> <sup>1)</sup>	-	-	-	-	+	+
<i>Rx+PVX</i> <sup>2)</sup>	-	-	+	+	-	+
<i>avrBsT</i> <sup>3)</sup>	(+)	+	+	+	+	+

In der Tabelle sind die Ergebnisse der *Silencing*-Experimente zusammengefasst. Die Experimente wurden dreimal mit ähnlichem Ergebnis wiederholt. In jedem Experiment wurden für jede Signalwegkomponente drei *N. benthamiana*-Pflanzen verwendet. Ein “+“ symbolisiert, dass nach dem *Silencing* der entsprechenden Signalwegkomponente noch eine HR durch die getesteten *R*-Gene bzw. des Effektors ausgebildet wurde. Ein “(+)“ bedeutet, dass die HR verzögert war und ein “-“ gibt an, dass keine HR ausgebildet wurde.

1) in Übereinstimmung mit den Daten aus Schornack et al. (2004)

2) in Übereinstimmung mit den Daten aus Peart et al. (2002a und 2002b)

3) in Übereinstimmung mit den Daten von R. Szczesny und U. Bonas, unveröffentlicht

Dabei ist zu erkennen, dass die Bs3-vermittelte HR nur von der Signalwegkomponente SGT1 abhängig ist. Bei allen anderen Signalwegkomponenten kommt es noch zu einer Ausbildung der Bs3-vermittelten HR, wobei diese in *Hsp90-gesilencten* Pflanzen etwa einen Tag langsamer als in WT- bzw. in *GFP-gesilencten* Pflanzen ist. Weiterführende Untersuchungen zu Effekten des *Silencings* der Signalwegkomponenten auf die *Bs3*-Induktion und die Bs3-Proteinmenge, sowie der Effizienz des *Silencings* sind Gegenstand der Doktorarbeit von Jana Piprek (J. Piprek und T. Lahaye, unveröffentlicht).

### 2.2.3.2 Das Bs3-Protein ist im Zytoplasma und Zellkern lokalisiert

Lokalisationsexperimente von Proteinen können Aufschluss über ihr Funktionsprinzip geben (Schornack et al., 2009). Die Lokalisation des Bs3-Proteins erfolgte mit einem C-terminalen GFP-Epitoptag (*Bs3<sub>Prom</sub>-Bs3<sub>kodierendeSequenz</sub>* im Vektor pGWB4; Bs3::GFP). Ein Problem war, dass die Bs3-vermittelte HR mit der Fluoreszenz von GFP interferiert, so dass die Analyse mittels des konfokalen Laser-Scanning-Mikroskop (LSM) vor der Ausbildung der HR-Symptome erfolgen musste. Daher erfolgte die Entnahme von 2 mm großen Blattsegmenten mit Hilfe eines Korkbohrers für die Lokalisationsstudien von Bs3::GFP mittels LSM und Elektronenmikroskopie 40 h nach *A. tumefaciens* basierter Transformation. Die Analyse erfolgte mit dem LSM510 (Zeiss, Jena, Deutschland) mit einem 505-530 nm Bandpass-Filter für GFP. Für die elektronenmikroskopischen Untersuchungen wurde das Blattmaterial hochdruck-gefrierfixiert, kryosubstituiert und Immunogold-markiert wie bei (Thieme et al., 2007) beschrieben. Die LSM und elektronenmikroskopischen Untersuchungen zeigten, dass Bs3::GFP im Zellkern und im Zytoplasma lokalisiert ist Abbildung 7B und C. Weiterführende Analysen, ob die Lokalisation in einem oder in den beiden Zellkompartimenten für die Ausbildung der HR notwendig sind, erfolgen im Rahmen der Doktorarbeit von Jana Piprek (J. Piprek und T. Lahaye, unveröffentlicht).

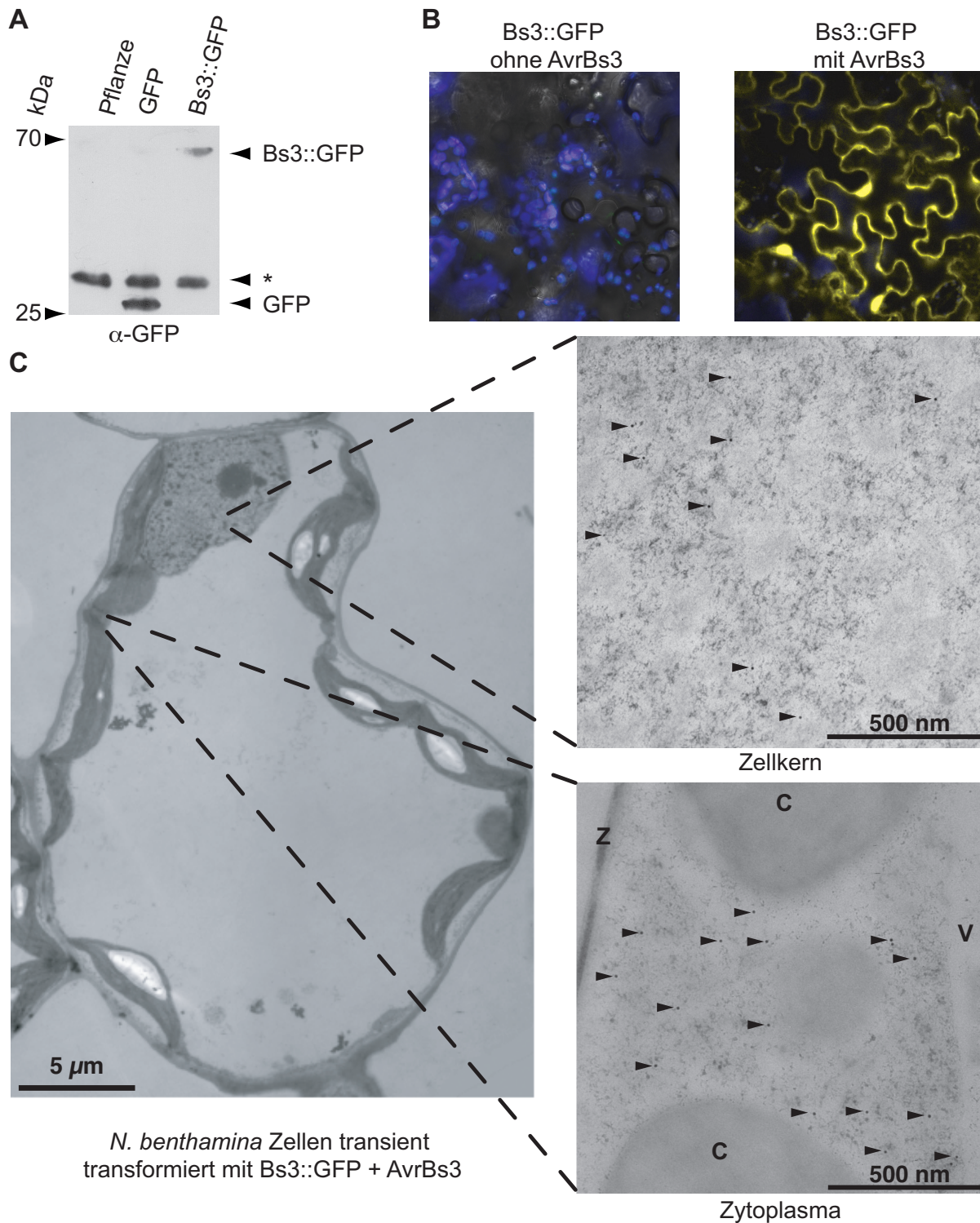


**Abbildung 7: Lokalisation von Bs3::GFP**

Für die Lokalisationsstudien von Bs3::GFP wurde der *A. tumefaciens*-Stamm GV3101 pGWB4:Bs3::GFP in Kombination mit dem Stamm GV3101 pVsF300 (35S:avrBs3) bzw. pCP60 (leerer Vektor) in *N. benthamiana* infiltriert. **A)** 40 h nach der Infiltration wurde Blattmaterial geerntet und die Gesamtproteinextrakte mittels SDS-PAGE (10%) und Westernblot unter Verwendung eines Anti-GFP-Antikörpers untersucht. Der Stern "\*" kennzeichnet eine unspezifische Hintergrundbande. **B)** 40 h nach der Infiltration wurde Blattmaterial geerntet und mikroskopisch am LSM analysiert. Dabei wurden spezifische Filter für EGFP verwendet. Die Autofluoreszenz der Chloroplasten ist blau und die GFP-Fluoreszenz von Bs3::GFP ist gelb dargestellt. **C)** Elektronenmikroskopie von Bs3::GFP in Kombination mit AvrBs3 40 h nach der Infiltration. Die Abbildung zeigt eine Übersicht und die Vergrößerung einzelner Zellkompartimente. Diese sind wie folgt gekennzeichnet C: Chloroplasten, V: Vakuole und Z: Zellwand. Die schwarzen Pfeile kennzeichnen die Immunogold-markierten Bs3::GFP Proteine. Die elektronenmikroskopischen Bilder wurden von Gerd Hause (Biozentrum Halle) angefertigt.

### 2.2.3.3 *Bs3*-Homologe aus *C. pubescens* vermitteln nicht die Erkennung von *AvrBs4*, jedoch die Erkennung von *AvrBs3Δrep16*

Das aus *C. annuum* ECW-30R isolierte *R*-Gen *Bs3* vermittelt die Erkennung des korrespondierenden Effektors *AvrBs3*. Die Erkennung von *AvrBs3* ist NLS- und AD-abhängig, da NLS- und AD-Deletionsderivate keine HR in ECW-30R Pflanzen induzieren (Van den Ackerveken et al., 1996).

Interessanterweise wird *AvrBs4*, das zu 97 % AS-identisch zu *AvrBs3* ist in der Paprika Linie *C. pubescens* PI 235047 in NLS- und AD-abhängiger Weise erkannt und induziert die HR. In der Paprika Linie *C. pubescens* PI 585270 erfolgt dagegen keine Erkennung von *AvrBs4*. Die Erkennung in *C. pubescens* PI 235047 wird offenbar nicht von einem *Bs4*-Homolog vermittelt, da diese AD- und NLS-unabhängig ist und bisher auch kein *Bs4*-Homolog aus der Paprikalinie *C. pubescens* PI 235047 isoliert werden konnte (D. Gürlebeck und U. Bonas, unveröffentlicht).

Um zu analysieren, ob die Erkennung von *AvrBs4* in *C. pubescens* PI 235047 von einem *Bs3*-Homologen in dieser Linie ausgeht, erfolgte die Amplifikation der *Bs3*-Allele aus den beiden *C. pubescens*-Linien mittels Phusion-Polymerase und den Oligonukleotiden A01-fwd und final-entry-02-rev. Die Sequenzanalyse der beiden *Bs3*-Allele aus *C. pubescens* ergab, dass sie in der kodierenden Sequenz identisch zueinander sind. Sie weisen aber 38 Polymorphismen zu der *Bs3-E*-Sequenz der Paprikalinie *C. annuum* ECW auf, die in 13 Aminosäureaustauschen resultieren (siehe Anhang Abbildung 17 und 18). Die Polymorphismen liegen jedoch alle außerhalb der konservierten Bereiche der FMOs und führen nicht zu einem frühzeitigen Stopp. Im 1023 Bp langen Promotorbereich unterscheiden sich die beiden *Bs3*-Allele aus *C. pubescens* durch eine 19-Bp Duplikation (Abbildung 8 und Anhang Abbildung 17).

Bs3-E	1	TAT	TATATAAACCTCTCT	TATTC	CACTAAACCATCCTCACAAC	TT-----
PI 235047	1	TAT	TATATAAACCTCTCT	TATTC	CACTAAACCATCCTCACAAC	CTT
PI 585270	1	TAT	TATATAAACCTCTCT	TATTC	CACTAAACCATCCTCACAAC	CTT
Bs3-E	46	-----	CAAGTTATCATCCCCTTTCTCTTTTCTCCTCTTGTTCTT			
PI 235047	61	CTT	-----	CAAGTTATCT	TCCCCTTTCTCTTTTCTCCTCTTGTTCTT	
PI 585270	61	CTT	TAAGTTATCCTCAAACCTT	CAAGTTATCT	TCCCCTTTCTCTTTTCTCCTCTTGTTCTT	
Bs3-E	82	GTCACCCGCTAAATCTATCAAAACACAAGTAGTCCTAGTTGCACATATATTTTCATGATGAA				
PI 235047	102	GTCACCC	ACTAAATCTATCAAAACACAAGTAGTCCTAGTTGCACATATATTTTCATGACGAA			
PI 585270	121	GTCACCC	ACTAAATCTATCAAAACACAAGTAGTCCTAGTTGCACATATATTTTCATGACGAA			

**Abbildung 8: Ausschnitt aus dem Sequenzvergleich der *Bs3*-Homologen von *C. pubescens* und *C. annuum***  
Dargestellt ist ein Teil der Promotoren und ein Teil der kodierenden Sequenz. Das ATG Startkodon ist blau unterlegt. Die 19-Bp Duplikation ist grün unterlegt und der Bereich, der dupliziert ist, wurde gelb markiert. Der rot gekennzeichnete Bereich stellt die  $UPT_{AvrBs3\Delta rep16}$ -Box dar.

Im Sequenzvergleich zu *Bs3-E* weisen die beiden Allele 21 Polymorphismen und drei Insertion unterschiedlicher Länge im Bereich des Promotors auf (Anhang Abbildung 17). Da vermutet

wurde, dass die 19-Bp Duplikation für den funktionalen Unterschied in der AvrBs4-Erkennung zuständig ist, wurden die Fragmente in den Vektor pGWB1 mittels LR-Rekombination transferiert. Die erhaltenen Plasmide wurden in *A. tumefaciens* GV3101 transformiert und dann erfolgte die transiente Koexpression der erhaltenen Konstrukte mit *35S:avrBs3*, *35S:avrBs4* oder *35S:avrBs3Δrep16* in *N. benthamiana*. Die Koexpression der *C. pubescens*-Allele ergab, dass die beiden Allele im transienten Assay keine HR mit *35S:avrBs4*-Konstrukten auslösen können. Aber beide Allele lösen nach der Koinfiltration mit *35S:avrBs3Δrep16* eine HR in *N. benthamiana* aus (siehe Abbildung 9). Genauere Sequenzanalysen der beiden *Bs3*-Allele aus *C. pubescens* ergaben, dass sie im Promotorbereich die gleiche  $UPT_{AvrBs3\Delta rep16}$ -Box wie *Bs3-E* enthalten (Abbildung 8). Es war deshalb zu erwarten, dass sie mit *avrBs3Δrep16* eine HR auslösen, wie in Abbildung 9 zu erkennen ist.

Die Kartierung der 19-Bp Duplikation auf eine vorhandene F<sub>2</sub>-Population (PI 235047 x PI 585270; D. Gürlebeck und U. Bonas, unveröffentlicht; siehe Anhang Tabelle 4) mit Hilfe des Marker „PR-Bs3“ (siehe 2.4) ergab, dass das *Bs3*-Homolog aus *C. pubescens* nicht mit der AvrBs4-induzierten HR gekoppelt ist, so dass man davon ausgehen kann, dass die *Bs3*-Homologen aus *C. pubescens* nicht für die AvrBs4-vermittelte Erkennung verantwortlich sind.

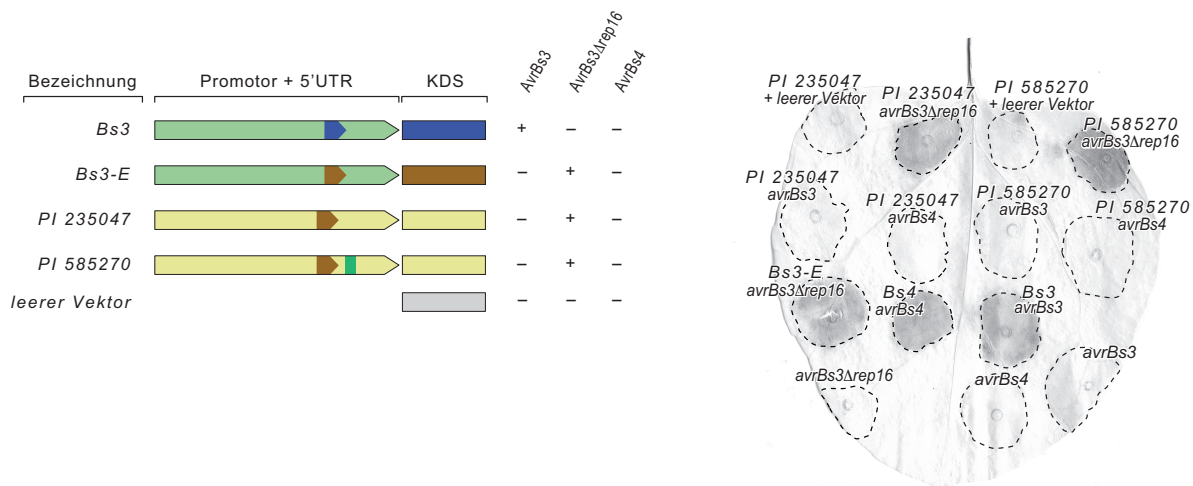


**Abbildung 9: Die *Bs3*-Allele aus *C. pubescens* vermitteln Erkennung von AvrBs3Δrep16**

Graphische Darstellung der verwendeten Konstrukte. Die grünen und gelben Pfeile symbolisieren die Promotoren der amplifizierten Gene mit den darin enthaltenen  $UPT_{AvrBs3}$ - und  $UPT_{AvrBs3\Delta rep16}$ -Boxen (blauer und braune Pfeile). Das grüne Rechteck im gelben Pfeil soll die 19-Bp Duplikation darstellen und das blaue, braune bzw. gelbe Rechteck steht für die kodierende Sequenz (KDS) der einzelnen *Bs3*-Allele. Ein „+“ gibt an, dass nach der Koexpression der Konstrukte eine HR ausgebildet wurde und ein „-“ zeigt an, dass keine HR nach der Koexpression der entsprechenden Konstrukte ausgebildet wurde. Die *Bs3*-Allele wurden in Kombination mit den T-DNAs, welche für ein *35S:avrBs3*-, ein *35S:avrBs3Δrep16*- oder ein *35S:avrBs4*-Gen kodieren transient mittels *Agrobacterium tumefaciens* GV3101 exprimiert. Die infiltrierten Bereiche sind mit gestrichelten Linien markiert. Vier Tage nach der Infiltration wurden die Blätter mit Ethanol entfärbt, um die HR (dunkle Bereiche) besser sichtbar zu machen. Anhand der Abbildung kann man erkennen, dass die beiden *C. pubescens*-Allele nur in Kombination mit AvrBs3Δrep16 eine HR in *N. benthamiana* auslösen.

#### 2.2.4 Zusammenfassung der Ergebnisse

Das *R*-Gen *Bs3* aus Paprika (*Capsicum annuum* ECW-30R) vermittelt die Erkennung von Stämmen des Pflanzenpathogens *Xcv*, die das korrespondierende Effektorprotein AvrBs3 translozieren. *Bs3* wurde über transiente-, *Agrobacterium*-vermittelte Komplementation mit Subfragmenten, eines den *Bs3*-Lokus überspannenden BAC-Klons, identifiziert. Das komplementierende BAC-Subfragment kodiert für ein 342 AS langes Protein, welches Homologien zu Flavin-abhängigen Monooxygenasen (FMOs) aufweist. Sequenzvergleiche zeigten, dass *Bs3* die höchste Homologie zu der FMO-Unterfamilie der *Arabidopsis* YUCCA-Proteine aufweist. Sequenzvergleiche der *Bs3*-Allele aus *C. annuum* ECW-30R (*Bs3*) und ECW (*Bs3-E*) ergaben, dass sie sich durch eine 13-Bp Insertion im Promotor und durch zwei Polymorphismen in der kodierenden Sequenz unterscheiden. Um zu klären, welcher Polymorphismus die unterschiedliche Erkennungsspezifität determiniert, wurde der *Bs3*-Promotor vor die kodierende Sequenz des *Bs3-E*-Gens und reziprok der *Bs3-E*-Promotor vor die kodierende Sequenz des *Bs3*-Gens kloniert. Transiente *Agrobacterium*-vermittelte Expression der chimären Gene zusammen mit AvrBs3 bzw. AvrBs3 $\Delta$ rep16 zeigten, dass die Unterschiede im Promotor die Erkennungsspezifität determinieren. Durch den Sequenzvergleich der Promotoren von *Bs3*, *Bs3-E* und den ebenfalls durch AvrBs3-induzierten Wirtsgenen *UPA10* und *UPA20* (Kay et al., 2007) konnte die *UPT*<sub>AvrBs3</sub>-Box (*upregulated by TALes*) mit dem Konsensus TATATAAACCN<sub>2-3</sub>CC definiert werden. Die Unterbrechung dieses Elements durch die 13-Bp Insertion im *Bs3-E*-Promotor resultiert in einem Verlust der Induzierbarkeit durch AvrBs3 und bedingt gleichzeitig spezifische Induzierbarkeit durch das AvrBs3-Deletionsderivat AvrBs3 $\Delta$ rep16. Mittels Chromatin-Immunopräzipitation konnte nachgewiesen werden, dass AvrBs3 in *planta* präferentiell an den *Bs3*-Promotor bindet (S. Hahn in Römer et al., 2007). In EMSA (*E*lectrophoretic *M*obility *S*hift *A*ssay)-Studien konnte gezeigt werden, dass AvrBs3 *in vitro* eine hohe Affinität zur *UPT*<sub>AvrBs3</sub>-Box des *Bs3*-Promotors aufweist, jedoch eine vergleichsweise geringe Affinität zur *UPT*<sub>AvrBs3 $\Delta$ rep16</sub>-Box des *Bs3-E*-Promotors hat (S. Hahn in Römer et al., 2007). Weiterhin wurde gezeigt, dass *Bs3* und *Bs3-E* nur durch ihre korrespondierenden TAL-Effektoren, aber nicht durch andere sequenzähnliche TAL-Effektoren oder im Verlauf der Bs1- oder Bs2-vermittelten Resistenzreaktionen induziert werden. Lokalisationsstudien zeigten, dass ein funktionales Bs3::GFP Fusionsprotein im Zellkern und Zytoplasma detektierbar ist. Analysen der Bs3-vermittelten Resistenzreaktion mittels Virus-induziertem Gen-*Silencings* zeigten, dass SGT1 eine essentielle Komponente der Bs3-vermittelten HR ist.



## 2.3 Mutationsbasierte Analyse des *Bs3*- und des *Bs3-E*-Promotors

### 2.3.1 Publikation 2

# Recognition of AvrBs3-Like Proteins Is Mediated by Specific Binding to Promoters of Matching Pepper *Bs3* Alleles<sup>1[W]</sup>

Patrick Römer, Tina Strauss, Simone Hahn, Heidi Scholze, Robert Morbitzer, Jan Grau, Ulla Bonas, and Thomas Lahaye\*

Institute of Biology, Department of Genetics (P.R., T.S., S.H., H.S., R.M., U.B., T.L.), and Institute of Informatics (J.G.), Martin Luther University Halle-Wittenberg, 06120 Halle (Saale), Germany

The pepper (*Capsicum annuum*) bacterial spot (*Bs*) resistance gene *Bs3* and its allelic variant *Bs3-E* mediate recognition of the *Xanthomonas campestris* pv *vesicatoria* type III effector protein AvrBs3 and its deletion derivative AvrBs3Δrep16. Recognition specificity resides in the *Bs3* and *Bs3-E* promoters and is determined by a defined promoter region, the *UPA* (for up-regulated by AvrBs3) box. Using site-directed mutagenesis, we defined the exact boundaries of the *UPA*<sub>AvrBs3</sub> box of the *Bs3* promoter and the *UPA*<sub>AvrBs3Δrep16</sub> box of the *Bs3-E* promoter and show that both boxes overlap by at least 11 nucleotides. Despite partial sequence identity, the *UPA*<sub>AvrBs3</sub> box and the *UPA*<sub>AvrBs3Δrep16</sub> box were bound specifically by the corresponding AvrBs3 and AvrBs3Δrep16 proteins, respectively, suggesting that selective promoter binding of AvrBs3-like proteins is the basis for promoter activation specificity. We also demonstrate that the *UPA*<sub>AvrBs3</sub> box retains its functionality at different positions within the pepper *Bs3* promoter and confers AvrBs3 inducibility in a novel promoter context. Notably, the transfer of the *UPA*<sub>AvrBs3</sub> box to different promoter locations is always correlated with a new transcriptional start site. The analysis of naturally occurring *Bs3* alleles revealed many pepper accessions that encode a nonfunctional *Bs3* variant. These accessions showed no apparent abnormalities, supporting the supposition that *Bs3* functions only in disease resistance and not in other developmental or physiological processes.

Plant pathogenic microbes deliver a cocktail of effector proteins into the host cytoplasm that collectively promote microbial growth (Kamoun, 2006; Block et al., 2008; Göhre and Robatzek, 2008; Cunnac et al., 2009; Hogenhout et al., 2009). Many effector proteins were first termed avirulence (Avr) proteins because their presence evoked a hypersensitive response (HR) in plants expressing a matching resistance (*R*) gene (Grant et al., 2006; Bent and Mackey, 2007). Although the appearance of an HR often correlates with disease resistance, its causal role in plant immunity has not been fully elucidated (Greenberg and Yao, 2004). Avr proteins were identified initially as activators of the plant immune reaction, but many were later found to contribute to pathogen virulence on host plants that lack a corresponding *R* gene (Jones and Dangl, 2006). Meanwhile, the in planta function of a number of effectors has been studied at the molec-

ular level, and some seem to function as enzymes (Mudgett, 2005; Abramovitch et al., 2006; Chisholm et al., 2006). Yet, some effectors of the bacterial genus *Xanthomonas* harbor nuclear localization signals and a transcriptional activation domain (Van den Ackerveken et al., 1996; Yang et al., 2000; Szurek et al., 2001) and have been termed transcription activator-like effector proteins (TALEs; Kay and Bonas, 2009). The prototype TALE, AvrBs3, was identified from *Xanthomonas campestris* pv *vesicatoria* (*Xcv*) based on its avirulence activity in pepper (*Capsicum annuum*; Bonas et al., 1989) and was later shown to contribute to bacterial virulence in susceptible pepper genotypes (Wichmann and Bergelson, 2004). The most characteristic structural feature of TALEs is a variable number of tandemly arranged, nearly perfect copies of a 34-amino acid motif that mediates binding of the TALE AvrBs3 to host target promoters (Kay et al., 2007).

Although TALEs are generally highly homologous to each other, their activity in plants is subject to exquisite specificity (Schornack et al., 2006). For example, the pepper *Bs3* and the tomato (*Solanum lycopersicum*) *Bs4* *R* genes mediate recognition of the 96.6% identical *Xcv* AvrBs3 and AvrBs4 proteins, respectively (Ballvora et al., 2001; Schornack et al., 2005; Römer et al., 2007). Tomato *Bs4* is expressed constitutively at low levels and encodes a nucleotide-binding Leu-rich repeat-type *R* protein (Schornack et al., 2004, 2005). By contrast, the pepper *Bs3* gene is transcriptionally induced by AvrBs3 and encodes a YUCCA-

<sup>1</sup> This work was supported by the Exzellenznetzwerk Biowissenschaften (Ministry of Culture of Saxonia-Anhalt), the 2Blades Foundation, and the Deutsche Forschungsgemeinschaft (grant nos. SFB 648, SPP 1212, and LA1338/2-2 to T.L. and grant no. SFB 648 to U.B.).

\* Corresponding author; e-mail lahaye@genetik.uni-halle.de.

The author responsible for distribution of materials integral to the findings presented in this article in accordance with the policy described in the Instructions for Authors ([www.plantphysiol.org](http://www.plantphysiol.org)) is: Thomas Lahaye (lahaye@genetik.uni-halle.de).

<sup>[W]</sup> The online version of this article contains Web-only data.

[www.plantphysiol.org/cgi/doi/10.1104/pp.109.139931](http://www.plantphysiol.org/cgi/doi/10.1104/pp.109.139931)

Römer et al.

like flavin monooxygenase (Römer et al., 2007). Thus, *Bs3*- and *Bs4*-mediated recognition are mechanistically distinct despite the fact that they mediate recognition of almost identical effector proteins.

Previously, we showed that the pepper *Bs3* gene mediates recognition of AvrBs3 but not of its deletion derivative AvrBs3Δrep16, which lacks repeat units 11 to 14 (Herbers et al., 1992). Reciprocally, the *Bs3-E* allele mediates recognition of AvrBs3Δrep16 but not of AvrBs3. Recent studies demonstrated that AvrBs3 and AvrBs3Δrep16 specifically activate the matching *Bs3* and *Bs3-E* promoters, respectively (Römer et al., 2007). The *Bs3-E* gene is an allele of *Bs3* that carries a 13-bp insertion in its promoter compared with *Bs3*. Comparison of the *Bs3* and other AvrBs3-inducible promoters from pepper revealed a conserved DNA element, the so-called *UPA* (for up-regulated by AvrBs3) box (Kay et al., 2007; Römer et al., 2007). Notably, the *Bs3-E*-specific 13-bp insertion is located within the *UPA* box of the *Bs3* promoter. Electrophoretic mobility shift assays (EMSA) showed that AvrBs3 has a higher affinity to the *Bs3* promoter as compared with the *Bs3-E* promoter. Yet, in EMSA, AvrBs3Δrep16 also had a higher affinity for the *Bs3* promoter than for the *Bs3-E* promoter. Thus, it seemed that promoter binding of AvrBs3 or AvrBs3Δrep16 is not the basis for promoter activation specificity (Römer et al., 2007).

In order to gain further insight into the molecular basis of TALE specificity and *Bs3*-mediated resistance, we have now carried out site-directed mutagenesis to define the exact boundaries of the *UPA* boxes of the *Bs3* promoter (herein designated *UPA*<sub>AvrBs3</sub> box) and the *Bs3-E* promoter (herein designated *UPA*<sub>AvrBs3Δrep16</sub> box). We present new EMSA results that demonstrate that promoter binding is indeed the basis for promoter activation specificity by TALEs. Finally, the analysis of a collection of naturally occurring *Bs3* alleles revealed that pepper accessions encoding nonfunctional *Bs3* variants are phenotypically normal. These data support the role of *Bs3* exclusively in disease resistance.

## RESULTS

### Mapping the Promoter Sequences Used for Activation by AvrBs3 and AvrBs3Δrep16

Previously, we showed that transcript abundance of the pepper *Bs3* resistance gene is increased 24 h post infection with *Xcv* strains that deliver AvrBs3 (Römer et al., 2007). We have now carried out semiquantitative reverse transcription (RT)-PCR to monitor *Bs3* transcript accumulation on *Xcv*-infected leaves in a time-course experiment. As shown in Figure 1A, *Bs3* transcript was detectable as early as 6 h post infection and peaks at 18 h post infection. Expression of *Bs3* and *Bs3-E* was also studied in uninfected leaf, flower, fruit, and root tissue. However, we were unable to detect *Bs3* or *Bs3-E* transcript in uninfected plant tissue (Fig. 1B).

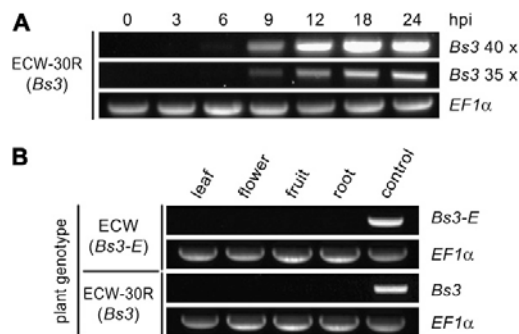


**Figure 1.** Analysis of *Bs3* and *Bs3-E* transcript abundance. Transcript abundance was determined by semiquantitative RT-PCR. The constitutively expressed gene elongation factor 1 $\alpha$  (*EF1 $\alpha$* ) served as a normalization control. **A**, An increase of *Bs3* transcript abundance was detectable 6 h post infection (hpi) with *Xcv* strain 85-10 expressing *avrBs3*. Leaves of 5- to 6-week-old plants of pepper cv ECW-30R (*Bs3* genotype) were inoculated with *Xcv* (OD<sub>600</sub> = 0.4) via blunt syringe. Inoculated leaf tissue was harvested at 0, 3, 6, 9, 12, 18, and 24 h post infection, and RNA was extracted and reverse transcribed into cDNA. To determine the earliest time point at which *Bs3* transcript was detectable, 35 and 40 PCR cycles were carried out. **B**, *Bs3* and *Bs3-E* transcripts were detectable only after infection with *Xcv* strains expressing the matching Avr protein. Tissue-specific analysis of *Bs3* and *Bs3-E* transcripts was performed on cDNA from uninfected leaf, flower, fruit, and root tissue of pepper ECW-30R (*Bs3*) and ECW (*Bs3-E*). As a positive control for RT-PCR, we used cDNA derived from ECW-30R and ECW leaves that were inoculated with *avrBs3*- and *avrBs3Δrep16*-expressing *Xcv* strains (OD<sub>600</sub> = 0.4), respectively.

To define the minimal *Bs3* and *Bs3-E* promoter regions, we generated progressive 5' deletions and fused these to the *Bs3* and *Bs3-E* coding sequences (cds). Functionality and specificity of corresponding T-DNA constructs were tested in leaves of *Nicotiana benthamiana* by *Agrobacterium tumefaciens*-mediated codelivery of a cauliflower mosaic virus 35S (35S) promoter-driven *avrBs3* (35S:*avrBs3*) or *avrBs3Δrep16* (35S:*avrBs3Δrep16*) gene, respectively (Fig. 2). Functional *Bs3* and *Bs3-E* promoter deletion derivatives were expected to be transcriptionally induced by AvrBs3 and AvrBs3Δrep16, respectively, resulting in the expression of the *Bs3* and *Bs3-E* proteins and triggering an HR.

Data observed with overexpression of bacterial effectors in a heterologous system generally need to be treated with caution. Yet, we have previously demonstrated that *Bs3*-mediated recognition specificity is unaffected even if highly related TALEs are expressed to high levels in a heterologous system (Schornack et al., 2005; Römer et al., 2007). Furthermore, our assay reflects the natural situation where activation of the *Bs3* promoter results in the HR (Römer et al., 2007).

Using *A. tumefaciens*-mediated delivery, it was found that *Bs3* promoter fragments containing 1,023, 343, or 166 bp upstream of the ATG start codon triggered the HR in combination with 35S:*avrBs3* but

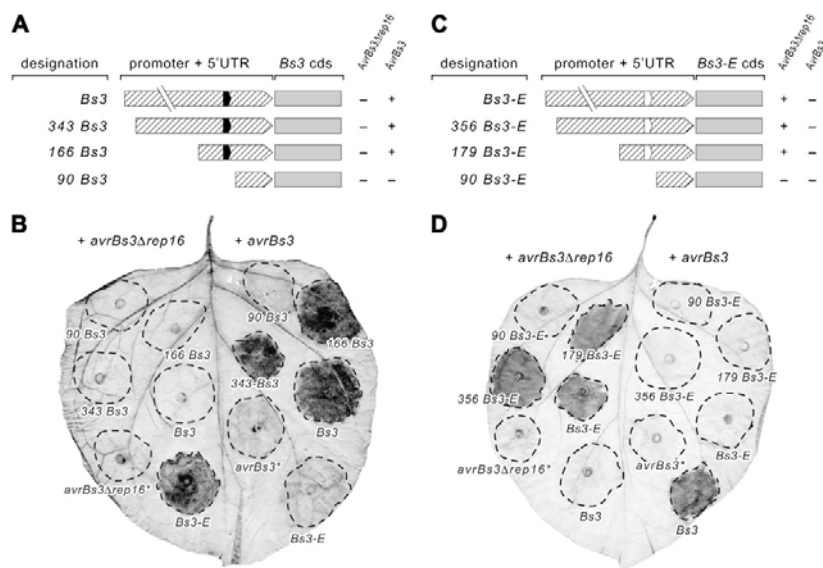


**Figure 2.** The UPA boxes of the *Bs3* and *Bs3-E* promoters are crucial to their inducibility by the matching AvrBs3 and AvrBs3 $\Delta$ rep16 proteins. To define the minimal *Bs3* and *Bs3-E* promoters, progressive 5' deletions of the *Bs3* promoter (343 *Bs3*, 166 *Bs3*, and 90 *Bs3*; A and B) and the *Bs3-E* promoter (356 *Bs3-E*, 179 *Bs3-E*, and 90 *Bs3-E*; C and D) were fused to the *Bs3* and *Bs3-E* cds, respectively. The *Bs3* and *Bs3-E* promoter constructs were delivered as denoted into *N. benthamiana* leaves via *A. tumefaciens* ( $OD_{600} = 0.8$ ) together with constructs containing the 35S promoter-driven *avrBs3 $\Delta$ rep16* (left side of the leaf; + *avrBs3 $\Delta$ rep16*) or *avrBs3* (right side of the leaf; + *avrBs3*) genes (B and D). In addition, *avrBs3* and *avrBs3 $\Delta$ rep16* were expressed individually in the absence of a *Bs3* or a *Bs3-E* promoter construct (*avrBs3\** or *avrBs3 $\Delta$ rep16\**). Dashed lines mark inoculated areas. Four days post infiltration (dpi), leaves were harvested and cleared with ethanol to visualize the HR (dark areas in B and D). Schemes in A and C show the length of the *Bs3* promoter (A) and the *Bs3-E* promoter (C) deletions examined. Promoter deletion constructs are designated according to the length of the respective promoter fragment with respect to the ATG start codon and are displayed to scale. The total length of promoter regions and the 5' UTR of *Bs3* and *Bs3-E* are 1,023 and 1,036 bp, respectively. All similarly sized *Bs3* and *Bs3-E* promoters are identical in their 5' and 3' ends but differ in size due to the presence of a 13-bp insertion/deletion polymorphism that is present in the *Bs3-E* promoter and absent from the *Bs3* promoter. Hatched boxes represent the promoter and the 5' UTR of the genes. Small white and black boxes represent the UPA boxes from the *Bs3* ( $UPA_{AvrBs3}$ ) and *Bs3-E* ( $UPA_{AvrBs3\Delta rep16}$ ) promoters, respectively. Note that the *Bs3* and *Bs3-E* promoters differ only within these UPA boxes but are otherwise identical and therefore are displayed in identical color. Gray boxes represent the cds of the *Bs3* and *Bs3-E* genes. + and - indicate the presence and absence of an HR in *N. benthamiana* (A and C).

not with 35S:*avrBs3 $\Delta$ rep16* (Fig. 2B). By contrast, a 90-bp *Bs3* promoter fragment, which lacks the previously predicted  $UPA_{AvrBs3}$  box (TATATAAACCN<sub>2-3</sub>CC; Kay et al., 2007), was not able to trigger the HR in *N. benthamiana* when codelivered with the 35S:*avrBs3* construct. In addition, we tested a set of equivalent *Bs3-E* promoter deletion derivatives (Fig. 2C; note that similarly sized *Bs3* and *Bs3-E* promoter deletions are identical at their 5' and 3' termini but differ in size due to a 13-bp insertion/deletion polymorphism). As observed with the *Bs3* promoter deletion derivatives, a *Bs3-E* promoter deletion that contains only 90 bp upstream of the ATG start codon (Fig. 2D; construct 90 *Bs3-E*) did not trigger HR when codelivered with a 35S:*avrBs3 $\Delta$ rep16* construct. The exact location of the  $UPA_{AvrBs3\Delta rep16}$  box of the *Bs3-E* promoter has not been defined; however, it likely will include the 13-bp insertion/deletion polymorphism present in the *Bs3-E* promoter and absent from the *Bs3* promoter, because

this is the only difference between the two promoters. Consistent with this region playing a role in activation is the result that the uninducible promoter derivatives 90 *Bs3* and 90 *Bs3-E* do not contain the regions that are polymorphic between *Bs3* and *Bs3-E*.

To determine if other sequences, apart from the predicted  $UPA_{AvrBs3}$  box, are crucial to AvrBs3-mediated transcriptional activation, we generated a set of *Bs3* promoter mutants carrying different deletions between the ATG start codon and the  $UPA_{AvrBs3}$  box (Fig. 3A). The *Bs3* promoter deletions were fused in front of the *Bs3* cds and were delivered into *N. benthamiana* leaves via *A. tumefaciens* T-DNA transfer together with a 35S:*avrBs3* gene (Fig. 3B). A *Bs3* promoter deletion derivative that lacks a 44-bp region 3' of the  $UPA_{AvrBs3}$  box (*Bs3 $\Delta$ 56-99*; Fig. 3A) was still capable of triggering an AvrBs3-dependent HR. By contrast, *Bs3* promoter mutants with deletions larger than 59 bp were not functional. These data suggest that

Römer et al.

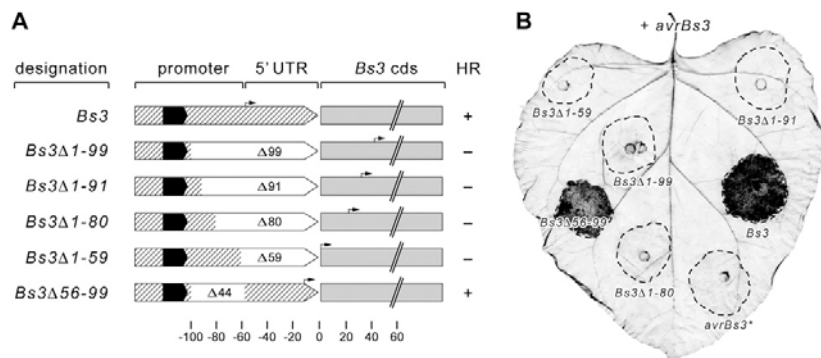


**Figure 3.** Extended *Bs3* promoter deletions 3' of the  $UPA_{AvrBs3}$  box suppress the AvrBs3-triggered and *Bs3*-mediated HR. To analyze if sequences apart from the  $UPA_{AvrBs3}$  box are needed for AvrBs3-mediated activation of the *Bs3* promoter, regions between the  $UPA_{AvrBs3}$  box and the ATG start codon were deleted. A, Graphical display of *Bs3* promoter deletion constructs. The designation of the deletions refers to the first and last deleted bp in the given promoter starting from the first bp 5' of the ATG start codon. Deletions are displayed as white boxes, and their size is indicated in bp (triangles). The *Bs3* promoter region, the  $UPA_{AvrBs3}$  box, and the *Bs3* cds are displayed as hatched, black, and gray boxes, respectively. The indicated 5' UTR refers to the *Bs3* wild-type gene. Arrows above the boxes mark the TSS of the given promoter. The scale at the bottom indicates the distances with respect to the ATG start codon. With the exception of the *Bs3* cds, all elements are drawn to scale. All deletions were fused individually in front of the *Bs3* cds. + and – indicate the presence and absence of an HR in *N. benthamiana* for each construct when being codelivered with a *35S:avrBs3* T-DNA. The sequences, deletions, and TSS of all promoters are also provided as Supplemental Data Set S1. B, Functional analysis of *Bs3* promoter deletion constructs. Individual deletion constructs were delivered together with *35S:avrBs3* via *A. tumefaciens* ( $OD_{600} = 0.8$ ) into *N. benthamiana* leaves. Dashed lines mark the inoculated areas. The leaves were harvested at 4 dpi and cleared with ethanol to visualize the HR (dark areas).

a minimum distance between the  $UPA_{AvrBs3}$  box and the ATG start codon is needed in order to generate a transcript that encodes a functional Bs3 protein. We carried out RACE to determine the transcriptional start site (TSS) of all constructs. As anticipated, most constructs that did not mediate an AvrBs3-dependent HR produced transcripts that lack the ATG start codon of the *Bs3* cds (constructs *Bs3Δ1-99*, *Bs3Δ1-91*, and *Bs3Δ1-80*; Fig. 3A; Supplemental Data Set S1). Construct *Bs3Δ1-59*, which also does not mediate an AvrBs3-dependent HR, produces a transcript that starts with the ATG start codon of the *Bs3* cds but that contains no 5' untranslated region (UTR). It seems likely that the absence of an HR with construct *Bs3Δ1-59* is due to the lack of a 5' UTR. Therefore, an essential aspect in the analysis of  $UPA$  box-containing promoters is to consider a spacing between the  $UPA$  box and the start of transcription.

While a deletion analysis is capable of coarse characterization of regulatory regions in a promoter, linker-scanning mutagenesis permits a higher resolution identification of short, defined sequence motifs and their effect on promoter activity (McKnight and Kingsbury, 1982). We analyzed a set of 12 linker-scanning *Bs3* promoter mutants. Each mutant contained a 15-bp insertion located between positions +31 and –191 relative to the TSS (Fig. 4, A and B; Supplemental Data Set S2). The *Bs3* promoter mutants were fused to the *Bs3* cds and were delivered via *A. tumefaciens* T-DNA transfer together with the *35S:avrBs3* construct into *N. benthamiana* leaves (Fig. 4C)

to test for HR induction. Two of the 12 mutants (T–46 and T–55) no longer triggered an HR. The insertions that affected *Bs3* promoter function are within (T–55) or adjacent to (T–46) the previously defined  $UPA_{AvrBs3}$  box (Fig. 4B) that spans a region from –47 to –61 bp. Given that the T–46 insertion is located adjacent to but not within the previously predicted  $UPA_{AvrBs3}$  box, the functionally relevant nucleotides of the box likely extend farther into the 3' region of the promoter. Given that all insertions that affected *Bs3* promoter function were located at or in the  $UPA_{AvrBs3}$  box, it seems likely that this is the only sequence motif that is crucial to AvrBs3-mediated promoter activation.

#### Recognition Specificity of the *Bs3-E* Promoter

The *Bs3* and *Bs3-E* promoters differ only by a 13-bp insertion (CTCTATTCCACTA) in *Bs3-E* compared with *Bs3* (Römer et al., 2007). Although it is conceivable that this polymorphic area defines recognition specificity, the particular sequences that contribute to specificity in the *Bs3-E* promoter remained unclear. We hypothesized that the 13-bp insertion in the *Bs3-E* promoter contains the complete  $UPA_{AvrBs3\Delta rep16}$  box of the *Bs3-E* promoter. Here, we tested this hypothesis by placing the 13-bp insertion of the *Bs3-E* promoter into two different locations of the *Bs3* promoter and fused the *Bs3* promoter derivatives (*Bs3 –20i* and *Bs3 +31i*) in front of the *Bs3* cds (Fig. 5A). We anticipated that *Bs3 –20i* and *Bs3 +31i* would be activated by both AvrBs3 and AvrBs3 $\Delta rep16$ . However, our data dem-

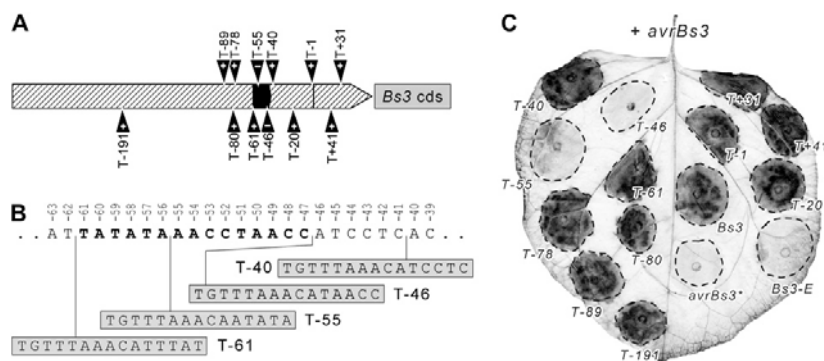


**Figure 4.** Linker-scanning mutagenesis of the *Bs3* promoter region identifies the  $UPA_{AvrBs3}$  box as a functionally crucial element. A, Distribution of transposon footprints in the *Bs3* promoter. To identify sequences that are crucial for AvrBs3-mediated transcriptional activation of the *Bs3* promoter, linker-scanning mutagenesis was carried out. Twelve transposon footprint mutants (T; black triangles above or below the hatched box) were obtained, containing a 15-bp insertion. Numbering of the mutants refers to the nucleotide that is adjacent to the 3' end of the respective transposon footprint with respect to the TSS. The *Bs3* promoter region and the 5' UTR are displayed as hatched areas. The transcriptional start site of the wild-type *Bs3* gene is indicated with a black horizontal line. The  $UPA_{AvrBs3}$  box and the *Bs3* cds are displayed as black and gray boxes, respectively. + and – indicate the presence and absence of an HR with each promoter construct in *N. benthamiana* leaves when codelivered with a *35S:avrBs3* T-DNA (+ *avrBs3*). *avrBs3\** denotes a tissue patch in which no *Bs3* promoter construct but only a *35S:avrBs3* T-DNA was delivered. The 5' UTR in the *Bs3* wild-type promoter is 59 bp in size, and thus insertions T + 31 and T + 41 are located in the 5' UTR. B, Insertions adjacent to or within the predicted  $UPA_{AvrBs3}$  box. The numbers above the nucleotide sequence indicate the distance with respect to the TSS. Boldface letters represent the predicted  $UPA_{AvrBs3}$  box. Sequences of transposon mutants are available as Supplemental Data Set S2. C, Functional analysis of linker-scanning-derived *Bs3* promoter mutants. Each mutant was fused in front of the *Bs3* cds and was delivered together with *35S:avrBs3* into *N. benthamiana* leaves via *A. tumefaciens* (OD<sub>600</sub> = 0.8). Dashed lines mark the inoculated areas. Leaves were harvested at 4 dpi and cleared with ethanol to visualize the HR (dark areas).

onstrated that only *35S:avrBs3* triggered the HR in combination with *Bs3* –20i and *Bs3* +31i, whereas *35S:avrBs3Δrep16* failed to trigger the HR with these promoter derivatives (Fig. 5B). Based on these data, it appears that the 13-bp insertion represents a part of, but not the complete,  $UPA_{AvrBs3Δrep16}$  box.

To further define the recognition specificity of the *Bs3-E* promoter, we placed insertions of one, two, or three nucleotides into the *Bs3* promoter instead of the 13-bp sequence (Fig. 6A). The *Bs3* promoter insertion mutants were fused to the *Bs3* cds and delivered via *A. tumefaciens* together with *35S:avrBs3Δrep16* or *35S:avrBs3* into *N. benthamiana* leaves. We found that only the insertions *Bs3*+CT, *Bs3*+CTA, and *Bs3*+CTC triggered the HR in combination with AvrBs3Δrep16 (Fig. 6). By contrast, all other insertions of one, two, and three nucleotides did not result in an AvrBs3Δrep16-responsive promoter (Fig. 6B). We concluded that the CTC motif at the 5' end of the 13-bp insertion in the *Bs3-E* promoter is part of the  $UPA_{AvrBs3Δrep16}$  box. Given that not only a CTC but also a CTA insertion triggered the AvrBs3Δrep16-dependent HR, it seems likely that the C nucleotide at the 3' terminal end can be functionally replaced by an A nucleotide. Since the *Bs3*+CT insertion is followed by an A nucleotide, this promoter mutant also contains a CTA motif at the 5' end of the insertion site. This probably explains why *Bs3*+CT is functionally identical to the *Bs3*+CTA construct.

#### Systematic Substitution Mutagenesis of the *Bs3* Promoter

Previously, the sequence of the  $UPA_{AvrBs3}$  box was determined to be TATATAAACCN<sub>2,3</sub>CC by comparing three different AvrBs3-inducible promoters (Kay et al., 2007; Römer et al., 2007). However, in this study, we found that the *Bs3* promoter mutant T–46, which contains an insertion adjacent to the 3' end of the predicted  $UPA_{AvrBs3}$  box, was no longer capable of triggering an AvrBs3-dependent HR (Fig. 4). This suggested that the  $UPA_{AvrBs3}$  box extends farther into the 3' direction than previously assumed. To determine the functionally relevant nucleotides of the  $UPA_{AvrBs3}$  box more precisely, we performed a systematic substitution mutagenesis of the *Bs3* promoter to permute each base from position –41 to –63 (Fig. 7A). The resulting 69 *Bs3* promoter substitution mutants were fused in front of the *Bs3* cds and were delivered via *A. tumefaciens* together with *35S:avrBs3Δrep16* or *35S:avrBs3* into *N. benthamiana* leaves. We identified three functionally distinct classes of substitution mutants. Forty-two substitution mutants were functionally identical to the *Bs3* wild-type promoter and triggered an HR in combination with *35S:avrBs3* but not in combination with *35S:avrBs3Δrep16* (Fig. 7B, light green boxes). Twenty substitution mutants produced no HR in combination with either *35S:avrBs3* or *35S:avrBs3Δrep16* (Fig. 7B, red boxes). The remaining

Römer et al.

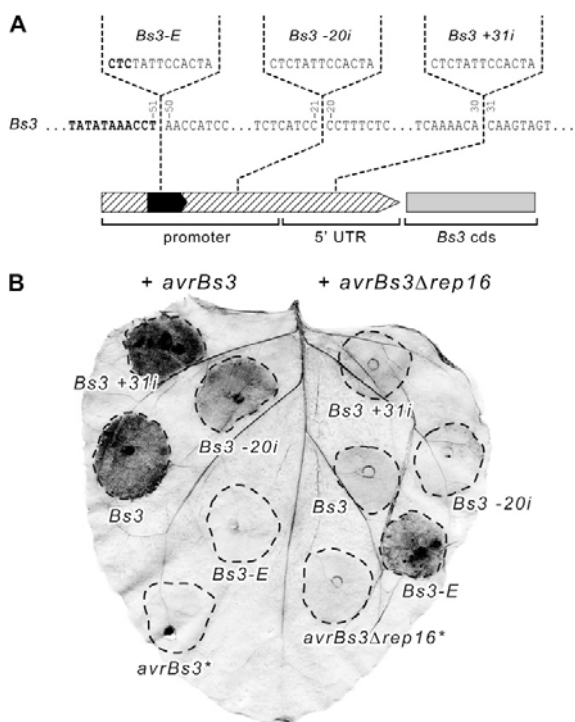


**Figure 5.** The *Bs3-E* promoter-specific 13-bp insertion exerts its function on recognition specificity in a position-dependent manner. A, The 13-bp insertion sequence (CTCTATTCCACTA) that is specific to the *Bs3-E* promoter (insertion at position  $-50$  of the *Bs3* promoter) was placed into the promoter and 5' UTR of the *Bs3* gene. Numbering of the corresponding mutant derivatives (*Bs3-20i* and *Bs3+31i*) refers to the nucleotide in the *Bs3* promoter that is adjacent to the 3' end of the 13-bp insertion. The nucleotide sequence highlighted in boldface letters represents the  $UPA_{AvrBs3\Delta rep16}$  box (see Fig. 7). The *Bs3* promoter region and the 5' UTR are displayed as a hatched box. The  $UPA_{AvrBs3}$  box and the *Bs3* cds are displayed as black and gray boxes, respectively. B, Functional analysis of the *Bs3* promoter derivatives *Bs3-20i* and *Bs3+31i*. Both *Bs3* promoter derivatives were fused to the *Bs3* cds and were codelivered with 35S promoter-driven *avrBs3* (+ *avrBs3*) or *avrBs3\Delta rep16* (+ *avrBs3\Delta rep16*) genes into *N. benthamiana* leaves via *A. tumefaciens* (OD<sub>600</sub> = 0.8). Leaf areas in which only a 35S:*avrBs3* or a 35S:*avrBs3\Delta rep16* T-DNA was delivered are marked as *avrBs3\** or *avrBs3\Delta rep16\**, respectively. Dashed lines mark the inoculated areas. Leaves were harvested at 4 dpi and cleared with ethanol to visualize the HR (dark areas).

seven substitution mutants showed a reduced HR phenotype (Fig. 7B, boxes with red and light green triangles). This reduced HR phenotype was observed in multiple repetitions and thus is highly reproducible. Inspection of the *Bs3* promoter substitution mutants revealed that functionally relevant nucleotides of the  $UPA_{AvrBs3}$  box span the region from  $-61$  to  $-44$ . Thus, the experimentally defined  $UPA_{AvrBs3}$  box (TATA-TAAACCTAACCATC) extends three nucleotides farther in the 3' direction as compared with the  $UPA_{AvrBs3}$

box described previously (TATATAAACCN<sub>2-3</sub>CC; Fig. 7; Kay et al., 2007). Based on the experimentally defined  $UPA_{AvrBs3}$  box, the *Bs3* promoter mutant T $-46$  (Fig. 4B) contains an insertion within and not adjacent to the  $UPA_{AvrBs3}$  box and explains why this insertion mutant is incapable of triggering the AvrBs3-dependent HR (Fig. 4C). Another notable observation of our systematic mutagenesis is that the functional consequences of substitutions in the  $UPA_{AvrBs3}$  box differ depending on which position is mutated. For example, any mutation at position  $-61$ ,  $-57$ , or  $-47$  abolished the AvrBs3-mediated HR (Fig. 7B). By contrast, none of the substitutions at positions  $-59$ ,  $-50$ ,  $-49$ ,  $-46$ , and  $-45$  had a detectable effect on the AvrBs3-mediated HR.

#### Substitution Mutagenesis of the *Bs3-E* Promoter

To analyze the  $UPA_{AvrBs3\Delta rep16}$  box, we carried out substitution mutagenesis of selected positions within the *Bs3-E* promoter (Fig. 7C). The observation that *Bs3* promoter mutants containing a 3-bp CTC insertion triggered an HR in combination with AvrBs3 $\Delta rep16$  (Fig. 6) suggests that this sequence motif defines the 3' end of the  $UPA_{AvrBs3\Delta rep16}$  box. In agreement with this hypothesis, we identified *Bs3-E* promoter substitution mutants in the CTC motif (positions  $-63$  to  $-61$ ) that do not mediate the HR in combination with AvrBs3 $\Delta rep16$  (Fig. 7C). All *Bs3-E* promoter mutants that contained substitutions located in the 3' direction of position  $-61$  were functionally identical to the *Bs3-E* wild-type promoter. By contrast, many *Bs3-E* promoter mutants that contained substitutions located in the 5' direction of the CTC motif lost the capability to mediate an AvrBs3 $\Delta rep16$ -triggered HR (Fig. 7C). Taken together, our data define the  $UPA_{AvrBs3\Delta rep16}$  box region as extending from position  $-74$  to position  $-61$  (TATATAAACCTCTC; Fig. 7C). Although it remains to be clarified if the  $UPA_{AvrBs3\Delta rep16}$  box extends at its 5' end beyond position  $-74$ , it seems evident that the  $UPA_{AvrBs3}$  and the  $UPA_{AvrBs3\Delta rep16}$  boxes overlap in at least 11 nucleotides (Fig. 7C). In this context, it is notable that substitution mutations in corresponding positions in the  $UPA_{AvrBs3}$  and  $UPA_{AvrBs3\Delta rep16}$  boxes ( $-61$  [*Bs3*] versus  $-74$  [*Bs3-E*],  $-57$  [*Bs3*] versus  $-70$  [*Bs3-E*], and  $-53$  [*Bs3*] versus  $-66$  [*Bs3-E*]) have almost identical functional consequences. For example, all substitutions in position  $-57$  of the *Bs3* promoter and in position  $-70$  of the *Bs3-E* promoter resulted in nonfunctional promoters (Fig. 7, B and C). Similarly, substitutions to an A nucleotide at position  $-53$  of the *Bs3* and position  $-66$  of the *Bs3-E* promoter had no obvious functional consequences, while mutations to G or T resulted in nonfunctional *Bs3* or *Bs3-E* promoter mutants.

#### DNA-Binding Specificity of AvrBs3 and AvrBs3 $\Delta rep16$

Previously, EMSA showed that AvrBs3 binds with high affinity to the *Bs3* promoter and weakly to the

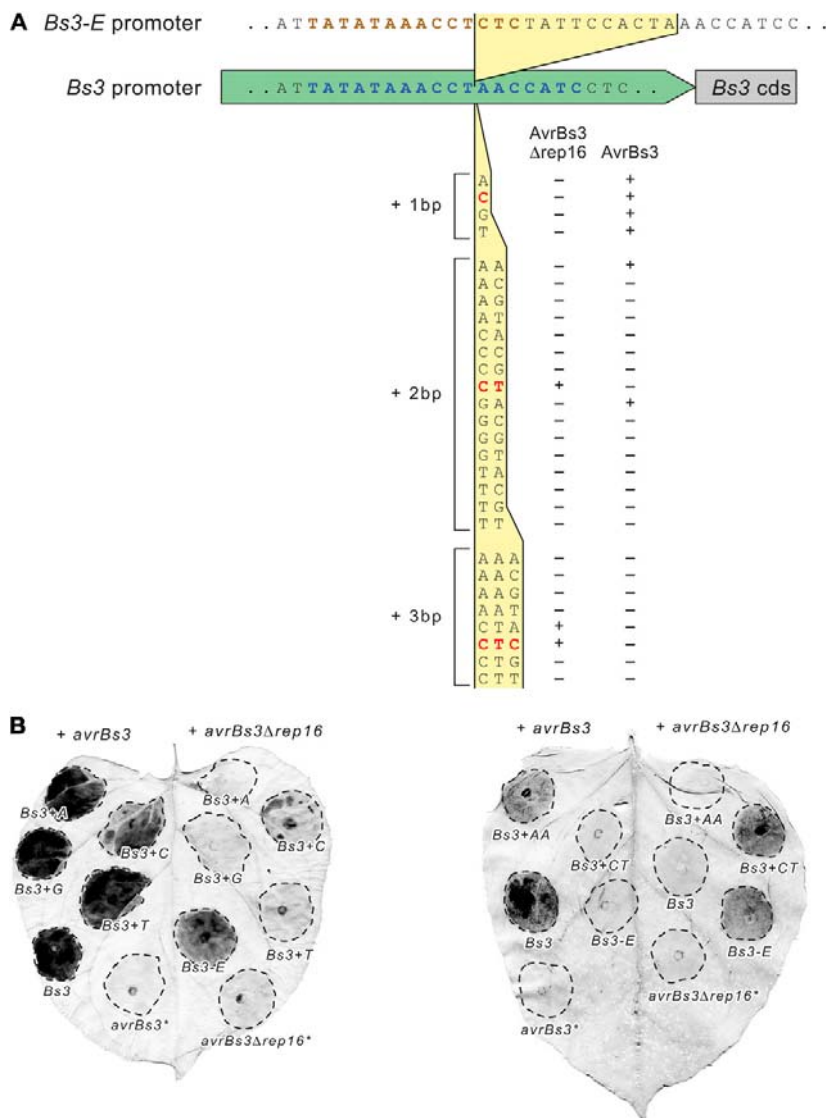


**Figure 6.** An insertion of 2 bp into the *Bs3* promoter causes a change in recognition specificity. A, Schematic representation of insertions that were placed into the *Bs3* promoter region. The 13-bp natural insertion of the *Bs3-E* promoter is displayed above the *Bs3* promoter with yellow background. Insertions were placed into the *Bs3-E* promoter at the position where the *Bs3-E* promoter contains the 13-bp insertion with respect to the *Bs3* promoter. Red letters highlight insertions corresponding to the 5' end of the 13-bp insertion in the *Bs3-E* promoter. Brown and blue letters display the predicted  $UPA_{AvrBs3}$  box of the *Bs3* promoter and the experimentally defined  $UPA_{AvrBs3\Delta rep16}$  box of the *Bs3-E* promoter, respectively (see Fig. 7). Green and gray boxes represent the *Bs3* promoter and the *Bs3* cds, respectively. + and - indicate the presence and absence of an HR in *N. benthamiana* leaves upon codelivery of each construct with a 35S promoter-driven *avrBs3* (*AvrBs3*) or *avrBs3 $\Delta$ rep16* (*AvrBs3 $\Delta$ rep16*) gene, respectively. B, Functional analysis of *Bs3* promoter insertion mutants. Representative mutants were expressed transiently in *N. benthamiana* leaves via *A. tumefaciens* ( $OD_{600} = 0.8$ ) together with T-DNA constructs containing 35S promoter-driven *avrBs3* (+ *avrBs3*) or *avrBs3 $\Delta$ rep16* (+ *avrBs3 $\Delta$ rep16*) genes. Leaf areas in which only a 35S:*avrBs3* or a 35S:*avrBs3 $\Delta$ rep16* T-DNA was delivered are marked as *avrBs3\** or *avrBs3 $\Delta$ rep16\**, respectively. Dashed lines mark the inoculated areas. Leaves were harvested at 4 dpi and cleared with ethanol to visualize the HR (dark areas).

*Bs3-E* promoter (Römer et al., 2007). Unexpectedly, EMSA showed also that *AvrBs3 $\Delta$ rep16* had a higher affinity to the *Bs3* promoter as compared with the *Bs3-E* promoter fragment (Römer et al., 2007). EMSA with *AvrBs3 $\Delta$ rep16* and *AvrBs3* was carried out with DNA probes of identical size that had identical sequence at their 3' end but not at their 5' end (Fig. 8A). Based on our data described above, it is now clear that the *Bs3-E* promoter probe did not span the complete  $UPA_{AvrBs3\Delta rep16}$  box, which likely accounts for the unexpected EMSA results (Römer et al., 2007). Therefore, we repeated the EMSA with *Bs3* and *Bs3-E* promoter-derived probes that are sequence identical at their 3' and 5' ends but that, due to the 13-bp insertion in the *Bs3-E* promoter, are not identical in size. Hence, the

new probe for the *Bs3-E* promoter is likely to contain the complete  $UPA_{AvrBs3\Delta rep16}$  box. As shown in Figure 8, *GST:AvrBs3 $\Delta$ rep16* bound with high affinity to the *Bs3-E*-derived and with low affinity to *Bs3*-derived promoter fragments (Fig. 8, B and C). Similarly, *GST:AvrBs3* binds with high and low affinity to the *Bs3*- and *Bs3-E*-derived promoter fragments, respectively. Competition assays with labeled *Bs3*-derived promoter fragments and nonlabeled *Bs3*- and *Bs3-E*-derived promoter fragments, and vice versa, further confirm that *AvrBs3* has high affinity to the *Bs3* promoter fragment and only low affinity to the *Bs3-E* promoter fragment (Fig. 8D). Competition assays for *AvrBs3 $\Delta$ rep16* showed that it binds with high affinity to the *Bs3-E* promoter fragment and with low

Römer et al.

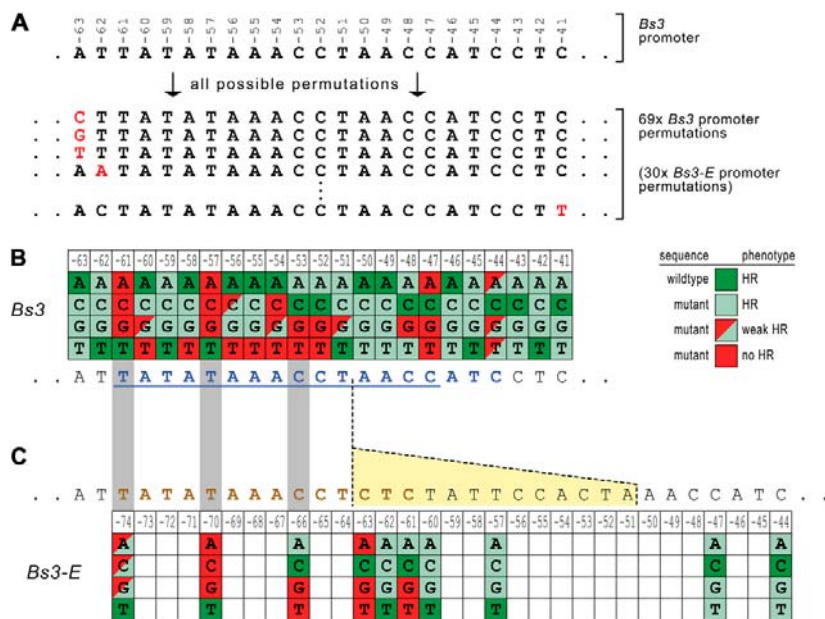


**Figure 7.** Substitution mutagenesis of the *Bs3* and *Bs3-E* promoters permits exact containment of the corresponding *UPA* boxes. A, Generation of *Bs3* and *Bs3-E* promoter substitution mutants. Individual nucleotides in the *Bs3* or *Bs3-E* promoter were replaced by all three alternative nucleotides via site-directed mutagenesis. The top sequence is part of the *Bs3* wild-type promoter. Nucleotide positions are relative to the TSS of the *Bs3* promoter. The five sequences below refer to representative substitution mutants. Mutagenized nucleotides are displayed in red letters. In total, 69 *Bs3* and 30 *Bs3-E* substitution mutants were generated. B, Functional analysis of *Bs3* promoter mutants. The 69 different *Bs3* promoter mutants and the wild-type *Bs3* promoter were fused to the *Bs3* cds and were codelivered with a 35S promoter-driven *avrBs3* construct into *N. benthamiana* leaves via *A. tumefaciens* (OD<sub>600</sub> = 0.8). The phenotypes were scored at 4 dpi. The colored boxes summarize the results of the phenotypic scoring. Nucleotide positions displayed in the top row are numbered relative to the TSS of *Bs3*. Green boxes display the wild-type *Bs3* promoter that triggers the HR. Each light green box represents a substitution mutant that triggers the HR. Substitution mutants that did not trigger the HR are displayed in red. Boxes representing substitution mutants with an intermediate phenotype (weak HR) are displayed as light green and red triangles. Please note that the collection of green boxes represents one data point (the wild-type *Bs3* promoter), while the other boxes represent the results that were observed with distinct substitution mutants. The *UPA*<sub>AvrBs3</sub> box deduced from this analysis is shown at bottom in blue letters. The underlined sequence represents the previously predicted *UPA*<sub>AvrBs3</sub> box (Kay et al., 2007). C, Functional analysis of *Bs3-E* promoter mutants. Thirty distinct *Bs3-E* promoter mutants and the wild-type *Bs3-E* promoter were fused to the *Bs3-E* cds and delivered with a 35S:*avrBs3Δrep16* construct into *N. benthamiana* leaves via *A. tumefaciens* (OD<sub>600</sub> = 0.8). The phenotypes were scored at 4 dpi. Color coding is as in B, with the difference that green boxes represent the *Bs3-E* promoter. Nucleotide positions that are displayed in the top row of boxes are relative to the TSS of *Bs3-E*. The deduced minimal *UPA*<sub>AvrBs3Δrep16</sub> box of *Bs3-E* is displayed in brown letters. Yellow background marks the *Bs3-E* promoter-specific 13-bp insertion. The gray background marks corresponding positions in the *Bs3* and *Bs3-E* promoters, which yielded almost identical results in the substitution mutant analysis.

affinity to the *Bs3* promoter fragment. Together, these data strongly suggest that, in contrast to our previous statements (Römer et al., 2007), specific binding of AvrBs3 or AvrBs3Δrep16 to their matching promoters is the basis for promoter activation specificity.

**A *Bs3* Promoter with an Inverted *UPA*<sub>AvrBs3</sub> Box Does Not Trigger the *Bs3*-Mediated HR**

To clarify if the *UPA*<sub>AvrBs3</sub> box acts in a directional manner, we generated a *Bs3* promoter derivative in which the *UPA*<sub>AvrBs3</sub> box is replaced by the reverse-

complement sequence (Fig. 9A). The corresponding *Bs3* promoter mutant (*Bs3* *UPA*<sub>rev</sub>) was fused to the *Bs3* cds and was delivered via *A. tumefaciens* together with 35S:*avrBs3* into *N. benthamiana* leaves. The *Bs3* *UPA*<sub>rev</sub> construct did not trigger the HR in combination with AvrBs3, suggesting that the *UPA*<sub>AvrBs3</sub> box acts in a directional manner (Fig. 9B).

**Functionality of the *UPA*<sub>AvrBs3</sub> Box Is Independent of the Promoter Context**

The 3' end of the *UPA*<sub>AvrBs3</sub> box in the *Bs3* promoter is located 44 bp upstream of the TSS and 102 bp



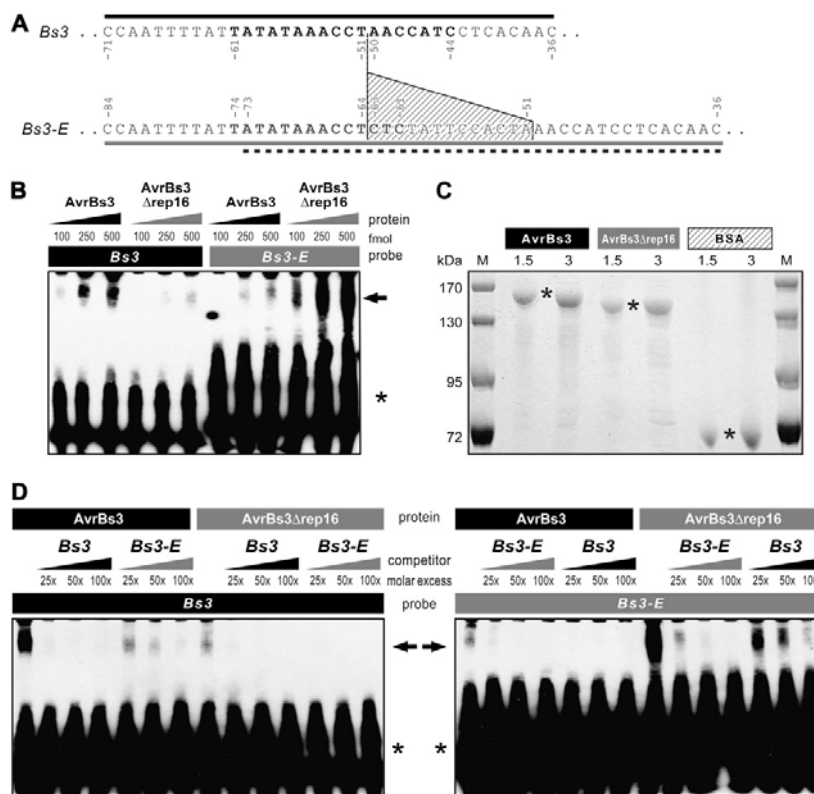


**Figure 8.** AvrBs3 and AvrBs3Δrep16 bind with high affinity to the *Bs3* and *Bs3-E* promoters, respectively. **A**, Probes derived from the *Bs3* and *Bs3-E* promoter sequences used in EMSA. The experimentally defined  $UPA_{AvrBs3}$  and  $UPA_{AvrBs3\Delta rep16}$  boxes of the *Bs3* and *Bs3-E* promoters (see Fig. 7) are displayed as boldface black and gray letters, respectively. Numbering is relative to the TSS of *Bs3* and *Bs3-E*, respectively. Note that the probe sequence used previously (dashed line) does not cover the entire  $UPA_{AvrBs3\Delta rep16}$  box (gray letters). **B**, EMSA of 100 fmol of biotin-labeled *Bs3*-derived (36 bp) and *Bs3-E*-derived (49 bp) probes incubated with 100, 250, and 500 fmol of GST:AvrBs3 (AvrBs3) and GST:AvrBs3Δrep16 (AvrBs3Δrep16) fusion proteins, respectively. Positions of bound and free probes are indicated: arrow, bound probe; asterisk, free probe. The top signals correspond to the slots. **C**, Coomassie Brilliant Blue-stained 8% SDS-PAGE. GST translational fusions to AvrBs3 and AvrBs3Δrep16 used for EMSA studies were expressed in *Escherichia coli*, purified, and quantified by Bradford analysis (Bradford, 1976). Subsequently, 1.5 and 3 μg of GST:AvrBs3, GST:AvrBs3Δrep16, and bovine serum albumin (BSA) standard were separated by SDS-PAGE and stained with Coomassie Brilliant Blue. Fragments of the expected size (GST:AvrBs3, 150.8 kD; AvrBs3Δrep16, 136.8 kD) are indicated by asterisks. Marker proteins (M) are indicated with their molecular masses in kD (PageRuler prestained protein ladder; Fermentas). **D**, EMSA competition assay of 100 fmol of biotin-labeled *Bs3* (left) or *Bs3-E* (right) probe incubated with 500 fmol of GST:AvrBs3 (AvrBs3) or GST:AvrBs3Δrep16 (AvrBs3Δrep16), respectively. A molar excess of nonlabeled *Bs3* and *Bs3-E* fragments of 25×, 50×, and 100× was used for competition. All experiments were repeated twice with similar results.

upstream of the ATG start codon. We wondered if the  $UPA_{AvrBs3}$  box retains its functionality when moved to other positions within the *Bs3* promoter. As starting material for this experiment, we used a *Bs3* promoter substitution mutant (designated *Bs3 UPA<sub>mut</sub>*; the wild-type T nucleotide at position -61 is replaced by an A nucleotide) that, when fused in front of the *Bs3* cds, did not trigger the HR in *N. benthamiana* leaves upon *A. tumefaciens*-mediated codelivery with *35S:avrBs3* (Fig. 10). Next, we inserted a wild-type  $UPA_{AvrBs3}$  box

into *Bs3 UPA<sub>mut</sub>* at a distance of 293 bp (*Bs3 UPA<sub>293</sub>*) or 424 bp (*Bs3 UPA<sub>424</sub>*) upstream of the ATG start codon. *Bs3 UPA<sub>293</sub>* and *Bs3 UPA<sub>424</sub>* promoter constructs were fused in front of the *Bs3* cds and were tested functionally via *A. tumefaciens*-mediated delivery. Both promoter constructs triggered an HR in *N. benthamiana* upon codelivery with *35S:avrBs3* (Fig. 10B). Thus, the  $UPA_{AvrBs3}$  box retains its functionality when moved within the *Bs3* promoter. Next, we tested if the  $UPA_{AvrBs3}$  box would retain its function when moved

Römer et al.

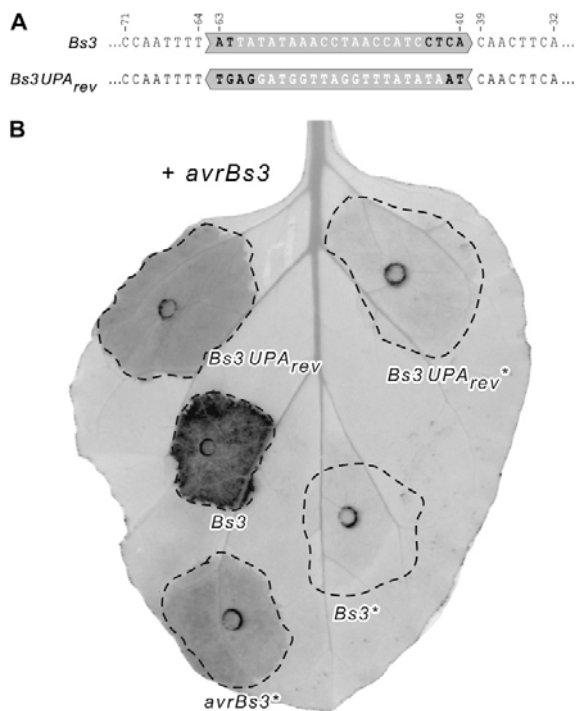


**Figure 9.** A *Bs3* promoter with an inversely orientated  $UPA_{AvrBs3}$  box does not trigger a *Bs3*-dependent HR. A, Part of the *Bs3* promoter wild-type sequence (*Bs3*) and a derivative with an inverted  $UPA_{AvrBs3}$  box (*Bs3 UPA<sub>rev</sub>*) are shown, highlighted with gray boxes. The experimentally determined  $UPA_{AvrBs3}$  box is shown in white letters (see Fig. 7). Numbering is relative to the TSS of *Bs3*. B, Functional analysis of the inverted box in the *Bs3* promoter. The promoters depicted in A were fused to the *Bs3* cds and delivered via *A. tumefaciens* ( $OD_{600} = 0.8$ ) alone (asterisks) or together with a 35S promoter-driven *avrBs3* gene (+ *avrBs3*) into *N. benthamiana* leaves. Dashed lines mark the inoculated areas. Leaves were harvested at 4 dpi and cleared with ethanol to visualize the HR (dark areas).

to a promoter context different from the pepper *Bs3* promoter. We used the promoter of the tomato *R* gene *Bs4*, which is transcribed constitutively at a low level (Schornack et al., 2005) and which does not trigger the HR when fused in front of the *Bs3* cds (Fig. 10B). We placed the  $UPA_{AvrBs3}$  box and a mutated box variant into the *Bs4* promoter (termed *Bs4 UPA* and *Bs4 UPA<sub>mut</sub>*, respectively) and fused these *Bs4* promoter derivatives in front of the *Bs3* cds. *A. tumefaciens*-mediated delivery of 35S:*avrBs3* triggered an HR in *N. benthamiana* leaves upon codelivery of the *Bs4 UPA* but not the *Bs4 UPA<sub>mut</sub>* promoter construct. Thus, the  $UPA_{AvrBs3}$  box retains its functionality not only in different locations within the pepper *Bs3* but also in the context of the tomato *Bs4* promoter.

The TSS of the *Bs3* promoter is 44 bp downstream of the 3' end of the  $UPA_{AvrBs3}$  box (Römer et al., 2007). We carried out RACE to determine the TSS generated in constructs that trigger the HR in combination with

35S:*avrBs3* (*Bs3 UPA<sub>293r</sub>*, *Bs3 UPA<sub>424r</sub>* and *Bs4 UPA*). As shown in Figure 10A, the TSS of *Bs3 UPA<sub>293r</sub>*, *Bs3 UPA<sub>424r</sub>* and *Bs4 UPA* were 46, 41, and 42 bp downstream of the 3' end of the respective  $UPA_{AvrBs3}$  boxes. Hence, the TSS in *AvrBs3*-inducible promoters appears to be dictated by the location of the  $UPA_{AvrBs3}$  box.

#### Naturally Occurring Nonfunctional *Bs3* Alleles

To study natural diversity of *Bs3* alleles, we examined accessions of the *Capsicum* species *C. annuum*, *C. baccatum*, and *C. chinense*. We determined the promoter sequences (244 bp 5' of the ATG start codon) and cds of 49 *Capsicum* accessions, identifying 23 different haplotypes (Table I; Supplemental Figs. S1 and S2; Supplemental Data Sets S3 and S4). The *Bs3-E* haplotype (defined as haplotype 1) was the most prevalent, found in nine of 49 sequenced accessions. Within the promoter region, 39 accessions constituting 14 haplotypes were identical to the *Bs3-E* haplotype. By contrast, we identified only two accessions that were sequence identical to the *Bs3* gene in promoter and cds (Table I). We identified two haplotypes (nos. 16 and 23) that carried mutations in the predicted  $UPA_{AvrBs3\Delta rep16}$  box (Supplemental Fig. S5). Infection experiments showed that neither *avrBs3*-expressing nor *avrBs3\Delta rep16*-expressing *Xcv* strains triggered the HR in pepper accessions corresponding to haplotypes 16 and 23 (Table I). We PCR amplified and cloned the two corresponding *Bs3* alleles (promoter and cds) and tested their functionality via *A. tumefaciens*-mediated transient expression in *N. benthamiana* leaves. Both alleles failed to trigger the HR when codelivered with 35S:*avrBs3\Delta rep16*. We also cloned the promoters of haplotypes 16 and 23 in front of the *Bs3-E* cds to test if the lack of functionality of these alleles is due to promoter polymorphisms. Indeed, transcriptional fusions of the *Bs3-E* cds to the promoters of haplotypes 16 and 23 did not mediate recognition of *AvrBs3\Delta rep16*. In a reciprocal experiment, we fused the strong constitutive 35S promoter in front of the cds of haplotypes 16 and 23. Functional analysis demonstrated that the cds of haplotype 23 but not of haplotype 16 triggered an HR. Inspection of the cds of haplotype 16 revealed a G-to-T substitution in the first exon that causes a Gly (GGC)-to-Val (GTC) exchange in a conserved Gly residue of the predicted FAD-binding domain of the *Bs3* protein (Table I; Supplemental Figs. S1A and S2). It is likely, therefore, that this difference renders haplotype 16 inactive. In addition to haplotype 16, we found 16 accessions (nine haplotypes [nos. 5, 8–13, 16, and 20]) that, due to polymorphisms in the cds, are unlikely to encode a functional *Bs3* protein. One remarkable finding in this context is an 11-bp deletion in exon 1 that is found in 12 accessions (six haplotypes [nos. 8–13]). This deletion results in a frameshift and an early stop codon in the cds (Supplemental Figs. S1A and S2). Similarly, we identified in haplotype 20 a C-to-G substitution in exon 1 that changes a Tyr (TAC) to a stop codon (TAG). We

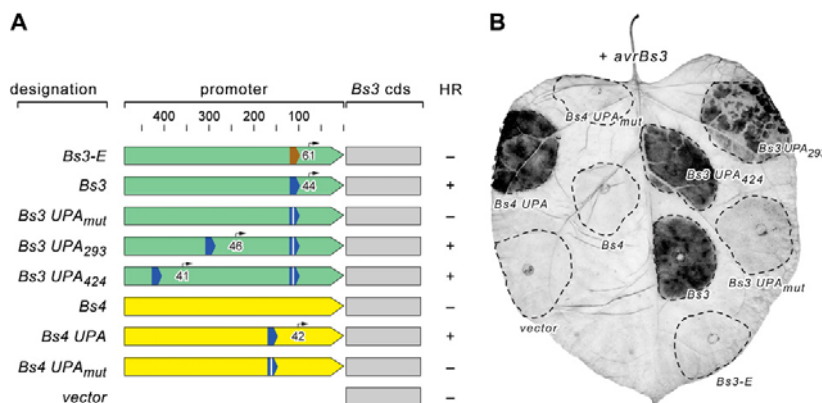


**Figure 10.** Functionality of the  $UPA_{AvrBs3}$  box is independent of its position and the promoter context. A, Graphical representation of promoter constructs tested. Mutations and insertions of  $UPA_{AvrBs3}$  boxes were made via site-directed mutagenesis. Green boxes represent the *Bs3* and *Bs3-E* promoters. Yellow boxes represent the *Bs4* promoter. Blue and brown boxes represent the  $UPA_{AvrBs3}$  and  $UPA_{AvrBs3\Delta rep16}$  boxes, respectively. Note that the *Bs3* and *Bs3-E* promoters differ only within and adjacent to their  $UPA$  boxes but are otherwise identical and therefore displayed in identical color. A white vertical line within the  $UPA_{AvrBs3}$  box represents a substitution mutation (T  $\rightarrow$  A at position  $-61$ ; see Fig. 7B) within the  $UPA_{AvrBs3}$  box. All promoter elements are displayed to scale. The numbers and horizontal lines above the promoters provide a scale and denote the distances with respect to the ATG start codon. Arrows above the promoter boxes mark the TSS of the given promoter. Numbers below the arrows denote the distance between the 3' end of the  $UPA_{AvrBs3}$  box and the respective TSS. Gray boxes represent the *Bs3* cds. + and - indicate the presence and absence of an HR in *N. benthamiana* upon codelivery of each promoter construct with a *35S:avrBs3* construct. B, Functional analysis of *Bs3* and *Bs4* promoter derivatives. The promoter constructs depicted in A were codelivered together with a *35S:avrBs3* construct (+ *avrBs3*) into *N. benthamiana* leaves via *A. tumefaciens* ( $OD_{600} = 0.8$ ). Dashed lines mark the inoculated areas. Four days after inoculation, the leaves were harvested and cleared with ethanol to better visualize the HR (dark areas).

expressed the cds of haplotype 20 and some representative haplotypes that are likely to encode nonfunctional *Bs3* proteins under the control of the 35S promoter and confirmed via *A. tumefaciens*-mediated transient expression that these alleles are indeed incapable of triggering an HR. Altogether, our data show that many *Capsicum* accessions contain a nonfunctional *Bs3* cds. None of these lines with nonfunctional *Bs3* alleles showed any observable morphological phenotypes.

## DISCUSSION

### *UPA* Boxes Matching to Different TALes Show No Obvious Sequence Homology

We wished to investigate how bacterial TALes specifically interact with and activate corresponding host plant promoters. To do so, we analyzed the *Bs3* and *Bs3-E* promoters to gain insights into how they are specifically activated by the highly related transcription activators *AvrBs3* and *AvrBs3 $\Delta$ rep16*, respectively. Using mutational analysis, we defined the  $UPA_{AvrBs3}$  box of the *Bs3* promoter and the  $UPA_{AvrBs3\Delta rep16}$  box of the *Bs3-E* promoter (Fig. 7). As both boxes overlap by at least 11 bp, it is unclear if the conserved sequence motif that is present in the  $UPA_{AvrBs3}$  and  $UPA_{AvrBs3\Delta rep16}$  boxes may also be part of  $UPA$  boxes that are targeted by TALes distinct from *AvrBs3* and *AvrBs3 $\Delta$ rep16*. Therefore, we inspected

the promoters of the rice (*Oryza sativa*) genes *Xa27*, *Os8N3*, *OsTFX1*, and *OsTFIIA $\gamma$ 1* that have been shown previously to be induced by the matching *Xanthomonas oryzae* pv *oryzae* TALes *AvrXa27*, *PthXo1*, *PthXo6*, and *PthXo7*, respectively (Gu et al., 2005; Chu et al., 2006; Yang et al., 2006; Sugio et al., 2007). None of these promoters contains a sequence that matches the 11-bp sequence present in the  $UPA_{AvrBs3}$  and  $UPA_{AvrBs3\Delta rep16}$  boxes. Thus, there is no evidence that  $UPA$  boxes matching different TALes share a consensus sequence. Our previous studies suggested that the hypervariable residues of TALes determine the promoter target sequence. This hypothesis is based on the analysis of *AvrHah1*, a TALE from *Xanthomonas gardneri*, which is recognized in pepper *Bs3* plants and thus likely activates the *Bs3* promoter. *AvrHah1* shares blocks of high homology with *AvrBs3* within the hypervariable repeat residues (Supplemental Fig. S3A; Schornack et al., 2008). Thus, comparative analysis of *AvrHah1* and *AvrBs3* suggested that TALes that share blocks of high homology within their hypervariable repeat residues are likely to target similar  $UPA$  boxes. Consistent with this idea is the fact that *AvrBs3* and *AvrBs3 $\Delta$ rep16* are identical in their first 10 repeat units (Supplemental Fig. S3A) and that the corresponding  $UPA_{AvrBs3}$  and  $UPA_{AvrBs3\Delta rep16}$  boxes are partially identical. Given that the hypervariable residues of *AvrXa27*, *PthXo1*, *PthXo6*, and *PthXo7* share no homology to *AvrBs3* within their hypervariable residues (Supplemental

Römer et al.

**Table 1.** Functional analysis of naturally occurring *Bs3* alleles

Haplotype No. <sup>a</sup>	Promoter Type	Promoter, Comments	Coding Sequence, Comments <sup>b</sup>	Functional Analysis <sup>c</sup>			
				<i>avrBs3</i> <sup>d</sup>	<i>avrBs3Δrep16</i> <sup>e</sup>	35S: <i>cds</i> <sup>f</sup>	Prom: <i>Bs3<sub>cds</sub></i> <sup>g</sup>
1*	<i>Bs3-E</i>			-/-	+/+	+	+
2	<i>Bs3-E</i>		DNA polymorphisms also present in <i>Bs3</i> cds	-/n	+/n		
3#	<i>Bs3</i>			+/+	-/-	+	-
4	<i>Bs3-E</i>		Cds identical to <i>Bs3</i> cds	-/-	+/+		
5	<i>Bs3-E</i>		Loss of function due to mutation in second exon (1,093, CCT[P] → CTT[L])	-/-	-/-	-	
6	<i>Bs3-E</i>			-/-	+/+		
7	<i>Bs3-E</i>			-/-	+/+		
8	<i>Bs3-E</i>		11-bp deletion in first exon (Δ595–605) results in a frameshift and thus an early stop codon (haplotypes 8–13)	-/-	-/-		
9	<i>Bs3-E</i>			-/-	-/-	-	
10	<i>Bs3-E</i>			-/-	-/-		
11	<i>Bs3-E</i>			-/-	-/-		
12	<i>Bs3-E</i>			-/-	-/-		
13	<i>Bs3-E</i>			-/-	-/-		
14	<i>Bs3-E</i>			-/-	+/+		
15	<i>Bs3-E</i>			-/-	+/+		
16	Unique	C → G (123) substitution in predicted <i>UPA<sub>AvrBs3Δrep16</sub></i> box	Loss of function due to mutation in first exon (366, GGT[G] → GTC[S])	-/-	-/-	-	-
17	<i>Bs3-E</i>			n/-	n/+	+	
18	Identical to no. 19	C → G (161) substitution		n/n	n/n		
19	Identical to no. 18	C → G (161) substitution		-/-	+/+		
20	Identical to no. 22	C → A (18) substitution	Substitution in first exon (472, TAC[Y] → TAG[stop]) results in a stop codon	-/-	-/-		
21	<i>Bs3-E</i>			-/-	-/+	+	
22	Identical to no. 20	C → A (18) substitution		n/-	n/+	+	+
23	Unique	Deletion (Δ199) and C → T (121) substitution in predicted <i>UPA<sub>AvrBs3Δrep16</sub></i> box		-/-	-/-	+	-

<sup>a</sup>Haplotypes 1 and 3 represent the *Bs3-E* (\*) and *Bs3* (#) alleles, respectively. *Capsicum* accessions corresponding to the haplotypes are provided in Supplemental Figure S1. <sup>b</sup>Polymorphic nucleotides are underlined, and the encoded amino acids are given in square brackets. Numbering of polymorphisms refers to Supplemental Figures S1 and S2. <sup>c</sup>Functionality of the *Bs3* alleles was analyzed via *Xcv* inoculation of the pepper accessions and via *A. tumefaciens*-mediated transient expression in *N. benthamiana*. Results are displayed in columns <sup>d</sup> and <sup>e</sup>, always with the data observed in pepper first and the data observed in *N. benthamiana* second. The presence or absence of an HR is indicated by + or -, respectively. n, Not tested. *Capsicum* accessions were tested with *Xcv* strains expressing either *avrBs3* (<sup>d</sup>) or *avrBs3Δrep16* (<sup>e</sup>). For *A. tumefaciens*-mediated transient expression in *N. benthamiana*, the cloned *Bs3* alleles (promoter and cds) were delivered in combination with a cauliflower mosaic virus 35S promoter-driven *avrBs3* (<sup>d</sup>) or *avrBs3Δrep16* (<sup>e</sup>) construct. <sup>f</sup>The cds of the given *Bs3* allele was expressed under the control of the 35S promoter (35S:*cds*). <sup>g</sup>The promoter of a given *Bs3* allele was fused in front of the *Bs3* wild-type cds and was delivered into *N. benthamiana* in combination with a 35S-driven *avrBs3Δrep16* T-DNA (*Prom:Bs3<sub>cds</sub>*).

Fig. S3, B and C), it is also expected that matching *UPA* boxes would not share homology with the *UPA<sub>AvrBs3</sub>* box. Taken together, these data indicate that no consensus *UPA* box exists.

Given that not only the *Bs3* but also the pepper *UPA10* and *UPA20* genes are induced by *AvrBs3* (Kay et al., 2007), these promoters should contain a *UPA<sub>AvrBs3</sub>* box. Indeed the *UPA10*, *UPA20*, and *Bs3* promoters share sequence conservation, which is pronounced in the 5' end of the corresponding *UPA<sub>AvrBs3</sub>* boxes (positions -61 to -52; Supplemental Fig. S4). Nucleotides at position -46 to -44 of the *Bs3* pro-

motor showed less sequence similarity to the corresponding promoter regions of *UPA10* and *UPA20*. In agreement with this observation, our substitution mutagenesis showed that sequence variation at positions -46 and -45 had no detectable effect and substitutions at position -44 had only a minor effect on the *Bs3*-mediated HR (Fig. 7; Supplemental Fig. S4). In this context, it is notable however, that the *Bs3* promoter transposon mutant T-46, which basically lacks the last three nucleotides of the *UPA<sub>AvrBs3</sub>* box (corresponding to positions -46 to -44; Fig. 4), did not trigger an HR. Mutant T-46 is equivalent to a "triple" substitution

mutant in which positions  $-46$ ,  $-45$ , and  $-44$  are mutated. Notably, the insertion mutant T $-46$  showed no Bs3-mediated HR (Fig. 4), while all single nucleotide substitution mutants at positions  $-46$  to  $-44$  showed no or only partial reduction of the Bs3 HR (Fig. 7). We conclude that the suppression of the Bs3 HR in T $-46$  is due to the additive effect of three substitutions. This implies that single nucleotide substitutions at positions  $-46$  and  $-45$  must affect the inducibility of the Bs3 promoter, although these substitutions had no detectable effect on the Bs3 HR.

Our mutational studies relied on a transient *A. tumefaciens*-mediated delivery system using constitutively expressed TALE genes in combination with Bs3 and Bs3-*E* promoter derivatives into *N. benthamiana*. This assay is useful for rapid analysis of in vitro-generated promoter derivatives. The assay also appears to be highly representative of the native interaction during infection, because naturally occurring Bs3 alleles by *Xcv* infection assay yielded identical results (see ECW, ECW-30R, PI593576, PI593491, PI631131, PI357635, PI593574, PI406948, PI631152, PI224415, PI599426, PI566809, PI181907, PI497971, CGN17230, CGN17227, PI593557, PI631137, CGN17042, and CGN17025 in Supplemental Fig. S1). Therefore, we are confident that our reporter system is an efficient and accurate assay to study interactions between TALEs and corresponding host promoters.

Sequence analysis of naturally occurring Bs3 alleles uncovered that haplotypes 16 and 23 carry mutations in the predicted  $UPA_{AvrBs3\Delta rep16}$  box (Supplemental Fig. S5). As anticipated, no HR was observed in either haplotype upon infection with *avrBs3\Delta rep16*-expressing *Xcv* strains as well as upon inoculation with an *A. tumefaciens* strain delivering a 35S promoter-driven *avrBs3\Delta rep16* gene (Table I). Furthermore, when promoters of both haplotypes were fused to the Bs3 wild-type cds, they were unable to trigger an AvrBs3 $\Delta rep16$ -induced HR. Notably, haplotype 16 carries a C-to-G substitution at position  $-63$  relative to the TSS (Supplemental Fig. S5) and thus resembles the C-to-G substitution mutant generated in this study (Fig. 7). By contrast, other haplotypes that contained promoter polymorphisms outside of the  $UPA_{AvrBs3\Delta rep16}$  box (e.g. haplotypes 19 and 22) were still capable of triggering an AvrBs3 $\Delta rep16$ -dependent HR (Table I). Thus, the definition of the  $UPA_{AvrBs3\Delta rep16}$  box by the aid of substitution mutants is supported by the functional analysis of naturally occurring Bs3 alleles.

#### What Defines the TSS in a Gene with a UPA Box?

We discovered that the  $UPA_{AvrBs3}$  box retained its function when moved to different locations within the pepper Bs3 promoter and also in the heterologous tomato Bs4 promoter (Fig. 10). We also determined that the placement of the  $UPA_{AvrBs3}$  box in different promoter locations changed the TSS. The distance between the TSS and the  $UPA_{AvrBs3}$  box was conserved in all constructs and was found to be between 41 and

46 bp with respect to the 3' end of the  $UPA_{AvrBs3}$  box. Thus, the TSS of AvrBs3-inducible genes seems to be dictated by the location of the  $UPA_{AvrBs3}$  box.

The initiation of mRNA synthesis in eukaryotic cells requires the assembly of general transcription factors and RNA polymerase II into a preinitiation complex at the core promoter. The only known sequence-specific DNA-binding protein among the general transcription factors is the TATA-binding protein, a subunit of the general transcription factor TFIID. Since AvrBs3 was shown to bind to the  $UPA_{AvrBs3}$  box-containing promoters (Kay et al., 2007; Römer et al., 2007) and since the TSS is dictated by the position of the  $UPA_{AvrBs3}$  box, it is possible that AvrBs3 replaces TATA-binding protein in its function as a sequence-specific DNA-binding protein in the preinitiation complex. Given that the  $UPA_{AvrBs3}$  box contains a TATA-like sequence motif, it is tempting to speculate that AvrBs3 binds to this promoter motif. However, mutational analysis of the  $UPA_{AvrBs3}$  box (Fig. 7B) did not provide any evidence that the TATA motif is functionally more important than other areas within the  $UPA_{AvrBs3}$  box.

The observation that the  $UPA_{AvrBs3}$  box works at different promoter locations and within different promoter contexts suggests that diverse UPA boxes corresponding to different TALEs may be arranged in tandem to make a complex promoter. If such a complex promoter is fused to the Bs3 cds, it should mediate recognition of multiple TALEs. Such a promoter may confer durable resistance against a range of pathogens containing a range of TALEs, as is the case of several *Xanthomonas* species, including *X. oryzae* pv *oryzae*, *X. oryzae* pv *oryzicola*, and *X. axonopodis* pv *citri*.

#### How Did Bs3 Evolve and Does it Have a Function aside from Resistance?

Previously, we showed that Bs3 and Bs3-*E* are transcriptionally induced by AvrBs3 and AvrBs3 $\Delta rep16$ , respectively, but not by the TALE AvrBs4 (Römer et al., 2007). Here, we show that Bs3 and Bs3-*E* transcripts are not detectable via RT-PCR in uninfected leaf, flower, fruit, or root tissue (Fig. 1B). This raises the question of whether the Bs3 protein has a biological function other than in recognition of TALEs. Given that expression of Bs3 triggers cell death, a potentially detrimental function that requires strict control of gene expression, one wonders how this gene evolved. The sequence analysis of Bs3 alleles from different *Capsicum* accessions provides some clues to these questions. About one-third of the analyzed *Capsicum* accessions (16 of 49) contained a Bs3 cds with a predicted early stop codon (Table I; Supplemental Figs. S1A and S2). It is known that cell death plays an important role not only in disease resistance but also in developmental processes (Lam, 2004). Thus, we wondered if the accessions that carry a nonfunctional Bs3 cds show any phenotypes that would be indicative of a contribution of Bs3 to developmental or physiological processes. Yet, we observed no altered phenotypes in

Römer et al.

these accessions other than the change in their response to bacterial effectors, indicating that *Bs3* is important only in the context of disease resistance.

More than three-quarters of the analyzed *Capsicum* accessions (38 of 49) were identical to the *Bs3-E* haplotype within their promoter sequences. About three-quarters of these *Bs3-E* promoter-containing accessions (29 of 38) differed from the *Bs3-E* haplotype in their cds. By contrast, the three accessions that contain the *Bs3* promoter were identical in their promoter and cds. The *Bs3-E* haplotype is more prevalent and possibly more ancient than the *Bs3* haplotype. Thus, the *Bs3* promoter is possibly the consequence of a 13-bp deletion in the *Bs3-E* promoter. Consistent with this hypothesis, haplotype 4 contains the *Bs3-E* promoter but is identical to the *Bs3* haplotype in its cds (Supplemental Fig. S1A) and thus might represent the progenitor of the *Bs3* haplotype.

The predicted *Bs3* protein is homologous to YUCCA-like proteins from *Arabidopsis* (*Arabidopsis thaliana*), some of which are involved in auxin biosynthesis (Schlauch, 2007; Chandler, 2009). Overexpression of YUCCA-like genes leads to phenotypes characteristic of auxin-overproducing mutants but not to an HR, as in the case of the *Bs3* cds (Zhao et al., 2001; Kim et al., 2007; Römer et al., 2007). Hence, YUCCA-like proteins and *Bs3* are functionally distinct. Yet, based on sequence homology, *Bs3* can be considered as a YUCCA deletion derivative because it lacks a stretch of approximately 70 amino acids present in all predicted YUCCA proteins (Römer et al., 2007). We speculated that the *Bs3* gene evolved from a YUCCA-like gene in pepper and anticipated that some *Capsicum* accessions would contain an ancestral *Bs3* gene that encodes a "full-length" YUCCA-like protein instead of the YUCCA deletion derivative. However, none of the *Capsicum* haplotypes analyzed here contained a *Bs3* cds that encodes a full-length YUCCA protein. Thus, the postulated deletion in the *Bs3* cds most likely preceded the speciation of *Capsicum*. Given that *Bs3* as a potential YUCCA deletion derivative triggers cell death, its expression must be strictly regulated. Therefore, it appears likely that a promoter mutation that made this promoter transcriptionally inactive preceded the deletion in the cds. In agreement with this idea, knockout mutations in *Arabidopsis* YUCCA-like genes produced no obvious phenotypes due to genetic redundancy (Schlauch, 2007). In summary, the analyses of *Capsicum* accessions suggest that the *Bs3* gene has no function aside from disease resistance and provide some insights into how and when this potentially detrimental gene evolved.

## MATERIALS AND METHODS

### Generation of Promoter Deletion Constructs of *Bs3* and *Bs3-E*

Progressive 5' promoter deletions of the *Bs3* gene were PCR amplified from genomic DNA of pepper (*Capsicum annuum* 'ECW-30R'; Minsavage et al.,

1990). The PCR was carried out with Phusion high-fidelity DNA polymerase (New England Biolabs) and the primers Prom-90 bp-fwd-PR (5'-CACCAGT-TATCATCCCCCTTTCTCTTTCTC-3'), Prom-179 bp-fwd-PR (5'-CACCG-CACACCCTGGTTAAACAATGAACACG-3'), and Prom-356 bp-fwd-PR (5'-CACCTCATAGTCAAGCTAACGAAACTTATGC-3') in combination with the primer Final-entry-02-rev (5'-CATTTGTCTTTCCAAATTTTGGCAATA-TCTTGTGCAAC-3'). PCR fragments were cloned into pENTR-D (Invitrogen), sequenced, and transferred into the T-DNA vector pGWB1 (Nakagawa et al., 2007) via Gateway recombination (Invitrogen). pGWB1 derivatives were transformed into *Agrobacterium tumefaciens* GV3101 (Holsters et al., 1980) for transient expression assays. The *Bs3-E* alleles were cloned in the same way using genomic DNA from pepper cv ECW as template.

Internal promoter deletions were generated by the Phusion site-directed mutagenesis kit (New England Biolabs). We used a *Bs3* gene (promoter and cds) cloned in pENTR-D (Invitrogen) as template (Römer et al., 2007) to create deletions. Primers that were used are available upon request. All constructs were sequenced and transferred by Gateway LR recombination into pGWB1 (Nakagawa et al., 2007). pGWB1 derivatives were transformed into *A. tumefaciens* GV3101 for transient expression assays.

### Creation of Promoter Substitution and Insertion Mutants

Substitution mutants in the *Bs3* promoter were generated via site-directed mutagenesis using the Phusion site-directed mutagenesis kit (New England Biolabs). We used a *Bs3* gene (promoter and cds) cloned in pENTR-D (Invitrogen) as template DNA (Römer et al., 2007). We employed primers that contain at a given position all nucleotides except the nucleotide present in the wild-type sequence. The different permutations were selected by sequence analysis of cloned fragments. The promoter constructs were transferred via Gateway LR recombination into pGWB4 (encodes a C-terminal GFP epitope tag; Nakagawa et al., 2007). pGWB4 derivatives were transformed into *A. tumefaciens* GV3101 for transient expression in planta. The same approach was used for creation of the *Bs3-E* promoter mutants, with the difference that we used a cloned *Bs3-E* gene as template DNA (Römer et al., 2007). For the insertion of nucleotides in the *Bs3* promoter, we used the Phusion site-directed mutagenesis kit (New England Biolabs) and the primers site-dir-02-N-fwd-PR (5'-CTGACCAATTTTATTATATAAACCTNAAACCATCCTCAC-3'), site-dir-02-NN-fwd-PR (5'-CTGACCAATTTTATTATATAAACCTNNAACCATCCTCAC-3'), site-dir-02-AA+N-fwd-PR (5'-CTGACCAATTTTATTATATAAACCTAANA-ACCATCCTCAC-3'), or site-dir-02-CT+N-fwd-PR (5'-CTGACCAATTTTATTATATAAACCTCTNAAACCATCCTCAC-3') in combination with the primer site-dir-02-rev-PR (5'-GCAACGTTGTCATTGTTTAAACCAGGGTG-3'). All primers used are phosphorylated at their 5' termini. We used a *Bs3* gene (promoter and cds) cloned in the vector pENTR-D (Invitrogen) as template DNA (Römer et al., 2007). After sequence analysis, cloned fragments were transferred into pGWB1 by Gateway LR recombination (Nakagawa et al., 2007). For insertion of a 13-bp sequence at different locations within the *Bs3* promoter, we used the Phusion site-directed mutagenesis kit (New England Biolabs) in combination with primers Prom-Bs3+13-20nU-fwd-PR (5'-CTC-TATTCCACTACCTTTCTTTCTCTCTCTTG-3') + Prom-Bs3+13-20nU-rev-PR (5'-GGATGATAACTTGAAGTTGTGGGATG-3') or primers Prom-Bs3+13+31UTR-fwd-PR (5'-CTCTATTCCACTACAAGTAGTCTAGTTGCACAT-3') + Prom-Bs3+13+31UTR-rev-PR (5'-TGTTTTGATAGATTAGCGGGTGAC-AAG-3'). A *Bs3* gene (promoter and cds) cloned in pENTR-D (Invitrogen) was used as template (Römer et al., 2007). For the insertion of a *UPA*<sub>AvrBs3</sub> box, we also used the Phusion site-directed mutagenesis kit. As template, we used pENTR-D, which contains a *Bs3* gene with a mutation (-61T is replaced by A) in the original *UPA*<sub>AvrBs3</sub> box. For the insertion of the *Bs3* *UPA*<sub>293</sub> box, we used primers box-02-293-fwd-PR (5'-CAATTTTATTATATAAACCTAACCATCCT-CACAACCAAGTAAACTCAAAGAATAATCATTGAAC-3') and box-02-293-rev-PR (5'-CATACTAATTCATATTTCCCTTGCCATAAG-3'). To insert the *Bs3* *UPA*<sub>424</sub> box, we used primers box-03-424-fwd-PR (5'-CAA-TTTTATTATATAAACCTAACCATCCTCACAACCACATAGATTGACTT-GCTTTTACCACAGATAC-3') and box-03-424-rev-PR (5'-TCATGTATCA-TTCGCATTTCAAAGTAAACTAAGG-3').

For the generation of *Bs4* *UPA* and *Bs4* *UPA*<sub>mut</sub> constructs, we used a *Bs4* promoter fragment of 302 bp (Schornack et al., 2005) in pENTR-D (Invitrogen). In the *Bs4* *UPA*<sub>mut</sub>, all C nucleotides in the *UPA*<sub>AvrBs3</sub> box are replaced by G nucleotides. The boxes were inserted via Phusion site-directed mutagenesis using primers *Bs3inBs4*-promfwd-PR (5'-CAATTTTATTATATAAACCTAAC-CATCCTCACACGTTTCAAGTGGTACTTGT-3') and *Bs3submlinBs4*-promfwd-PR (5'-CAATTTTATTATATAAAGGTAAGGATCCTCACACACAGTTCAGTGG-TACTTGT-3') in combination with the primer *Bs3in4*-promrev-PR (5'-GTG-

AAAGCTTGATTAACATTCGCTTTG-3'). After sequence analysis, the promoter constructs were transferred by Gateway LR recombination into the T-DNA vector pK7-GW-Bs3. pK7-GW-Bs3 was generated on the basis of pK7FWG2 (Karimi et al., 2002). We removed the *Hind*III and *Bam*HI fragments by restriction digest from pK7FWG2 (contains the cauliflower mosaic virus 35S promoter, the Gateway *attR* cassette, and the GFP cds) and replaced it by a synthesized DNA fragment that contains *Sac*I and *Eco*RV restriction sites followed by the cauliflower mosaic virus 35S terminator. Next, a Gateway *attR* cassette was placed into the *Eco*RV site, resulting in pK7-GW. The *Bs3* cds was amplified from genomic DNA of pepper cv ECW-30R using the primers final-entry-*Sac*I-01-fwd-PR (5'-GGGGGAGCTCATGATGAATCAGAAATTCCTTAATCTTGTC-3') and final-entry-*Sac*I-02-rev-PR (5'-GGGGGAGCTCCATTGTTCTTTCCAAATTTGGCAATATC-3'). These primers add a *Sac*I restriction site on both ends of the *Bs3* cds. The *Bs3* cds was cloned into the *Sac*I restriction site of pK7-GW, resulting in pK7-GW-Bs3.

### Linker-Scanning Mutagenesis of the *Bs3* Promoter

For insertion mutagenesis, we used the GPS-LS Linker Scanning System (New England Biolabs). As template, we used pENTR-D containing 343 bp 5' of the ATG start codon of the *Bs3* gene fused to the *Bs3* cDNA. This plasmid was created by splicing using overlap extension PCR. The promoter was amplified from genomic DNA of ECW-30R pepper plants using primers Prom-356 bp-fwd-PR (5'-CACCTCATAGTCAAGCTAACGAAACT-TATGC-3') and B5-rev-PR (5'-CATACGGAACACTGTATTGCTTAAGG-3'). For cDNA synthesis, pepper ECW-30R plants were inoculated with a blunt syringe using *Xanthomonas campestris* pv *vesicatoria* strain 85-10 expressing *avrBs3* (pDS300F; optical density at 600 nm [OD<sub>600</sub>] = 0.4). RNA extraction and cDNA synthesis were done as described previously (Römer et al., 2007). The *Bs3* cDNA was amplified with Phusion high-fidelity DNA polymerase and the primers Final-entry-01-fwd-PR (5'-ATGATGAATCAGAAATGCTT-TAATCTTGTC-3') and Final-entry-01-rev-PR (5'-CTACATTGTTCTTTC-CAAAATTTGGCAATATCTTGTC-3'). PCR products of the cDNA and the promoter region were mixed in a 1:1 ratio and PCR amplified using Prom-356 bp-fwd-PR and Final-entry-01-rev-PR primers. The PCR product was cloned into pENTR-D (Invitrogen), sequenced, and used for the transposon mutagenesis. Transposon insertions in the promoter region were identified via PCR. The identified transposon mutants were treated according to the manual, so that only the 15-bp insertion of the transposon was left. The resulting transposon mutants were sequenced and then recombined into pGWB1.

### Plant Material and Infection Assays

Pepper and *Nicotiana benthamiana* plants were grown as described previously (Römer et al., 2007). Pepper germplasm was supplied by the U.S. Department of Agriculture (accessions preceded by "PI" or "Grif") and the Plant Genetic Resources cluster of the Centre for Genetic Resources, The Netherlands (accessions preceded by CGN). Information on corresponding pepper accessions is available at [http://www.ars-grin.gov/npgs/acc/acc\\_queries.html](http://www.ars-grin.gov/npgs/acc/acc_queries.html) and <http://www.cgn.wur.nl/UK/CGN+Plant+Genetic+Resources/>. *Agrobacterium*-mediated transient transformation of *N. benthamiana* leaves, *Xcv* infection assays of *Capsicum* species, RT-PCR, RACE, and EMSA were carried out as described previously (Römer et al., 2007). Generally, *Xanthomonas* and *Agrobacterium* infection assays were routinely carried out at three independent time points. At each time point, each bacterial strain or combination of strains was inoculated into four different leaves. *Agrobacterium* strains delivering T-DNAs that encode bacterial effector genes were generally used in multiple infiltrations, always including an appropriate positive and negative control on each inoculated leaf.

### Supplemental Data

The following materials are available in the online version of this article.

**Supplemental Figure S1.** Nucleotide polymorphisms of *Bs3* alleles.

**Supplemental Figure S2.** Proteins that are encoded by naturally occurring *Bs3* alleles.

**Supplemental Figure S3.** Sequence comparison of TALE hypervariable residues.

Plant Physiol. Vol. 150, 2009

**Supplemental Figure S4.** Comparison of *UPA*<sub>AvrBs3</sub> boxes of different AvrBs3-inducible promoters.

**Supplemental Figure S5.** Alignment of *UPA*<sub>AvrBs3Δrep16</sub> box variants in naturally occurring *Bs3* alleles.

**Supplemental Data Set S1.** *Bs3* promoter deletions.

**Supplemental Data Set S2.** Nucleotide sequences of linker-scanning *Bs3* promoter mutants.

**Supplemental Data Set S3.** Nucleotide sequences of naturally occurring *Bs3* alleles in Fasta format.

**Supplemental Data Set S4.** Sequence alignment of naturally occurring *Bs3* alleles.

### ACKNOWLEDGMENTS

We are grateful to Diana Horvath, Annett Strauss, and Christoph Peterhänsel for helpful comments on earlier versions of the manuscript. We acknowledge the technical support of Sabine Recht, Jens Hausner, Carola Kretschmer, Bianca Rosinsky, and Marina Schulze. Seeds were obtained from the U.S. Department of Agriculture-Agricultural Research Service National Genetic Resources Program and the Centre for Genetic Resources (Wageningen University and Research Centre).

Received April 14, 2009; accepted May 11, 2009; published May 15, 2009.

### LITERATURE CITED

- Abramovitch RB, Anderson JC, Martin GB (2006) Bacterial elicitation and evasion of plant innate immunity. *Nat Rev Mol Cell Biol* 7: 601–611
- Ballvora A, Pierre M, Van den Ackerveken G, Schomack S, Rossier O, Ganai M, Lahaye T, Bonas U (2001) Genetic mapping and functional analysis of the tomato *Bs4* locus, governing recognition of the *Xanthomonas campestris* pv. *vesicatoria* AvrBs4 protein. *Mol Plant Microbe Interact* 14: 629–638
- Bent AE, Mackey D (2007) Elicitors, effectors, and *R* genes: the new paradigm and a lifetime supply of questions. *Annu Rev Phytopathol* 45: 399–436
- Block A, Li G, Fu ZQ, Alfano JR (2008) Phytopathogen type III effector weaponry and their plant targets. *Curr Opin Plant Biol* 11: 396–403
- Bonas U, Stall RE, Staskawicz B (1989) Genetic and structural characterization of the avirulence gene *avrBs3* from *Xanthomonas campestris* pv. *vesicatoria*. *Mol Gen Genet* 218: 127–136
- Bradford MM (1976) A rapid and sensitive method for the quantitation of microgram quantities of protein utilizing the principle of protein-dye binding. *Anal Biochem* 72: 248–254
- Chandler JW (2009) Local auxin production: a small contribution to a big field. *Bioessays* 31: 60–70
- Chisholm ST, Coaker G, Day B, Staskawicz BJ (2006) Host-microbe interactions: shaping the evolution of the plant immune response. *Cell* 124: 803–814
- Chu Z, Yuan M, Yao J, Ge X, Yuan B, Xu C, Li X, Fu B, Li Z, Bennetzen JL, et al (2006) Promoter mutations of an essential gene for pollen development result in disease resistance in rice. *Genes Dev* 20: 1250–1255
- Cunnac S, Lindeberg M, Collmer A (2009) *Pseudomonas syringae* type III secretion system effectors: repertoires in search of functions. *Curr Opin Microbiol* 12: 53–60
- Göhre V, Robatzek S (2008) Breaking the barriers: microbial effector molecules subvert plant immunity. *Annu Rev Phytopathol* 46: 189–215
- Grant SR, Fisher EJ, Chang JH, Mole BM, Dangl JL (2006) Subterfuge and manipulation: type III effector proteins of phytopathogenic bacteria. *Annu Rev Microbiol* 60: 425–449
- Greenberg JT, Yao N (2004) The role and regulation of programmed cell death in plant-pathogen interactions. *Cell Microbiol* 6: 201–211
- Gu K, Yang B, Tian D, Wu L, Wang D, Sreekala C, Yang F, Chu Z, Wang GL, White FF, et al (2005) *R* gene expression induced by a type-III effector triggers disease resistance in rice. *Nature* 435: 1122–1125
- Herbers K, Conrads-Strauch J, Bonas U (1992) Race-specificity of plant

Römer et al.

- resistance to bacterial spot disease determined by repetitive motifs in a bacterial avirulence protein. *Nature* **356**: 172–174
- Hogenhout SA, Van der Hoorn RA, Terauchi R, Kamoun S (2009) Emerging concepts in effector biology of plant-associated organisms. *Mol Plant Microbe Interact* **22**: 115–122
- Holsters M, Silva B, Van Vliet F, Genetello C, De Block M, Dhaese P, Depicker A, Inzé D, Engler G, Villarreal R, et al (1980) The functional organization of the nopaline *A. tumefaciens* plasmid pTiC58. *Plasmid* **3**: 212–230
- Jones JD, Dangl JL (2006) The plant immune system. *Nature* **444**: 323–329
- Kamoun S (2006) A catalogue of the effector secretome of plant pathogenic oomycetes. *Annu Rev Phytopathol* **44**: 41–60
- Karimi M, Inze D, Depicker A (2002) GATEWAY vectors for *Agrobacterium*-mediated plant transformation. *Trends Plant Sci* **7**: 193–195
- Kay S, Bonas U (2009) How *Xanthomonas* type III effectors manipulate the host plant. *Curr Opin Microbiol* **12**: 37–43
- Kay S, Hahn S, Marois E, Hause G, Bonas U (2007) A bacterial effector acts as a plant transcription factor and induces a cell size regulator. *Science* **318**: 648–651
- Kim JJ, Sharkhuu A, Jin JB, Li P, Jeong JC, Baek D, Lee SY, Blakeslee JJ, Murphy AS, Bohnert HJ, et al (2007) *yucca6*, a dominant mutation in *Arabidopsis*, affects auxin accumulation and auxin-related phenotypes. *Plant Physiol* **145**: 722–735
- Lam E (2004) Controlled cell death, plant survival and development. *Nat Rev Mol Cell Biol* **5**: 305–315
- McKnight SL, Kingsbury R (1982) Transcriptional control signals of a eukaryotic protein-coding gene. *Science* **217**: 316–324
- Minsavage GV, Dahlbeck D, Whalen MC, Kearny B, Bonas U, Staskawicz BJ, Stall RE (1990) Gene-for-gene relationships specifying disease resistance in *Xanthomonas campestris* pv. *vesicatoria*-pepper interactions. *Mol Plant Microbe Interact* **3**: 41–47
- Mudgett MB (2005) New insights to the function of phytopathogenic bacterial type III effectors in plants. *Annu Rev Plant Biol* **56**: 509–531
- Nakagawa T, Kurose T, Hino T, Tanaka K, Kawamukai M, Niwa Y, Toyooka K, Matsuoka K, Jinbo T, Kimura T (2007) Development of series of Gateway binary vectors, pGWBs, for realizing efficient construction of fusion genes for plant transformation. *J Biosci Bioeng* **104**: 34–41
- Römer P, Hahn S, Jordan T, Strauss T, Bonas U, Lahaye T (2007) Plant-pathogen recognition mediated by promoter activation of the pepper *Bs3* resistance gene. *Science* **318**: 645–648
- Schlauch NL (2007) Flavin-containing monooxygenases in plants: looking beyond detox. *Trends Plant Sci* **12**: 412–418
- Schorneck S, Ballvora A, Gürlebeck D, Peart J, Baulcombe D, Baker B, Ganai M, Bonas U, Lahaye T (2004) The tomato resistance protein Bs4 is a predicted non-nuclear TIR-NB-LRR protein that mediates defense responses to severely truncated derivatives of AvrBs4 and overexpressed AvrBs3. *Plant J* **37**: 46–60
- Schorneck S, Meyer A, Römer P, Jordan T, Lahaye T (2006) Gene-for-gene mediated recognition of nuclear-targeted AvrBs3-like bacterial effector proteins. *J Plant Physiol* **163**: 256–272
- Schorneck S, Minsavage GV, Stall RE, Jones JB, Lahaye T (2008) Characterization of AvrHah1 a novel AvrBs3-like effector from *Xanthomonas gardneri* with virulence and avirulence activity. *New Phytol* **179**: 546–556
- Schorneck S, Peter K, Bonas U, Lahaye T (2005) Expression levels of *avrBs3*-like genes affect recognition specificity in tomato *Bs4* but not in pepper *Bs3* mediated perception. *Mol Plant Microbe Interact* **18**: 1215–1225
- Sugio A, Yang B, Zhu T, White FF (2007) Two type III effector genes of *Xanthomonas oryzae* pv. *oryzae* control the induction of the host genes *OsTFIIAγ1* and *OsTFX1* during bacterial blight of rice. *Proc Natl Acad Sci USA* **104**: 10720–10725
- Szurek B, Marois E, Bonas U, Van den Ackerveken G (2001) Eukaryotic features of the *Xanthomonas* type III effector AvrBs3: protein domains involved in transcriptional activation and the interaction with nuclear import receptors from pepper. *Plant J* **26**: 523–534
- Van den Ackerveken G, Marois E, Bonas U (1996) Recognition of the bacterial avirulence protein AvrBs3 occurs inside the host plant cell. *Cell* **87**: 1307–1316
- Wichmann G, Bergelson J (2004) Effector genes of *Xanthomonas axonopodis* pv. *vesicatoria* promote transmission and enhance other fitness traits in the field. *Genetics* **166**: 693–706
- Yang B, Sugio A, White FF (2006) *Os8N3* is a host disease-susceptibility gene for bacterial blight of rice. *Proc Natl Acad Sci USA* **103**: 10503–10508
- Yang B, Zhu W, Johnson LB, White FF (2000) The virulence factor AvrXa7 of *Xanthomonas oryzae* pv. *oryzae* is a type III secretion pathway-dependent nuclear-localized double-stranded DNA-binding protein. *Proc Natl Acad Sci USA* **97**: 9807–9812
- Zhao Y, Christensen SK, Fankhauser C, Cashman JR, Cohen JD, Weigel D, Chory J (2001) A role for flavin monooxygenase-like enzymes in auxin biosynthesis. *Science* **291**: 306–309

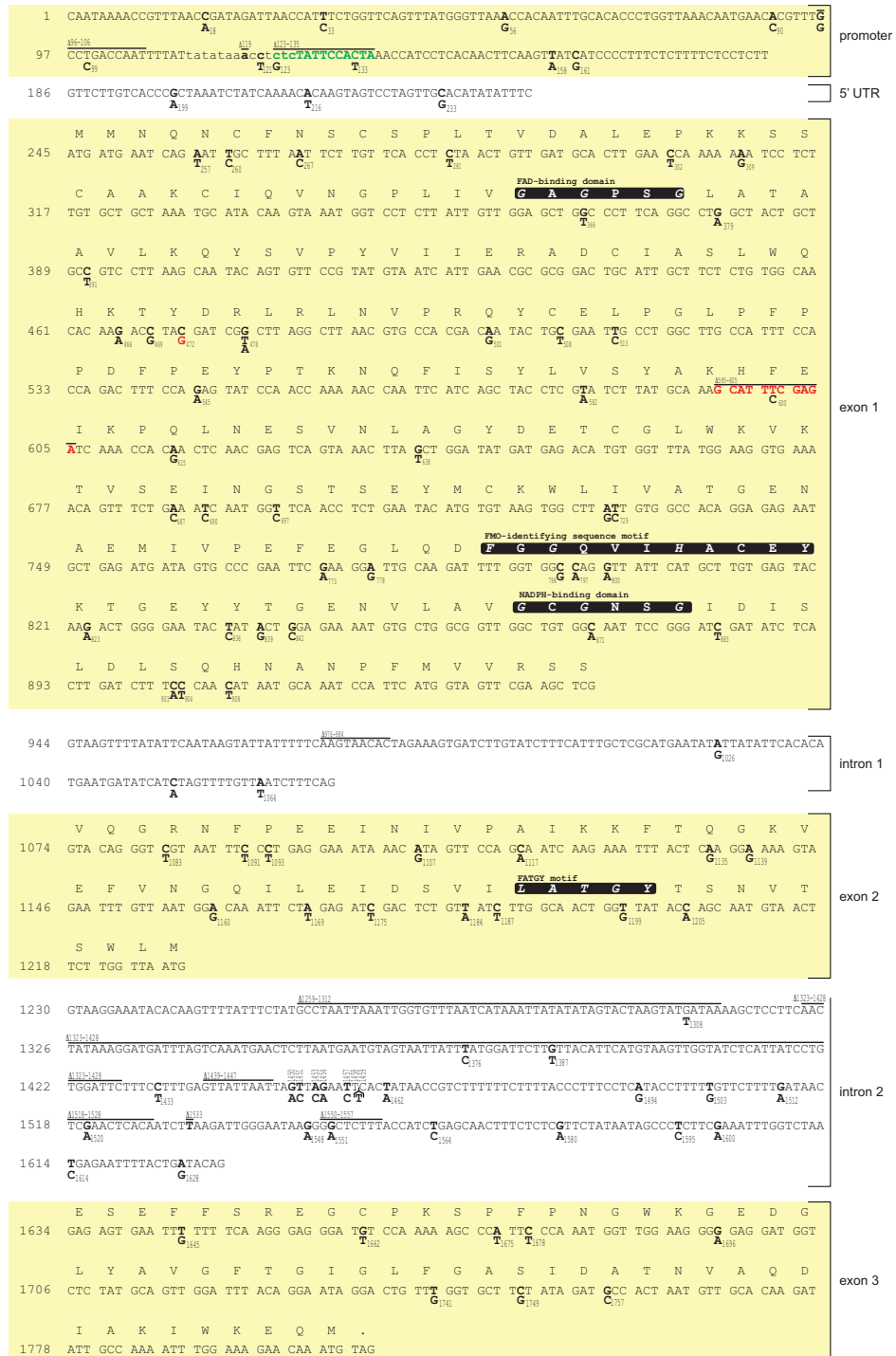






Supplementary Figure 2

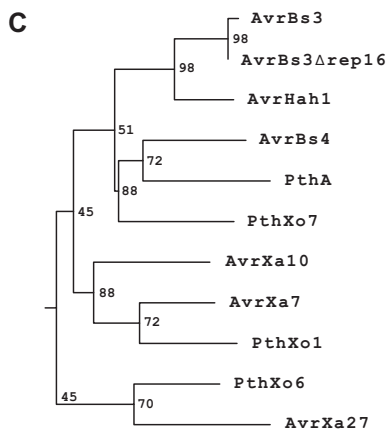
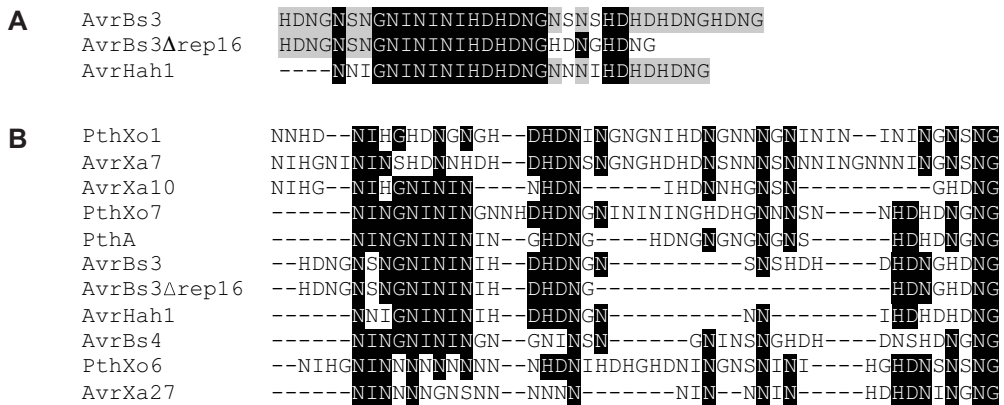
Figure legend, see next page



**Supplementary Figure 2. (see preceding page) Proteins that are encoded by naturally occurring *Bs3* alleles.**

Nucleotide and predicted amino acid sequences of *Bs3* alleles. Black boxes with white letters highlight the conserved residues of the FAD-binding domain (GXGXXG), the FMO-identifying sequence motif, (FXGXXXHXXX[Y/F]), the NADPH-binding domain (GXGXX[G/A]) and the conserved FATGY motif ([L/F]ATGY). Bold letters indicate polymorphisms with respect to the *Bs3-E* allele. The numbers next to the bold letters refers to the numbering of Supplementary Figure 1 Online and Supplementary Data Set 4 Online. Red letters indicate polymorphisms that result in early stop codons. Horizontal bars indicate deletions. The sequence in green letters represents the 13-bp sequence that is present in the *Bs3-E* but absent from the *Bs3* promoter. The predicted *UPA*<sub>AvrBs3Δrep16</sub> box is displayed in lower case letters.

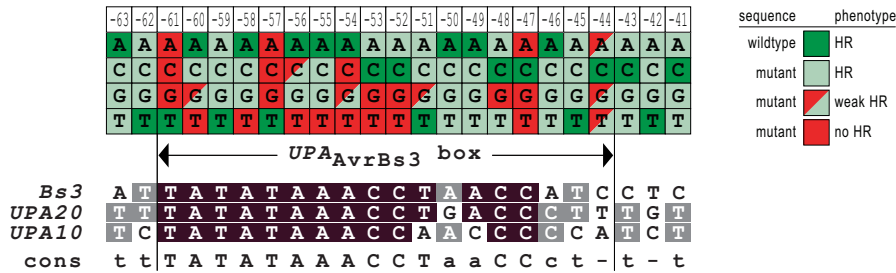
**Supplementary Figure 3**



**Sequence comparison of TAL effector hypervariable residues**

(A) AvrBs3, AvrBs3Δrep16 and AvrHah1 share blocks of high homology within the hypervariable repeat unit residues 12 and 13. Hypervariable residues of AvrBs3, AvrBs3Δrep16 and AvrHah1 were assembled as contiguous stretches and subjected to ClustalW analysis. Gray and black shading indicates residues that are conserved between two or all TAL effectors, respectively. (B) Alignment of the hypervariable residues of a set of representative TAL effectors. The hypervariable residues were assembled as contiguous stretches and subjected to ClustalW analysis. Black shading indicates residues that share high homology among different TAL effectors. (C) AvrBs3 is closely related to AvrBs3Δrep16 and AvrHah1. A neighbor-joining tree of the hypervariable residues of AvrBs3 and related proteins was generated using ClustalX. The branch length is proportional to divergence. Bootstrap values are based on 100 replications and are indicated as numbers at branching points.

**Supplementary Figure 4**



**Supplementary Figure 4. Comparison of *UPA<sub>AvrBs3</sub>* boxes of different AvrBs3-inducible promoters.** *UPA<sub>AvrBs3</sub>* boxes of the AvrBs3-inducible *Bs3*, *UPA10* and *UPA20* promoters are compared. Gray and black shading indicates nucleotides that are conserved between two or all promoters, respectively. The graphics above the alignment summarizes the results of the substitution mutagenesis (details are given in Figure 7B).

**Supplementary Figure 5**



**Supplementary Figure 5. Alignment of *UPA<sub>AvrBs3Δrep16</sub>*-box variants in naturally occurring *Bs3* alleles** The experimentally determined *UPA<sub>AvrBs3Δrep16</sub>* box of *Bs3-E* and the corresponding sequences of two *Bs3* alleles that are not transcriptionally activated by AvrBs3Δrep16 are compared. Black shading marks nucleotides that are conserved between different haplotypes. Vertical numbers at the top indicate the corresponding nucleotide position in the pepper cultivar ECW (see also Supplementary Figure 1 Online). Red numbers indicate the position of the nucleotides with respect to the transcriptional start site in the *Bs3-E* promoter. The G polymorphism in haplotype 16 results in a non-functional *UPA<sub>AvrBs3Δrep16</sub>* box, (see also Figure 7). The two polymorphisms in haplotype 23 result also in a non-functional *UPA<sub>AvrBs3Δrep16</sub>* box.

### 2.3.3 Zusammenfassung der Ergebnisse

In der Veröffentlichung konnte mittels RT-PCR gezeigt werden, dass *Bs3*-Transkripte bereits sechs Stunden nach Inokulation AvrBs3-translozierender *Xcv*-Stämme nachweisbar sind. Im Rahmen dieses Manuskriptes wurde gezeigt, dass *Bs3*- und *Bs3-E*-Transkripte mittels RT-PCR nicht in nicht-infizierten Blatt-, Blüten-, Stängel- und Wurzelgewebe detektierbar sind. Durch Deletionsstudien der *Bs3*- und *Bs3-E*-Promotoren konnten Minimalpromotoren von 166 Bp (*Bs3*) und 179 Bp (*Bs3-E*) definiert werden, welche durch die korrespondierende TAL-Effektoren AvrBs3 und AvrBs3Δrep16 induzierbar sind. RACE-Analysen von Promotorderivaten, die Deletionen unterschiedlicher Größe zwischen der  $UPT_{AvrBs3}$ -Box (*upregulated by TALes*) und dem ATG-Startkodon aufweisen zeigten, dass sich der Transkriptionsstart (TSS) in Abhängigkeit von der Position der  $UPT_{AvrBs3}$ -Box ändert und dass der Abstand zwischen der  $UPT_{AvrBs3}$ -Box und dem TSS 41 - 46 Bp beträgt. Die Verschiebung der 13-Bp Insertion des *Bs3-E*-Promotors an zwei andere Positionen im *Bs3*-Promotor zeigte, dass der Sequenzkontext der Insertion wichtig für die AvrBs3Δrep16 vermittelte Promotoraktivierung ist. Die Insertion von je 1, 2 bzw. 3 Bp in den *Bs3*-Promotor an die Position, wo sich im *Bs3-E*-Promotor die 13-Bp Insertion befindet ergab, dass drei zusätzliche Nukleotide (CTC oder CTA) ausreichen, um den AvrBs3-induzierbaren *Bs3*-Promotor in einen AvrBs3Δrep16-induzierbaren Promotor zu konvertieren. Somit konnte gezeigt werden, dass die 13-Bp Insertion im *Bs3-E*-Promotor nur ein Teil der  $UPT_{AvrBs3\Delta rep16}$ -Box ist. Durch die Substitutionsmutagenese des *Bs3*- und des *Bs3-E*-Promotors war es möglich die 5' und 3' Termini der  $UPT_{AvrBs3}$ - und die  $UPT_{AvrBs3\Delta rep16}$ -Box zu definieren. Durch EMSA-Analysen konnte ermittelt werden, dass AvrBs3 spezifisch an den *Bs3*-Promotor und dass AvrBs3Δrep16 spezifisch an den *Bs3-E*-Promotor bindet. Demnach ist die spezifische Bindung von TAL-Effektoren an ihre korrespondierenden Promotoren wahrscheinlich die Grundlage für die Induktion der Resistenzreaktion ist. Die Analyse einer invertierten  $UPT_{AvrBs3}$ -Box im *Bs3*-Promotor zeigte, dass diese nicht AvrBs3 induzierbar ist, was darauf hinweist das die  $UPT$ -Boxen direktional agieren. In der korrekten Orientierung war die  $UPT_{AvrBs3}$ -Box an verschiedenen Stellen des Paprika *Bs3*- und auch im Kontext des Tomaten *Bs4*-Promotors funktional. Die Analyse von 51 verschiedenen *Capsicum*-Species ergab, dass zahlreiche der untersuchten Linien auf Grund von Nukleotidpolymorphismen und Deletionen kein Voll-längen-Bs3-Protein bilden. Da die entsprechenden Genotypen keine offensichtlichen morphologischen Veränderungen im Vergleich zu Genotypen mit Voll-längen-Bs3-Protein aufweisen, muss man annehmen, dass Bs3 neben der Resistenzvermittlung keine weitere Funktion zukommt.

## 2.4 Etablierung eines diagnostischen *Bs3*-Markers

### 2.4.1 Publikation 3

Plant Breeding  
© 2010 Blackwell Verlag GmbH

doi:10.1111/j.1439-0523.2009.01750.x

#### Short Communication

### Identification and application of a DNA-based marker that is diagnostic for the pepper (*Capsicum annuum*) bacterial spot resistance gene *Bs3*

P. RÖMER<sup>1,2</sup>, T. JORDAN<sup>1,3</sup> and T. LAHAYE<sup>1,2,4</sup>

<sup>1</sup>Institute of Genetics, Martin-Luther-Universität Halle-Wittenberg, 06099; Halle (Saale), Germany; <sup>2</sup>Present address: Institute of Genetics, University of Munich (LMU), 82152 Martinsried, Germany; <sup>3</sup>Present address: Institute of Plant Biology, University of Zürich, 8008 Zürich, Switzerland; <sup>4</sup>Corresponding author, E-mail: lahaye@biologie.uni-muenchen.de

With 1 figure and 1 table

Received August 20, 2009/Accepted November 10, 2009

Communicated by T. Debener

#### Abstract

The pepper (*Capsicum annuum*) disease resistance gene *Bs3* mediates recognition of *avrBs3*-expressing strains of the bacterial spot pathogen *Xanthomonas campestris* pv. *vesicatoria*. We established the co-dominant DNA marker PR-*Bs3* that detects a functional nucleotide polymorphism in the *Bs3* promoter. Analysis of 20 F<sub>2</sub> segregants demonstrated complete linkage between PR-*Bs3* and *Bs3* resistance. Furthermore the analysis of 17 *Capsicum* accessions from diverse geographical origins demonstrated that PR-*Bs3* was diagnostic for *Bs3* resistance in all cases. Given that marker PR-*Bs3* allows the identification of *Bs3* resistant lines in a co-dominant fashion it will be a valuable tool for marker assisted selection of *Bs3* resistant lines in bacterial spot resistance breeding programs.

**Key words:** pepper — PCR — *Xanthomonas euvesicatoria* or *Xanthomonas axonopodis* pv. *vesicatoria*

Bacterial spot disease of tomato (*Solanum lycopersicon*) and pepper (*Capsicum annuum*), caused by *Xanthomonas campestris* pv. *vesicatoria* (*Xcv*; also referred to as *X. euvesicatoria* or *X. axonopodis* pv. *vesicatoria*) (Vauterin et al. 1995, Jones et al. 2004), can be devastating to production of these crops in areas with high humidity and heavy rainfall. Copper compounds and streptomycin have been used for several decades to control bacterial spot disease. However, tolerant *Xcv* strains have become prevalent and have reduced the efficacy of copper- and streptomycin-based bactericides (Basim et al. 2005). Considerable efforts were devoted to identify, characterize and employ genetic resistance to bacterial spot disease. In this context *Xcv* strains have been classified into races 1–10 according to their ability to cause bacterial spot on pepper lines that contain the resistance (*R*) gene *Bs1*, *Bs2*, *Bs3*, or *Bs4*, respectively (Stall et al. 2009). These dominantly inherited *Bs* genes trigger a hypersensitive response (HR) upon recognition of the matching *Xcv* avirulence proteins AvrBs1 (Ronald and Staskawicz 1988, Swanson et al. 1988), AvrBs2 (Minsavage et al. 1990), AvrBs3 (Bonas et al. 1989, Herbers et al. 1992) and AvrBs4 (formerly also known as AvrBsP or AvrBs3-2) (Canteros et al. 1991, Bonas et al. 1993, Minsavage et al. 1999), respectively. Thus far, only *Bs2* and *Bs3* have been cloned (Tai et al. 1999, Römer et al. 2007). The predicted *Bs2* and *Bs3* proteins share no sequence homology. *Bs2* belongs

to the large family of nucleotide-binding leucine-rich-repeat (NB-LRR) proteins (Tai et al. 1999) while *Bs3* shows homology to YUCCA-like flavin-dependent monooxygenases (Römer et al. 2007).

AvrBs2 is a widespread bacterial effector protein within the genus *Xanthomonas* and corresponding mutant strains are reduced in virulence (Kearney and Staskawicz 1990). Thus, the corresponding *R* gene *Bs2* promised to be durable and hence was introgressed into most commercial pepper cultivars. However, *Xanthomonas* strains that carry mutated *avrBs2* genes have been detected in the field since the mid-1990s, which is most likely the consequence of high selection pressure (Wichmann and Bergelson 2004). Subsequently, breeders generated pepper varieties that combined *Bs1* and *Bs2* resistance. Yet, in the last four years *Xcv* strain 4 has defeated the *Bs1* and *Bs2* resistance along the entire east coast of the U.S. (Jordan et al. 2006). The *R* gene *Bs3* provides resistance against *Xanthomonas* races 0, 1, 4, 7 and 9 and is thus far not prevalent in commercial varieties. Therefore the *Bs3* gene is a potentially useful new resistance resource against bacterial spot disease. However, efficient introgression of *Bs3* via marker-assisted selection (MAS; Collard and Mackill 2008) does require a diagnostic marker, which is not available thus far. In this study we present the identification and application of a DNA marker that is diagnostic to *Bs3* resistance.

#### Materials and Methods

**Plant material and resistance scoring:** Pepper (*Capsicum annuum*) plants of cultivar 'Early California Wonder' (ECW), the near isogenic line ECW-30R containing the resistance gene *Bs3* and all other pepper genotypes (Table 1) were grown in the greenhouse under standard conditions: day/night temperatures 24°C/19°C, 16 h light-period, and 60–70% relative humidity. Pepper cultivar ECW and the near isogenic line ECW-30R seeds were provided by R. E. Stall (University of Florida, Gainesville, FL, USA). Seeds of other *Capsicum* accessions were provided by USDA, ARS, National Germplasm Resources Laboratory (Beltsville, MD, USA). Pepper accessions CGN17230 and 17227 were provided by the Plant Genetic Resources cluster of the Centre for Genetic Resources, The Netherlands. Plants were inoculated with *xanthomonads* as described previously (Bonas et al. 1989). Resistance, indicated by an HR, was scored over a period of 2–3 days postinoculation.

2

RÖMER, JORDAN and LAHAYE

Table 1: *Capsicum annuum* lines used to study the diagnostic value of the PR-Bs3 marker with respect to *Bs3* resistance

Plant genotype	Collection site	Resistance phenotype <sup>1</sup>	Marker genotype <sup>2</sup>
Early California Wonder <sup>3</sup> (ECW) (cultivar)	not applicable	–	S
ECW-30R <sup>4</sup> (cultivar)	not applicable	+	R
PI <sup>5</sup> 159226	United States	–	S
PI <sup>5</sup> 433216	Australia	–	S
PI <sup>5</sup> 433215	Australia	–	S
PI <sup>5</sup> 432836	China	–	S
PI <sup>5</sup> 432835	China	–	S
PI <sup>5</sup> 640513	Mexico	+	R
PI <sup>5</sup> 631130	Bulgaria	–	S
PI <sup>5</sup> 631128	Russian Federation	–	S
PI <sup>5</sup> 432833	China	–	S
PI <sup>5</sup> 432832	China	–	S
PI <sup>5</sup> 432830	China	–	S
PI <sup>5</sup> 432827	China	–	S
PI <sup>5</sup> 432825	China	–	S
PI <sup>5</sup> 432818	China	–	S
PI <sup>5</sup> 593597	India	+	R
PI <sup>5</sup> 432813	China	–	S
PI <sup>5</sup> 432812	China	–	S

<sup>1</sup> +, resistance reaction (HR) after inoculation with *Xcv* expressing *avrBs3*, –, susceptible phenotype (no HR) after inoculation with *Xcv* expressing *avrBs3*.

<sup>2</sup> S represents the fragment present in all lines that do not contain the *Bs3* gene. R represents the fragment that is present in all *Bs3* resistant lines.

<sup>3</sup> Early California Wonder (ECW) is a cultivated pepper genotype.

<sup>4</sup> The *Bs3* gene was introgressed from PI 271322 into ECW and several times backcrossed to ECW yielding the near isogenic line ECW-30R.

<sup>5</sup> Info on the plant introduction (PI) lines are available at [http://www.ars-grin.gov/npgs/acc/acc\\_queries.html](http://www.ars-grin.gov/npgs/acc/acc_queries.html).

**Marker analysis:** Primer Prom.+2-fwd (GCACACCCTGGTTA-AACAATGAACACG) and Prom.+2-rev (GATGATAACTTG-AAGTTGTGAGGATGG) were used to screen segregants and *Capsicum* accessions. PCR reactions were carried out on 5 µl (1/5 diluted) miniprep DNA of pepper leaves (Edwards et al. 1991) in a 20 µl PCR reaction. The PCR conditions were as follows: denaturation at 94°C for 2 min, followed by 35 cycles of 94°C for 10 s, 58°C for 15 s, 72°C for 45 s, and in addition 72°C for 5 min as a final extension. PCR fragments were separated on a 3% Metaphor-agarose gel (Cambrex Bioscience, Rockland, ME, USA) and visualized under UV light.

## Results and Discussion

Recent studies showed that the *Xcv* effector protein AvrBs3 binds to an 18-bp promoter motif, the so-called *UPA* (upregulated by AvrBs3) box, that is present in the promoter of the pepper (*Capsicum annuum*) *Bs3* gene (Kay et al. 2007, Römer et al. 2009b). Binding of AvrBs3 causes transcriptional activation of the *Bs3* promoter, expression of the *Bs3* protein and results in *Xcv* resistance (Römer et al., 2007, 2009b). Analysis of 51 *Capsicum* accessions revealed that all accessions that mediate AvrBs3 recognition contain an *UPA* box (Römer et al., 2007, 2009b). In contrast the *Capsicum* accessions that did not show an AvrBs3 dependent HR contained an insertion of 13 bp in the *UPA* box (Römer et al. 2009b). Given that the *UPA* box in the *Bs3* promoter is the functional element that determines AvrBs3 recognition it seemed possible that this functional polymorphism could provide the basis to generate a diagnostic marker for *Bs3* resistance.

We designed primers that flank the *UPA* box of the *Bs3* promoter and tested if the corresponding PCR marker, designated PR-Bs3, would be diagnostic for *Bs3* resistance. To determine the diagnostic value of PR-Bs3 we first analysed 20 plants of a segregating F<sub>2</sub> population that is derived from a cross between the *Bs3* resistant cultivar ECW-30R and its near isogenic line ECW that does not show an AvrBs3-dependent HR. We inoculated the parental lines and all F<sub>2</sub> segregants with an *Xcv* strain that contains *avrBs3* and scored each plant for the presence or absence of an HR. Subsequently we isolated DNA of the parental lines and the F<sub>2</sub> segregants and carried out a PCR reaction with primers Prom.+2-fwd and Prom.+2-rev that flank the *UPA* box of the *Bs3* promoter. The corresponding amplicons were resolved on a high percentage agarose gel in order to distinguish PCR products with and without the 13-bp insertion in the *Bs3* promoter. As shown in Fig. 1a the PCR marker PR-Bs3 produced fragments of discernable size in the resistant (ECW-30R) and the susceptible (ECW) parental lines. Analysis of 20 F<sub>2</sub> segregants demonstrated that occurrence of an AvrBs3-dependent HR perfectly correlated with the presence of the shorter amplicon that was predicted to be diagnostic for the presence of the *Bs3* resistance gene. Reciprocally all F<sub>2</sub> segregants that did not show an HR upon infection with AvrBs3 expressing *Xcv* showed only the longer PR-Bs3 amplicon that is derived from the susceptible parent ECW. Taken together marker PR-Bs3 allowed a clear co-dominant scoring of segregants that either contain or lack the *Bs3* resistance gene.

Next we wanted to clarify the diagnostic value of PR-Bs3 in a collection of pepper accessions from diverse geographic origin (Table 1). As positive controls we included in our analysis two *Capsicum* accessions that were shown previously to contain the *Bs3* gene (PI 640513 and PI 593597) (Römer et al. 2009b). In addition we tested 15 pepper accessions that did not show an HR upon inoculation with AvrBs3 expressing *Xcv* strains. All tested *Capsicum* genotypes showed a strict correlation between bacterial spot resistance and the presence of the smaller PCR fragment, indicative for the *Bs3* allele (Fig. 1b). This finding suggests that PR-Bs3 is a valuable tool to screen *Capsicum* germplasm for *Bs3* resistant accessions.

The diagnostic value of PR-Bs3 is based on a 13-bp insertion/deletion (InDel) polymorphism. Due to this polymorphism amplicons from *Bs3* resistant accessions are 13 bp shorter than amplicons from susceptible accessions. However, other InDel polymorphisms that are not functionally relevant in the context of *Bs3* resistance but that are within the marker locus PR-Bs3 could obviously affect the diagnostic value of PR-Bs3. Previously we identified one haplotype, present in *Capsicum* accessions CGN17230 and CGN17227, that contains an 11-bp deletion 16 bp 5' of the diagnostic 13-bp InDel polymorphism (Römer et al. 2009b). As a consequence of this 11-bp InDel polymorphism PR-Bs3 amplicons derived from the susceptible *Capsicum* accessions CGN17230 and CGN17227 are almost indiscernible to PR-Bs3 amplicons derived from *Bs3* resistant *Capsicum* accessions (see Fig. 1c). However, the 11-bp deletion results in the loss of an internal *Tsp509I* recognition sequence. Thus incubation of the PR-Bs3 amplicons with *Tsp509I* and subsequent agarose gel electrophoresis allowed a clear discrimination between amplicons from *Bs3* resistant accessions on one hand and the susceptible pepper accessions CGN17230 and CGN17227 on the other hand (Fig. 1c).



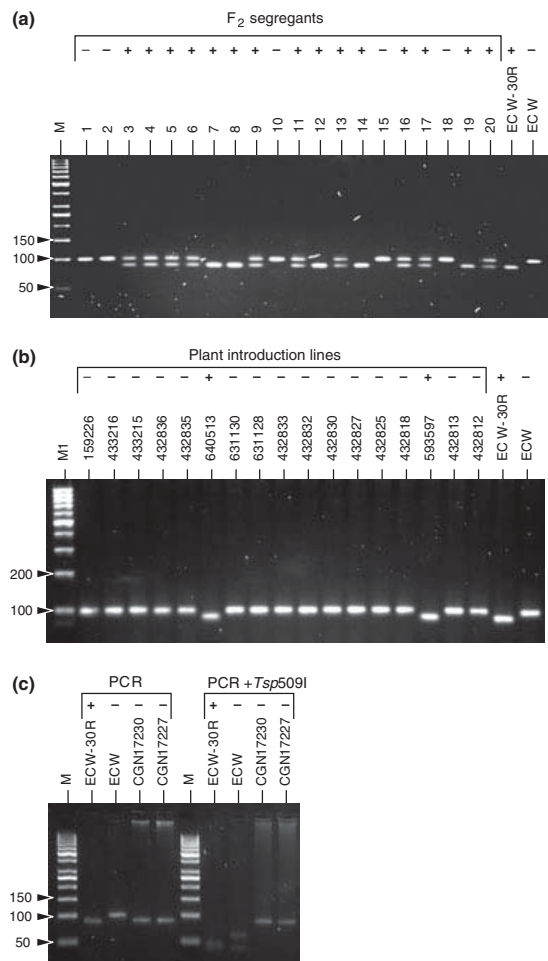


Fig. 1: The marker PR-Bs3 is diagnostic for *Bs3* resistant plants. (a) The DNA marker PR-Bs3 identifies *Bs3* resistant F<sub>2</sub> segregants in a co-dominant fashion. Ethidium bromide-stained 3% Metaphor agarose gel displaying PR-Bs3 amplicons derived from resistant (+) and susceptible (-) F<sub>2</sub> segregants (ECW × ECW-30R). ECW-30R, resistant parent; ECW, near-isogenic line of ECW-30R that lacks the *Bs3* allele. Amplification was carried out as described in materials and methods. M, GeneRuler 50 bp DNA Ladder (Fermentas, St. Leon-Rot, Germany). Arrowheads indicate DNA fragments of defined size in basepairs (bp). (b) The marker PR-Bs3 is diagnostic for *Bs3* resistant germplasm. Ethidium bromide-stained 3% Metaphor agarose gel displaying amplicons derived from different *Capsicum* accessions. Numbers on top denote the tested plant introduction lines. ECW-30R, resistant parent; (c) Similar-sized PCR products from *Bs3* and *bs3* accessions are diagnostic upon *Tsp509I* cleavage. Ethidium bromide-stained 3% Metaphor agarose of PR-Bs3 amplicons derived from the *Bs3* resistant line ECW-30R and the susceptible lines ECW, CGN17230 and CGN17227 (PCR). Differences in the amplicons of the *Bs3* resistant cultivar ECW-30R and the susceptible *Capsicum* accessions CGN17230 and CGN17227 are visible only upon cleavage of the PCR products with *Tsp509I* (PCR + *Tsp509I*). Plus (+) and minus (-) indicate plant genotypes that respond or do not respond with a hypersensitive response upon inoculation with *avrBs3* containing strains of *Xanthomonas campestris* pv. *vesicatoria*. Amplification was carried out as described in materials and methods. M, GeneRuler 50 bp DNA Ladder; M1, GeneRuler 100 bp DNA Ladder (Fermentas). Arrowheads indicate DNA fragments of defined size in base pairs (bp)

We have developed PR-Bs3, a co-dominant DNA marker that is diagnostic for the bacterial spot resistance gene *Bs3*. Primary motivation for developing this marker was to provide the basis for MAS of *Bs3*-mediated bacterial spot resistance. In the course of the map-based isolation of the pepper *Bs3* gene we developed a large number of DNA markers that were diagnostic between the pepper cultivar ECW-30R (*Bs3*) and the pepper accession PI-197409 (Pierre et al. 2000, Jordan et al. 2006) that were used for genetic mapping of the *Bs3* locus. To establish diagnostic markers for *Bs3*, we tested these markers on a collection of *C. annuum* cultivars that did not contain the *Bs3* gene. However the observed fragment patterns of all tested *C. annuum* cultivars were identical to the *Bs3* resistant cultivar ECW-30R and thus the markers were not diagnostic for *Bs3* resistance (data not shown).

Ideally diagnostic markers should detect polymorphisms that are connected to the function of the gene. Such functional nucleotide polymorphism (FNP) that differentiate resistant and susceptible genotypes have been established for the rice *xa5* (Iyer-Pascuzzi and McCouch 2007) the rice *Pi-ta* (Jia et al. 2002) and the wheat *Pm3* resistance gene (Tommasini et al. 2006). The development of a FNP requires that the gene that is responsible for the given trait has been isolated. The molecular isolation of the pepper *Bs3* gene (Römer et al. 2007) thus provided the basis to establish a FNP for *Bs3*.

The rice resistance *Xa27* is transcriptionally activated by the matching AvrBs3-like AvrXa27 protein from *Xanthomonas oryzae* pv. *oryzae* (*Xoo*) (Gu et al. 2005; Römer et al. 2009a). Furthermore it has been shown that both AvrBs3 and AvrXa27 bind to and activate the promoters of the matching *R* genes (Römer et al. 2009a). Thus it seems possible if not likely that the rice *R* genes *Xa7* and *Xa10* that mediate recognition of the AvrBs3-like AvrXa7 and AvrXa10 proteins from *Xoo* are also transcriptionally upregulated and that corresponding resistant and susceptible rice lines differ in the composition of their promoters. Thus in case of *R* genes that mediate recognition of AvrBs3-like proteins functionally, relevant promoter polymorphisms potentially provide a basis to establish diagnostic markers.

#### Acknowledgements

We would like to acknowledge contributions and technical support by C. Kretschmer, B. Rosinsky, S. Recht and M. Schulze. This work was supported by an EMBO short-term fellowship to T. J. (ASTF 54.00-03) and by grants from the "Exzellenznetzwerk Biowissenschaften" (Ministry of culture of Saxonia-Anhalt), the 2Blades Foundation and the Deutsche Forschungsgemeinschaft (SFB 648, SPP 1212 and LA1338/2-2) to T.L.

#### References

- Basim, H., G. V. Minsavage, R. E. Stall, J.-F. Wang, S. Shanker, and J. B. Jones, 2005: Characterization of a unique chromosomal copper resistance gene cluster from *Xanthomonas campestris* pv. *vesicatoria*. *Appl. Environ. Microbiol.* **71**, 8284–8291.
- Bonas, U., R. E. Stall, and B. Staskawicz, 1989: Genetic and structural characterization of the avirulence gene *avrBs3* from *Xanthomonas campestris* pv. *vesicatoria*. *Mol. Gen. Genet.* **218**, 127–136.
- Bonas, U., J. Conrads-Strauch, and I. Balbo, 1993: Resistance in tomato to *Xanthomonas campestris* pv. *vesicatoria* is determined by alleles of the pepper-specific avirulence gene *avrBs3*. *Mol. Gen. Genet.* **238**, 261–269.

- Canteros, B., G. Minsavage, U. Bonas, D. Pring, and R. Stall, 1991: A gene from *Xanthomonas campestris* pv. *vesicatoria* that determines avirulence in tomato is related to *avrBs3*. *Mol. Plant-Microbe Interact.* **4**, 628–632.
- Collard, B. C. Y., and D. J. Mackill, 2008: Marker-assisted selection: an approach for precision plant breeding in the twenty-first century. *Philos. Trans. R. Soc. B Biol. Sci.* **363**, 557–572.
- Edwards, K., C. Johnstone, and C. Thompson, 1991: A simple and rapid method for the preparation of plant genomic DNA for PCR analysis. *Nucl. Acids Res.* **19**, 1349.
- Gu, K., B. Yang, D. Tian, L. Wu, D. Wang, C. Sreekala, F. Yang, Z. Chu, G. L. Wang, F. F. White, and Z. Yin, 2005: *R* gene expression induced by a type-III effector triggers disease resistance in rice. *Nature* **435**, 1122–1125.
- Herbers, K., J. Conrads-Strauch, and U. Bonas, 1992: Race-specificity of plant resistance to bacterial spot disease determined by repetitive motifs in a bacterial avirulence protein. *Nature* **356**, 172–174.
- Iyer-Pascuzzi, A. S., and S. R. McCouch, 2007: Recessive resistance genes and the *Oryza sativa*-*Xanthomonas oryzae* pv. *oryzae* pathosystem. *Mol. Plant-Microbe Interact.* **20**, 731–739.
- Jia, Y. L., Z. H. Wang, and P. Singh, 2002: Development of dominant rice blast *Pi-ta* resistance gene markers. *Crop Sci.* **42**, 2145–2149.
- Jones, J. B., G. H. Lacy, H. Bouzar, R. E. Stall, and N. W. Schaad, 2004: Reclassification of the xanthomonads associated with bacterial spot disease of tomato and pepper. *Syst. Appl. Microbiol.* **27**, 755–62.
- Jordan, T., P. Römer, A. Meyer, R. Szczesny, M. Pierre, P. Piffanelli, A. Bendahmane, U. Bonas, and T. Lahaye, 2006: Physical delimitation of the pepper *Bs3* resistance gene specifying recognition of the AvrBs3 protein from *Xanthomonas campestris* pv. *vesicatoria*. *Theor. Appl. Genet.* **113**, 895–905.
- Kay, S., S. Hahn, E. Marois, G. Hause, and U. Bonas, 2007: A bacterial effector acts as a plant transcription factor and induces a cell size regulator. *Science* **318**, 648–651.
- Kearney, B., and B. J. Staskawicz, 1990: Widespread distribution and fitness contribution of *Xanthomonas campestris* avirulence gene, *avrBs2*. *Nature* **346**, 385–386.
- Minsavage, G., J. Jones, R. Stall, S. Miller, and D. Ritchie, 1999: Hypersensitive resistance in *Capsicum pubescens* PI 235047 to *Xanthomonas campestris* pv. *vesicatoria* (*Xcv*) is elicited by *avrBs3-2*. *Phytopathology* **89**, S53.
- Minsavage, G. V., D. Dahlbeck, M. C. Whalen, B. Kearny, U. Bonas, B. J. Staskawicz, and R. E. Stall, 1990: Gene-for-gene relationships specifying disease resistance in *Xanthomonas campestris* pv. *vesicatoria*-pepper interactions. *Mol. Plant-Microbe Interact.* **3**, 41–47.
- Pierre, M., L. Noël, T. Lahaye, A. Ballvora, J. Veuskens, M. Ganal, and U. Bonas, 2000: High-resolution genetic mapping of the pepper resistance locus *Bs3* governing recognition of the *Xanthomonas campestris* pv. *vesicatoria* AvrBs3 protein. *Theor. Appl. Genet.* **101**, 255–263.
- Römer, P., S. Hahn, T. Jordan, T. Strauß, U. Bonas, and T. Lahaye, 2007: Plant-pathogen recognition mediated by promoter activation of the pepper *Bs3* resistance gene. *Science* **318**, 645–648.
- Römer, P., S. Recht, and T. Lahaye, 2009a: A single plant resistance gene promoter engineered to recognize multiple TAL effectors from disparate pathogens. *Proc. Natl. Acad. Sci. USA*, **106**, 20526–20531.
- Römer, P., T. Strauß, S. Hahn, H. Scholze, R. Morbitzer, J. Grau, U. Bonas, and T. Lahaye, 2009b: Recognition of AvrBs3-like proteins is mediated by specific binding to promoters of matching pepper *Bs3* alleles. *Plant Physiol.* **150**, 1697–1712.
- Ronald, P. C., and B. J. Staskawicz, 1988: The avirulence gene *avrBs1* from *Xanthomonas campestris* pv. *vesicatoria* encodes a 50-kDa protein. *Mol. Plant-Microbe Interact.* **1**, 191–198.
- Stall, R. E., J. B. Jones, and G. V. Minsavage, 2009: Durability of resistance in tomato and pepper to xanthomonads causing bacterial spot. *Annu. Rev. Phytopathol.* **47**, 265–284.
- Swanson, J., B. Kearney, D. Dahlbeck, and B. J. Staskawicz, 1988: Cloned avirulence gene of *Xanthomonas campestris* pv. *vesicatoria* complements spontaneous race-change mutants. *Mol. Plant-Microbe Interact.* **1**, 5–9.
- Tai, T. H., D. Dahlbeck, E. T. Clark, P. Gajiwala, R. Pasion, M. C. Whalen, R. E. Stall, and B. J. Staskawicz, 1999: Expression of the *Bs2* pepper gene confers resistance to bacterial spot disease in tomato. *Proc. Natl. Acad. Sci. USA* **96**, 14153–14158.
- Tommasini, L., N. Yahiaoui, P. Srichumpa, and B. Keller, 2006: Development of functional markers specific for seven *Pm3* resistance alleles and their validation in the bread wheat gene pool. *Theor. Appl. Genet.* **114**, 165–175.
- Vauterin, L., B. Hoste, K. Kersters, and J. Swings, 1995: Reclassification of *Xanthomonas*. *Int. J. Syst. Bacteriol.* **45**, 472–489.
- Wichmann, G., and J. Bergelson, 2004: Effector genes of *Xanthomonas axonopodis* pv. *vesicatoria* promote transmission and enhance other fitness traits in the field. *Genetics* **166**, 693–706.

## 2.4.2 Zusammenfassung der Ergebnisse

Wie in den vorangegangenen Publikationen gezeigt werden konnte, bindet der TAL-Effektor AvrBs3 aus *Xcv* an ein 18-Bp langes Sequenzmotiv im *Bs3*-Promotor, das als  $UPT_{AvrBs3}$ -Box bezeichnet wird (Römer et al., 2007; Römer et al., 2009b). *Bs3*-Allele, die AvrBs3- bzw. AvrBs3 $\Delta$ rep16-Erkennung vermitteln, unterscheiden sich in einem 13-Bp Insertions-/Deletionspolymorphismus (InDel) im Promotor (Römer et al., 2007; Römer et al., 2009b). In der hier vorgelegten Veröffentlichung konnte gezeigt werden, dass dieser InDel im Promotor für die Differenzierung zwischen *Bs3*-resistenten und -suszeptiblen Pflanzen genutzt werden kann. Dafür erfolgte mit Hilfe von Oligonukleotiden, die die  $UPT_{AvrBs3}$ -Box flankieren die Generierung des PCR-gestützten Markers "PR-Bs3". Getestet wurde dieser PCR-Marker zunächst auf einer Population von 20 F<sub>2</sub>-Pflanzen aus einer Kreuzung von *Bs3*-resistenten (ECW-30R) und -suszeptiblen (ECW) *C. annuum* Pflanzen, die bezüglich der *Bs3*-Resistenz aufspalten. Dabei wurde festgestellt, dass der Marker "PR-Bs3" kodominant ist und zuverlässig zwischen homo- und heterozygoten *Bs3*-resistenten F<sub>2</sub>-Segreganten differenziert. Ein Test auf eine Auswahl von 17 Paprikaakzessionen zeigte außerdem, dass dieser Marker eine zuverlässige Identifizierung von AvrBs3-responsiven Akzessionen ermöglicht. Zusammenfassend konnte gezeigt werden, dass der etablierte DNA-Marker diagnostisch bezüglich AvrBs3-aktivierbarer *Bs3*-Allele ist.

## 2.5 Erstellung eines komplexen Promotors

### 2.5.1 Publikation 4

# A single plant resistance gene promoter engineered to recognize multiple TAL effectors from disparate pathogens

Patrick Römer, Sabine Recht, and Thomas Lahaye<sup>1</sup>

Institute of Biology, Department of Genetics, Martin-Luther-University Halle-Wittenberg, D-06099 Halle (Saale), Germany

Edited by Jeffery L. Dangl, University of North Carolina, Chapel Hill, NC, and approved October 2, 2009 (received for review August 6, 2009)

Plant pathogenic bacteria of the genus *Xanthomonas* inject transcription-activator like (TAL) effector proteins that manipulate the hosts' transcriptome to promote disease. However, in some cases plants take advantage of this mechanism to trigger defense responses. For example, transcription of the pepper *Bs3* and rice *Xa27* resistance (*R*) genes are specifically activated by the respective TAL effectors *AvrBs3* from *Xanthomonas campestris* pv. *vesicatoria* (*Xcv*), and *AvrXa27* from *X. oryzae* pv. *oryzae* (*Xoo*). Recognition of *AvrBs3* was shown to be mediated by interaction with the corresponding *UPT* (*UP*regulated by TAL effectors) box *UPT*<sub>AvrBs3</sub> present in the promoter *R* gene *Bs3* from the dicot pepper. In contrast, it was not known how the *Xoo* TAL effector *AvrXa27* transcriptionally activates the matching *R* gene *Xa27* from the monocot rice. Here we identified a 16-bp *UPT*<sub>AvrXa27</sub> box present in the rice *Xa27* promoter that when transferred into the *Bs3* promoter confers *AvrXa27*-dependent inducibility. We demonstrate that polymorphisms between the *UPT*<sub>AvrXa27</sub> box of the *AvrXa27*-inducible *Xa27* promoter and the corresponding region of the noninducible *xa27* promoter account for their distinct inducibility and affinity, with respect to *AvrXa27*. Moreover, we demonstrate that three functionally distinct *UPT* boxes targeted by separate TAL effectors retain their function and specificity when combined into one promoter. Given that many economically important xanthomonads deliver multiple TAL effectors, the engineering of *R* genes capable of recognizing multiple TAL effectors provides a potential approach for engineering broad spectrum and durable disease resistance.

*AvrBs3* | *AvrXa27* | transcription-activator like effector proteins | *Xanthomonas*

Plant pathogens are a major threat to crop production worldwide and durable disease resistance is a major goal in plant biotechnology (1–3). A key to achieving durable disease resistance is to elucidate the function of effector proteins that various microbial pathogens (bacteria, fungi, oomycetes, and nematodes) secrete into their hosts (4, 5). Although the primary function of microbial effectors is in virulence, some are known to trigger plant resistance (*R*) gene mediated resistance and have therefore been termed avirulence (*Avr*) proteins. For example, *AvrBs3* from the bacterial phytopathogen *Xanthomonas campestris* pv. *vesicatoria* (*Xcv*) confers both virulence (6) and avirulence (7). *AvrBs3*-like proteins have been identified in many pathovars of *Xanthomonas* (8) and *Ralstonia solanacearum* (9). Owing to their homology to eukaryotic transcription factors, *AvrBs3*-like proteins are also termed transcription-activator like (TAL) effectors (10–12). A characteristic central domain of TAL effectors is comprised of a variable number of tandemly-arranged, near-perfect copies of a 34/35-amino acid motif and determines virulence and avirulence specificity (8). In addition, TAL effector proteins generally contain C-terminal nuclear localization signals (NLSs) and an acidic transcriptional activation domain (AAD) (8, 11–13). The repeat domain of the TAL effector *AvrBs3* interacts with a corresponding *UPA* (*UP*regulated by *AvrBs3*) box in the promoter of the pepper transcription

factor *UPA20*, which induces hypertrophy (i.e., enlargement) of mesophyll cells, as well as to the promoters of other host genes that appear to contribute to susceptibility (14). In addition, *AvrBs3* triggers a programmed cell death response, referred to as the hypersensitive response (HR), in pepper plants that contain the cognate *R* gene *Bs3* (15, 16). Certain pepper lines have an allele of *Bs3* known as *Bs3-E*, which confers resistance to strains carrying the *AvrBs3* derivative *AvrBs3Δrep16* that has a deletion of repeat units 11–14 (15, 17). *AvrBs3* and *AvrBs3Δrep16* were found to interact specifically with distinct boxes in the *Bs3* and *Bs3-E* promoters, respectively (16). For clarity we herein refer to these binding sites collectively as *UPT* (*UP*regulated by TAL effectors), with a subscript designation for the specific TAL effector that targets it. Interaction of *AvrBs3* or *AvrBs3Δrep16* with their respective *UPT* sites, *UPT*<sub>AvrBs3</sub>, and *UPT*<sub>AvrBs3Δrep16</sub>, induces transcription of the *Bs3* or *Bs3-E* coding sequence (cgs), leading to HR. Previously we analyzed multiple *in vitro* generated *UPT*<sub>AvrBs3</sub> box mutants and uncovered three *AvrBs3Δrep16* inducible box derivatives (16). Notably, the recognition specificity of the mutated boxes always correlated with a loss of the *AvrBs3* mediated inducibility and did not result in *UPT* boxes with dual recognition specificity.

Transcription of the rice *R* gene *Xa27* is specifically induced by *AvrXa27*, a TAL effector from *X. oryzae* pv. *oryzae* (*Xoo*) (18). The products of rice *Xa27* and pepper *Bs3* share no sequence homology. However, transcriptional activation of these *R* genes by their matching TAL effectors suggests that this mechanism of disease resistance is common to both mono- and dicotyledonous plant species.

In the present study, we wanted to clarify if activation of the rice *Xa27* promoter by the matching *Xoo* TAL effector *AvrXa27* is mechanistically similar to activation of the pepper *Bs3* promoter by the *Xcv* TAL effector *AvrBs3*. Furthermore we test if *UPT* boxes matching distinct TAL effectors retain their specificity and functionality when combined into one complex promoter.

## Results

**The Pepper *Bs3* and Rice *Xa27* Resistance Genes Use Identical Mechanisms for Detection of Their Matching TAL Effectors.** Previously we showed that *AvrBs3* binds to the pepper *Bs3* promoter, resulting in transcriptional activation of the *Bs3* cgs and subsequent triggering of HR (15, 16). In the current study, we investigated if the combination of the *Xcv* *AvrBs3* protein and the pepper *Bs3* promoter can be functionally substituted by the *Xoo* *AvrXa27* protein and the rice *Xa27* promoter to facilitate *Bs3* gene

Author contributions: P.R. and T.L. designed research; P.R. and S.R. performed research; and P.R. and T.L. wrote the paper.

The authors declare no conflict of interest.

This article is a PNAS Direct Submission.

Freely available online through the PNAS open access option.

<sup>1</sup>To whom correspondence should be addressed. E-mail: lahaye@genetik.uni-halle.de.

This article contains supporting information online at [www.pnas.org/cgi/content/full/0908812106/DCSupplemental](http://www.pnas.org/cgi/content/full/0908812106/DCSupplemental).

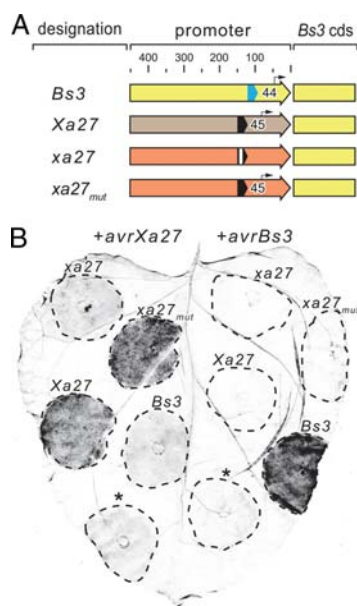


**Fig. 1.** AvrXa27 activates the rice *Xa27* promoter and triggers a *Bs3*-dependent HR in *N. benthamiana*. (A) Graphical representation of constructs used for promoter analysis. The *Bs3*, *Xa27*, *xa27*, and the *xa27*<sup>mut</sup> promoters are displayed as yellow, brown, and orange arrows, respectively. A yellow box represents the *Bs3* cds. The *UPT*<sub>AvrBs3</sub> and *UPT*<sub>AvrXa27</sub> boxes are shown as blue and black boxes, respectively. A black box with a white bar represents the *UPT*<sub>AvrXa27+</sub> box of the *xa27* promoter. Black arrows represent transcription start sites (TSS). The scale indicates distances from the ATG start codon. Numbers below the arrows denote the distances between the 3' end of a *UPT* box and its TSS. The *Bs3* cds is not drawn to scale. (B) The promoter-*Bs3* cds and the 35S promoter-driven *avr* constructs (*avrXa27* [Left] or *avrBs3* [Right]) were expressed transiently in *N. benthamiana* leaves via *A. tumefaciens*. Asterisks (\*) mark areas in which the *avr* construct but no promoter construct was infiltrated. Dashed lines mark the inoculated areas. Four days after infiltration, the leaves were cleared with ethanol to visualize the HR (dark areas).

activation. To do so, we placed the *Bs3* cds under transcriptional control of the rice *Xa27* or the rice *xa27* promoter and tested if these genes were transcriptionally activated by AvrXa27. The constructs (Fig. 1A) were cloned into a plant transformation vector and delivered into *Nicotiana benthamiana* leaves using *Agrobacterium tumefaciens* mediated transient transformation, along with *avrXa27* or *avrBs3* genes driven by the constitutive cauliflower mosaic virus 35S (35S) promoter (Fig. 1B). In previous studies, *Xa27* but not *xa27* was found to be transcriptionally activated by *Xoo* strains delivering AvrXa27 (18). Consistent with this observation, we found that delivery of *avrXa27* triggered HR in *N. benthamiana* only in the presence of the *Xa27* promoter-driven *Bs3* cds, but not in the presence of the *xa27* promoter-driven *Bs3* cds. Furthermore, delivery of the *Xa27* promoter-driven *Bs3* cds did not mediate an HR when coexpressed with *avrBs3* (Fig. 1B), confirming that recognition was specific for the particular promoter-TAL effector combination, despite >90% identity between the AvrBs3 and AvrXa27 proteins (8). In summary, these findings demonstrate that the combination of the *Xcv* TAL effector AvrBs3 and the pepper *Bs3* promoter can be functionally replaced by the *Xoo* TAL effector AvrXa27 and the rice *Xa27* promoter to activate expression of the *Bs3* cds.

#### Functionally-Relevant Nucleotide Polymorphisms Between the *Xa27* and *xa27* Promoters Are Located Adjacent to the Predicted TATA Box.

The promoters of the pepper *Bs3* and *Bs3-E* genes differ by a single 13-bp insertion-deletion (InDel) polymorphism that determines the recognitional specificity of the *R* genes (Fig. S1) (15). In contrast, the 1.5 kb putative promoter regions of the rice *Xa27* and the *xa27* alleles differ by 16 polymorphisms (Figs. S2 and S3). Because the *Bs3/Bs3-E* InDel is located in the vicinity of the TATA box (Fig. S1), we hypothesized that the functionally relevant *Xa27/xa27* promoter polymorphism might have a similar location. Using site-directed mutagenesis, we replaced the polymorphic nucleotides adjacent to the TATA box (one 3-bp InDel polymorphism and an adenine to cytosine substitution) (Fig. S2) in the *xa27* promoter by the corresponding nucleotides from the *Xa27* promoter. The mutated *xa27* promoter (*xa27*<sup>mut</sup>) was fused to the *Bs3* cds and the transgene coexpressed with *avrXa27* or *avrBs3*. The *xa27*<sup>mut</sup> promoter construct triggered HR in *N. benthamiana* when codelivered with *avrXa27*, but not when codelivered with *avrBs3* (Fig. 1B). This indicates that the *xa27*<sup>mut</sup> promoter is functionally identical to the *Xa27* promoter and that the specificity-determinant in the *Xa27/xa27* promoter is located adjacent to the predicted TATA box. Furthermore, these observations suggest that the *xa27* promoter region containing the polymorphisms constitutes the *UPT*<sub>AvrXa27</sub> box.

#### The *UPT*<sub>AvrXa27</sub> Box from the Rice *Xa27* Promoter Retains Its Function in the Context of the Pepper *Bs3* Promoter.

Previously we delimited the *UPT*<sub>AvrBs3</sub> box of the *Bs3* promoter to an interval of 18 nucleotides and showed that the box retains its function if placed at different positions within the promoters of the pepper *Bs3* or tomato *Bs4* genes (16). Here, we wanted to test if the *UPT*<sub>AvrXa27</sub> box from the *Xa27* promoter retains its function when transferred into another promoter context. To this end, we introduced the regions encompassing the *UPT*<sub>AvrXa27</sub> box of *Xa27* or the *UPT*<sub>AvrXa27+</sub> box of *xa27* into the *Bs3* promoter and inserted these sequences in front of the *Bs3* cds (Fig. 2A). The former transgene (*Xa27/Bs3* [*UPT*<sub>AvrXa27</sub> box of *Xa27* in *Bs3* promoter]) mediated HR in *N. benthamiana* when cotransformed with the *avrXa27* gene (Fig. 2B). In contrast, cotransformation with the other construct containing the *UPT*<sub>AvrXa27+</sub> box of *xa27* in the *Bs3* promoter (*xa27/Bs3*) did not trigger an AvrXa27 dependent HR (Fig. 2B). These data demonstrate that the *UPT*<sub>AvrXa27</sub> box can function within different promoter contexts, like the *UPT*<sub>AvrBs3</sub> box and that the *Xa27* promoter but not the *xa27* promoter contains a functional *UPT*<sub>AvrXa27</sub> box.

#### The *UPT*<sub>AvrXa27</sub> Minimal Box Covers 16 Bps.

Next we determined the boundaries of the *UPT*<sub>AvrXa27</sub> box by deletion analysis. Of the constructs containing 5' deletions of the *UPT*<sub>AvrXa27</sub> box, A-03, A-06, and A-09 still triggered an AvrXa27 dependent HR in *N. benthamiana*, while A-12 did not (Fig. 2B). Of the constructs containing 3' deletions, B-03, B-06, B-09, B-10, and B-12 triggered an AvrXa27 dependent HR, while B-13 did not (Fig. 2B). As a result of this deletion analysis, the *UPT*<sub>AvrXa27</sub> box was delimited to 16 nucleotides (Fig. 2A).

#### AvrXa27 Binds with High and Low Affinity to the *Xa27* and *xa27* Promoters, Respectively.

Next we wanted to investigate why AvrXa27 activates the *Xa27* promoter but not the *xa27* promoter. Electrophoretic mobility shift assays (EMSAs) with a N-terminal 6xHistidine (His)-tagged AvrXa27 fusion protein and biotin-labeled *Xa27* and *xa27* promoter fragments (Fig. 3A and Fig. S4) showed that AvrXa27 indeed binds with high affinity to the *Xa27* promoter fragment and with much lower affinity to the *xa27* promoter fragment (Fig. 3B). Importantly, binding of AvrXa27 to labeled *Xa27* promoter fragments could be readily out-competed by nonlabeled *Xa27* promoter fragments, whereas even a 100-fold excess of nonlabeled *xa27* promoter fragments could not out-compete the binding (Fig. 3B). These data demonstrate that AvrXa27 has a significantly higher affinity to the *Xa27* promoter

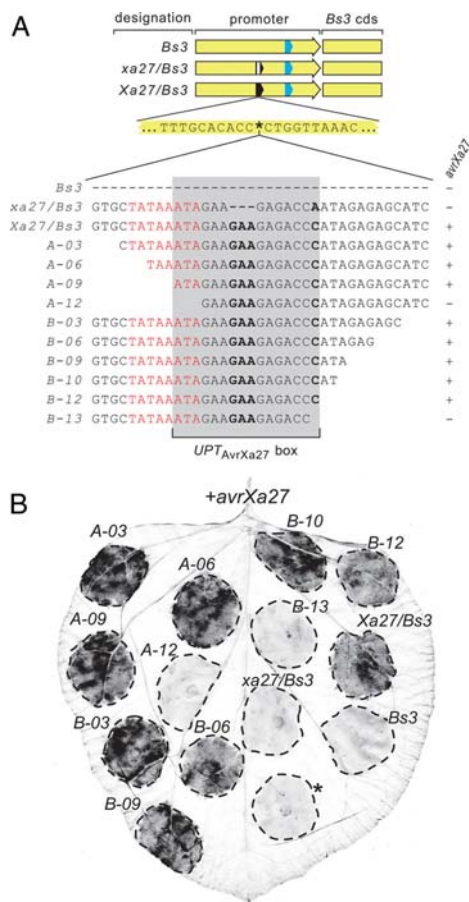


**Fig. 2.** A 16-bp fragment of the rice *Xa27* promoter mediates transcriptional activation via *AvrXa27*. (A) Graphical representation of the analyzed promoter constructs. Yellow arrows and boxes represent the *Bs3* promoter and cds, respectively. The *UPT<sub>AvrBs3</sub>* and *UPT<sub>AvrXa27</sub>* boxes are shown as blue and black boxes, respectively. A black box with a white bar marks the *UPT<sub>AvrXa27</sub>* box of the *xa27* promoter. Letters on yellow background represent *Bs3* promoter sequence. The asterisk (\*) marks the position where *Xa27/xa27* promoter sequences were inserted. Bold-face black letters mark nucleotide polymorphisms between *Xa27* and *xa27*. Red letters mark the predicted TATA box. The gray background highlights the minimal *UPT<sub>AvrXa27</sub>* box. “+” and “-” indicates the presence or absence of an HR in *N. benthamiana* upon codelivery of 35S promoter-driven *avrXa27* gene. (B) *In planta* analysis of *UPT<sub>AvrXa27</sub>* box deletion constructs. Promoter constructs were delivered together with a 35S promoter-driven *avrXa27* gene via *A. tumefaciens* into *N. benthamiana* leaves. Asterisks mark areas where only the *avr* but no *R* promoter constructs were infiltrated. Dashed lines mark the inoculated areas. Four days after inoculation, the leaves were harvested and cleared with ethanol to visualize the HR (dark areas).

than to the *xa27* promoter. It is likely that these differing affinities of *AvrXa27* for the *Xa27* or *xa27* promoters provide the molecular basis for the specificity of promoter activation.

**AvrXa27 Binds to the Rice *Xa27* Promoter But Not to the Pepper *Bs3* Promoter.** We demonstrated that the *Xcv* TAL effector *AvrBs3* and the *Xoo* TAL effector *AvrXa27* specifically activate the pepper *Bs3* and the rice *Xa27* promoters, respectively (Figs. 1 and 2). Further EMSA experiments were undertaken to clarify if promoter activation specificity is due to interaction of the TAL

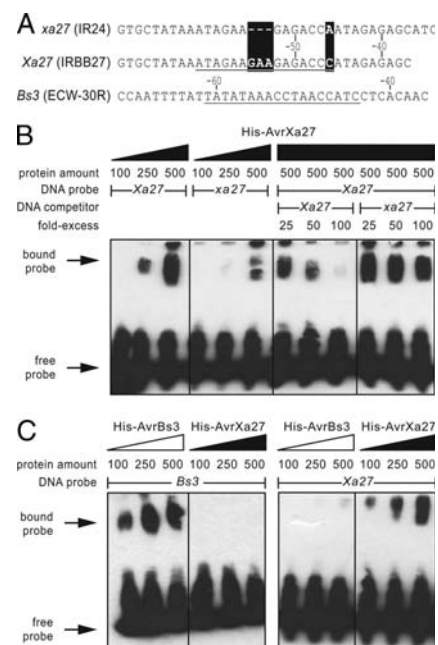


**Fig. 3.** *AvrXa27* binds specifically to the *Xa27* promoter. (A) Probes derived from *Xa27*, *xa27*, and *Bs3* promoters used in EMSAs. Numbering is relative to the transcription start site (TSS). The polymorphisms between the *Xa27* and *xa27* promoter are shown by white letters and black background. The *UPT<sub>AvrXa27</sub>* box of the *Xa27* and the *UPT<sub>AvrBs3</sub>* box of the *Bs3* promoter are underlined (B) *AvrXa27* binds with high and low affinity to the *Xa27* and *xa27* promoters, respectively. EMSA with *AvrXa27* and *Xa27*- or *xa27*-derived probes and competition experiment between *AvrXa27* and different amounts (in fmol) of a nonlabeled competitor probe in a 6% nondenaturing polyacrylamide gel. Positions of the bound and free probe are indicated on the left. (C) *AvrXa27* and *AvrBs3* bind specifically to the *Xa27* and *Bs3* promoters, respectively. EMSA with *AvrBs3* and *AvrXa27* and *Xa27*- and *Bs3*-derived probes in a 6% nondenaturing polyacrylamide gel. Protein amounts are in fmol. Positions of the bound and free probe are indicated on the left.

effectors with their matching plant promoters. These experiments demonstrated that *AvrBs3* interacts with the pepper *Bs3* promoter but not with the rice *Xa27* promoter (Fig. 3C). Conversely, *AvrXa27* interacted with the rice *Xa27* promoter but not the pepper *Bs3* promoter (Fig. 3C). These data indicate that specific binding to the promoter is the basis for promoter activation in the *AvrBs3-Bs3* and the *AvrXa27-Xa27* promoter interactions.

**UPT Boxes Matching to Distinct TAL Effectors Retain Their Function When Combined into One Complex Promoter.** The finding that the *UPT<sub>AvrBs3</sub>* and *UPT<sub>AvrXa27</sub>* boxes can each retain their functions when moved into another promoter suggested that it might be possible to combine functionally distinct *UPT* boxes to generate a single promoter capable of recognizing multiple *Avr* proteins. The *Bs3* promoter constructs used to delimit the *UPT<sub>AvrXa27</sub>* box provided an opportunity to test this hypothesis, because these constructs also contain an *UPT<sub>AvrBs3</sub>* box (Fig. 2A). All of these constructs produced an HR in *N. benthamiana* when coexpressed with *avrBs3*, irrespective of which *Xa27* or *xa27* promoter fragment was inserted into the *Bs3* promoter (Fig. S5), demonstrating that *UPT* boxes with distinct TAL effector specificities can indeed be combined into one complex promoter.

We further explored this concept by introducing the *UPT<sub>AvrXa27</sub>* box from the rice *Xa27* promoter, the *UPT<sub>AvrXa27</sub>* box

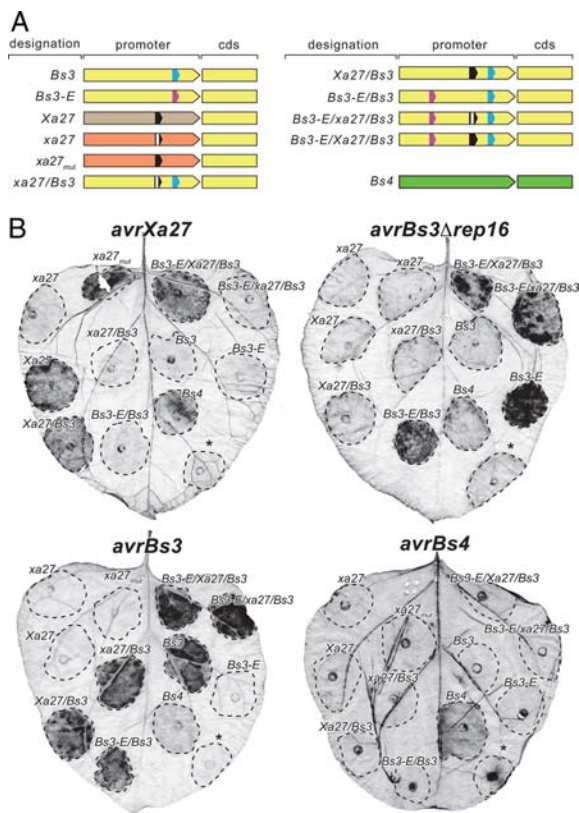


**Fig. 4.** Tandemly-arranged *UPT* boxes with distinct TAL effector specificity retain their function when combined into a single promoter. (A) Graphical representation of promoter constructs. Yellow arrows and boxes represent the promoters and cds, respectively of the *Bs3* and *Bs3-E* genes. *Bs3* and *Bs3-E* promoters differ only in their *UPT* boxes and are therefore displayed in identical color. Green, brown, and orange color represents the promoters (arrows) and cds (boxes) of the tomato *Bs4*, rice *Xa27*, and rice *xa27* genes, respectively. Pink, black and blue boxes represent the *UPT*<sub>AvrBs3Δrep16</sub>, *UPT*<sub>AvrXa27</sub>, and *UPT*<sub>AvrBs3</sub> boxes, respectively. The black box with the white vertical line represents the nonfunctional *UPT*<sub>AvrXa27\*</sub> box of the rice *xa27* gene. With exception of the *Bs3* cds all elements are drawn to scale. (B) *In planta* analysis of the promoter constructs. The promoter constructs depicted in (A) were codelivered together with 35S promoter-driven *avr* genes into *N. benthamiana* leaves (displayed in boldface letters above each leaf) via *A. tumefaciens*. Asterisks (\*) mark areas in which *A. tumefaciens* containing only a TAL effector gene were infiltrated. Dashed lines mark the inoculated areas. Four days after inoculation, the leaves were harvested and cleared with ethanol to visualize the HR (dark areas).

from the rice *xa27* promoter and the *UPT*<sub>AvrBs3Δrep16</sub> box from the pepper *Bs3-E* promoter, alone or in different combinations, into the pepper *Bs3* promoter containing the *UPT*<sub>AvrBs3</sub> box, and inserted these promoters in front of the *Bs3* cds (Fig. 4A). We used *A. tumefaciens* mediated delivery in *N. benthamiana* leaves to study recognition specificity of these promoter constructs and found that *avrBs3*, *avrBs3Δrep16*, and *avrXa27* triggered an HR only when coexpressed with the *R* gene constructs containing the matching *UPT* boxes (Fig. 4B). For example, AvrBs3 triggered HR in combination with the promoter constructs *Bs3*, *xa27/Bs3*, *Xa27/Bs3*, *Bs3-E/Bs3*, *Bs3-E/Xa27/Bs3*, and *Bs3-E/xa27/Bs3* but not in combination with the promoter constructs *xa27*, *xa27<sub>mut</sub>*, *Xa27*, and *Bs3-E*. None of the promoter constructs produced an HR in combination with AvrBs4 (Fig. 4B), which is 96.6%

identical to AvrBs3 (8). As expected however, *avrBs4* triggered an HR when expressed with its cognate *R* gene *Bs4* (Fig. 4B), which encodes a nucleotide-binding site (NB) leucine rich repeat (LRR) type tomato R protein (19).

We have shown that the placement of the *UPT*<sub>AvrBs3</sub> box determines the position of the transcription start site (TSS), such that the distance between the TSS and the 3' end of *UPT*<sub>AvrBs3</sub> box remains approximately constant (16). On this basis, we anticipated that the complex *Bs3-E/Xa27/Bs3* promoter containing the *UPT*<sub>AvrBs3Δrep16</sub>, *UPT*<sub>AvrXa27</sub>, and *UPT*<sub>AvrBs3</sub> boxes would produce different TSSs in combination with the respective TAL effectors AvrBs3Δrep16, AvrXa27, and AvrBs3. Rapid amplification of cDNA ends (RACE) showed that the TSSs of the *Bs3-E/Xa27/Bs3* promoter was 311-, 119-, and 59-bp upstream of ATG start codon when coexpressed with AvrBs3Δrep16, AvrXa27, and AvrBs3, respectively (Figs. S6 and S7). The distances between the 3' end of the *UPT* boxes and the given TSSs was 45- to 46-, 53- to 54-, and 44-bp for AvrBs3Δrep16, AvrXa27, and AvrBs3, respectively. Notably, these distances observed with the complex *Bs3-E/Xa27/Bs3* promoter were not significantly different from the respective distances observed with the native *Bs3-E*, *Xa27*, and the *Bs3* promoters (Table S1), indicating that the position of the *UPT* boxes rather than the promoter context defines the TSSs. Taken together, our data indicate that *UPT* boxes from different plant promoters can be assembled *in vitro* into one complex promoter in which each *UPT* box retains its TAL effector specificity.

## Discussion

**Promoter-Activation Mediated Recognition-The Default Mechanism of Plant R Genes to Detect Matching TAL Effectors?** We have studied the molecular basis of how the TAL effector proteins AvrBs3, AvrBs3Δrep16, and AvrXa27 are recognized by the pepper *Bs3*, *Bs3-E*, and rice *Xa27* *R* genes. We determined that these *R* genes contain distinct promoter motifs (*UPT* boxes) that are the site of direct physical interaction with and activation by the matching TAL effector proteins. Notably, neither the *UPT* boxes nor the coding regions of pepper *Bs3* and rice *Xa27* share any sequence homology, indicating that this mechanism of disease resistance evolved independently in both mono- and dicotyledonous plant species.

With the mechanism of activation elucidated, it is now evident why mutant derivatives of AvrBs3 and AvrXa27 lacking either the NLS or AAD domains fail to activate the *Bs3* and *Xa27* mediated defense response (18, 20). The dominantly inherited TAL effector *R* genes *Xa7* and *Xa10*, from rice, also recognize TAL effector proteins but not their NLS and AAD mutant derivatives (21, 22). Thus, *Xa7* and *Xa10*, and possibly other TAL effector *R* genes, maybe transcriptionally activated by their matching TAL effectors as is the case for pepper *Bs3* and rice *Xa27*.

Transcriptional activation of *R* promoters is possibly the default mechanism for recognition of TAL effectors by plant immune systems. However, a notable aberration is the tomato *R* gene *Bs4* that mediates recognition of but is not transcriptionally activated by the matching TAL effector AvrBs4 (19, 23). Yet, tomato *Bs4* is clearly an exceptional case since it is the only known plant *R* gene that mediates recognition of NLS-deprived TAL effector mutants (19, 24).

A notable peculiarity of the *Bs3* and *Xa27* proteins is that they lack any sequence homology to each other or to NB-LRR type *R* proteins, which appear to represent the most common type of *R* proteins. Although rice *Xa7* and *Xa10* are not isolated yet, the physical genomic intervals that contain these *R* genes have been defined (25, 26). Notably, these intervals lack any genes for NB-LRR proteins or proteins resembling pepper *Bs3* or rice *Xa27* (25, 26). Thus it seems that TAL effector *R* proteins are structurally extraordinarily diverse.

These mechanistic insights into how plant *R* genes mediate

recognition of matching TAL effectors suggests alternate cloning strategies for this type of *R* gene. For example, transcript profiling could be used to identify candidate *R* genes by virtue of the fact that they are upregulated only upon delivery of a corresponding TAL effector. Chromatin immunoprecipitation (ChIP) and yeast-one hybrid (Y1H) screens might be complementary approaches to identify TAL effector *R* gene candidates since our studies have shown that a strong interaction between TAL effector and matching *UPT* box is a prerequisite for transcriptional activation of the *Bs3* and *Xa27* promoter (Fig. 3). In summary, differential transcript profiling, Y1H screens, and ChIP technology may provide shortcuts to laborious positional cloning methods for the isolation of plant *R* genes that mediate recognition of TAL effectors.

**Recognition of Multiple Pathogen Races Can Be Achieved via a Single Construct.** Most plant *R* genes are transcribed constitutively and encode NB-LRR proteins that mediate both the recognition of effector proteins, as well as the execution of the defense response. In contrast, the pepper *Bs3* and rice *Xa27* *R* genes show a separation of these functions, since recognition of the microbial effectors is mediated through interaction with the *UPT* box promoter elements, while instigation of the plant's defense response is carried out by the *Bs3* and *Xa27* proteins. Given that TAL effector *R* proteins are involved only in the execution of the defense response, but not in Avr perception, may explain their high structural diversity. The molecular basis of NB-LRR mediated Avr recognition is so far poorly elucidated and it has not been possible to combine multiple Avr specificities into one NB-LRR protein. However, with TAL effectors we have now demonstrated that the *UPT* boxes of three distinct *R* genes can be combined into one complex *R* promoter (Fig. 4). A priori, there is no reason to suspect that more than three *UPT* boxes could not be functionally combined into one complex promoter. Furthermore our approach does not necessarily rely on *UPT* boxes from known *R* gene promoters. For example, the *Xoo* TAL effectors PthXo1, PthXo6, and PthXo7 transcriptionally activate the rice *Os8N3*, *OsTFX1*, and *OsTFIIAγ1* genes in the context of a compatible interaction (27, 28) and thus, these promoters are likely to contain matching *UPT* boxes that can be combined into complex *R* gene promoters. Most recent studies also uncovered how target DNA-specificity of TAL effectors is encoded (29, 30) and thus *UPT* boxes can now also be predicted *in silico*, which substantially simplifies the generation of complex promoters. Because several economically significant xanthomonads including *Xoo*, *X. oryzae* pv. *oryzicola*, and *X. citri* contain multiple TAL effectors it would appear feasible to engineer such a complex *R* promoter to confer potentially durable disease resistance.

## Materials and Methods

**Generation of Expression Clones Containing the *Bs3* Gene with Promoter Regions of *Xa27* and *xa27*.** The *Xa27* and the *xa27* promoters were PCR-amplified from genomic rice DNA of the cultivar IRBB27 and IR24, respectively. The amplification was carried out with *Phusion* high-fidelity DNA polymerase (New England Biolabs) and the primers *Xa27*-01-fwd-CACC-PR (CACCTG-CAGCTGAACCAACAGTTTGTAGCTCCATCG) and *Xa27*-01-rev-PR (CACACT-GAGACACCAAGAAGCTGCCTCC). The PCR fragments were cloned into pENTR-D (Invitrogen), sequenced and transferred into the binary-vector pK7-GW-Bs3 (16) by LR recombination (Invitrogen). The promoter *xa27*<sub>mut</sub> was created by *Phusion* site directed mutagenesis kit (New England Biolabs) using the primers *Xa27*-mut-01-fwd-PR (AGTGCTATAAATAGAAGAAGAGAC-CCATAG) *Xa27*-mut-01-rev-PR (AGTAGTCGTAGTCAACCAATTCACAAG), that are phosphorylated at their 5' termini. After sequencing the construct was transferred via LR-recombination in the binary vector pK7-GW-Bs3. pK7-GW-Bs3-derivatives were transformed into *A. tumefaciens* GV3101 (32) for transient expression assays.

**Insertion and Limitation of *UPT* Boxes.** For the insertion of the *UPT*<sub>AvrXa27</sub> box, the *UPT*<sub>AvrXa27+</sub> box and the *UPT*<sub>AvrBs3.3rep16</sub> box 5' upstream of the *UPT*<sub>AvrBs3</sub> box we used the *Phusion* site directed mutagenesis kit (New England Biolabs). As template we used a pENTR-D, which contains *Bs3* promoter and coding sequence (15). For the insertion of the *UPT*<sub>AvrXa27</sub> box and the *UPT*<sub>AvrXa27+</sub> box we used the primers *Xa27*-IRBB27inBs3-02-fwd-PR (GTGCTATAAATAGAA-GAAGAGACCCATAGAGAGCATCTGGTTAAACAATGAACACGTTTG) and *xa27*-IR24inBs3-01-fwd-PR (GTGCTATAAATAGAAGAAGACCAATAGAGAG-CATCTGGTTAAACAATGACACGTTTG) in combination with the primer *xa27*-in3-01-rev-PR (GGTGTGCAAATGTGGTTAAACCATAAACTG). For the insertion of the *UPT*<sub>AvrBs3.3rep16</sub> box we used the primers 293-bp-ECW-01-fwd-PR (CAATTTTATATATAAACTCTCTATTCCTAAACCATCCTCAC-ACCAAGTAAACTCAAAGAATAATCATTGAAC) and box-02-293-rev-PR (CATACTAATTCATATTTCCCTGCATAAG). The limitation of the *UPT*<sub>AvrXa27</sub> box was done using a pENTR-D, which contains the *Bs3* promoter with the inserted *UPT*<sub>AvrXa27</sub> box and the *Bs3* coding sequence. The limitation of the 5' parts of the *UPT*<sub>AvrXa27</sub> box was also done by site directed mutagenesis using the primers *Xa27*-Mut-A-3bp-fwd-PR (CTATAAATAGAAGAAGAGAGAC-CCATAG), *Xa27*-Mut-A-6bp-fwd-PR (TAAATAGAAGAAGAGACCCATA-GAGAG), *Xa27*-Mut-A-9bp-fwd-PR (ATAGAAGAAGAGACCCATAGAG), *Xa27*-Mut-A-12bp-fwd-PR (GAAGAAGAGACCCATAGAGAG) in combination with the primer *Xa27*-Mut-A-01-rev-PR (GGTGTGCAAATGTGGTTAAACCC). The limitation of the 3' parts of the *UPT*<sub>AvrXa27</sub> box was done by site directed mutagenesis using the primers *Xa27*-Mut-B-3bp-rev-PR (GCCTCTAT-GGGTCTCTCTTC), *Xa27*-Mut-B-6bp-rev-PR (CTCTATGGGTCTCTCTTC), *Xa27*-Mut-B-9bp-rev-PR (TATGGGTCTCTCTCTCTATTATAGCAC), *Xa27*-Mut-B-12bp-rev-PR (GGGTCTCTCTCTCTATTATAGCAC) in combination with the primer *Xa27*-Mut-B-02-fwd-PR (CTGGTTAAACCAATGAACACGTTTGCC). All primers used are phosphorylated at their 5' termini. After sequencing the constructs were transferred by LR-recombination in the binary-vector pGWB1 (31). pGWB1-derivatives were transformed into *A. tumefaciens* GV3101 for transient expression assays.

**A. *tumefaciens* Mediated Transient Expression in *N. benthamiana*.** *Agrobacterium* strains were grown overnight in yeast extract broth (YEB) medium (5 g bacto beef extract, 1 g bacto yeast extract, 5 g bacto peptone, 5 g sucrose, and 2 mM MgSO<sub>4</sub>, pH 7.2, per liter) containing 100 µg/mL each of rifampicin and kanamycin, collected by centrifugation, resuspended in inoculation medium (10 mM MgCl<sub>2</sub>, 5 mM Mes, pH 5.3, 150 µM acetosyringone) and adjusted to an OD<sub>600</sub> of 0.8. Equal amounts of *A. tumefaciens* strains containing a 35S-promoter driven TAL effector gene and a given promoter construct (fused to the *Bs3* coding sequence) were mixed and infiltrated into *N. benthamiana* leaves by blunt-end syringe infiltration. Leaves were harvested about 4 days post infiltration. For better visualization of the HR, leaves were cleared by incubation in ethanol at 60°C and were dried and photographed.

**Electrophoretic Mobility Shift Assay (EMSA).** EMSAs were done as described earlier (15) with the difference that we used a N-terminal 6xHistidine (His) tag instead of a N-terminal GST tag for purification of TAL effector proteins. TAL effector proteins were purified from *E. coli* BL21-AL with Ni-NTA agarose (Qiagen).

**Generation of a Binary Vector that Contains an *avrXa27* Gene.** For the generation of a binary vector that contains *avrXa27* we used a pKSAvrXa27 (provided by Zhongchao Yin, Temasek, Life Sciences Laboratory) that contains *avrXa27*. From this vector we amplified the C-terminal *Bam*HI-fragment with the *Phusion* high-fidelity DNA polymerase (New England Biolabs) using the primers *Bam*HI+CACC+ATG-01-fwd-PR CACCATGGATCCTGGTACGCC-CATCGCTGCCGA and *Bam*HI-02-rev-woS-PR GATCGTCCCTCCGACTGAGCT-GACTGAG. The amplified fragment that is flanked by *Bam*HI sites was cloned into pENTR-D (Invitrogen), resulting in pENTR-D-*Bam*HI-*avrXa27*. After sequencing, the *Bam*HI fragment of pKSAvrXa27 was transferred into pENTR-D-*Bam*HI-*avrXa27* resulting in the pENTR-D-*avrXa27*. The *avrXa27* gene was then transferred via LR recombination in the binary vectors pGWB2 or pGWB5 (31). pGWB2 and pGWB5-derivatives were transformed into *A. tumefaciens* GV3101 for transient expression assays. For EMSA we transferred *avrXa27* from pENTR-D-*avrXa27* via recombination into pDEST17 (Invitrogen).

**ACKNOWLEDGMENTS.** We thank Nick Collins and Diana Horvath for helpful comments on earlier versions of the manuscript; Zhongchao Yin for providing the *avrXa27* gene construct; and Tina Strauß, Carola Kretschmer, Bianca Rosinsky, and Marina Schulze for technical support. This work was funded in part by the 2Blades Foundation and the Deutsche Forschungsgemeinschaft Grants SFB 648 and SPP 1212 (to T.L.).



1. Jones JD, Dangl JL (2006) The plant immune system. *Nature* 444:323–329.
2. Anderson PK, et al. (2004) Emerging infectious diseases of plants: Pathogen pollution, climate change, and agrotechnology drivers. *Trends Ecol Evol* 19:535–544.
3. Michelmore R (2003) The impact zone: Genomics and breeding for durable disease resistance. *Curr Opin Plant Biol* 6:397–404.
4. Hogenhout SA, Van der Hoorn RAL, Terauchi R, Kamoun S (2009) Emerging concepts in effector biology of plant-associated organisms. *Mol Plant-Microbe Interact* 22:115–122.
5. Oliver R (2009) Plant breeding for disease resistance in the age of effectors. *Phyto-parasitica* 37:1–5.
6. Wichmann G, Bergelson J (2004) Effector genes of *Xanthomonas axonopodis* pv. *vesicatoria* promote transmission and enhance other fitness traits in the field. *Genetics* 166:693–706.
7. Bonas U, Stall RE, Staskawicz B (1989) Genetic and structural characterization of the avirulence gene *avrBs3* from *Xanthomonas campestris* pv. *vesicatoria*. *Mol Gen Genet* 218:127–136.
8. Schornack S, Meyer A, Römer P, Jordan T, Lahaye T (2006) Gene-for-gene mediated recognition of nuclear-targeted AvrBs3-like bacterial effector proteins. *J Plant Physiol* 163:256–272.
9. Heuer H, Yin Y-N, Xue Q-Y, Smalla K, Guo J-H (2007) Repeat domain diversity of *avrBs3/pthA*-like genes in *Ralstonia solanacearum* strains and association with host preferences in the field. *Appl Environ Microbiol* 73:4379–4384.
10. Kay S, Bonas U (2009) How *Xanthomonas* type III effectors manipulate the host plant. *Curr Opin Microbiol* 12:37–43.
11. White FF, Yang B (2009) Host and pathogen factors controlling the rice/*Xanthomonas oryzae* interaction. *Plant Physiol* 150:1677–1686.
12. Saijo Y, Schulze-Lefert P (2008) Manipulation of the eukaryotic transcriptional machinery by bacterial pathogens. *Cell Host Microbe* 4:96–99.
13. Niño-Liu D, Ronald PC, Bogdanove AJ (2006) *Xanthomonas oryzae* pathovars: model pathogens of a model crop. *Mol Plant Pathol* 7:303–324.
14. Kay S, Hahn S, Marois E, Hause G, Bonas U (2007) A bacterial effector acts as a plant transcription factor and induces a cell size regulator. *Science* 318:648–651.
15. Römer P, et al. (2007) Plant-pathogen recognition mediated by promoter activation of the pepper *Bs3* resistance gene. *Science* 318:645–648.
16. Römer P, et al. (2009) Recognition of AvrBs3-like proteins is mediated by specific binding to promoters of matching pepper *Bs3* alleles. *Plant Physiol* 150:1697–1712.
17. Herbers K, Conrads-Strauch J, Bonas U (1992) Race-specificity of plant resistance to bacterial spot disease determined by repetitive motifs in a bacterial avirulence protein. *Nature* 356:172–174.
18. Gu K, et al. (2005) *R* gene expression induced by a type-III effector triggers disease resistance in rice. *Nature* 435:1122–1125.
19. Schornack S, et al. (2004) The tomato resistance protein *Bs4* is a predicted non-nuclear TIR-NB-LRR protein that mediates defense responses to severely truncated derivatives of *AvrBs4* and overexpressed *AvrBs3*. *Plant J* 37:46–60.
20. Van den Ackerveken G, Marois E, Bonas U (1996) Recognition of the bacterial avirulence protein *AvrBs3* occurs inside the host plant cell. *Cell* 87:1307–1316.
21. Yang B, Zhu W, Johnson LB, White FF (2000) The virulence factor *AvrXa7* of *Xanthomonas oryzae* pv. *oryzae* is a type III secretion pathway-dependent nuclear-localized double-stranded DNA-binding protein. *Proc Natl Acad Sci USA* 97:9807–9812.
22. Zhu WG, Yang B, Chittoor JM, Johnson LB, White FF (1998) *AvrXa10* contains an acidic transcriptional activation domain in the functionally conserved C terminus. *Mol Plant-Microbe Interact* 11:824–832.
23. Schornack S, Peter K, Bonas U, Lahaye T (2005) Expression levels of *avrBs3*-like genes affect recognition specificity in tomato *Bs4* but not in pepper *Bs3* mediated perception. *Mol Plant-Microbe Interact* 18:1215–1225.
24. Ballvora A, et al. (2001) Genetic mapping and functional analysis of the tomato *Bs4* locus, governing recognition of the *Xanthomonas campestris* pv. *vesicatoria* *AvrBs4* protein. *Mol Plant-Microbe Interact* 14:629–638.
25. Gu K, Sangha JS, Li Y, Yin Z (2008) High-resolution genetic mapping of bacterial blight resistance gene *Xa10*. *Theor Appl Genet* 116:155–163.
26. Chen S, et al. (2008) High-resolution mapping and gene prediction of *Xanthomonas oryzae* pv. *oryzae* resistance gene *Xa7*. *Mol Breed* 22:433–441.
27. Sugio A, Yang B, Zhu T, White FF (2007) Two type III effector genes of *Xanthomonas oryzae* pv. *oryzae* control the induction of the host genes *OstFIIAγ1* and *OstTFX1* during bacterial blight of rice. *Proc Natl Acad Sci USA* 104:10720–10725.
28. Yang B, Sugio A, White FF (2006) *Os8N3* is a host disease-susceptibility gene for bacterial blight of rice. *Proc Natl Acad Sci USA* 103:10503–10508.
29. Moscou MJ, Bogdanove AJ (2009) A simple cipher governs TAL effector-DNA recognition. *Science*, in press.
30. Boch J, et al. (2009) Breaking the code of DNA-binding specificity of TAL-type III effectors. *Science*, in press.
31. Nakagawa T, et al. (2007) Development of series of Gateway binary vectors, pGWBs, for realizing efficient construction of fusion genes for plant transformation. *J Biosci Bioeng* 104:34–41.
32. Koncz C, Schell J (1986) The promoter of TL-DNA gene 5 controls the tissue-specific expression of chimeric genes carried by a novel type of *Agrobacterium* binary vector. *Mol Gen Genet* 204:383–396.

## 2.5.2 Anlagen zur Publikation 4

Das folgende „*Supporting Online Material*” (SOM) (veröffentlicht unter: [www.pnas.org/content/106/48/20526/suppl/DCSupplemental](http://www.pnas.org/content/106/48/20526/suppl/DCSupplemental)) enthält Zusatzinformationen zu Kapitel 2.5.1: die „*Supplemental Figures*” 1-7 und die Tabelle S1.

```

Bs3-E    1  CTGGTTCAGTTTATGGGTTAAACCACAATTTGCACACCCTGGTTAAACAATGAACACGTT
Bs3     1  CTGGTTCAGTTTATGGGTTAAACCACAATTTGCACACCCTGGTTAAACAATGAACACGTT

Bs3-E   61  TGCCTGACCAATTTTAT TATATAAA CCT CTCTATTCCACTA AACCATCCTCACAACCTCA
Bs3     61  TGCCTGACCAATTTTAT TATATAAA CCT ----- AACCATCCTCACAACCTCA

Bs3-E   121 AGTTATCATCCCCTTTCTCTTTTCTCCTCTTGTCTTGTGTCACCCGCTAAATCTATCAAAA
Bs3    108 AGTTATCATCCCCTTTCTCTTTTCTCCTCTTGTCTTGTGTCACCCGCTAAATCTATCAAAA

Bs3-E   181 CACAAGTAGTCCTAGTTGCACATATATTTCA ATG
Bs3    168 CACAAGTAGTCCTAGTTGCACATATATTTCA ATG

```

**Fig. S1.** Nucleotide differences between the pepper *Bs3* and *Bs3-E* promoter. The 13-bp insertion/deletion polymorphism adjacent to the predicted TATA box (red letters) is highlighted as yellow letters (in *Bs3-E* promoter) or as yellow background (in *Bs3* promoter). The  $UPT_{AvrBs3}$  box as determined in ref. 1 is shown in italics.

1. Römer P, et al. (2009) Recognition of AvrBs3-like proteins is mediated by specific binding to promoters of matching pepper *Bs3* alleles. *Plant Physiol* 150:1697–1712.

```

xa27 960 GTAAAGTGGCACACACAGAGGAAAAATCCTGGATTGTCACCTGCCATCAACATCTGCTT
Xa27 950 GTAAAGTGGCACACACAGAGGAAAAATCCTGGATTGTCACCTGCCATCAACATCTGCTT

xa27 1020 TCGCCTCCCAATTCCTGCTTTCTGAAATCTGCTTTTCGCCGAATTCATGCCTTCTTGAATT
Xa27 1010 TCGCCTCCCAATTCCTGCTTTCTGAAATCTGCTTTTCGCCGAATTCATGCCTTCTTGAATT

xa27 1080 ATGCTTTCTTAGACCCTCTTTAGATGAGACTAAAACCTTTTACTCTCTATCACATCGGATG
Xa27 1070 ATGCTTTCTTAGACCCTCTTTAGATGAGACTAAAACCTTTTACTCTCTATCACATCGGATG

xa27 1140 TTTGGACACTAATTATAAATATTAACGCTAGACTATTAATAAAACCCATCTATAATCTTG
Xa27 1130 TTTGGACACTAATTATAAATATTAACGCTAGACTATTAATAAAACCCATCTATAATCTTG

xa27 1200 TATTAATTCGCGTGACGAATCTATTGAGCCTAATTAATCCATGATTAGCCTATGTGATGC
Xa27 1190 TATTAATTCGCGTGACGAATCTATTGAGCCTAATTAATCCATGATTAGCCTATGTGATGC

xa27 1260 TATAATAACATTTCTCTAATTATAAATTAATTGGGCTTAAAAAATTTGTCTCGCGTATTA
Xa27 1250 TATAATAACATTTCTCTAATTATAAATTAATTGGGCTTAAAAAATTTGTCTCGCGTATTA

xa27 1320 GCTTTCATTTATGTAATTAGTTTTTATAAATAGTCTATATTTAATACTCTAAATTAGTGTC
Xa27 1310 GCTTTCATTTATGTAATTAGTTTTTATAAATAGTCTATATTTAATACTCTAAATTAGTGTC

xa27 1380 TAAATACAGGGACTAAAGTTAAGTCCCTGGATCCAAACGCCACCTAAGGTTTTCTTGTGT
Xa27 1370 TAAATACAGGGACTAAAGTTAAGTCCCTGGATCCAAACGCCACCTAAGGTTTT-----

xa27 1440 ACTTGTGAATTGTGGTTTTCTTGTGTACTTGTGAATTGTGGTTGACTACGACTACGAGTGC
Xa27 1423 -----CTTGTGTACTTGTGAATTGTGGTTGACTACGACTACTAGTGC

xa27 1500 TATAAATAGAAGA---GACCAATAGAGAGCATCAGAGCAAAGTACTCCTAAAAGACAGCC
Xa27 1465 TATAAATAGAAGAAGAGACCCATAGAGAGCATCAGAGCAAAGTACTCCTAAAAGACAGCC

xa27 1557 ACACACACTGAGACACCCAAGAAGCTGCCTCCAATG
Xa27 1525 ACACACACTGAGACACCCAAGAAGCTGCCTCCAATG

```

**Fig. S2.** Sequence alignment of the rice *Xa27* promoter from the rice cultivar IRBB27 (gi 66735941 gb AY986491.1) and the *xa27* promoter from the rice cultivar IR24 (gi 66735943 gb AY986492.1). The ATG start codon is displayed in boldface green. Nucleotides that are identical in *Xa27* and *xa27* are displayed as white letters on black background. The predicted TATA box (2) is displayed in boldface red letters. The residues of the *xa27* promoter that were replaced in the *xa27<sub>mut</sub>* promoter by the corresponding nucleotides from the *Xa27* promoter are highlighted by yellow color. The FASTA files of the *Xa27* and *xa27* nucleotide sequences are given in Fig. S3.

- Gu K, et al. (2005) *R* gene expression induced by a type-III effector triggers disease resistance in rice. *Nature* 435:1122–1125.

>Xa27 (IRBB27 allele); gj|66735943|gb|AY986492.1|

CTGCAGCTGAACCAAACAGTTTTAGCTCCATCGAAGAAAGGAGTTATACTGATTGGAATGCTCTCACAGTAAAAAAAACAAGGAAGTAGA  
GCTGGATTTTAGACAGTTCTACAAGAAGTTAGAACTCTACCAAAATGGAATTTGGATGATGGTCTTTAAAAACTCGATTGCAGGAAT  
AAAATTTTACGGCTTGAACCTTACAAAATGATTAGAAAAGATAACATGCCTCAGCGATTGTAAAAAGTGAACAAATAAAAACTACAA  
TACCCTAAACTATTGCTTTATTTGGGGACATTGCTTACCATTGAAAAACAACCTAACCGTAAATACGAACACCCATATCAAAATATACT  
ATCACTGATAAAAATAATCAATTGTAATTCAGCACACATATTAGTATAGTACTTTAACTCGATTGGATAGAAGAAACCTAACCTAATTTA  
AGCTATGCCTCACAAACAAAAGGTATAAATTTTTTAAGGCTTCTTTTTTTTCTTGCCTTGTAGTTTATGCTTTTAAAGTGTTTATAC  
CTTTTACTCCCTCATTCCTGTTTAAATACAATGGGAATTAGTGAAATCAATGAGAGTTCAAACCTCGAAACACTGAATACATGTTATT  
TTGGATTGAAATCAAATCGAATCAGTCAAATTCAAATAGGAGGAGGAACATAGGCATTCTTCTTTCTCAGCGGGCACCATTGAATCA  
GATACTGCTTCGCCTAGTCTCTGTCCAAGACTCCACATTTCTGATGGTGATGGGAACCTCTGAAACTATAGGAGGAAGAAATAAATGAA  
GAATGCAGAAATGAATAGTAATTTGTGTTTTTAATCTTCTTCAATCCACCTTAGGATCCAACCTCAGTCCAATCCAAAGTAATGCA  
ACTGCCACTAGATCAGGCTAGAGCTTCAAATTCAACTCCAAAAACCTCCGTAAGTGCCACACACAGAGGAAAAATCCTGGATTTCGTAC  
TGCCCTCAACATCTGCTTCGCCTCCCAATTCCTGCTTCTGAAATCTGCTTTCGCCGAATTCATGCCTTCTGAAATATGCTTTCTTA  
GACCCCTTTAGATGGGACTAAAACCTTTACTCTCTATCACATCGGATGTTGGACACTAATTATAAATAATTAACGTAGACTATTAATA  
AAACCCATCTATAATCTTGTATTAATTCGCGAGACGAATCTATTGACCTAATTAATCCATGATTAGCCTATGTGATGCTATAATAAACA  
TTCTCTAATATAAATAATTTGGGCTTAAAAAATTTGTCTCGCGTATTAGCTTTCATTTATATAAATAGTTTTATAAATAGTCTATATTT  
AATACTCTAATTAGTGTCTAATAACAGGGACTAAAGTTAAGTCACTGGATCCAAACACCCTAAGGTTTTCTTGTGACTTGTGAAAT  
GTGGTTGACTACCACTACTA**GTGCTATAAATA**GAAGAAGAGACC**ATAGAGAGCATC**AGAGCAAAGTACTCCTAAAAAGACAGCCACAC  
ACTGAGACACCAAGAAGCTGCCTCCA**ATG**

>xa27 (IR24 allele); gj|66735941|gb|AY986491.1|

CTGCAGCTGAACCAAACAGTTTTAGCTCCATCGAAGAAAGGAGTTATACTGATTGGAATGCTCACAGTAAAAAAAACAAGGAAGTAGAG  
CTGGATTTTAGACAGTTCTATAAGAAGTTAGAACTCTACCAACCGGATAGTTAATGGAATTTGGATGATGGTCTTTAAAAACTCGAT  
TGCAGGAATAAAATTTTACGGCTTGAACCTTACAAAATGATTAGAAAAGATAACATGCCTCAGCGATTGTAAAAAGTGAACAAATAAA  
AATCTACAATACCCTAAACTATTGCTTTATTTTGGGGACATTGCTTACCATTGAAAAACAACCTAACCGTAAATACGAACACCCATGTC  
AAATATACTATCACTGATAAAAATAATCAATTTGTAATTCAGCACACATATTAGTATAGTACTTTAACTCGATTGGATAGAAGAAACCTA  
ACTAATTTAAGCTATGCCTCACAAACAAAAGGTATAAATTTTTTAAGGCTTCTTTTTTTTTCTTGCCTTGTGCTTTATGCTTTTAAG  
ATGTTTATACTTTTTACTCCCTCATTCCTGTTTAAATACAATGGGAATTAGTGAAATCAATGAGAGTTCAAACCTCGAAACACTGAAT  
ACATGTTATTTGGATTGAAATCAAATCGAATCAGTCAAATTCAAATAGGAGGAGGAACATAGGCATTCTTCTTTCTCAGCGGGCACC  
ATTGAATTCAGATACTGCTTCGCCTAGTCTCTGTCCAAGACTCCACATTTCTGATGGTGATGGGAACTCTGAAACTATAGGAGGAAGA  
ATAAAAAGAAGATGCAGAAATGAATAGTAATTTGTGTTTTTAATCTTCTTCAATCCACCTTAGGATCCAACCTCAGTCCAATCCA  
AAGTAATGCAACTGCCACTAGATCAGGCTAGAGCTTCAAATTCAACTCCAAAAACCTCCGTAAGTGCCACACACAGAGGAAAAATCCTG  
GATTCGTCAGTACGCTTCGCCTAGTCTCTGTCCAAGACTCCACATTTCTGATGGTGATGGGAACTCTGAAACTATAGGAGGAAGA  
TGCTTTCTTAGACCTCTTTAGATGAGACTAAAACCTTTACTCTCTATCACATCGGATGTTGGACACTAATTATAAATAATTAACGTAG  
ACTATTAATAAAACCCATCTATAATCTTGTATTAATTCGCGTGACGAATCTATTGAGCCTAATTAATCCATGATTAGCCTATGTGATGCT  
ATAATAAACACTCTCTAATATAAATAATTTGGGCTTAAAAAATTTGTCTCGCGTATTAGCTTTCATTTATGTAATAGTTTTATAAATA  
GTCTATATTTAATCTCTAATTAGTGTCTAATAACAGGGACTAAAGTTAAGTCCCTGGATCCAAACGCCACCTAAGGTTTTCTTGTGTA  
CTTGTGAAATGTGGTTTTCTTGTGACTTGTGAATTTGGTTGACTACGACTACGA**GTGCTataaata**GAAGAAGAGACC**AATAGAGAGCA**  
**TC**AGAGCAAAGTACTCCTAAAAAGACAGCCACACACACTGAGACACCAAGAAGCTGCCTCCA**ATG**

Fig. S3. Nucleotide sequences of the rice Xa27 and xa27 alleles. The ATG start codon is displayed in green letters. The primers that were used for amplification of the promoter region are underlined. The predicted TATA box of Xa27 (2) is displayed in bold red letters. The region of the Xa27 and xa27 promoters that was transferred to the Bs3 promoter (see also Fig. 2) is highlighted by yellow background. The minimal UPT<sub>AvrXa27</sub> box is displayed in italics.

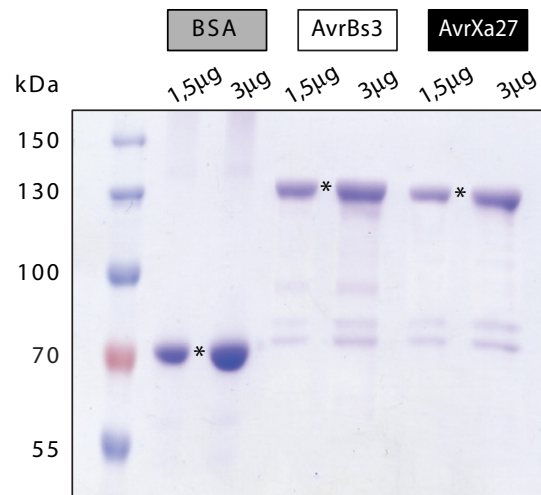


**Fig. S4.** Purified His:AvrXa27 and His:AvrBs3 fusion proteins. Coomassie-stained 8% SDS polyacrylamide gel (PAGE). His translational fusions to AvrBs3 and AvrXa27 used for EMSA studies were expressed in *E. coli* BL21-AI, purified and quantified by Bradford assay (3). Subsequently 1.5 and 3 µg of His:AvrBs3, His:AvrXa27 and BSA standard were separated by SDS PAGE and stained with Coomassie. Fragments of expected size (His:AvrBs3 [123 kDa], His:AvrXa27 [120 kDa]) are indicated by asterisk (\*). Marker proteins (M) are indicated with their molecular masses in kDa (PageRuler™ prestained protein ladder, Fermentas).

3. Bradford MM (1976) A rapid and sensitive method for the quantitation of microgram quantities of protein utilizing the principle of protein-dye binding. *Anal Biochem* 72:248–254.

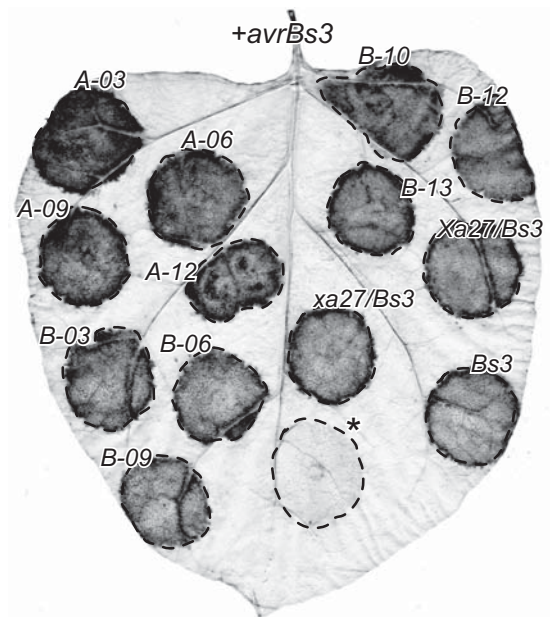


Fig. S5. The  $UPT_{avrBs3}$  box retains its function irrespective of which *Xa27* or *xa27* promoter fragment was inserted into the *Bs3* promoter. The promoter constructs depicted in Fig. 2A were delivered together with a 35S promoter-driven *avrBs3* gene into *N. benthamiana* leaves via *A. tumefaciens*. Asterisks (\*) mark areas in which *A. tumefaciens* delivering only the *avrBs3* gene were infiltrated. Dashed lines mark the inoculated areas. Four days after inoculation, the leaves were harvested and cleared with ethanol to visualize the HR (dark areas).

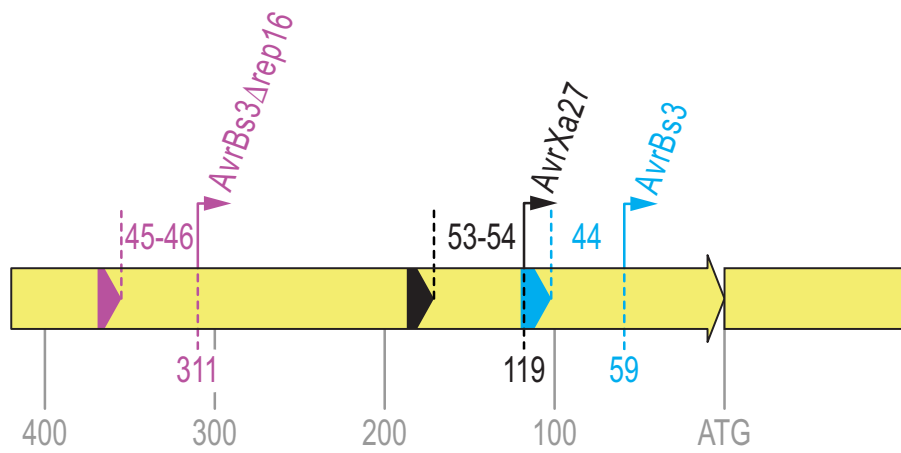


Fig. 56. Transcription start sites (TSSs) in the *Bs3-E/Xa27/Bs3* promoter. Yellow arrows and boxes represent the *Bs3* promoter and cds, respectively. Pink, black, and blue boxes represent the  $UPT_{AvrBs3\Delta rep16}$ ,  $UPT_{AvrXa27}$ , and  $UPT_{AvrBs3}$  minimal boxes, respectively. Pink, black and blue arrows above the boxes mark the TSSs of the *Bs3-E/Xa27/Bs3* promoter in combination with *AvrBs3Δrep16*, *AvrXa27*, and *AvrBs3*, respectively. Numbers above the arrows denote the distance between the 3' end of the given *UPT* minimal box and the respective TSSs. Numbers below the *UPT* boxes denote the distance between the ATG start codon and the given TSSs. With exception of the *Bs3* cds all elements are drawn to scale.

CTACGGAATAGCAGCATTAAAGGCACATCAGAGATTTTTGGGTGTTAAGTTGTGCATGAAACCTGATGCCTCCACAGGAA  
 CTGTCAATCTCATGTGTCTTGGCTCTGGTTTTTCAGAAATTTATCCAGAAAAGTATCATGATAAATTAATGGTGTCTGTGTT  
 TGGTGGCTTAGAGTGACGGCTAGATCAACATCTTTGGGATGCCTTGTGGAGTGAAATCAAGCATACTTTATCATAGGGGA  
 AATTTTTTGTGTGGTTTGTCTTGAATGAGAGAGTGATATAGGAAGCAAATGTGGAGATCACATTTGTCTCATCTCCT  
 TGTGCGTTGAACTTTTGGTGTCAAGAGTTCTAATTCACATGTATTTGAAGATTCCTCATATGCTGCTTTTGTCTTAA  
 TTATTTTTCTAGTAAGAAAACATTTGTCTCGAGTTTCCAACCTAGAAAAAATATCAAGTAAATAGAATTCATCATT  
 TCCCTTACCAACGCTTGGTACTGCCAACCCGAACAAAGAATTAATGCAAAACAACAGTCTATTAATATCAACCTAGACTA  
 AACTCCTTAGTTTTACTTTGAAATGCGAATGATACATGACACATTAGATTGTACTTGTCTTTTACCACAGATACAACGAT  
 ACATTTGTATATCTTTTCCCTTATAGCAAACCTAATATATCATAGTCAAGCTAACGAACTTATGCAAGGGAATATGA  
 AATTAGTATGCAATTTTATTATATAAACCTCTCTATTCCACTAAACCATCCTCACAAACCAAGTAAACTCAAAGAACT**AA**  
 CATTGAACTGAAAGATCAATATATCAAAAAAAAAAAAAAAAAAACAATAAAACCCTTTAACCGATAGATTAACCATTCTGGTT  
 CAGTTTATGGGTTAAACCACAATTTGCACACC**GTGCTATAAATAGAAGAAGAGACCCATAGAGAGCATC**CTGGTTAAACA  
 ATGAACACGTTTGGCTGACCAATTTTAT**TTATAAACCTAACCAATC**CTCACAACTTCAAGTTATCATCCCTTTCTCTTT  
 TCCTCTTT**CTTCTT**GCACCCGCTAAATCTATCAAAACACAAGTAGTCTAGTTGCACATATATTT**CATG**ATGAATCAG  
 AATTGCTTTAAATCTTGTTCACCTCTAACTGTTGATGCACTTGAACCAAAAAAAAAATCCTCTTGTGCTGCTAAATGCATACA  
 AGTAAATGGTCTCTTATTGTTGGAGCTGGCCCTCAGGCTGGTACTGCTGCCGTCTTAAGCAATACAGTGTCCCGT  
 ATGTAATCATTGAACGCGGGACTGCATTTGCTTCTGTGGCAACACAAGACCTACGATCGGCTTAGGCTTAACGTTGCA  
 CGACAATCTGCGAATGCTGGCTTGCATTTCCACCAGACTTTCCAGAGTATCCAACCAAAACCAATTCATCAGCTA  
 CCTCGTATCTTATGCAAAGCATTTGAGATCAAACCACAACCTCAACGAGTCAAGTAACTTAGCTGGATATGATGAGACAT  
 GTGGTTTATGGAAGGTGAAAACAGTTTCTGAAATCAATGGTTCAACCTCTGAATACATGTGTAAGTGGCTTATTGTGGCC  
 ACAGGAGAGAATGCTGAGATGATAGTGCAGGAAATCGAAGGATTGCAAGATTTGGTGGCCAGGTTATTCATGCTTGTGA  
 GTACAAGACTGGGGAATACTATACTAGGAGAAAATGTGCTGGCGGTTGGCTGTGGCAATTCGGGATCGATATCTCACTTG  
 ATCTTTCCCAACATAATGCAATCCATTCATGGTAGTTCGAAGCTCGGTAAGTTTATATTTCAATAAGTATTATTTTTCA  
 AGTAACTAGAAAGTATCTTGTATCTTTCATTTGCTCGCATGAATATATATATTCACACATGAATGATATCATCTAG  
 TTTGTTAATCTTTCAGGTACAGGTCGTAATTTCCCTGAGGAAATAAACATAGTTCCAGCAATCAAGAAATTTACTCAA  
 GGAAAAGTAGAATTTGTTAATGGACAAATCTAGAGATCGACTCTGTTATCTTGGCAACTGGTTATACCAGCAATGTAAC  
 TTCTTGGTAAATGGTAAGGAAATACACAAGTTTATTTCTATGCCTAATTAATTTGGTGTAAATCATAAATTTATATA  
 GTACTAAGTATGATAAAGCTCCTCAACTATAAAGGATGATTTAGTCAAAATGAAGTCTTAATGAATGATGATTAATTT  
 ATGGATTTCTGTTACATTCATGTAAGTTGGTATCTCATTATCCTGTGGATTCTTCTTCTTGGATTATTAATTTAGTTAGAA  
 TTCACTATAACCGTCTTTTTCTTTTACCCTTTCCATACCTTTTTGTTCTTTTGTATACTCGAACTCACAATCTTAAG  
 ATTGGGAATAAGGGCTCTTTACCATCTGAGCAACTTCTCTCGTTCTATAATAGCCCCCTCGAAATTTGGTCTAATGA  
 GAATTTTACTGATACAGGAGAGTGAATTTGTTTCAAGGGAGGGATGTCCAAAAAGCCATTCCTCAATGGTTGGAGGGG  
 GAGGATGGTCTATGCAGTTGGATTTACAGGAATAGGACTGTTTGGTGTCTTATAGATGCCACTAATGTTGCACAAGA  
 TATTGCCAAAATTTGAAAGAACAATG

**Fig. S7.** Nucleotide sequence of the complex *Bs3-E/Xa27/Bs3* promoter. The sequences of the *Bs3-E* and the *Xa27* promoter that were inserted into the *Bs3* promoter are displayed in purple and red letters, respectively. The  $UPT_{AvrBs3}$  box from the *Bs3* promoter is shown in blue letters. The minimal  $UPT_{AvrBs3\Delta rep16}$ ,  $UPT_{AvrXa27}$ , and  $UPT_{AvrBs3}$  boxes are underlined in purple, red, and blue. The transcription start sites that were observed with *AvrBs3* $\Delta rep16$ , *AvrXa27*, and *AvrBs3* are highlighted by purple-, red-, and blue-background. The ATG start codon of the *Bs3* coding sequence is shown in green bold letters.



**Table S1. Distances between the 3' end of a given *UPT* box and the corresponding TSS is mostly independent of the promoter context**

TAL effector	Native promoters with a single <i>UPT</i> box	<i>Bs3-E/Xa27/Bs3</i> promoter
AvrBs3	44 ( <i>Bs3</i> )*	44 <sup>‡</sup>
AvrBs3Δrep16	61 ( <i>Bs3-E</i> ) <sup>†</sup>	45–46 <sup>‡</sup>
AvrXa27	45 ( <i>Xa27</i> )*	53–54 <sup>‡</sup>

Given is the distance between the 3' end of the given *UPT* boxes and the TSSs in promoters with a single *UPT* box as compared to the complex *Bs3-E/Xa27/Bs3* promoter.

\*See Fig.1 and ref. 1.

<sup>†</sup>See ref. 1.

<sup>‡</sup>see Fig. 4.

### 2.5.3 Zusammenfassung der Ergebnisse

In der Publikation von Gu und Kollegen (Gu et al., 2005) wurde gezeigt, dass das Reis *R*-Gen *Xa27* durch den korrespondierenden TAL-Effektor *AvrXa27* aus *Xoo* transkriptionell aktiviert wird. Der molekulare Mechanismus der Aktivierung war bislang jedoch nicht geklärt. In der hier dargelegten Publikation konnte gezeigt werden, dass *AvrXa27* an den *Xa27*-Promotor bindet. Somit funktioniert die Erkennung des *R*-Gens *Xa27* aus Reis prinzipiell wie die des Paprika *Bs3*-Gens. Weiterhin war es möglich zu zeigen, dass ein Konstrukt, in dem der *Xa27*-Promotor vor die kodierende Region des *Bs3*-Gens fusioniert wurde, eine *AvrXa27*-abhängige HR induziert. Ein Sequenzvergleich, der 1,5 Kb langen Promotorregionen des *AvrXa27*-induzierbaren *Xa27*-Allels (Reis Kultivar IRBB27) und des nicht durch *AvrXa27*-induzierbaren *xa27*-Allels (Reis Kultivar IR24) ergab 16 Nukleotidpolymorphismen. Aus diesen wurden die zwei Polymorphismen identifiziert, die den funktionellen Unterschied zwischen diesen beiden *R*-Allelen bedingen. Mittels Promotordeletionsderivaten konnte außerdem die  $UPT_{AvrXa27}$ -Box im *Xa27*-Promotor definiert werden. EMSA-Analysen zeigten, dass *AvrXa27* mit hoher Affinität an den *Xa27*-Promotor und mit signifikant geringerer Affinität an den *xa27*-Promotor bindet. Diese Daten weisen darauf hin, dass die spezifische Bindung von TAL-Effektoren an ihre korrespondierenden Promotoren die Grundlage für die Aktivierung der dahinter liegenden Gene ist. Durch die Kombination der  $UPT_{AvrBs3\Delta rep16^-}$ , der  $UPT_{AvrXa27}$ - und der  $UPT_{AvrBs3}$ -Boxen im *Bs3*-Promotor konnte ein komplexer Promotor generiert werden, welcher durch drei verschiedene TAL-Effektoren aus unterschiedlichen *Xanthomonas*-Spezies aktiviert wird. Derart komplexe Promotoren könnten die Grundlage für die Erzeugung von Breitspektrum- und stabilen Resistenzen sein.

## 2.6 Promotoren von Reissuszeptibilitätsgenen werden von korrespondierenden TAL-Effektoren gebunden und aktiviert

### 2.6.1 Publikation 5



Research

# Promoter elements of rice susceptibility genes are bound and activated by specific TAL effectors from the bacterial blight pathogen, *Xanthomonas oryzae* pv. *oryzae*

Patrick Römer<sup>1,2\*</sup>, Sabine Recht<sup>1,2\*</sup>, Tina Strauß<sup>1,2</sup>, Janett Elsaesser<sup>1,2</sup>, Sebastian Schornack<sup>1,3</sup>, Jens Boch<sup>1</sup>, Shiping Wang<sup>4</sup> and Thomas Lahaye<sup>1,2</sup>

<sup>1</sup>Institute of Biology, Martin-Luther-University Halle-Wittenberg, 06099 Halle (Saale), Germany; <sup>2</sup>Present address: Institute of Genetics, University of Munich (LMU), Großhaderner Straße 2, 82152 Martinsried, Germany; <sup>3</sup>The Sainsbury Laboratory, Norwich, NR4 7UH, UK; <sup>4</sup>National Key Laboratory of Crop Genetic Improvement, National Center of Plant Gene Research (Wuhan), Huazhong Agricultural University, Wuhan 430070, PR China

### Summary

Author for correspondence:  
Thomas Lahaye  
Tel: +49 (0)89 2180 7470  
Email: lahaye@bio.lmu.de

Received: 20 November 2009  
Accepted: 11 January 2010

New Phytologist (2010)  
doi: 10.1111/j.1469-8137.2010.03217.x

**Key words:** AvrBs3, AvrXa27, Bs3, PthXo1, UPA (up-regulated by AvrBs3), Xa13, *Xanthomonas*.

- Plant pathogenic bacteria of the genus *Xanthomonas* inject transcription activator-like effector (TALE) proteins that bind to and activate host promoters, thereby promoting disease or inducing plant defense. TALEs bind to corresponding *UPT* (up-regulated by TALE) promoter boxes via tandemly arranged 34/35-amino acid repeats. Recent studies uncovered the TALE code in which two amino acid residues of each repeat define specific pairing to *UPT* boxes.
- Here we employed the TALE code to predict potential *UPT* boxes in TALE-induced host promoters and analyzed these via  $\beta$ -glucuronidase (GUS) reporter and electrophoretic mobility shift assays (EMSA).
- We demonstrate that the *Xa13*, *OsTFX1* and *Os11N3* promoters from rice are induced directly by the *Xanthomonas oryzae* pv. *oryzae* TALEs PthXo1, PthXo6 and AvrXa7, respectively. We identified and functionally validated a *UPT* box in the corresponding rice target promoter for each TALE and show that box mutations suppress TALE-mediated promoter activation. Finally, EMSA demonstrate that code-predicted *UPT* boxes interact specifically with corresponding TALEs.
- Our findings show that variations in the *UPT* boxes of different rice accessions correlate with susceptibility or resistance of these accessions to the bacterial blight pathogen.

### Introduction

Microbial plant pathogens deliver effector proteins into the host's cytoplasm to promote their virulence or to suppress plant innate immunity (Göhre & Robatzek, 2008; Boller & He, 2009; Hogenhout *et al.*, 2009). After delivery, microbial effectors are targeted to different subcellular compartments of the host cell. Recently it has become evident that the nucleus is targeted by effectors from various classes of plant microbial pathogens, including nematodes (Elling *et al.*, 2007), oomycetes (Kanneganti *et al.*, 2007), fungi (Kemen *et al.*, 2005) and bacteria (Deslandes *et al.*, 2003;

Nissan *et al.*, 2006; Bai *et al.*, 2009). Transcription activator-like effectors (TALEs) from the plant pathogenic bacterial genus *Xanthomonas* are among the most intensively studied class of nuclear-targeted microbial effectors (Kay & Bonas, 2009; White *et al.*, 2009). The most characteristic structural feature of TALEs is the central repeat domain that is composed of a variable number of tandemly arranged, imperfect copies of a 34/35-amino acid motif (Schornack *et al.*, 2006). Differences between individual repeat units are found primarily at positions 12 and 13, the so-called repeat-variable diresidues (RVDs) (Moscou & Bogdanove, 2009). The repeat domain of the prototype TALE, AvrBs3, from *Xanthomonas campestris* pv. *vesicatoria* (*Xcv*), has been shown to interact with a corresponding promoter element,

\*These authors contributed equally to this work.

termed an *UPA* (up-regulated by AvrBs3) box, that is present in the promoter of the pepper transcription factor *UPA20*, a host susceptibility gene that appears to support bacterial spread (Kay *et al.*, 2007). The presence of a *UPA* box in a promoter results in AvrBs3-mediated expression of the given host gene (Kay *et al.*, 2009; Römer *et al.*, 2009b). The promoter of the pepper resistance (*R*) gene *Bs3* also contains a *UPA* box and thus is transcriptionally activated by AvrBs3 (Römer *et al.*, 2007, 2009b). Expression of *Bs3* triggers a cell death reaction, referred to as the hypersensitive response (HR), and results in resistance against *Xcv*. Thus, the *R* gene *Bs3* represents a 'promoter trap' that coopts AvrBs3's function in promoting virulence. Similarly, transcription of the rice *R* gene *Xa27* is specifically induced by AvrXa27, a TALE from the bacterial blight pathogen, *X. oryzae* pv. *oryzae* (*Xoo*) (Gu *et al.*, 2005). Recent studies uncovered that the *Xoo* TALE AvrXa27 binds to a matching promoter motif in the rice *Xa27* promoter (Römer *et al.*, 2009a). Thus the *R* genes *Bs3* and *Xa27* use identical mechanisms to detect their matching TALEs. Promoter motifs that mediate TALE transcriptional activation have been collectively defined as *UPT* (up-regulated by TALEs) boxes, with a subscript designation to define the specific TALE that targets the given *UPT* box (Römer *et al.*, 2009a).

Although it was long known that TALE target specificity is defined by the number and order of repeat units that together form the repeat domain (Herbers *et al.*, 1992), it was not clear how the repeat domain conferred target specificity at the molecular level. Recent studies demonstrated that RVDs specify the nucleotide target site of a given TALE with one RVD pairing to one specific *UPT* box nucleotide (Boch *et al.*, 2009; Moscou & Bogdanove, 2009). This pairing code defined the interaction of TALEs to colinear binding sites and was used to deduce functional *UPT* boxes for such TALEs for which a corresponding host target promoter was not available (Boch *et al.*, 2009).

Recently, a number of genes have been identified in rice that are targeted and transcriptionally activated by specific *Xoo* TALEs to promote virulence of *Xoo* (Chu *et al.*, 2006; Yang *et al.*, 2006; Sugio *et al.*, 2007; Antony *et al.*, 2009; Yuan *et al.*, 2009). The *UPT* boxes in the promoters of these rice genes have been predicted (Boch *et al.*, 2009; Moscou & Bogdanove, 2009) by the use of the TAL code but not functionally validated. In the present study we analyzed if code predicted *UPT* boxes in the TALE-induced rice promoters of *Xa13* (also known as *Os8N3*), *OsTFX1* and *Os11N3* are crucial to transcriptional activation by matching TALEs. Furthermore we tested via electrophoretic mobility shift assay (EMSA) if TALEs physically interact with the corresponding *UPT* boxes and how box mutations affect the TALE–DNA interaction. Our results show that resistance and susceptibility to *Xoo* in rice are influenced by *UPT* box sequences.

## Materials and Methods

### Generation of the promoter *uidA* fusion constructs

Promoter regions of *OsTFX1*, *Os11N3*, and *Xa13* were PCR-amplified from genomic rice (*Oryza sativa*) DNA of cv IR24. The *xal3* promoter region was amplified from genomic rice DNA of cv IRBB13. Amplification was carried out with Phusion high-fidelity DNA polymerase (New England Biolabs, Frankfurt, Germany) and primers provided in Supporting Information (Fig. S1). The PCR fragments were cloned into pENTR-D (Invitrogen GmbH, Karlsruhe, Germany), sequenced and transferred into the T-DNA vector pGWB3 (Nakagawa *et al.*, 2007) by LR recombination (Invitrogen). pGWB3 derivatives were transformed into *Agrobacterium tumefaciens* GV3101 (Koncz & Schell, 1986) for *in planta* analysis.

### Generation of the TALE constructs

For the generation of T-DNA vectors that contain *avrXa7*, *pthXo1* or *pthXo6*, we used the vector pENTR-D-*Bam*HI-*avrXa27* (Römer *et al.*, 2009a). The *Bam*HI fragments of *avrXa7*, *pthXo1* and *pthXo6* were transferred into pENTR-D-*Bam*HI-*avrXa27*, resulting in the pENTR-D-*avrXa7*, pENTR-D-*pthXo1* and pENTR-D-*pthXo6*, respectively. The TALE genes were transferred via LR recombination in the binary vectors pGWB2 or pGWB5 (Nakagawa *et al.*, 2007). pGWB2 and pGWB5 derivatives were transformed into *A. tumefaciens* GV3101 for *in planta* analysis. For EMSA we transferred *pthXo1* and *pthXo6* from pENTR-D-*pthXo1* and pENTR-D-*pthXo6* via LR recombination into pDEST17 (Invitrogen).

### Insertion of *UPT* boxes in the *Bs3* promoter

For the insertion of the predicted *UPT* boxes in the *Bs3* promoter 5' upstream of the *UPT*<sub>AvrBs3</sub> box we used primers Xa13in30R-fwd-01-PR GATATNCATCTCCCCCTACTGTACACCACCAACTGGTTAAACAATGAACACGTTTGC, Xa13in30R-fwd-02-T-PR GATAGCATCTCCCCCTACTGTACACCACCAACTGGTTAAACAATGAACACGTTTGC, OsTFX1in30R-fwd-01-PR ACCCTATAAAAAGGCCCTCACCAACCCATCGCCTGGTTAAACAATGAACACGTTTGC, OsTFX1in30R-fwd-02-T-PR ACCCATAAAAGGCCCTCACCAACCCATCGCCTGGTTAAACAATGAACACGTTTGC, Os11N3in30R-fwd-03-PR GCACTATATAAAACCCCTCCAACAGGTGCTAAGCTCCTGGTTAAACAATGAACACG, Os11N3in30R-fwd-04-T-PR GCACATATAAACCCCTCCAACAGGTGCTAAGCTCCTGGTTAAACAATGAACACG in combination with the primer 4in30R-rev-02-PR GGTGTGCAAATTGTGGTTAACCC. All primers used are phosphorylated at their 5' termini. Insertion was

done using the Phusion site directed mutagenesis kit (New England Biolabs). As a template, we used pENTR-D containing 343 bp 5' of the ATG start codon of the *Bs3* gene. The promoter was amplified from genomic DNA of ECW-30R pepper plants using the Phusion high-fidelity DNA polymerase. After sequencing, the promoter constructs were transferred by LR recombination in the binary vector pGWB3 (Nakagawa *et al.*, 2007). pGWB3 derivatives were transformed into *A. tumefaciens* GV3101 (Koncz & Schell, 1986) for *in planta* analysis.

#### Electrophoretic mobility shift assay (EMSA)

Electrophoretic mobility shift assays were carried out as described earlier (Römer *et al.*, 2009a).

#### $\beta$ -Glucuronidase (GUS) measurements

Leaves of three *Nicotiana benthamiana* plants were inoculated with a mixture of *Agrobacterium* delivering constructs for expression of TALEs and the promoter-GUS reporter. Twenty-seven or 48 h postinoculation, two leaf discs (1 cm diameter) from separate infiltration spots of the same constructs on one plant were combined, ground in liquid nitrogen, and GUS assays were done as described previously (Kay *et al.*, 2007). Samples were measured in a plate reader at 360 nm (excitation) and 465 nm (emission) with 4-methyl-umbelliferon (MU) (Carl Roth, Karlsruhe, Germany) dilutions as standard. Proteins were quantified using Bradford assays (Bio-Rad). Triplicate samples from three different plants were combined into one data point. In parallel, leaf discs from inoculated areas were sampled and incubated overnight in X-Gluc staining solution (Schornack *et al.*, 2005). Leaf discs were cleared in 100% ethanol and dried using cellulose foil. Experiments were performed at least twice with similar results.

## Results

The promoters of the rice genes *Xa13*, *OsTFX1* and *Os11N3* are direct targets of the *Xoo* TALEs PthXo1, PthXo6 and AvrXa7, respectively

Recent studies uncovered that the *Xoo* TALEs PthXo1, PthXo6 and AvrXa7 transcriptionally activate the rice *Xa13* (synonym: *Os8N3*), *OsTFX1* and *Os11N3* genes, respectively (Chu *et al.*, 2006; Yang *et al.*, 2006; Sugio *et al.*, 2007; Antony *et al.*, 2009; Yuan *et al.*, 2009). To test if the rice *OsTFX1*, *Os11N3* and *Xa13* promoters are direct TALE targets, we amplified the corresponding promoter fragments from rice genomic DNA and cloned these in a T-DNA vector in front of an *uidA* reporter gene (Figs 1a, S1). The promoter::*uidA* fusion constructs were delivered into *N. benthamiana* leaves via transient *A. tumefaciens*-mediated

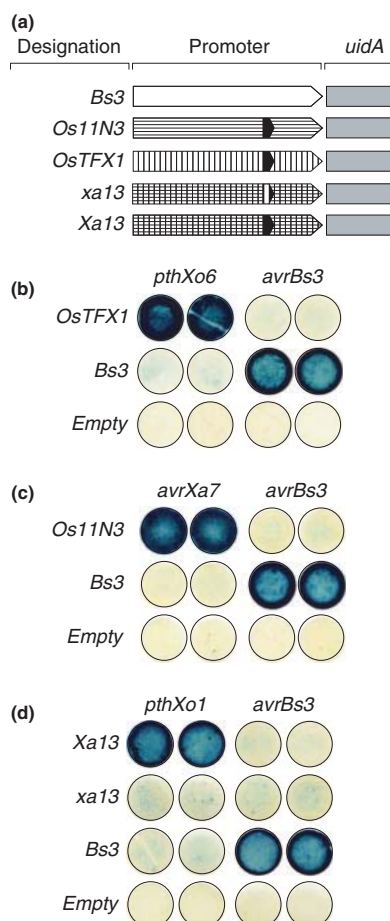


**Fig. 1** Promoters of *Xoo* susceptibility genes in rice are transcriptionally activated by their matching transcription activator-like effector (TALE) proteins. (a) Graphical display of the studied promoter::*uidA* reporter constructs. Arrows represent the rice promoters *Os11N3*, *OsTFX1*, *Xa13*, *xa13* and the pepper *Bs3* gene. Nucleotide sequences of the rice promoters are provided in Supporting Information, Fig. S1. The corresponding *UPT*<sub>AvrXa7</sub>, *UPT*<sub>PthXo6</sub>, *UPT*<sub>PthXo1</sub> and *UPT*<sub>AvrBs3</sub> boxes are shown as black boxes. A black box with a white bar represents the nonfunctional *UPT*<sub>PthXo1</sub> box of the *xa13* promoter from the rice cv IRBB13. A gray box represents the *uidA* reporter gene, encoding the  $\beta$ -glucuronidase (GUS) protein. (b–d) *In planta* functional analysis of rice promoters and their matching TALEs. *uidA* T-DNA constructs under transcriptional control of the depicted plant promoters were delivered via *Agrobacterium tumefaciens* into *Nicotiana benthamiana* leaves in combination with either an empty T-DNA vector (empty) or the 35S-promoter-driven TALE genes of *avrBs3*, *pthXo6*, *avrXa7* and *pthXo1*. Leaf discs were stained with 5-bromo-4-chloro-3-indolyl- $\beta$ -D-glucuronic acid, cyclohexylammonium salt (X-Gluc) to visualize activity of the GUS reporter. Samples were taken at 27 hpi (b, d) or 48 hpi (c).

T-DNA transformation (agroinfiltration) in combination with the cauliflower mosaic virus 35S (35S) promoter-driven TALE genes *pthXo1*, *pthXo6*, *avrXa7* and *avrBs3*. GUS

## 4 Research

assays showed that the rice *OsTFX1* and *Os11N3* promoters are activated specifically by the matching *Xoo* TALEs PthXo6 and AvrXa7, respectively, but not by the related *Xcv* TALE AvrBs3 (Fig. 1b,c). Furthermore, the GUS assays showed that the *Xoo* TALE PthXo1 transcriptionally activates only the rice *Xa13* promoter from the rice cv IR24 but not the allelic *xa13* promoter from the *Xoo*-resistant rice cv IRBB13 (Fig. 1d). Our GUS assays are in agreement with previous studies showing that *Xoo* delivering PthXo1 activates only expression of *Xa13* but not *xa13* alleles (Chu *et al.*, 2006; Yuan *et al.*, 2009). In our GUS assays, the pepper *Bs3* promoter was not activated by any of the *Xoo* TALEs but it was activated by the *Xcv* TALE AvrBs3 (Fig. 1b–d). These data demonstrate that the *OsTFX1*, *Os11N3* and *Xa13* promoters are direct targets of the *Xoo* TALEs PthXo6, AvrXa7 and PthXo1, respectively.

TALEs target the *in silico* predicted UPT boxes

We used the TALE code (Boch *et al.*, 2009; Moscou & Bogdanove, 2009) to predict the  $UPT_{PthXo6}$ ,  $UPT_{AvrXa7}$  and  $UPT_{PthXo1}$  boxes of the rice *OsTFX1*, *Os11N3* and *Xa13* promoters, respectively (Figs S1, S2, Table S1). Regions potentially encompassing the distinct UPT boxes were introduced into the pepper *Bs3* promoter and cloned in front of an *uidA* reporter gene. The *Bs3* promoter-embedded UPT boxes were agroinfiltrated into *N. benthamiana* leaves in combination with the 35S promoter-driven TALE genes *pthXo1*, *pthXo6*, *avrXa7* or *avrBs3*. GUS assays showed that a *Bs3* promoter derivative containing a given UPT box is transcriptionally activated only by the matching *Xoo* TALE (Figs 2–4). For example, insertion of the  $UPT_{PthXo6}$  box from the rice *OsTFX1* into the pepper *Bs3* promoter (*OsTFX1* in *Bs3*, Fig. 2b) made this promoter PthXo6- but not PthXo1-inducible. By contrast, the *Bs3* wild-type promoter (*Bs3*) that lacks the  $UPT_{PthXo6}$  box was only AvrBs3- but not PthXo6-inducible. Similarly, insertion of the  $UPT_{AvrXa7}$  and  $UPT_{PthXo1}$  boxes into the *Bs3* promoter resulted in promoter constructs that were AvrXa7- and PthXo1-inducible, respectively (Figs 3b, 4b). All *Bs3* promoter derivatives contain the  $UPT_{AvrBs3}$  box and thus were AvrBs3-inducible, irrespective of whether or not a *Xoo* TALE box was present (Figs 2b, 3b, 4b). In summary, the TALE code enabled the identification of UPT boxes from rice promoters that are transcriptionally up-regulated by corresponding *Xoo* TALEs.

## Mutation of the conserved 5' terminal T nucleotide of UPT boxes results in reduced TALE-mediated inducibility

All UPT boxes that have been predicted with the TALE code are preceded by a 5' terminal T nucleotide (Boch *et al.*, 2009; Moscou & Bogdanove, 2009). Mutations in

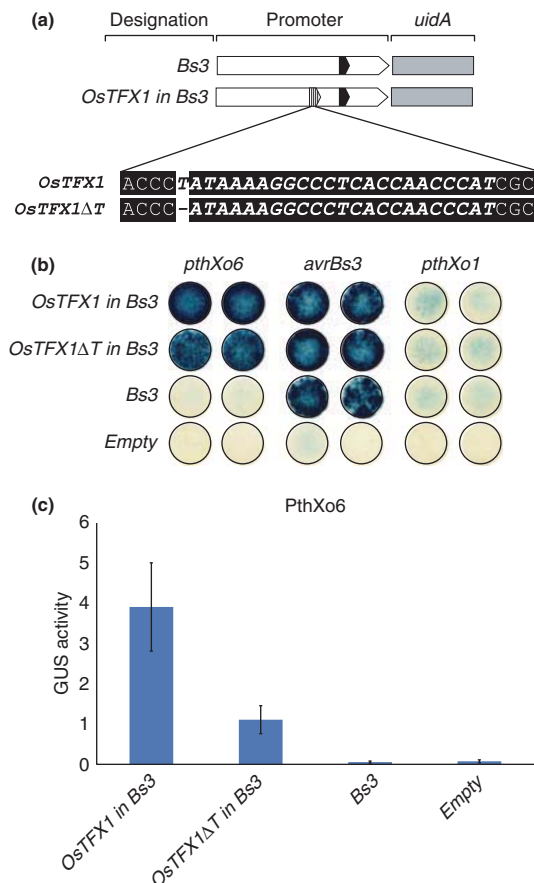


**Fig. 2** The transcription activator-like effector (TALE) PthXo6 transcriptionally activates promoters containing the  $UPT_{PthXo6}$  box of the rice *OsTFX1* promoter. (a) Graphical display of promoter::*uidA* reporter constructs. The white arrow represents the pepper *Bs3* promoter. A gray box represents the β-glucuronidase (GUS)-encoding *uidA* reporter gene. The  $UPT_{AvrBs3}$  and  $UPT_{PthXo6}$  boxes are displayed as black and hatched arrows, respectively, with their nucleotide sequences depicted below. Bold italic letters represent the core  $UPT_{PthXo6}$  box (*OsTFX1*). A dash represents the deleted 5' terminal T nucleotide of the mutated  $UPT_{PthXo6}$  box (*OsTFX1ΔT*). (b) PthXo6 targets specifically the  $UPT_{PthXo6}$  but not the  $UPT_{AvrBs3}$  box. A fragment of the *OsTFX1* promoter containing the  $UPT_{PthXo6}$  box was placed into the context of pepper *Bs3* promoter (*OsTFX1* in *Bs3*). '*OsTFX1ΔT* in *Bs3*' denotes a *OsTFX1* promoter fragment with a mutated  $UPT_{PthXo6}$  box that lacks the 5' terminal T nucleotide of the core box. The different reporter constructs were delivered into *Nicotiana benthamiana* leaves via *Agrobacterium tumefaciens* with either an empty T-DNA vector (empty) or 35S-promoter-driven TALE genes *avrBs3*, *pthXo6* or *pthXo1*. (c) Deletion of the 5' terminal T nucleotide of the  $UPT_{PthXo6}$  box significantly reduces its PthXo6-dependent inducibility. GUS activity (pmol 4-MU min<sup>-1</sup> μg<sup>-1</sup> protein) was determined 27 h after *A. tumefaciens*-mediated co-delivery of the depicted reporter constructs in combination with a 35S-promoter-driven *pthXo6* gene. Error bars denote standard deviations.

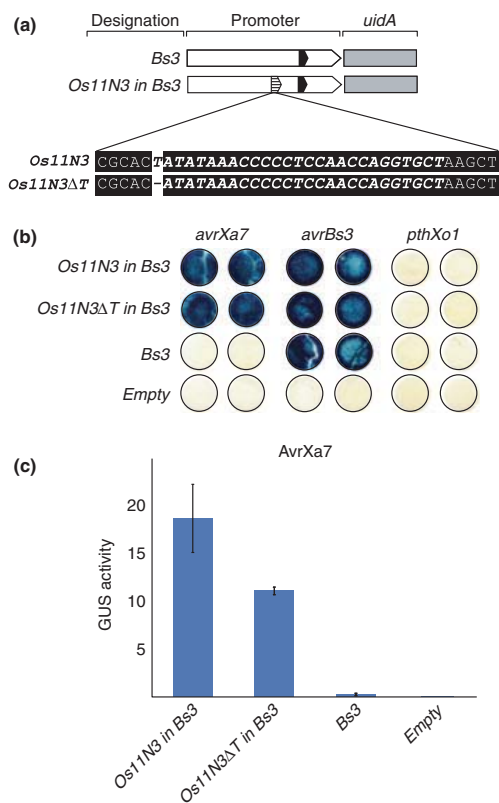


**Fig. 3** The transcription activator-like effector (TALE) AvrXa7 transcriptionally activates promoters containing the  $UPT_{AvrXa7}$  box of the rice *Os11N3* promoter. (a) Graphical display of promoter::*uidA* reporter constructs. The white arrow represents the pepper *Bs3* promoter. The  $UPT_{AvrBs3}$  and  $UPT_{AvrXa7}$  boxes are displayed as black and hatched boxes, respectively. A gray box represents the *uidA* reporter gene, encoding the  $\beta$ -glucuronidase (GUS) protein. The letters below the boxes represent the nucleotides of the *Os11N3* promoter that were inserted into the *Bs3* promoter. Bold italic letters represent the core  $UPT_{AvrXa7}$  box (*Os11N3*). The dash represents the deleted nucleotide of the mutated  $UPT_{AvrXa7}$  box (*Os11N3ΔT*). (b) AvrXa7 targets specifically the  $UPT_{AvrXa7}$  but not the  $UPT_{AvrBs3}$  box. A fragment of the *Os11N3* promoter containing the  $UPT_{AvrXa7}$  box was placed into the context of pepper *Bs3* promoter (*Os11N3 in Bs3*). '*Os11N3ΔT in Bs3*' denotes an *Os11N3* promoter fragment with the mutated  $UPT_{AvrXa7}$  box. The different reporter constructs were delivered into *Nicotiana benthamiana* leaves via *Agrobacterium tumefaciens* in combination with either an empty T-DNA vector (empty) or the 35S-promoter-driven TALE genes *avrBs3*, *avrXa7* or *pthXo1*. (c) The deletion of the 5' terminal T nucleotide of the  $UPT_{AvrXa7}$  box significantly reduces its AvrXa7-dependent inducibility. GUS activity in *N. benthamiana* is taken as a measure of the AvrXa7-dependent inducibility of the given promoter. GUS activity ( $\text{pmol } 4\text{-MU min}^{-1} \mu\text{g}^{-1} \text{ protein}$ ) was determined 48 h after *A. tumefaciens*-mediated co-delivery of the depicted reporter constructs in combination with a 35S-promoter-driven *avrXa7* gene. Error bars denote standard deviations.

the 5' terminal T nucleotide of the  $UPT_{AvrBs3}$  or  $UPT_{Hax3}$  box resulted in reduced inducibility by the matching TALE (Boch *et al.*, 2009; Römer *et al.*, 2009b). To study the functional importance of the 5' terminal T nucleotide of the  $UPT_{PthXo6}$ ,  $UPT_{AvrXa7}$  and  $UPT_{PthXo1}$  boxes, we created T deletion mutants ( $\Delta T$ ) of the corresponding *Bs3*-promoter-embedded  $UPT$  boxes and cloned these in front of an *uidA* reporter gene. The  $UPT$  box  $\Delta T$  mutants were delivered into *N. benthamiana* leaves via agroinfiltration in combination with the 35S promoter-driven TALE genes *pthXo6*, *avrXa7*, *pthXo1* or *avrBs3*. Qualitative GUS assays showed that promoters containing the  $\Delta T$  mutants of the  $UPT_{PthXo6}$ ,  $UPT_{AvrXa7}$  or  $UPT_{PthXo1}$  boxes were still induced by their matching TALEs (*OsTFX1ΔT in Bs3* (Fig. 2b), *Os11N3ΔT in Bs3* (Fig. 3b) and *Xa13ΔT in Bs3* (Fig. 4b)). However, quantitative GUS assays demonstrated that the three tested  $\Delta T$  mutants in all cases produced a significantly reduced GUS activity in comparison to the wild-type  $UPT$  boxes (Figs 2c, 3c, 4c). Thus the 5' terminal T nucleotide is important to the function of the  $UPT_{PthXo6}$ ,  $UPT_{AvrXa7}$  and  $UPT_{PthXo1}$  boxes.

#### Rice *Xa13* and *xa13* alleles differ in the predicted $UPT_{PthXo1}$ box

Molecular analysis of a collection of rice *xa13* and *Xa13* rice genotypes uncovered that the *pthXo1* expressing *Xoo* strain PXO99 transcriptionally activates only *Xa13* but not *xa13* genotypes (Chu *et al.*, 2006; Yuan *et al.*, 2009). We anticipated that *Xa13* and *xa13* genotypes are likely to differ in their  $UPT_{PthXo1}$  box region. Sequence analysis revealed that the PthXo1-inducible *Xa13* alleles from rice cvs IR24, IR64, Nipponbare, Minghui and 93-11 were sequence identical within the  $UPT_{PthXo1}$  box (Figs S3, S4). By contrast, all studied *xa13* alleles differed from the *Xa13* alleles within the  $UPT_{PthXo1}$  box. In several *xa13* alleles, the integrity of the  $UPT_{PthXo1}$  box was lost as a result of nucleotide insertions or deletions. For example, the *xa13* allele from rice cv AC 19-1-1 and Kalimekri 77-5 have lost 3' terminal nucleotides of the  $UPT_{PthXo1}$  box as a result of a 34 bp deletion with respect to the IR24 *Xa13* allele (Fig. S4). We also identified five *xa13* genotypes (Tepa1, BJ1, Chinsurah 11484, Chinsurah 11760 and Chinsurah 50930) that showed only a G  $\rightarrow$  T substitution in the second box nucleotide with respect to the  $UPT_{PthXo1}$  box from IR24 (Fig. S4a). According to the TALE code the second nucleotide of the  $UPT_{PthXo1}$  box is bound by the first PthXo1 repeat unit, which contains an NN-type RVD. Experimental studies with an *in vitro* constructed TALE consisting of NN-type RVDs only have shown that NN recognizes preferentially G (Boch *et al.*, 2009). To clarify how polymorphisms in the second nucleotide of the  $UPT_{PthXo1}$  box influence PthXo1-mediated promoter activation, we replaced the G nucleotide of the *Xa13* allele by A, C or T

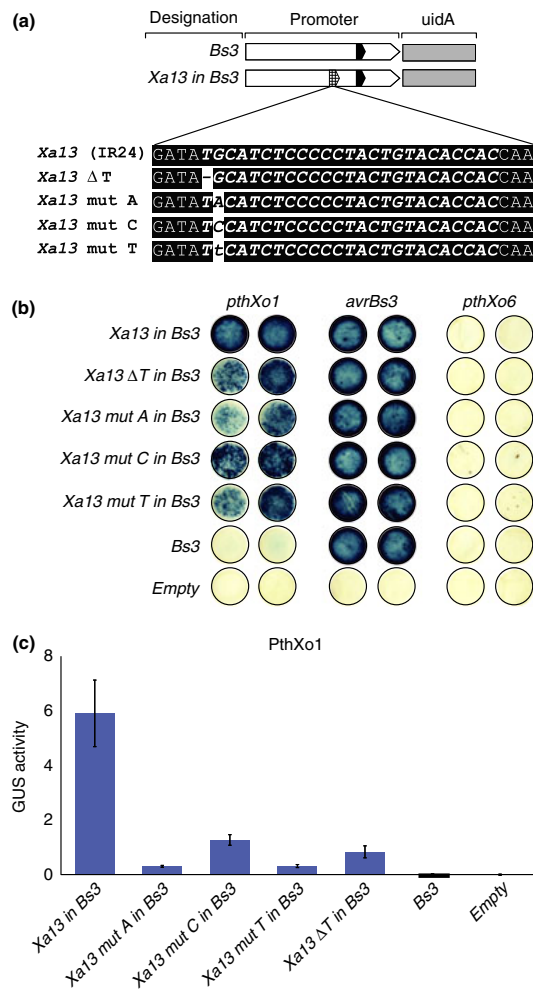


**Fig. 4** The transcription activator-like effector (TALE) PthXo1 transcriptionally activates promoters containing the  $UPT_{PthXo1}$  box of the rice *Xa13* promoter. (a) Graphical display of promoter::uidA reporter constructs. The white arrow represents the pepper *Bs3* promoter. The  $UPT_{AvrBs3}$  and  $UPT_{PthXo1}$  boxes are displayed as black and hatched boxes, respectively. A gray box represents the *uidA* reporter gene, encoding the  $\beta$ -glucuronidase (GUS) protein. Letters below the boxes represent the nucleotides of the *Xa13* promoter that were inserted into the *Bs3* promoter. Bold italic letters represent the core  $UPT_{PthXo1}$  box of the *Xa13* promoter from rice cv IR24. A dash represents the deleted 5' terminal T nucleotide of the mutated  $UPT_{PthXo1}$  (*Xa13*ΔT). Black letters on white background represent mutations with respect to the *Xa13* allele of the rice cv IR24. The G → T exchange that is present in several *xa13* alleles is displayed in lower case. (b) PthXo1 targets specifically the  $UPT_{PthXo1}$  but not the  $UPT_{AvrBs3}$  box. A fragment of the *Xa13* promoter containing the  $UPT_{PthXo1}$  box was placed into the context of pepper *Bs3* promoter (*Xa13* in *Bs3*). '*Xa13* in *Bs3*' and derivatives with mutations in the  $UPT_{PthXo1}$  box were delivered into *Nicotiana benthamiana* leaves via *Agrobacterium tumefaciens* in combination with either an empty T-DNA vector (empty) or the 35S-promoter-driven TALE genes *pthXo6*, *avrBs3* or *pthXo1*. (c) Mutations within the first and the second nucleotide of the  $UPT_{PthXo1}$  box significantly reduce the PthXo1-dependent inducibility. GUS activity (pmol 4-MU min<sup>-1</sup> μg<sup>-1</sup> protein) in *N. benthamiana* is taken as a measure of the PthXo1-dependent inducibility of the given promoter. GUS activity was determined 27 h after *A. tumefaciens*-mediated co-delivery of the depicted reporter constructs in combination with a 35S-promoter-driven *pthXo1* gene. Error bars denote standard deviations.

nucleotides and tested the activity of these boxes in the context of the *Bs3* promoter (Fig. 4c). Quantitative GUS assays showed that G → A, G → C or G → T exchanges of the second box nucleotide resulted in significantly reduced PthXo1 inducibility in comparison to the nonmutated IR24  $UPT_{PthXo1}$  box (Fig. 4c). Thus these experimental findings provide further support for the TALE code.

**PthXo1 and PthXo6 bind in EMSA to matching UPT boxes**

Previous studies have shown that the TALEs AvrBs3, AvrBs3Δrep16 and AvrXa27 bind specifically to their matching UPT boxes (Römer *et al.*, 2009a,b). Here we carried out EMSA to clarify if PthXo1 and PthXo6 would also bind specifically to their matching UPT boxes. EMSA showed that a His::PthXo1 fusion protein binds to a biotin-

labeled *Xa13* (cv IR24) promoter fragment containing the  $UPT_{PthXo1}$  box and, to a lesser extent, to the corresponding promoter region of the *xa13* allele (cv IRBB13) (Fig. 5). Importantly, binding of His::PthXo1 to biotin-labeled *Xa13* promoter fragments could be readily out-competed by nonlabeled *Xa13* promoter fragments, whereas even a 100-fold excess of nonlabeled *xa13* promoter fragments could not out-compete the binding (Fig. 5). Similarly, His::PthXo6 binds in EMSA to a biotin-labeled *OsTFX1* promoter fragment containing the  $UPT_{PthXo6}$  box and, to a much lesser extent, to a mutated *OsTFX1* promoter fragment (*OsTFX1*ΔT) that lacks the 5' terminal T nucleotide of the  $UPT_{PthXo6}$  box (Fig. 6). Competition assays with biotin-labeled *OsTFX1*-derived promoter fragments and unlabeled *OsTFX1* and *OsTFX1*ΔT promoter fragments further confirmed that His::PthXo6 has high affinity to the  $UPT_{PthXo6}$  box and only a very low affinity to a  $UPT_{PthXo6}$  box mutant variant that lacks the 5' terminal T nucleotide (Fig. 6). Together these findings indicate that PthXo1 and PthXo6 bind specifically to their matching UPT boxes.

**Discussion**

**The TALE code and its limitations**

We have demonstrated that the rice promoters *Xa13*, *OsTFX1* and *Os11N3* are activated by the *Xoo* TALEs



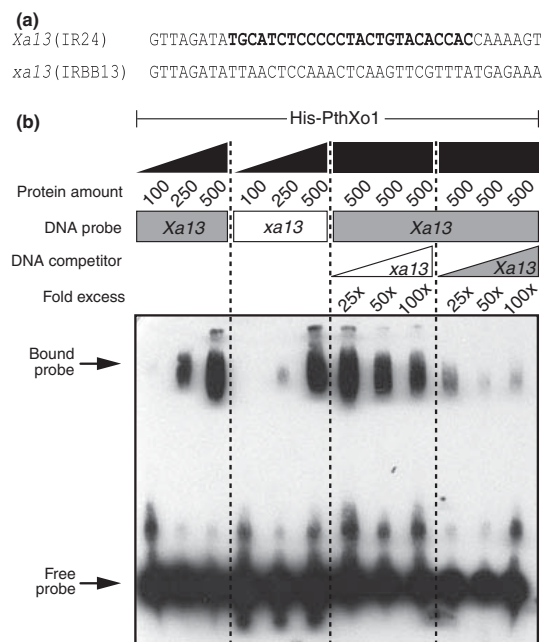


**Fig. 5** The transcription activator-like effector (TALe) PthXo1 binds to the  $UPT_{PthXo1}$  box of the *Xa13* promoter. (a) Probes derived from *Xa13* (cv IR24) and *xa13* (cv IRBB13) promoters used in electrophoretic mobility shift assays (EMSAs). The predicted  $UPT_{PthXo1}$  box of the *Xa13* promoter is shown in bold letters. (b) PthXo1 binds with higher affinity to the *Xa13* promoter (gray boxes) than to the *xa13* promoter (white boxes). EMSA with PthXo1 and *Xa13*- or *xa13*-derived probes or competitor DNA. A molar excess of nonlabeled *Xa13* or *xa13* fragments of 25 $\times$ , 50 $\times$  and 100 $\times$  were used for competition experiments. Protein amounts are in fmol. Positions of the bound and free probes are indicated.

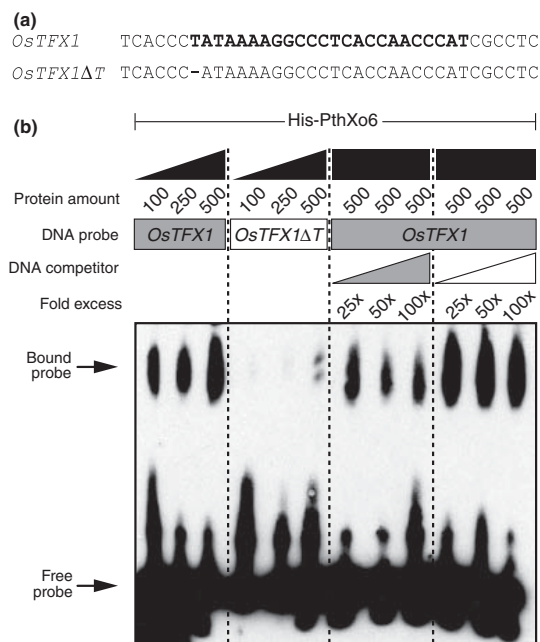


**Fig. 6** The transcription activator-like effector (TALe) PthXo6 binds to the  $UPT_{PthXo6}$  box of the *OsTFX1* promoter. (a) Probes derived from the *OsTFX1* promoter and a mutant derivative (*OsTFX1* $\Delta$ T) were used in electrophoretic mobility shift assays (EMSAs). The predicted  $UPT_{PthXo6}$  box of the *OsTFX1* promoter is shown in bold letters. A dash '-' indicates a deletion. (b) A deletion of the first nucleotide of the  $UPT_{PthXo6}$  box strongly reduces its affinity to PthXo6. EMSA with PthXo6 and *OsTFX1*-derived probes or competitor DNA. A molar excess of nonlabeled *OsTFX1*- and *OsTFX1* $\Delta$ T-fragments of 25 $\times$ , 50 $\times$ , and 100 $\times$  was used for competition experiments. Protein amounts are in fmol. Positions of the bound and free probes are indicated.

PthXo1, PthXo6 and AvrXa7, respectively (Fig. 1). Furthermore, we demonstrated that code-predicted  $UPT$  boxes are functional in the context of the pepper *Bs3* promoter (Figs 2–4) and that TALes interact physically with code-predicted  $UPT$  boxes (Figs 5, 6). Given that functional  $UPT$  boxes could be reliably predicted for promoters that are known to be activated by given TALes, the question arises whether functional  $UPT$  boxes can also be identified from sequenced host genomes. One obvious limitation of the current version of the TALe code is that RVDs with low frequency of occurrence in sequenced TALes (e.g. HI, SS, NQ, NC and NV) have not yet been deciphered, although their specificity should be readily determined. The major limitation of the TALe code, then, is the uncertainty of the functional consequences of mismatches between  $UPT$  box nucleotides and individual RVDs. In this context it needs to be noted that our previous study on the TALe code (Boch *et al.*, 2009) was focused on *in vitro* generated  $UPT$  boxes that show no or very few mismatches with respect to the given TALe. By contrast, all identified natural  $UPT$

boxes in plant promoters and their matching TALes contain many mismatches. For example, the TALe PthXo1 contains three NI-type RVDs that do not match the code-predicted A in the  $UPT_{PthXo1}$  box of the PthXo1-inducible *Xa13* promoter (see PthXo1 repeat units 10 (NI  $\rightarrow$  C), 19 (NI  $\rightarrow$  C) and 21 (NI  $\rightarrow$  C); Fig. S2). Whereas some mismatches have little effect on the magnitude of transcription activation, other mismatches have proved to be critical to TALe-mediated promoter activation. One striking example is the PthXo1-inducible *Xa13* gene from the rice cv IR24 and the allelic, non PthXo1-inducible *xa13* gene from the rice cv Tepas1. These *Xa13/xa13* alleles differ only in a G  $\rightarrow$  T substitution of the second nucleotide of the  $UPT_{PthXo1}$  box which pairs to a NN-type repeat (Figs S2, S4). Reverse transcription polymerase chain reaction (RT-PCR) analysis of rice leaf tissue that was infected with a *pthXo1*-expressing *Xoo* strain revealed transcriptional activation of the IR24 *Xa13* but not the Tepas1 *xa13* allele (Chu *et al.*, 2006). Similarly, agroinfiltration assays revealed a sig-

nificantly reduced PthXo1-mediated transcriptional activation of the Tepa1 *xa13* allele as compared with induction of the IR24 *Xa13* allele (Fig. 4c; the Tepa1 *xa13* allele corresponds to 'Xa13 mut T in B3'). This strong effect of a single mismatched NN-type repeat is somewhat unexpected considering that the  $UPT_{PthXo1}$  box of the IR24 *Xa13* promoter, which mediates PthXo1-mediated promoter activation, contains seven mismatches compared with the code-predicted  $UPT_{PthXo1}$  box (Fig. S2). Thus it seems that correct pairing of the second (NN-type) repeat of PthXo1 is crucial in the context of the PthXo1– $UPT$  box interaction than correct pairing of other RVDs.

We postulate that the sum of RVDs that pair to code-predicted nucleotides determines the overall affinity of a TALE to a given  $UPT$  box, with a minimum number of matching RVDs required to promote TALE-mediated transcriptional activation. This hypothesis is supported by the observation that longer TALEs appear to tolerate more mismatches than shorter TALEs. For example, AvrXa7 (26 repeat units) and PthXo1 (24 repeats units) transcriptionally activate the rice *Os11N3* and *Xa13* promoter despite the fact that there are eight and seven mismatches in the corresponding  $UPT_{AvrXa7}$  (*Os11N3* promoter) and  $UPT_{PthXo1}$  (IR24 *Xa13* promoter) boxes, respectively (Fig. S2). By contrast, the  $UPT$  boxes that are targeted by the shorter TALEs AvrHah1 (14 repeats units; activates *B3* promoter) (Schornack *et al.*, 2008) and AvrBs3 $\Delta$ rep16 (14 repeats units; activates *B3-E* promoter) (Römer *et al.*, 2007, 2009b; Boch *et al.*, 2009; Moscou & Bogdanove, 2009) each contains a single mismatch as compared with the code-predicted  $UPT$  boxes.

Although longer TALEs seem to target  $UPT$  boxes with multiple mismatches, it is conceivable that longer TALEs also require a minimum number of RVDs that pair to matching nucleotides in order to promote transcriptional activation. Given that the  $UPT_{PthXo1}$  box from the IR24 *Xa13* promoter contains seven mismatches as compared with the code-predicted  $UPT_{PthXo1}$  box (Fig. S2), one might speculate that any additional mismatch will result in reduced inducibility of the given box. Thus the reduced inducibility of the Tepa1 *xa13* allele (G  $\rightarrow$  T substitution of the second nucleotide of the  $UPT_{PthXo1}$  box) might be a consequence of the reduced overall affinity of PthXo1 to the Tepa1 *xa13* allele and does not necessarily imply that correct pairing of this particular RVD is crucial to the TALE– $UPT$  box interaction.

In summary, TALEs target not only code-predicted  $UPT$  boxes but also closely related boxes. However, the functional consequences of mismatches between  $UPT$  box nucleotides and corresponding RVDs remain, to some extent, unpredictable. It remains to be clarified if all RVDs make an equal contribution to the TALE–DNA interaction or if certain RVDs are of particular importance. Obviously a crystal structure of a TALE and its matching  $UPT$  box will

help to give further insights into the molecular basis of this interaction.

The 5' terminal T of the  $UPT$  boxes is crucial to transcriptional activation by, and interaction with, its matching TALE

Previous studies uncovered that all functional  $UPT$  boxes contain a conserved, invariant 5' terminal T nucleotide (Boch *et al.*, 2009; Moscou & Bogdanove, 2009). Mutational studies of the conserved T in the  $UPT$  boxes of the TALEs AvrBs3 and Hax3 resulted in reduced induction of the corresponding promoter mutant derivatives as compared with the promoters containing the conserved T nucleotide (Boch *et al.*, 2009; Römer *et al.*, 2009b). Analogously, our studies showed that a mutation in the conserved 5' terminal T nucleotide of the PthXo1, PthXo6 and AvrXa7  $UPT$  boxes also resulted in reduced inducibility of the corresponding rice *Xa13*, *OsTFX1* and *Os11N3* promoters (Figs 2c, 3c, 4c). Thus the functional relevance of the conserved 5' terminal T nucleotide has by now been confirmed for five different TALEs, suggesting that the invariant T is crucial to the function of most, or possibly all,  $UPT$  boxes.

Previous EMSAs on the TALE AvrBs3 $\Delta$ rep16 suggested that the 5' terminal T nucleotide of the corresponding pepper *B3-E* promoter  $UPT_{AvrBs3\Delta rep16}$  box makes a significant contribution to the TALE–DNA interaction (Römer *et al.*, 2007, 2009b). However, an EMSA-based comparison of identical DNA fragments that contain or lack the conserved 5' terminal T nucleotide of a  $UPT$  box had not yet been carried out. We compared by EMSA the affinities of the wild-type  $UPT_{PthXo6}$  box from the rice *OsTFX1* promoter and a corresponding mutant box lacking the conserved T nucleotide (*OsTFX1* $\Delta$ T), and found a drastically reduced interaction between PthXo6 and the mutant box as compared with the wild-type  $UPT_{PthXo6}$  box (Fig. 6). These findings demonstrate that the 5' terminal T nucleotide of the  $UPT_{PthXo6}$  box is crucial to physical interaction between PthXo6 and the  $UPT_{PthXo6}$  box. Given that similar findings have been observed for the TALE AvrBs3 $\Delta$ rep16 (Römer *et al.*, 2007, 2009b), it seems likely that, in general, the 5' terminal T nucleotide of a  $UPT$  box is crucial to its physical interaction with a corresponding TALE. Future studies will have to clarify which TALE residues pair to the conserved T. Once this question is resolved, we may be able to modify TALEs in such a way that pairing to nucleotides other than a 5' terminal T is possible.

## Acknowledgements

We thank Bing Yang and Frank White for providing *Xoo* TALE genes. We would like to acknowledge the technical

support of Carola Kretschmer, Bianca Rosinsky, Marina Schulze and Heidi Scholze. Work in our laboratory has been supported by grants of the 2Blades foundation, the Exzellenznetzwerk Biowissenschaften (Ministry of Culture of Saxonia-Anhalt) and the Deutsche Forschungsgemeinschaft (SPP1212, SFB 648 and LA1338/2-2). We are grateful to Diana Horvath for helpful comments on the manuscript.

## References

- Antony G, Yang B, White FF. 2009. The alternate major effector AvrXa7 in bacterial blight of rice evades host resistance by targeting an alternate major host susceptibility gene. *Phytopathology* 99: S5. (abstract).
- Bai XD, Correa VR, Toruno TY, Ammar ED, Kamoun S, Hogenhout SA. 2009. AY-WB phytoplasma secretes a protein that targets plant cell nuclei. *Molecular Plant-Microbe Interactions* 22: 18–30.
- Boch J, Scholze H, Schornack S, Landgraf A, Hahn S, Kay S, Lahaye T, Nickstadt A, Bonas U. 2009. Breaking the code of DNA-binding specificity of TAL-type III effectors. *Science* 326: 1509–1512.
- Boller T, He SY. 2009. Innate immunity in plants: an arms race between pattern recognition receptors in plants and effectors in microbial pathogens. *Science* 324: 742–744.
- Chu Z, Yuan M, Yao J, Ge X, Yuan B, Xu C, Li X, Fu B, Li Z, Bennetzen JL *et al.* 2006. Promoter mutations of an essential gene for pollen development result in disease resistance in rice. *Genes and Development* 20: 1250–1255.
- Deslandes L, Olivier J, Peeters N, Feng DX, Khounlotham M, Boucher C, Somssich I, Genin S, Marco Y. 2003. Physical interaction between RRS1-R, a protein conferring resistance to bacterial wilt, and PopP2, a type III effector targeted to the plant nucleus. *Proceedings of the National Academy of Sciences, USA* 100: 8024–8029.
- Elling AA, Davis EL, Hussey RS, Baum TJ. 2007. Active uptake of cyst nematode parasitism proteins into the plant cell nucleus. *International Journal for Parasitology* 37: 1269–1279.
- Göhre V, Robatzek S. 2008. Breaking the barriers: microbial effector molecules subvert plant immunity. *Annual Review of Phytopathology* 46: 189–215.
- Gu K, Yang B, Tian D, Wu L, Wang D, Sreekala C, Yang F, Chu Z, Wang GL, White FF *et al.* 2005. *R* gene expression induced by a type-III effector triggers disease resistance in rice. *Nature* 435: 1122–1125.
- Herbers K, Conrads-Strauch J, Bonas U. 1992. Race-specificity of plant resistance to bacterial spot disease determined by repetitive motifs in a bacterial avirulence protein. *Nature* 356: 172–174.
- Hogenhout SA, Van der Hoorn RAL, Terauchi R, Kamoun S. 2009. Emerging concepts in effector biology of plant-associated organisms. *Molecular Plant-Microbe Interactions* 22: 115–122.
- Kanneganti TD, Bai X, Tsai CW, Win J, Meulia T, Goodin M, Kamoun S, Hogenhout SA. 2007. A functional genetic assay for nuclear trafficking in plants. *Plant Journal* 50: 149–158.
- Kay S, Bonas U. 2009. How *Xanthomonas* type III effectors manipulate the host plant. *Current Opinion in Microbiology* 12: 37–43.
- Kay S, Hahn S, Marois E, Hause G, Bonas U. 2007. A bacterial effector acts as a plant transcription factor and induces a cell size regulator. *Science* 318: 648–651.
- Kay S, Hahn S, Marois E, Wieduwild R, Bonas U. 2009. Detailed analysis of the DNA recognition motifs of the *Xanthomonas* type III effectors AvrBs3 and AvrBs3Arep16. *Plant Journal* 59: 859–871.
- Kemen E, Kemen AC, Rafiqi M, Hempel U, Mendgen K, Hahn M, Voegelé RT. 2005. Identification of a protein from rust fungi transferred from haustoria into infected plant cells. *Molecular Plant-Microbe Interactions* 18: 1130–1139.
- Koncz C, Schell J. 1986. The promoter of TL-DNA gene 5 controls the tissue-specific expression of chimeric genes carried by a novel type of *Agrobacterium* binary vector. *Molecular and General Genetics* 204: 383–396.
- Moscou MJ, Bogdanove AJ. 2009. A simple cipher governs DNA recognition by TAL effectors. *Science* 326: 1501.
- Nakagawa T, Kurose T, Hino T, Tanaka K, Kawamukai M, Niwa Y, Toyooka K, Matsuoka K, Jinbo T, Kimura T. 2007. Development of series of gateway binary vectors, pGWBs, for realizing efficient construction of fusion genes for plant transformation. *Journal of Bioscience and Bioengineering* 104: 34–41.
- Nissan G, Manulis-Sasson S, Weinthal D, Mor H, Sessa G, Barash I. 2006. The type III effectors HsvG and HsvB of gall-forming *Pantoea agglomerans* determine host specificity and function as transcriptional activators. *Molecular Microbiology* 61: 1118–1131.
- Römer P, Hahn S, Jordan T, Strauß T, Bonas U, Lahaye T. 2007. Plant-pathogen recognition mediated by promoter activation of the pepper *B3* resistance gene. *Science* 318: 645–648.
- Römer P, Recht S, Lahaye T. 2009a. A single plant resistance gene promoter engineered to recognize multiple TAL effectors from disparate pathogens. *Proceedings of the National Academy of Sciences, USA* 106: 20526–20531.
- Römer P, Strauß T, Hahn S, Scholze H, Morbitzer R, Grau J, Bonas U, Lahaye T. 2009b. Recognition of AvrBs3-like proteins is mediated by specific binding to promoters of matching pepper *B3* alleles. *Plant Physiology* 150: 1697–1712.
- Schornack S, Meyer A, Römer P, Jordan T, Lahaye T. 2006. Gene-for-gene mediated recognition of nuclear-targeted AvrBs3-like bacterial effector proteins. *Journal of Plant Physiology* 163: 256–272.
- Schornack S, Minsavage GV, Stall RE, Jones JB, Lahaye T. 2008. Characterization of AvrHah1 a novel AvrBs3-like effector from *Xanthomonas gardneri* with virulence and avirulence activity. *New Phytologist* 179: 546–556.
- Schornack S, Peter K, Bonas U, Lahaye T. 2005. Expression levels of *avrBs3*-like genes affect recognition specificity in tomato *B4* but not in pepper *B3* mediated perception. *Molecular Plant-Microbe Interactions* 18: 1215–1225.
- Sugio A, Yang B, Zhu T, White FF. 2007. Two type III effector genes of *Xanthomonas oryzae* pv. *oryzae* control the induction of the host genes *OsTFIIAγ1* and *OsTFX1* during bacterial blight of rice. *Proceedings of the National Academy of Sciences, USA* 104: 10720–10725.
- White FF, Potnis N, Jones JB, Koebnik R. 2009. The Type III effectors of *Xanthomonas*. *Molecular Plant Pathology* 10: 749–766.
- Yang B, Sugio A, White FF. 2006. *Ox8N3* is a host disease-susceptibility gene for bacterial blight of rice. *Proceedings of the National Academy of Sciences, USA* 103: 10503–10508.
- Yuan M, Chu Z, Li X, Xu C, Wang S. 2009. Pathogen-induced expression loss of function is the key factor in race-specific bacterial resistance conferred by a recessive *R* gene *xa13* in rice. *Plant and Cell Physiology* 50: 947–955.

## Supporting Information

Additional supporting information may be found in the online version of this article.

**Fig. S1** Nucleotide sequence of the promoter fragments that were amplified from genomic DNA to analyze recognition specificity.

## 10 Research

New  
Phytologist

**Fig. S2** Alignment of the predicted and naturally occurring *UPT* (up-regulated by transcription activator-like effectors) boxes in the different rice promoters.

**Fig. S3** FASTA files of rice *Xa13* and *xa13* alleles from different rice genotypes.

**Fig. S4** Alignment of the *Xa13/xa13* promoters.

**Table S1** Amino acids of repeat unit residues 12 and 13 and predicted target DNA specificities.

Please note: Wiley-Blackwell are not responsible for the content or functionality of any supporting information supplied by the authors. Any queries (other than missing material) should be directed to the *New Phytologist* Central Office.

## 2.6.2 Anlagen zur Publikation 5

Das folgende „*Supporting Online Material*” (SOM) (veröffentlicht unter: [www3.interscience.wiley.com/journal/123325166/supinfo](http://www3.interscience.wiley.com/journal/123325166/supinfo)) enthält Zusatzinformationen zu Kapitel 2.6.1: die „*Supplemental Figures*” 1, 2 und 4 und die Tabelle S1. Die „*Supplemental Figure*” 3 wurde aus Platz gründen nicht in die Arbeit aufgenommen.

### SUPPORTING INFORMATION

#### Fig. S1

Nucleotide Sequence of the promoter fragments that were amplified from genomic DNA to analyze recognition specificity. The primer binding sites are marked by yellow background colour. The predicted *UPT* boxes of the promoter constructs are marked as boldface red letters.

```
>Bs3-promoter (UPTAvrBs3 box); pepper cultivar ECW-30R; GenBank: EU078684
TCATAGTCAAGCTAACGAACTTATGCAGGGAAATATGAAATTAGTATGCAAGTAACTCAAAGAACTAATC
ATTGAACTGAAAGATCAATATATCAAAAAAAAAAAAAAAAAACAATAAACCGTTTAAACCGATAGATTAACCATTT
CTGGTTCAGTTTATGGGTAAACCACAATTTGCACACCCTGGTTAAACAATGAACACGTTTGCCTGACCAATT
TTATTATATAAACCTAACCATCCTCACAACCTCAAGTTATCATCCCCCTTCTCTTTCTCCTCTTGTCTTGT
CACCCGCTAAATCTATCAAAACACAAGTAGTCCTAGTTGCACATATATTTCC

>Os11N3 (UPTAvrXa7 box); rice cultivar: IR24; GenBank: Os11g0508600
ATTGGCACTTTCTGTCTATGCATGGGTGCTGATGATTATCTTGTATCTAATTTAATCAATCCCATGGCTGTGAT
TGATCAGGAATAGTTTTGTGTGTCAGCTATATGCTTATTGGTGTCCAGGGTCACACACCATAAGGGCATGCA
TGTCAGCAGCTGGTCAATGTGTGCCCTTTTCATCCCTTCTCTCCTCCTAGCACTATATAAACCCCTCCAACCA
GGTGTTAAGCTCATCAAGCCTTCAAGCAAAGCAAAGCTCAAGTAGTAGCTGATTACCAGCTCTTCTCTCTTCTC
ATTGAGAAGAGGGAAATTAAGTTTTGATCTCTGCTTTATTGGCTGATCATCTCTTGTACTTGAAGCAAGAA
CAGTAGTGTACTGTGCCCTATTGATCTCCTCCCAACCTCTCTCTCTCTCATATTTCCGAGCTAGCTA
GTTAATCAAGATCTTGCTGCA

>Xa13; (UPTPthXo1 box); rice cultivar: IR24; GenBank: DQ421396
AACCTATATGAGAGCTCCAGCTCTCCAAATGGCAACAGACACACTGAGTGGTCATACGTGTCATATTGCCCT
CAGTTATGCATTCATATGACCACATATTCAGAGTAGTGGAGAGAGGGACAGATCTAGAGGTAGAAAAAGAAAA
TTCATATAAATGATATATCAGAGTGAAAAAGAAATATCAAGCACAAGAAAAAAGCAAAGGTTAGATATT
AACTCCAAACTCAAGTTCGTTTTATGAGAAACAAAAAGACAAATTTTCAGGTGAATAGTGTCTCTACTATTC
ACCTGAAATTTGTCTTTTTTGTACTCCTAAACGAAGTTGAGTTTGAACCTTGAGATTTGGTGAGAAATGATTT
CATATCTACACCTATCTCTAGTATTTTTTTCATGAATTTATAAACTTTTAGGTATGATTTTCACGAGTTTTTC
AACACTTAGCTCATTTCACCGGATATGTCCTCCTCAACTATATAAACTGAGCCATGGCCAGGCCAAAC
CACACATGCAGTTGTAGTAGCACTTAAGCCTTCTCTCTAGCTAGCATCTCTTGTGTGTCAGGAAGTTGGAAGGG
ATTTCTGGCTAGTTTCTAGCTGGTGTCTCTCTCTCTCTCTCTCTCTCTCTCTCTCTCTCTCTCTCTCTCTCTCT
GTTAATAACCTTCATCACCAGTAGCAATGGCAGGAGGTTTCTTGTCC

>xa13; rice cultivar: IRBB13; Genbank: DQ421394
AACCTATATGAGAGCTCCAGCTCTCCAAATGGCAACAGACACACTGAGTGGTCATACGTGTCATATTGCCCT
CAGTTATGCATTCATATGACCACATATTCAGAGTAGTGGAGAGAGGGACAGATCTAGAGGTAGAAAAAGAAAA
TTCATATAAATGATATATCAGAGTGAAAAAGAAATATCAAGCACAAGAAAAAAGCAAAGGTTAGATATT
AACTCCAAACTCAAGTTCGTTTTATGAGAAACAAAAAGACAAATTTTCAGGTGAATAGTGTCTCTACTATTC
ACCTGAAATTTGTCTTTTTTGTACTCCTAAACGAAGTTGAGTTTGAACCTTGAGATTTGGTGAGAAATGATTTT
CATATCTACACCTATCTCTAGTATTTTTTTCATGAATTTATAAACTTTTAGGTATGATTTTCACGAGTTTTTC
AACACTTAGCTCATTTCACCGGATATGTCCTCCTCAACTATATAAACTGAGCCATGGCCAGGCCAAAC
CACACATGCAGTTGTAGTAGCACTTAAGCCTTCTCTCTAGCTAGCATCTCTTGTGTGTCAGGAAGTTGGAAGGG
ATTTCTGGCTAGTTTCTAGCTGGTGTCTCTCTCTCTCTCTCTCTCTCTCTCTCTCTCTCTCTCTCTCTCTCTCT
GTTAATAACCTTCATCACCAGTAGCAATGGCAGGAGGTTTCTTGTCC

>OsTFX1 (UPTPthXo6 box); Genbank: Os09g0474000
ATTGTTGGCGAAAAGCTCACCGTCATGGCCATGTACCAAAATCGACAAAATTAAGCTACCAAATTTCTACAAA
ACAAGGAGGGGTGGAGAGGAGAGAAAGGTTGGTCTCTCTCTAGTCTCTAGCCATAGGCAATCAAAGCAC
CTTTTCTCACCCTTATAAAGGCCCTCACCAACCATCGCCTCCTCCGCTCAGAGAGAGCAAATTTCTCAGTAA
GCAGAAATCAAAGCAGATTAACCTCATCTACTTCTGGCCCTCTAAGAGTTCTCCACTAAGCAAGCGAAAACAG
CC
```

**Primers used to amplify rice promoter sequences:**

xa13Prom500 CACCfwd/SaR:	CACCAACCTATATGAGAGCTCCAGC
xa13Prom rev/SaR:	GGACAAGAAACCTCCTGCCATTGC
OsTFX1_FW1_CACC	CACCATTGTTGGCGAAAAGCTCAC
OsTFX1_REV3	GGCTGTTTTTCGCTTAGTGGAGAACTCTTAG
Os11N3_CACC_Prom_02_FWD_PR	CACCATTGGCACTTTCTGTCATGC
Os11N3_Prom_Rev_01_PR	TGCAGCAAGATCTTGATTAAGTAGCTAGCTC
Prom-356 bp-fwd-PR	CACCTCATAGTCAAGCTAACGAACTTATGC
Promotor-1-rev-PR	GAAATATATGTGCAACTAGGACTACTTGTG

**Fig. S2**

Alignment of the predicted and naturally occurring *UPT* boxes in the different rice promoters. Red letters mark positions where the predicted *UPT* boxes differ from the naturally occurring ones. The asterisk (\*) indicates nucleotides that pair to the 0<sup>th</sup> repeat due to the deletion of a T nucleotide. Nucleotide polymorphisms that were shown to result in a reduced TAL-effector mediated inducibility are highlighted in bold blue letters. A mutation in the *OsTFX1* box that resulted in reduced affinity to PthXo6 in EMSA is underlined.

#### *Os11N3* is induced by AvrXa7:

repeat unit number	0	1	2	3	4	5	6	7	8	9	10	11	12	13	14	15	16	17	18	19	20	21	22	23	24	25	26	
residues 12 and 13		NI	HG	NI	NI	NS	HD	NN	HD	HD	NS	NG	NG	HD	HD	NS	NS	NN	NN	NI	NG	NN	NI	NG	NS	NG		
predicted <i>UPT</i> <sub>AvrXa7</sub> box		T	A	T	A	A	N	C	AG	C	C	N	T	T	C	C	N	N	AG	AG	A	T	AG	A	T	N	T	
<i>Os11N3</i> box		T	A	T	A	<b>T</b>	A	A	C	C	C	C	<b>C</b>	T	C	C	A	A	<b>C</b>	<b>C</b>	A	A	<b>G</b>	<b>G</b>	<b>T</b>	<b>G</b>	<b>C</b>	<b>T</b>
<i>Os11N3ΔT</i> box		<b>C</b> *	A	T	A	<b>T</b>	A	A	C	C	C	C	<b>C</b>	T	C	C	A	A	<b>C</b>	<b>C</b>	A	A	<b>G</b>	<b>G</b>	<b>T</b>	<b>G</b>	<b>C</b>	<b>T</b>

#### *Xa13* is induced by PthXo1:

repeat unit number	0	1	2	3	4	5	6	7	8	9	10	11	12	13	14	15	16	17	18	19	20	21	22	23	24	
residues 12 and 13		NN	HD	NI	HG	HD	NG	NG	HD	HD	NI	NG	NG	NI	HD	NG	NN	NG	NI	NI	NI	NI	NI	NG	NS	NG
predicted <i>UPT</i> <sub>PthXo1</sub> box		T	AG	C	A	T	C	T	T	C	C	A	T	T	A	C	T	AG	T	A	A	A	A	T	N	T
<i>Xa13</i> box (IR24)		T	G	C	A	T	C	T	<b>C</b>	<b>C</b>	<b>C</b>	<b>C</b>	<b>C</b>	<b>T</b>	A	C	T	G	T	A	<b>C</b>	<b>A</b>	<b>C</b>	<b>A</b>	<b>C</b>	<b>C</b>
<i>Xa13</i> box mut A		T	<b>A</b>	C	A	T	C	T	<b>C</b>	<b>C</b>	<b>C</b>	<b>C</b>	<b>C</b>	<b>T</b>	A	C	T	G	T	A	<b>C</b>	<b>A</b>	<b>C</b>	<b>A</b>	<b>C</b>	<b>C</b>
<i>Xa13</i> box mut C		T	<b>G</b>	C	A	T	C	T	<b>C</b>	<b>C</b>	<b>C</b>	<b>C</b>	<b>C</b>	<b>T</b>	A	C	T	G	T	A	<b>C</b>	<b>A</b>	<b>C</b>	<b>A</b>	<b>C</b>	<b>C</b>
<i>Xa13</i> box mut T (Tepal)		T	<b>T</b>	C	A	T	C	T	<b>C</b>	<b>C</b>	<b>C</b>	<b>C</b>	<b>C</b>	<b>T</b>	A	C	T	G	T	A	<b>C</b>	<b>A</b>	<b>C</b>	<b>A</b>	<b>C</b>	<b>C</b>
<i>Xa13ΔT</i> box		<b>A</b> *	G	C	A	T	C	T	<b>C</b>	<b>C</b>	<b>C</b>	<b>C</b>	<b>C</b>	<b>T</b>	A	C	T	G	T	A	<b>C</b>	<b>A</b>	<b>C</b>	<b>A</b>	<b>C</b>	<b>C</b>

#### *OsTFX1* is induced by PthXo6

repeat unit number	0	1	2	3	4	5	6	7	8	9	10	11	12	13	14	15	16	17	18	19	20	21	22	23	
residues 12 and 13		NI	HG	NI	NN	NN	NN	NN	HD	NI	HD	NI	HD	HG	HD	NI	NG	NS	NI	NI	HG	HD	NS	NS	NG
predicted <i>UPT</i> <sub>PthXo6</sub> box		T	A	T	A	AG	AG	AG	AG	C	A	C	T	C	A	T	N	A	A	T	C	N	N	T	
<i>OsTFX1</i> box		T	A	T	A	A	A	A	G	G	C	<b>C</b>	<b>C</b>	<b>C</b>	<b>T</b>	<b>C</b>	<b>A</b>	<b>C</b>	<b>A</b>	<b>A</b>	<b>C</b>	<b>A</b>	<b>C</b>	<b>A</b>	<b>T</b>
<i>OsTFX1ΔT</i> box		<b>C</b> *	A	T	A	A	A	A	G	G	C	<b>C</b>	<b>C</b>	<b>C</b>	<b>T</b>	<b>C</b>	<b>A</b>	<b>C</b>	<b>A</b>	<b>A</b>	<b>C</b>	<b>A</b>	<b>C</b>	<b>A</b>	<b>T</b>

**Bs3 is induced by AvrBs3**

repeat unit number 0 1 2 3 4 5 6 7 8 9 10 11 12 13 14 15 16 17 18  
 residues 12 and 13 HD NG NS NG NI NI NI HD HD NG NS HD HD HD NG HD NG  
 predicted  $UPT_{AvrBs3}$  box T C T A T A A A C C T A A C C C T C T  
 Bs3 box T A T A T A A A C C T A A C C A T C C

**Xa27 is induced by AvrXa27**

repeat unit number 0 1 2 3 4 5 6 7 8 9 10 11 12 13 14 15 16 17  
 residues 12 and 13 NI NN NG NS NN NN NN NI NN NI NG HD HD NI NG  
 predicted  $UPT_{AvrXa27}$  box T A AG T T A AG AG A AG A T C C A T T  
 Xa27 box T A G A A A G A G A C C C C A T

**Bs3 is induced by AvrHah1**

repeat unit number 0 1 2 3 4 5 6 7 8 9 10 11 12 13 14  
 residues 12 and 13 NN IG NI NI NI HD HD NG NN NI HD HD HD NG  
 predicted  $UPT_{AvrHah1}$  box AG T A A A C C T AG A C C C T  
 Bs3 box T A T A A A C C T A A C C A T

**Bs3-E is induced by AvrBs3 $\Delta$ rep16**

repeat unit number 0 1 2 3 4 5 6 7 8 9 10 11 12 13 14  
 residues 12 and 13 HD NG NS NG NI NI NI HD HD NG HD NG HD NG  
 pred.  $UPT_{AvrBs3\Delta rep16}$  box T C T N T A A A C C T C T C T  
 Bs3-E box T A T A T A A A C C T C T C T



**Fig. S4a**

Alignment of the *Xa13/xa13* promoters. The predicted  $UPT_{PthXo1}$  box of the IR24 *Xa13* promoter and box nucleotides that are identical in other promoters are shown in bold red letters. Green background colour highlights a G→T substitution within the  $UPT_{PthXo1}$  boxes that causes that the corresponding promoters are not PthXo1-inducible.

IR24	( <i>Xa13</i> )	73	AAAAAAAAAGCAAAGGTTAGATA <b>TGCATCTCCCCTACTGTACACCAC</b> AAAAAGTGGAGGGTCTCCAACATA
IR64	( <i>Xa13</i> )	73	AAAAAAAAAGCAAAGGTTAGATA <b>TGCATCTCCCCTACTGTACACCAC</b> AAAAAGTGGAGGGTCTCCAACATA
Nipponbare	( <i>Xa13</i> )	71	AAAAAAAGCAAAGGTTAGATA <b>TGCATCTCCCCTACTGTACACCAC</b> AAAAAGTGGAGGGTCTCCAACATA
Minghui 63	( <i>Xa13</i> )	73	AAAAAAAGCAAAGGTTAGATA <b>TGCATCTCCCCTACTGTACACCAC</b> AAAAAGTGGAGGGTCTCCAACATA
93-11	( <i>Xa13</i> )	72	AAAAAAAGCAAAGGTTAGATA <b>TGCATCTCCCCTACTGTACACCAC</b> AAAAAGTGGAGGGTCTCCAACATA
BJ1	( <i>xa13</i> )	73	AAAAAAAGCAAAGGTTAGATA <b>TGCATCTCCCCTACTGTACACCAC</b> AAAAAGTGGAGGGTCTCCAACATA
Chinsurah 11484	( <i>xa13</i> )	73	AAAAAAAGCAAAGGTTAGATA <b>TGCATCTCCCCTACTGTACACCAC</b> AAAAAGTGGAGGGTCTCCAACATA
Chinsurah 11760	( <i>xa13</i> )	73	AAAAAAAGCAAAGGTTAGATA <b>TGCATCTCCCCTACTGTACACCAC</b> AAAAAGTGGAGGGTCTCCAACATA
Chinsurah 50930	( <i>xa13</i> )	73	AAAAAAAGCAAAGGTTAGATA <b>TGCATCTCCCCTACTGTACACCAC</b> AAAAAGTGGAGGGTCTCCAACATA
Tepa	( <i>xa13</i> )	73	AAAAAAAGCAAAGGTTAGATA <b>TGCATCTCCCCTACTGTACACCAC</b> AAAAAGTGGAGGGTCTCCAACATA
Aus 274	( <i>xa13</i> )	70	AAAAAAAGCAAAGTGGAGGGT <b>TGCATCTCCCCTACTGTACACCAC</b> AAAAAGTGGAGGGTCTCCAACATA
AC 19-1-1	( <i>xa13</i> )	37	AAAAAAAGCAAAGGTTAGATA <b>TGCATCTCC</b> -----AACTATA
Kalimekri 77-5	( <i>xa13</i> )	37	AAAAAAAGCAAAGGTTAGATA <b>TGCATCTCC</b> -----AACTATA

**Fig. S4b**

Alignment of the *Xa13/xa13* promoters from the rice cultivars IR24 (*Xa13*), IRBB13 (*xa13*) and, Long grain (*xa13*). The predicted  $UPT_{PthXo1}$  box of the IR24 *Xa13* promoter and box nucleotides that are identical in the IRBB13 or Long Grain promoters are shown in bold red letters. Green background colour highlights a G→T substitution within the  $UPT_{PthXo1}$  box that is also found in the promoters of other *xa13* alleles (see supplementary figure S1).

IR24	( <i>Xa13</i> )	110	CACAAGAAAAAAAAAGCAAAGGTTAGATA <b>TGCATC</b> -----
IRBB13	( <i>xa13</i> )	325	CACAAGAAAAAAAAAGCAAAGGTTAGATA <b>TGA</b> ACTCCAACTCAAGTTCGTTTATGAGAAACAAAAAGACA
Long Grain	( <i>xa13</i> )	325	CACAAGAAAAAAAAAGCAAAGGTTAGATA <b>TGA</b> ACTCCAACTCAAGTTCGTTTATGAGAAACAAAAAGACA
IR24	( <i>Xa13</i> )	74	----- <b>TCCCCCTACTGTACACCAC</b> AA----- <b>AGT</b> G
IRBB13	( <i>xa13</i> )	252	AATTCAGGTGAATAGT <b>TCCCTGTACTATTACCT</b> GAAATTTGCTTTTTTGTACTCCTAAACGAAGTTGA
Long Grain	( <i>xa13</i> )	252	AATTCAGGTGAATAGT <b>TCCCTGTACTATTACCT</b> GAAATTTGCTTTTTTGTACTCCTAAACGAAGTTGA
IR24	( <i>Xa13</i> )	45	G-----GGT-----
IRBB13	( <i>xa13</i> )	179	GTTTGAAGT <b>TGAGATTGGTGAGAATGTATTT</b> CATA <b>TCTACACCTA</b> CTCTAGATTTTTTTCATGAATTTAT
Long Grain	( <i>xa13</i> )	179	GTTTGAAGT <b>TGAGATTGGTGAGAATGTATTT</b> CATA <b>TCTACACCTA</b> CTCTAGATTTTTTTCATGAATTTAT
IR24	( <i>Xa13</i> )	41	-----CTCCAACT
IRBB13	( <i>xa13</i> )	106	AAAAC <b>TTTTAGGTATGATTTT</b> CACGAGTTT <b>TCAACACTTAGCTCATTTT</b> CACCGGATAT <b>GC</b> CCCC <b>TTCCAAC</b> T
Long Grain	( <i>xa13</i> )	106	AAAAC <b>TTTTAGGTATGATTTT</b> CACGAGTTT <b>TCAACACTTAGCTCATTTT</b> CACCGGATAT <b>GC</b> CCCC <b>TTCCAAC</b> T
IR24	( <i>Xa13</i> )	33	<b>ATATAAACTGAGCCATGGCCAAGGCCAAACC</b>
IRBB13	( <i>xa13</i> )	33	<b>ATATAAACTGAGCCATGGCCAAGGCCAAACC</b>
Long Grain	( <i>xa13</i> )	33	<b>ATATAAACTGAGCCATGGCCAAGGCCAAACC</b>

Table S1. Amino acids of repeat unit residues 12 and 13 and predicted target DNA specificities\*

Residue 12 and 13	HD	NI	NG	NS	NN	IG
Predicted nucleotide match	C	A	T	N	A/G	T

\*Table according to Boch *et al.* (2009).

### 2.6.3 Zusammenfassung der Ergebnisse

TAL-Effektorproteine aus dem bakteriellen Reispathogen *Xoo* aktivieren Wirtsgene transkriptionell, die für die Virulenz des Pathogens essentiell sind (Yang und White, 2004; Yang et al., 2006; Sugio et al., 2007; Antony et al., 2009). Um zu prüfen, ob der molekulare Mechanismus der Promotoraktivierung bei den Suszeptibilitätsgenen *OsTFX1*, *Os8N3* und *Os11N3* ähnlich wie bei den *R*-Genen *Bs3* und *Xa27* ist, wurden im Rahmen des Manuskriptes die Promotorregionen der verschiedenen Suszeptibilitätsgene aus Reis vor ein *uidA*-Reporter gen (Gen der  $\beta$ -Glucuronidase) kloniert und mittels Nachweis des X-Glucuronid-Substratumsatzes (Blaufärbung) detektiert. Basierend auf dem TAL-Effektor-CODE konnten die *UPT*-Boxen in den Promotoren der Suszeptibilitätsgene *OsTFX1*, *Os8N3* und *Os11N3* aus Reis vorhergesagt werden (Boch et al., 2009; Moscou und Bogdanove, 2009). Der Transfer dieser vorhergesagten *UPT*-Boxen in den *Bs3*-Promotor zeigte, dass die Boxen Induzierbarkeit durch korrespondierende TAL-Effektoren im heterologen Promotorkontext vermitteln. Durch EMSA-Studien wurde ermittelt, dass diese vorhergesagten *UPT*-Boxen spezifisch mit ihren korrespondierenden TAL-Effektoren interagieren. Mutationsstudien, bei denen einzelne Basenpaare in den *UPT*-Boxen verändert wurden, ergaben, dass das 5' terminale und konservierte TA-Basenpaar in den *UPT*-Boxen wichtig für die TAL-Effektor Bindung und die TAL-Effektor-vermittelte Induktion ist. Durch den Vergleich von *Xoo* resistenten *xa13*- und *Xoo* suszeptiblen *Xa13* (synonym: *Os8N3*)-Allelen konnten Genotypen identifiziert werden, die sich nur in einem Basenpaar in der postulierten *UPT*-Box unterscheiden. Funktionale Analysen dieser beiden Promotorvarianten zeigten, dass dieser Polymorphismus in der Tat die differentielle, TAL-Effektor-vermittelte Induzierbarkeit der beiden Promotorvarianten bedingt. Zusammenfassend wurde gezeigt, dass die Promotoren der Suszeptibilitätsgene *Os8N3*, *Os11N3* und *OsTFX1* aus Reis nach dem gleichen Erkennungsprinzip wie die Promotoren der *R*-Gene *Bs3* aus Paprika und *Xa27* aus Reis funktionieren und dass die spezifische Bindung von TAL-Effektoren an ihre korrespondierenden Promotoren die Grundlage für die Aktivierung der Gene ist.

### 3 Diskussion

#### 3.1 *Bs3* kodiert für ein neuartiges R-Protein

Das in dieser Arbeit isolierte *R*-Gen *Bs3* umfasst 3 Exons und 2 Introns und kodiert für ein 342 AS langes Protein, welches Homologie zu Flavin-abhängigen Monooxygenasen (FMOs) und im speziellen zu den YUCCA Proteinen aus *Arabidopsis* aufweist (Römer et al., 2007). *Bs3* weist die typischen konservierten Bereiche von FMOs auf. Im N-terminalen Bereich befindet sich die FAD (Flavinadenindinukleotid)-Bindedomäne (GxGxxG), dann folgt das FMO-Identifizierungsmotiv (FxGxxxH-xxxY/F) und im Zentrum befindet sich, wie bei allen FMOs, die NADPH (Nikotinsäureamidadenindinukleotidphosphat)-Bindedomäne (GxGxxG) (Choi et al., 2003; Abbildung 10A). Typisch für FMOs ist im C-terminalen Bereich ein FATGY-Motiv, welches die AS Phenylalanin, Alanin, Threonin, Glycin und Tyrosin umfasst (Schlauch, 2007). In Bakterien, Hefe und den tierischen FMOs ist das FATGY Motiv konserviert und es wird vermutet, dass es in Proteinen vorkommt, die Stickstoff oxidieren (Stehr et al., 1998). Wie bei den *Arabidopsis* YUCCA-Proteinen ist bei *Bs3* das Phenylalanin (F) des FATGY-Motivs durch ein Leucin (L) ersetzt, wodurch ein LATGY-Motiv entsteht (Stehr et al., 1998; Schlaich, 2007). Für das konservierte NADPH-Motiv von *Bs3* konnte im Rahmen der Diplomarbeit von Tina Strauß gezeigt werden, dass das darin enthaltene konservierte Glycin (G212) für das Auslösen der *Bs3*-vermittelten HR in *N. benthamiana* notwendig ist. Weitere mutationsanalytische Studien in der Diplomarbeit von Tina Strauß zeigten, dass auch Bereiche außerhalb der konservierten Struktur motive der FMOs wichtig für die Ausbildung der *Bs3*-abhängigen HR sind (T. Strauß und T. Lahaye, unveröffentlicht). Damit war es möglich zu zeigen, welche Bereiche in *Bs3* bedeutend für die Ausbildung der HR in *N. benthamiana* sind. Jedoch war es bis jetzt nicht möglich, die Substrate und den möglichen Reaktionsweg dieser besonderen FMO zu identifizieren. Es könnte sein, dass im Verlauf der *Bs3*-bedingten HR reaktive Sauerstoffspezies (*reactive oxygen species*, ROS) entstehen, oder dass die HR durch den Elektronen- und Sauerstofftransfer, wie er im FMO-Reaktionszyklus beschrieben wurde, ausgebildet wird (Schlauch, 2007; Abbildung 10B). Obwohl *Bs3* charakteristische Struktur motive von FMOs enthält (Abbildung 10A), ist es sowohl strukturell als auch funktionell unterschiedlich zu den YUCCA-Proteinen und der FMO1 aus *Arabidopsis*. *Bs3* enthält im Gegensatz zu den *YUCCAs*, die 4 Exons enthalten, nur 3 Exons. Bei *Bs3* befindet sich im Bereich des 3. Exons der *YUCCAs* eine 216-Bp große Deletion (Römer et al., 2007). Dieser Befund wirft die Frage auf, ob es einen gemeinsamen

Vorläufer von *Bs3* und den *YUCCAs* gibt. In den bisher durchgeführten Analysen, bei denen aus 51 *Capsicum* spp. *Bs3*-Allele sequenziert und funktionell charakterisiert wurden, konnte jedoch kein *Bs3*-Allel identifiziert werden, welches für ein Vollängen-YUCCA-Protein kodiert (T. Strauß in Römer et al., 2009b). Erstaunlich ist auch, dass in der vollständig annotierten Version des Tomatengenoms zwar Proteine mit Homologie zu YUCCA-Proteinen vorhergesagt werden, jedoch keines der Proteine die für *Bs3* typische Deletion aufweist (<http://solgenomics.net>). Dies deutet darauf hin, dass das *Bs3*-Protein ausschließlich in *Capsicum* spp. entstanden ist.

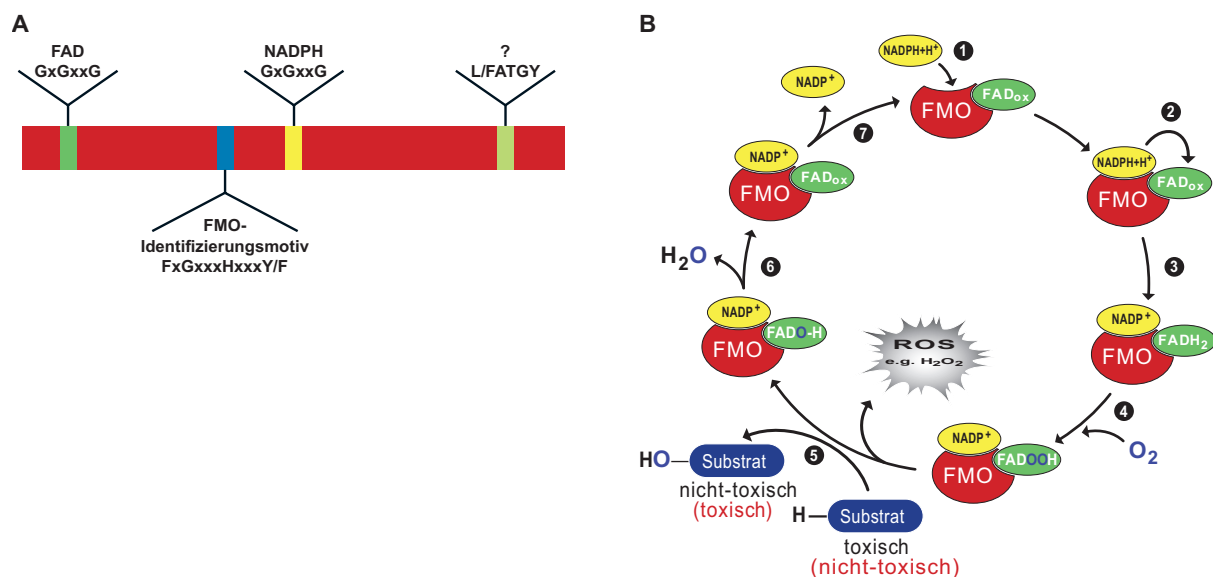


#### Abbildung 10: Struktur und möglicher Reaktionszyklus der FMOs

**A)** Schematische Darstellung der konservierten Motive in FMOs aus *Arabidopsis*. Abgebildet sind die konservierten AS der jeweiligen Motive bzw. die variablen AS (x). Das Fragezeichen (?) zeigt an, dass für dieses Motiv die Funktion noch nicht eindeutig geklärt ist. **B)** Möglicher Reaktionszyklus von FMOs. Der katalytische Reaktionszyklus der FMOs beginnt mit der Bindung von  $NADPH+H^+$  (1). Danach erfolgt der Wasserstofftransfer von  $NADPH+H^+$  auf FAD, wodurch dieses zu  $FADH_2$  reduziert wird (2+3). Anschließend erfolgt die Bindung von molekularem Sauerstoff und die Oxidation von  $FADH_2$  (4). Durch  $FADOOH$  wird das Substrat oxidiert (5). Dabei ist es möglich, dass ein toxisches in ein nicht-toxisches Substrat (schwarze Schrift) oder dass ein nicht-toxisches in ein toxisches Substrat umgewandelt wird (rote Schrift). Eine mögliche Nebenreaktion von Schritt 5 ist die Bildung von reaktiven Sauerstoffspezies (ROS). In den Schritten 6 und 7, die die limitierenden Schritte darstellen (Ziegler, 2002; Phillips und Shephard, 2008), kommt es zur Freisetzung von Wasser- und  $NADP^+$ . Um die toxische Wirkung von *Bs3* zu erklären, ist es denkbar, dass die ROS-Bildung die Ausbildung einer HR bedingt und/oder dass ein nicht-toxisches in ein toxisches Substrat umgewandelt wird, wodurch die HR entsteht. Die Abbildung wurde modifiziert nach Schlaich (2007).

Neben den genannten strukturellen Unterschieden gibt es auch funktionelle Unterschiede zwischen *Bs3*, den YUCCA-Proteinen und der *FMO1* aus *A. thaliana*. Die *FMO1* wird sowohl durch virulente als auch avirulente *Pseudomonas*-Stämme induziert (Bartsch et al., 2006; Koch et al., 2006), *Bs3* dagegen nur durch *Xcv*, welche *AvrBs3* translozieren. Durch andere TAL-Effektoren (*AvrBs4*, *AvrBs3Δrep16*) und auch durch andere Abwehrreaktionen (*Bs1*- und *Bs2*-vermittelte Resistenzreaktion) wird die Expression von *Bs3* nicht induziert (Römer et al., 2007). Ein weiterer funktioneller Unterschied von *Bs3* im Vergleich zur *FMO1* ist, dass

die 35S-Promotor-vermittelte Überexpression von *Bs3* eine Zelltodreaktion induziert, während die Überexpression der *FMO1* Breitspektrumresistenz verleiht (Bartsch et al., 2006; Römer et al., 2007). Die Tabakrattle-Virus (TRV)-basierten *Gen-Silencing*-Analysen der Signalwegkomponenten Rar1, SGT1, NDR1, Hsp90 und EDS1 in *N. benthamiana* ergab, dass die *Bs3*-vermittelte HR nur durch *Silencing* der Signalwegkomponente SGT1 beeinflusst wird, jedoch nicht durch *Silencing* der Signalwegkomponente EDS1. Im Gegensatz dazu ist die *FMO1*-vermittelte Resistenz EDS1-abhängig (Bartsch et al., 2006).

Zusammenfassend läßt sich feststellen, dass *Bs3* zwar Homologie zu den FMOs aufweist, jedoch sowohl strukturell als auch funktionell unterschiedlich zu den anderen bekannten pflanzlichen und tierischen FMOs ist.

### **3.2 Kernlokalisierung von *Bs3* ist für das Auslösen der Resistenzreaktion nötig**

Die subzellulären Lokalisationsstudien eines *Bs3::GFP* Fusionsproteins zeigten, dass GFP-Fluoreszenz im Zellkern und im Zytoplasma nachweisbar war (siehe 2.2.3.2). Daraus ergab sich die Frage, ob für die Auslösung der *Bs3*-vermittelten HR die Lokalisation in einem oder in beiden Zellkompartimenten notwendig ist. Für andere R-Proteine (N, MLA1, MLA10 und RPS4) wurde gezeigt, dass obwohl sie in mehreren Zellkompartimenten nachweisbar sind, die Lokalisation im Zellkern für die Auslösung der Resistenzreaktion notwendig ist (Burch-Smith et al., 2007; Shen et al., 2007; Wirthmueller et al., 2007). Diese Proteine gehören zu der großen Klasse der NB-LRR-Proteine. NB-LRR-Proteine haben im Gegensatz zu *Bs3*, eine Funktion bei der Pathogenerkennung und der Signalweiterleitung (Rafiqi et al., 2009). Obwohl es formal noch nicht nachgewiesen ist, scheint es wahrscheinlich, dass die Translokation der NB-LRR-Proteine in den Kern primär für die Signalweiterleitung erfolgt. Das *Bs3*-Protein ist nicht in die Pathogenerkennung involviert, da diese Funktion durch den *Bs3*-Promotor vermittelt wird. Ob das *Bs3*-Protein im Zellkern die Signalweiterleitung vermittelt oder eine HR direkt durch seine enzymatische Funktion auslöst, ist nicht geklärt. Arbeiten im Rahmen der Doktorarbeit von Jana Piprek lieferten jedoch erste Hinweise, dass *Bs3* wie N, MLA1 und MLA10 im Kern lokalisiert sein muss, um eine Resistenzreaktion auslösen zu können (Burch-Smith et al., 2007; Shen et al., 2007; J. Piprek und T. Lahaye, unveröffentlicht). In diesem Zusammenhang ist es interessant, dass *Xa27* aus Reis, welches auf transkriptioneller Ebene wie *Bs3* funktioniert, nicht im Zellkern nachgewiesen werden konnte (Wu et al., 2008). Die bisher durchgeführten Studien zeigten, dass *Xa27* im Apoplasten lokalisiert ist und dass diese Lokalisation für das Auslösen der Resistenzreaktion essentiell ist (Wu et al., 2008). Vermutlich löst *Xa27* die Resistenzreaktion über einen mechanistisch anderen Weg aus als

Bs3. Die Erkennung und die Nutzung des *R*-Genpromotors als Immunrezeptor ist jedoch bei diesen beiden *R*-Genen konserviert (Römer et al., 2009a).

### 3.3 Bs3-vermittelte Resistenz: Ein Beispiel für das *Decoy*-Modell

Bisher wurden für die Erkennung von Effektoren durch korrespondierende R-Proteine drei Modelle aufgestellt (siehe 1.3). Das konzeptionell einfachste, das Rezeptor-Liganden-Modell postuliert, dass Erkennung des Effektorproteins durch eine direkte Interaktion mit dem R-Protein ausgelöst wird. Da die Erkennung des TAL-Effektors AvrBs3 nicht durch das Bs3-Protein, sondern über den *Bs3*-Promotor erfolgt, entspricht die Bs3-Resistenz konzeptionell nicht dem Rezeptor-Liganden-Modell, da dieses eine Protein-Protein Interaktion postuliert. Vielmehr erfolgt die Erkennung von AvrBs3 durch den Promotor von *Bs3* als Immunrezeptor nach dem *Decoy*-Modell (Van der Hoorn und Kamoun, 2008). Grundlage für diese Schlussfolgerung ist, dass der *Bs3*-Promotor, ein definiertes Sequenzmotiv, die  $UPT_{AvrBs3}$ -Box enthält. Eine fast identische  $UPT_{AvrBs3}$ -Box befindet sich in den Promotoren von zahlreichen *UPA*-Genen (*upregulated by AvrBs3*) (Kay et al., 2007; Kay et al., 2009). Für das *UPA*-Gen *UPA20* konnte gezeigt werden, dass es notwendig und ausreichend für das Auslösen der Hypertrophie ist, wodurch die Pflanzenzelle zum Vorteil von *Xcv* manipuliert wird (Kay et al., 2007). *Bs3* wird wie *UPA20* durch AvrBs3 induziert, da es im Promotor eine  $UPT_{AvrBs3}$ -Box enthält (Kay et al., 2007; Römer et al., 2007). Dem *Bs3*-Gen kommt in der Interaktion mit *Xcv* jedoch keine bekannte Virulenzfunktion zu. Daher stellt es kein Pathogenitätstarget im Sinne des *Guard*-Modells dar. Außerdem "überwacht" das *Bs3*-Genprodukt auch nicht den Zustand eines pflanzlichen Pathogenitätstargets und ist daher kein *Guard* im Sinne des *Guard*-Modells. Vielmehr ist der *Bs3*-Promotor eine Mimikry des AvrBs3 Pathogenitätstargets, der  $UPT_{AvrBs3}$ -Box in den Virulenz-assoziierten *UPA*-Genen.

Ein ähnlicher Sachverhalt wurde auch für andere *R*-Gene nachgewiesen. Ein Beispiel für ein weiteres *Decoy*-*R*-Gen ist *Xa27*. Wie im Fall von *Bs3* wurde auch hier gezeigt, dass es durch den korrespondierenden TAL-Effektor AvrXa27 aktiviert wird (Gu et al., 2005). AvrXa27 bindet an den *Xa27*-Promotor (Römer et al., 2009a). Ein Virulenztarget für AvrXa27 ist bis jetzt nicht bekannt (Gu et al., 2005; Tian und Yin, 2009). Alternativ zum *Decoy*-Modell könnte die Interaktion von TAL-Effektoren und ihren korrespondierenden Promotoren aber auch als direkte Interaktion im Sinne des Rezeptor-Liganden-Modell interpretiert werden. Die Spezifität wird dabei von der *Repeat*-Region der TAL-Effektoren bestimmt (Herbers et al., 1992; Kay et al., 2007). Allerdings müsste das Rezeptor-Liganden-Modell dahingehend

erweitert werden, dass statt der üblichen Protein-Protein-Interaktionen auch Protein-DNA-Interaktionen integrierbar sind.

### 3.4 Die Funktion von *Bs3* ist nur die Generierung von Resistenz gegen *Xcv*

Die überwiegende Mehrzahl der *R*-Gene kodiert für NB-LRR-Proteine (Liu et al., 2007) (Sacco und Moffett, 2009). Diese haben eine wesentliche Funktion in der Pathogenerkennung und der Signalweiterleitung (Caplan et al., 2008; Padmanabhan et al., 2009; Swiderski et al., 2009). Bis jetzt konnte nur für wenige NB-LRR-Proteine eine Funktion neben der des Immunrezeptors gezeigt werden. In den meisten Fällen handelt es sich dabei um Signalfunktionen für einen anderen Immunrezeptor. Beispiele hierfür sind *NRC1* (NB-LRR protein required for HR-associated cell death 1) und *NRG1* (N requirement gene 1) (Tameling und Joosten, 2008). *NRC1* ist für die Ausbildung der Cf-4 abhängigen HR in Tomate notwendig (Gabriels et al., 2006) und *NRG1* ist für die Resistenzreaktion von N in N-transgenen *N. benthamiana* erforderlich (Peart et al., 2005).

Da *Bs3* nicht für ein NB-LRR-Protein kodiert, wurde untersucht ob *Bs3* noch eine andere Funktion als die der Resistenzvermittlung hat. Um diesen Sachverhalt zu hinterfragen, erfolgte die Analyse von 51 *Bs3*-Allelen aus verschiedenen *Capsicum* spp. Die Sequenzierung ergab, dass 42 dieser Allele Nukleotidpolymorphismen aufwiesen. Diese führten bei 13 Allelen zu frühen Stopps in der Sequenz, wodurch verkürzte Proteine entstehen (Römer et al., 2009b). Die funktionelle Analyse der verkürzten Allele in *N. benthamiana* ergab, dass sie nicht in der Lage waren, eine *Bs3*-vermittelte HR auszulösen, was darauf schließen lässt, dass es sich tatsächlich um Nullallele handelt (Römer et al., 2009b). Die Paprikapflanzen, die diese Allele enthalten, wiesen phänotypisch und entwicklungspezifisch keine Unterschiede zu Pflanzen auf, welche die Wildtyp-Allele von *Bs3* oder *Bs3-E* tragen (Römer et al., 2009b), so dass *Bs3* bis jetzt keine Funktion neben der der Resistenzvermittlung zugewiesen werden kann. Unterstützend konnte festgestellt werden, dass *Bs3*-Transkripte in keinem der getesteten pflanzlichen Gewebe ohne Induktion durch AvrBs3 detektierbar waren (siehe 2.3.1). Bemerkenswerterweise war für *Bs3* auch keine Basallevelexpression nachweisbar, wodurch es sich von den anderen *UPA*-Genen abgrenzt (Kay et al., 2007; Römer et al., 2007; Kay et al., 2009; Römer et al., 2009b). Zusammenfassend lässt sich feststellen, dass *Bs3* obwohl es kein NB-LRR-Protein ist, höchstwahrscheinlich nur für die Generierung von Resistenz gegen *Xcv*, die AvrBs3 tranlozieren, notwendig ist. Dadurch ist es funktionell gesehen sehr ähnlich zu den meisten NB-LRR-Proteinen, welche auch ausschließlich in der Resistenzvermittlung involviert sind.

### 3.5 Spezifische Promotorbindung ist die Grundlage für TAL-Effektor vermittelte Promotoraktivierung

Für die TAL-Effektoren AvrBs3 und AvrBs3 $\Delta$ rep16 wurde gezeigt, dass sie jeweils spezifisch an Promotorelemente in *Bs3* bzw. *Bs3-E* binden (Römer et al., 2009b) und dass eine 13-Bp Insertion im *Bs3-E*-Promotor die Grundlage der differentiellen Promotoraktivierung von *Bs3* durch AvrBs3 und von *Bs3-E* durch AvrBs3 $\Delta$ rep16 ist (Römer et al., 2007). Auch für die *Xoo* TAL-Effektoren AvrXa7, AvrXa27, PthXo6 und PthXo1 konnte gezeigt werden, dass diese sequenzspezifisch an DNA binden (Yang et al., 2000; Römer et al., 2009a; Römer et al., 2010). Für AvrXa27 wurde durch EMSA (*Electrophoretic Mobility Shift Assay*)-Studien geklärt, dass es mit hoher Affinität an den *Xa27*-Promotor der Reislinie IRBB27 jedoch nur schwach an den *xa27*-Promotor der Reislinie IR24 bindet (Römer et al., 2009a). Auch hier korreliert die Affinität der TAL-Effektoren mit der Aktivierung, denn nur *Xa27* und nicht *xa27* wird durch AvrXa27 induziert (Gu et al., 2005; Römer et al., 2009a). EMSA-Studien mit PthXo1 zeigten, dass es stark an den *Xa13*-Promotor aus der Reislinie IR24 und schwach an den *xa13*-Promotor der Reislinie IRBB13 bindet (Römer et al., 2010). Auch für diese TAL-Effektor-Promotor-Kombination korreliert die Bindungsstärke mit der Induktion durch den korrespondierenden TAL-Effektor (Chu et al., 2006; Yang et al., 2006; Yuan et al., 2009; Römer et al., 2010). Damit wird deutlich, dass das Prinzip der Promotorbindung durch TAL-Effektoren in mono- und dikotyledonen Pflanzen funktionell konserviert ist und dass die spezifische Promotorbindung generell die Grundlage für die Induktion der Gene ist. Da bislang keines der durch TAL-Effektoren induzierten *R*-Gene für ein NB-LRR-Protein kodiert, sind vermutlich die Reis-*R*-Gene *Xa7* und *Xa10*, die die Erkennung der TAL-Effektoren AvrXa7 und AvrXa10 vermitteln, auch keine NB-LRR-Proteine. In Übereinstimmung mit dieser Hypothese wurden in den physikalischen Zielintervallen der beiden kartierten *R*-Gene weder ein NB-LRR kodierendes Gen identifiziert, noch wurden in diesen Bereichen Homologe anderer bekannter *R*-Gene detektiert (Chen et al., 2008; Gu et al., 2008). Damit scheint der Mechanismus der Promotorbindung durch den korrespondierenden TAL-Effektor vermutlich der vorwiegend genutzte Mechanismus zur Perzeption von TAL-Effektoren zu sein. Obwohl die Promotor-vermittelte Erkennung von TAL-Effektoren konserviert ist, so sind jedoch die *R*-Proteine, die die Resistenzreaktion auslösen, strukturell divers (*Bs3* und *Xa27*) (Gu et al., 2005; Römer et al., 2007; Römer et al., 2009a). Der klassische Weg, die direkte oder indirekte Bindung an ein *R*-Protein, scheint die Ausnahme zu sein. Bislang wurde nur für den TAL-Effektor AvrBs4 ein NB-LRR-Protein isoliert (Ballvora et al., 2001b; Schornack et



al., 2004), wobei bis heute nicht geklärt ist, wie diese Erkennung auf molekularer Ebene abläuft. Es war zwar möglich zu zeigen, dass die Bs4-vermittelte Erkennung von AvrBs4 in NLS- und AD-unabhängiger Weise erfolgt und dass sogar AvrBs4-Deletionskonstrukte erkannt werden, die aus nur 3,5 *Repeat*-Einheiten bestehen. Aber bis jetzt war es nicht möglich, eine direkte oder indirekte Interaktion von Bs4 und AvrBs4 nachzuweisen (Bonas et al., 1993; Ballvora et al., 2001a; Schornack et al., 2004).

### 3.6 Funktionell austauschbare TAL-Effektoren

Durch Mutations- und anschließende Komplementationsanalysen konnten in *Xanthomonas*-Stämmen TAL-Effektoren identifiziert werden, die funktionell austauschbar sind (Yang und White, 2004; Yang et al., 2005). Auf Basis des aktuellen Wissensstandes stellt sich die Frage, was die molekulare Basis für diese funktionell austauschbaren TAL-Effektoren ist. Eine naheliegende Erklärung für die funktionelle Austauschbarkeit ist, dass diese TAL-Effektoren sehr ähnliche oder identische hypervariable AS 12 und 13 (*repeat variable diresidue*, RVD) aufweisen und folglich identische Bereiche in Zielpromotoren angesteuert werden (Schornack et al., 2008; Boch et al., 2009; Moscou und Bogdanove, 2009).

Ein solches Beispiel sind AvrBs3 aus *Xcv* und der TAL-Effektor AvrHah1 (avirulence (*avr*) gene homologous to *avrBs3* and *hax2*, No. 1) aus dem Tomatenpathogen *Xanthomonas gardneri* (*Xg*). AvrHah1 löst wie AvrBs3 eine HR in der *Bs3*-resistenten Paprikalinie ECW-30R aus (Schornack et al., 2008). AvrBs3 (17,5 *Repeat*-Einheiten) und AvrHah1 (13,5 *Repeat*-Einheiten) weisen größere Blöcke von hintereinander geordneten identischen RVDs auf (Schornack et al., 2008). Insgesamt sind 10 der 14 *Repeat*-Einheiten an den Positionen der RVDs zwischen AvrBs3 und AvrHah1 identisch (Schornack et al., 2008; Abbildung 11).

Repeat-Nummer:		1	2	3	4	5	6	7	8	9	10	11	12	13	14			
AvrHah1				<b>NN IG</b>	<b>NI NI NI</b>	<b>HD HD NG</b>				NN	<b>NI</b>	<b>HD HD</b>	<b>HD NG</b>					
AvrBs3	HD NG	NS NG		<b>NI NI NI</b>	<b>HD HD NG</b>					NS NS	<b>HD HD</b>	<b>HD NG</b>		HD NG				
Repeat-Nummer:	1	2	3	4	5	6	7	8	9	10	11	12	13	14	15	16	17	18

#### Abbildung 11: Vergleich der RVDs der TAL-Effektoren AvrBs3 und AvrHah1

AvrBs3 und AvrHah1 sind innerhalb der RVDs sehr homolog (schwarzer Hintergrund). Fettgedruckte Buchstaben markieren die 35 AS *Repeat*-Einheiten in AvrHah1. Die Nummern ober- und unterhalb des Sequenzvergleichs geben die *Repeat*-Nummer von AvrHah1 bzw. AvrBs3 an.

Weiterführende Analysen haben gezeigt, dass AvrHah1 wie AvrBs3 an den *Bs3*-Promotor bindet und diesen aktiviert (S. Recht und T. Lahaye, unveröffentlicht). Aufgrund der geringeren Anzahl von *Repeat*-Einheiten von AvrHah1, im Vergleich zu AvrBs3, ist die  $UPT_{AvrHah1}$ -Box 4 Bp kleiner als die  $UPT_{AvrBs3}$ -Box (S. Recht und T. Lahaye,

unveröffentlicht). Damit wird von beiden TAL-Effektoren eine überlagerte *UPT*-Box angesteuert.

Doch nicht nur AvrBs3 und AvrHah1 weisen große identische Bereiche auf, sondern auch AvrBs3 und das AvrBs3-Deletionsderivat AvrBs3 $\Delta$ rep16 (13,5 *Repeat*-Einheiten) sind in den *Repeat*-Einheiten 1-10 identisch (siehe Abbildung 12). Interessanterweise bedingen hier jedoch drei unterschiedliche *Repeat*-Einheiten (11, 12 und 14) eine differentielle Affinität und eine differentielle Aktivierung von *Bs3* durch AvrBs3 bzw. von *Bs3-E* durch AvrBs3 $\Delta$ rep16 (Römer et al., 2007; Römer et al., 2009b). Somit scheint nicht nur die Anzahl an „passenden“ RVDs wichtig zu sein, sondern auch deren Position innerhalb der *Repeat*-Struktur. Da für eine Promotoraktivierung die physikalische Nähe der Aktivierungsdomäne zur DNA essentiell ist, wäre es naheliegend, dass *Repeat*-Einheiten, die im C-terminalen Bereich unmittelbar vor der Aktivierungsdomäne liegen, Schlüsselpositionen für die Funktionalität eines TAL-Effektors darstellen.

Repeat-Nummer:	1	2	3	4	5	6	7	8	9	10	11	12	13	14	15	16	17	18
AvrBs3 $\Delta$ rep16	HD	NG	NS	NG	NI	NI	NI	HD	HD	NG	HD	NG	HD	NG				
AvrBs3	HD	NG	NS	NG	NI	NI	NI	HD	HD	NG	NS	NS	HD	HD	HD	NG	HD	NG

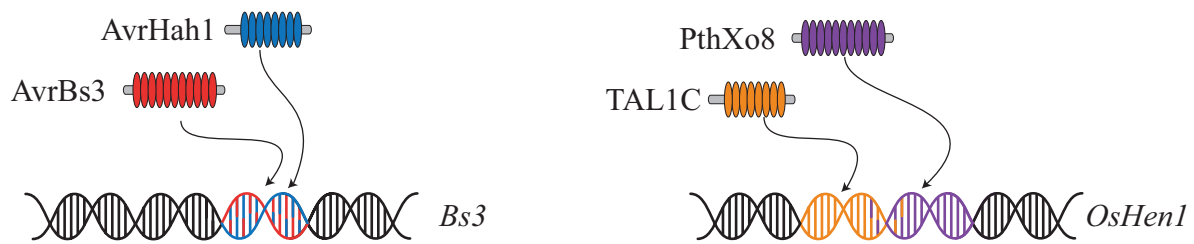
**Abbildung 12: Vergleich der RVDs der TAL-Effektoren AvrBs3 und AvrBs3 $\Delta$ rep16**

AvrBs3 und AvrBs3 $\Delta$ rep16 sind innerhalb der RVDs sehr homolog (schwarzer Hintergrund). Die Nummern oberhalb des Sequenzvergleichs geben die Nummer der jeweiligen *Repeat*-Einheit an.

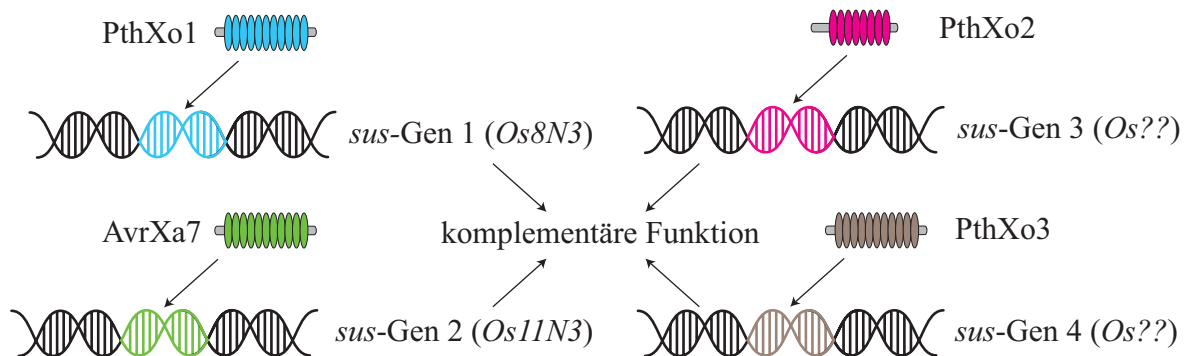
Auch für die TAL-Effektoren PthXo8 und TAL1c, die aus verschiedenen *Xoo*-Stämmen isoliert wurden, konnte gezeigt werden, dass sie beide das Reisgen *OsHen1* aktivieren (Moscou und Bogdanove, 2009; Ryan et al., 2009). Im Gegensatz zu AvrBs3 und AvrHah1 weisen PthXo8 und TAL1c keine großen Übereinstimmungen im Bereich der RVDs auf. Durch Anwendung des TAL-Effektor-CODEs wird jedoch ersichtlich, dass PthXo8 und TAL1c vermutlich unterschiedliche Bereiche im *OsHen1*-Promotor ansteuern, die an ihrem Ende überlappen (Abbildung 13A; *OsHen1*).

Funktionell austauschbare TAL-Effektoren müssen jedoch nicht zwangsläufig die selben Promotoren aktivieren, sondern könnten auch sequenzverschiedene Promotoren von funktionell redundanten Mitgliedern einer Genfamilie ansteuern (siehe Abbildung 13B). So steuern beispielsweise die funktionell austauschbaren TAL-Effektoren PthXo1 und AvrXa7 jeweils spezifisch die Promotoren der Reisgene *Os8N3* bzw. *Os11N3* an (Yang et al., 2006; Antony et al., 2009; Römer et al., 2010). In diesem Fall ist die funktionelle Austauschbarkeit der TAL-Effektoren durch die funktionellen Ähnlichkeiten der *Os8N3*- und *Os11N3*-Genprodukte bedingt.

### A. Verschiedene Effektoren steuern überlappende Boxen an



### B. Verschiedene *sus*-Gene mit ähnlicher Funktion



### C. Gleiche Boxen werden von unterschiedlichen Effektoren angesteuert und verschiedene *sus*-Gene mit komplementärer Funktion

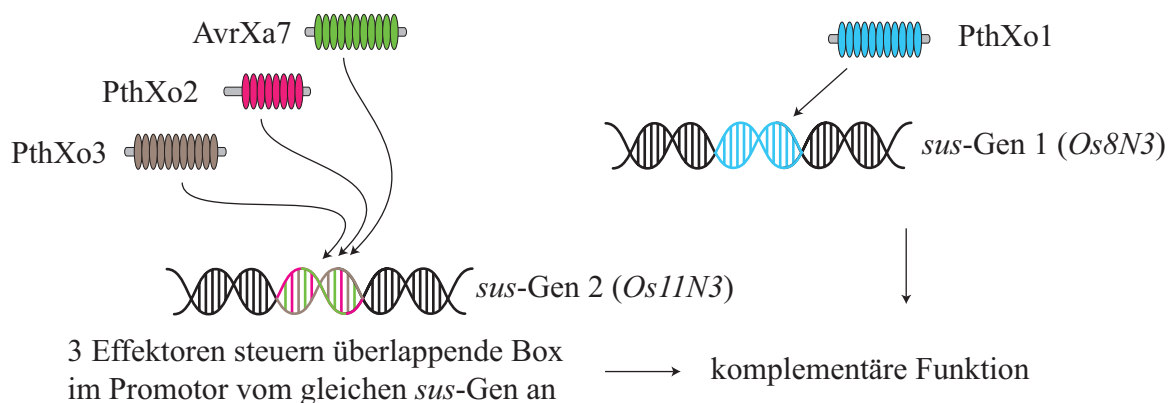


**Abbildung 13: Modell der Wirkungsweise von TAL-Effektoren mit ähnlicher Repeat-Struktur**

A) Sowohl AvrBs3 als auch AvrHah1 binden an eine sich überschneidende  $UPT_{AvrBs3}$ -Box im *Bs3*-Promotor und induzieren damit die Expression des *Bs3*-Gens. B) PthXo1 bindet und aktiviert den *Os8N3*-Promotor. AvrXa7 bindet und aktiviert den *Os11N3*-Promotor. PthXo2 und PthXo3 binden an Promotoren von Genen, welche eine ähnliche Funktion wie *Os8N3* und *Os11N3* haben. Die Funktion von *Os8N3* wird durch die ähnliche Funktion der anderen aktivierten Gene komplementiert. C) AvrXa7, PthXo2 und PthXo3 binden an eine andere Promotorbox als PthXo1 und induzieren die Expression eines gemeinsamen Suszeptibilitäts (*sus*)-Gens (*Os11N3*). *Os11N3* hat eine ähnliche Funktion wie *Os8N3* und komplementiert dadurch den Virulenzphänotyp. Grundlage für die Hypothese, dass PthXo2, PthXo3 und AvrXa7 an die gleiche Box binden ist, dass sie die gleiche Virulenzfunktion und sehr ähnliche RVDs haben (Yang und White, 2004).

Neben dem TAL-Effektor AvrXa7 können auch die TAL-Effektoren PthXo2 und PthXo3 die Virulenzfunktion von PthXo1 komplementieren (Yang und White, 2004). Es ist möglich, dass alle vier TAL-Effektoren unterschiedliche Promotorboxen von verschiedenen Genen

ansteuern, deren Genprodukte funktionelle Homologien aufweisen (siehe Abbildung 13B). Eine weitere Möglichkeit besteht darin, dass PthXo1 an einen anderen Bereich im Promotor oder an einen anderen Promotor bindet als die drei anderen TAL-Effektoren (Abbildung 13C), da die RVDs der drei TAL-Effektoren untereinander sehr ähnlich, aber im Vergleich zu denen von PthXo1 doch unterschiedlich sind.

Durch die ähnliche Funktion, welche von den beiden Suszeptibilitäts (*sus*)-Genen ausgeübt wird, kommt es dann zu einer Kompensation des von PthXo1 bedingten Virulenzphänotyps (Abbildung 13C). Die Möglichkeit, dass PthXo1 und die anderen drei Effektoren an eine identische Sequenz im gleichen Promotor binden und es dadurch zur Aktivierung desselben Genes kommt, ist sehr unwahrscheinlich, weil die in dieser Arbeit getesteten Promotoren keine Kreuzaktivierbarkeit aufgewiesen haben, d.h. *Os8N3* war nur durch PthXo1 und *Os11N3* war nur durch AvrXa7 aktivierbar (siehe 2.6.1) und *Os8N3* wurde auch in Reis nur durch PthXo1 und nicht durch AvrXa7 induziert (Yang et al., 2006).

### 3.7 Der “CODE“ erklärt Einiges in der Promotor-TAL-Effektorinteraktion

Die Korrelation zwischen Anzahl der *Repeat*-Einheiten und der Länge der korrespondierenden *UPT*-Boxen konnte in der hier vorliegenden Arbeit, sowie in anderen Studien gezeigt werden. Durch die Substitutionsmutagenese des *Bs3*-Promotors konnte ermittelt werden, dass die *UPT*<sub>AvrBs3</sub>-Box 18 Bp umfasst (Römer et al., 2009b). Für AvrHah1 konnte eine *UPT*<sub>AvrHah1</sub>-Box im *Bs3*-Promotor von 14 Bp bestimmt werden (S. Recht und T. Lahaye, unveröffentlicht). Mit AvrBs3 $\Delta$ rep16 wurde eine *UPT*<sub>AvrBs3 $\Delta$ rep16</sub>-Box von 14 Bp identifiziert (Römer et al., 2009b) und für AvrXa27 konnte eine *UPT*<sub>AvrXa27</sub>-Box von 16 Bp ermittelt werden (Römer et al., 2009a). Somit korreliert die Länge der getesteten *UPT*-Boxen mit der Anzahl an vorhandenen *Repeat*-Einheiten in den jeweiligen TAL-Effektoren.

Weiterführende Analysen haben gezeigt, dass nicht nur die Anzahl der *Repeat*-Einheiten, sondern auch die Art der hypervariable AS-Dipeptide 12 und 13 (*repeat variable diresidue*, RVD), die Erkennung von bestimmten Promotorboxen definieren. So konnte ermittelt werden, dass spezifische RVDs immer zu bestimmten Basenpaaren in den Promotorboxen passen (Boch et al., 2009; Moscou und Bogdanove, 2009). Die Korrelation zwischen RVDs und den dazu passenden Nukleotiden im oberen Strang der DNA (betrachtet in der 5'  $\rightarrow$  3' Richtung vor dem Gen) ist in Tabelle 3 dargestellt. Aufgrund der Tatsache, dass bestimmte RVDs mit spezifischen Basenpaaren paaren, konnten für TAL-Effektoren kompatible Promotorboxen generiert werden und reziprok für Promotorsequenzen korrespondierende TAL-Effektoren erstellt werden (Boch et al., 2009; R. Morbitzer und T. Lahaye, unveröffentlicht). Vergleicht

man die basierend auf den TAL-Effektor-CODE (“CODE“) vorhergesagte Box für AvrBs3 mit der natürlich vorkommenden  $UPT_{AvrBs3}$ -Box im *Bs3*-Promotor, so ist zu erkennen, dass es an drei Positionen Unterschiede gibt (Abbildung 14). Auch für die TAL-Effektoren AvrXa27, AvrXa7, PthXo1, PthXo6, AvrHah1 und AvrBs3 $\Delta$ rep16 konnte eine Diskrepanz zwischen “CODE“ vorhergesagten und den natürlich vorhandenen *UPT*-Boxen in den Promotoren der korrespondierenden Gene ermittelt werden (Römer et al., 2010). Dabei stellt sich die Frage, ob diese theoretischen Idealboxen im Vergleich zu den natürlich vorkommenden Boxen Unterschiede bezüglich ihrer Induzierbarkeit aufweisen oder nicht. Um diesen Sachverhalt zu analysieren, müssten die natürlich vorkommenden und die idealen “CODE“-*UPT*-Boxen vergleichend untersucht werden. Idealerweise sollte hierfür ein System zur Anwendung kommen, das quantifizierbar ist und dadurch eine genaue Aussage zulassen würde, wie z.B. quantitative GUS-Analysen oder qRT-PCR.

**Tabelle 3: Der “CODE“ der TAL-Effektoren**

		RVDs					
		HD	NG	NI	NN	NS	HG
Häufigkeit		75 x	65 x	53 x	32 x	21 x	10 x
Frequenz in Prozent	A	9	6	<b>87</b>	<b>41</b>	<b>62</b>	0
	C	<b>90</b>	26	9	19	29	20
	G	0	3	0	<b>34</b>	9	0
	T	1	<b>65</b>	4	6	0	<b>80</b>

Zusammenfassung der RVDs-Basenpaarung nach Boch und Moscou (Boch et al., 2009; Moscou und Bogdanove, 2009) und als zusätzlichen Effektor AvrXa7 mit *Os11N3* als getesteten Promotor (siehe Tabelle 5 im Anhang). Bestimmte RVDs passen zu bestimmten Nukleotiden im oberen Strang. Die Häufigkeit gibt an, wie oft RVDs in den analysierten TAL-Effektoren vorkommen. Die gleichen Hintergrundfarben sollen verdeutlichen, welche RVDs bevorzugt zu welchem Nukleotid im oberen Strang der DNA passen. Die am häufigsten von bestimmten RVDs gebundenen Nukleotide im oberen Strang der DNA sind fett und mit grauem Hintergrund dargestellt. Für die RVDs NK, HI, IG und ND wurden jeweils nur 1-2 Fälle gefunden und deshalb wurden sie nicht in die Tabelle aufgenommen. Für NS erfolgte keine Zuordnung, da hierfür schon gezeigt wurde, dass es alle 4 Nukleotide im oberen Strang aktiviert (Boch et al., 2009). Für NN wurden sowohl A und G als präferentielle Nukleotide angegeben, da sie fast gleich oft vorkommen. Die Daten in der hier vorliegenden Arbeit zeigen allerdings, dass für NN an bestimmten Positionen im Promotor von *Xa13* nur ein G Nukleotid im oberen Strang der DNA erlaubt ist (siehe 2.6.1).

Der TAL-Effektor-CODE sagt voraus, dass unterschiedliche RVDs jeweils spezifisch an ein A-, C-, G- oder T-Nukleotid im oberen Strang der DNA binden (siehe Tabelle 3). Dieser “CODE“ ist nicht positionsspezifisch, d.h., dass beispielweise die Spezifität eines NI in allen Positionen eines TAL-Effektors gleich sein sollte (Moscou und Bogdanove, 2009). Die Substitutionsmutagenese des *Bs3*-Promotors hat jedoch gezeigt, dass Mutationen an unterschiedlichen Positionen der  $UPT_{AvrBs3}$ -Box unterschiedlich starke Effekte auf die Aktivierbarkeit des *Bs3*-Promotors haben, auch wenn diese Mutationen die gleichen RVDs

betreffen. Ein Beispiel hierfür sind die Positionen -57 und -45 im *Bs3*-Promotor (Abbildung 14). Bei beiden Positionen paart ein T-Nukleotid im oberen Strang der DNA, mit dem RVD NG. Alle Permutationen an Position -45 haben keinen Einfluss auf die Promotoraktivität im HR-Assay (Römer et al., 2009b). Im Gegensatz dazu bedingen alle Permutationen an Position -57 den Verlust der Promotoraktivierung im HR-Assay (Römer et al., 2009b; Abbildung 14). Es gibt jedoch noch weitere Positionen in der  $UPT_{AvrBs3}$ -Box des *Bs3*-Promotors, die an identische RVDs paaren und die bei der Substitutionsmutagenese unterschiedliche Effekte auf die Aktivierbarkeit des *Bs3*-Promotors zeigten. Ein weiteres Beispiel für identische RVDs, die bei der Substitutionsmutagenese unterschiedliche Effekte auf die Aktivierbarkeit des *Bs3*-Promotors zeigten, sind die Positionen -47 und -46, die an die RVDs des HD-Typs der *Repeat*-Einheiten 14 und 15 paaren (Abbildung 14). An der Position -47 bedingt jeglicher Austausch einen Verlust der AvrBs3-vermittelten Induktion, wohingegen an der Position -46 Austausche in alle drei anderen Varianten keinen signifikanten Einfluss auf die Aktivierbarkeit des Promotors haben (Abbildung 14A). Eine mögliche Erklärung für das unterschiedliche Verhalten dieser HD-*Repeat*-Einheiten in der Substitutionsmutagenese wäre die Position innerhalb der *Repeat*-Struktur. Möglicherweise gibt es Positionen, welche auf Grund der benachbarten *Repeat*-Einheiten Mutationen in der Sequenz des korrespondierenden Promotors tolerieren und andere nicht.

Für die  $UPT_{AvrBs3}$ -Boxen der *UPA20*- und *Bs3*-Promotoren wurden neben den Einzelmutanten auch zahlreiche Mutanten mit multiplen Veränderungen in der  $UPT_{AvrBs3}$ -Box erstellt. Dabei konnte festgestellt werden, dass die meisten Mehrfachmutationen in einem Verlust der Aktivierbarkeit durch AvrBs3 resultieren (Kay et al., 2007; Kay et al., 2009; Römer et al., 2009b). Anscheinend sind Einzelmutationen tolerierbar, wohingegen Mehrfachmutationen sehr häufig zum Funktionsverlust führen (Boch et al., 2009; Kay et al., 2009; Römer et al., 2009b). Wahrscheinlich entstehen durch die Mehrfachmutationen additive Effekte. Dass Einzelmutationen toleriert werden, zeigen auch die bekannten  $UPT_{AvrBs3}$ -Boxen in den Promotoren der *UPA*-Gene, die zwar ähnlich zueinander sind, sich aber an einigen Positionen unterscheiden (Kay et al., 2007; Kay et al., 2009; Abbildung 14C). Bei dem Sequenzvergleich der  $UPT_{AvrBs3}$ -Boxen ist auffällig, dass die meisten Positionen, die in der Substitutionsmutagenese des *Bs3*-Promotors nicht veränderbar waren, ohne dass es zum Verlust in der Aktivierbarkeit kam, auch in den natürlich vorkommenden  $UPT_{AvrBs3}$ -Boxen konserviert sind (Abbildung 14A und C). Interessant wäre es herauszufinden, warum an bestimmten Positionen Mutationen erlaubt sind und an anderen wiederum nicht. Wahrscheinlich spielt dabei die Länge des jeweiligen TAL-Effektors eine Rolle, denn in

längeren TAL-Effektoren gibt es mehr Unterschiede zwischen “CODE“ vorhergesagten und natürlich vorkommenden *UPT*-Boxen (Römer et al., 2010). Es wäre aber auch möglich, dass die anderen variablen AS (4, 16, 17 und 24) eine Bedeutung bei der Erkennungsspezifität haben und es deshalb zu Positionseffekten innerhalb von TAL-Effektoren kommt.

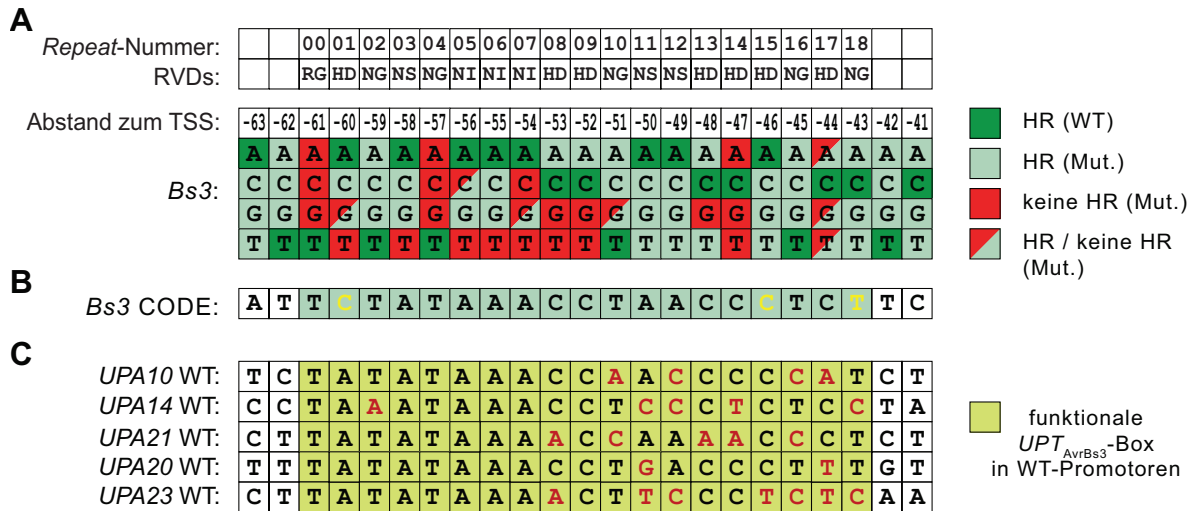


**Abbildung 14: Einige Positionen in den *UPT*<sub>AvrBs3</sub>-Boxen sind nicht durch den “CODE“ erklärbar**

**A)** Zusammenfassung der Inokulationsstudien der Einzelmutanten im *Bs3*-Promotor. Die *Bs3*-Promotorvarianten wurden in Kombination mit einem *35S:avrBs3*-Gen transient mittels *A. tumefaciens* in *N. benthamiana* exprimiert. Die Auswertung der Phänotypen erfolgte 4 Tage nach der Infiltration. Die grünen Vierecke geben die Wildtyp- (WT)-Situation an (Ausbildung einer HR nach der Koexpression mit *35S:avrBs3*). Hellgrüne Kästchen geben die Mutanten an, die eine HR wie der WT ausbilden und die roten Kästchen die Mutanten, die keine HR mehr induzieren. Die hellgrün/roten Kästchen stellen die Mutanten dar, welche manchmal eine HR nach der Koexpression mit einem *35S:avrBs3*-Gen auslösten und manchmal nicht. Alle dunkelgrünen Kästchen stellen die WT-Situation (einen Datenpunkt) dar. Alle anderen Kästchen symbolisieren das Ergebnis der jeweiligen Promotormutante und sind alles Einzeldatenpunkte. Die *Repeat*-Nummer bezeichnet die Position der *Repeat*-Einheiten innerhalb von *AvrBs3* und die RVDs symbolisieren die *Repeat variable diresidue* der jeweiligen *Repeat*-Einheit. **B)** Nach dem “CODE“ vorhergesagte ideale *UPT*<sub>AvrBs3</sub>-Box im *Bs3*-Promotor. Die gelben Nukleotide symbolisieren die Unterschiede zu der natürlich vorkommenden WT-*UPT*<sub>AvrBs3</sub>-Box des *Bs3*-Promotors. **C)** Sequenzvergleich von einigen natürlich vorkommenden *UPT*<sub>AvrBs3</sub>-Boxen aus verschiedenen *UPA*-Genpromotoren. Der grün hinterlegte Bereich stellt die experimentell bestimmte und durch den “CODE“ vorhergesagte Größe der *UPT*<sub>AvrBs3</sub>-Box dar. Sequenzunterschiede, die von der theoretischen Konsensussequenz abweichen, sind als rote Buchstaben markiert.

Es kann aber auch sein, dass es Schlüsselpositionen innerhalb der Promotor-TAL-Effektor Interaktion gibt und dass deshalb bestimmte Positionen so strikt festgelegt sind. Eine sogenannte Schlüsselposition ist das T-Nukleotid im oberen Strang der DNA, das wahrscheinlich von der “0.“ *Repeat*-Einheit gebunden wird. So ergab sowohl die Substitutionsmutagenese von natürlich vorkommenden *UPT*-Boxen als auch die Erstellung von *UPT*-Boxen für vorhandene TAL-Effektoren, dass dieses T-Nukleotid im oberen Strang entscheidend für die Bindung und die Induktion durch TAL-Effektoren ist (Boch et al., 2009; Römer et al., 2009b; Römer et al., 2010). Die Frage, warum es so entscheidend ist und warum es in allen *UPT*-Boxen konserviert ist (Moscou und Bogdanove, 2009), konnte bis jetzt nicht geklärt werden. Auch war es bis jetzt nicht möglich die exakten AS innerhalb der “0.“ *Repeat*-

Einheit zu bestimmen, welche dieses T-Nukleotid im oberen Strang der DNA binden. Diesen Sachverhalt zu analysieren und im Detail zu hinterfragen, wäre sicherlich wichtig um den "CODE" noch besser zu verstehen und anwenden zu können.

### 3.8 Die Interaktion von *UPT*-Boxen mit TAL-Effektoren

Die Analyse von acht *UPA*-Genen zeigte, dass der Abstand zwischen den *UPT*<sub>AvrBs3</sub>-Boxen und dem Transkriptionsstart (*transcriptional start site*, TSS) generell ähnlich ist und dass sich die *UPT*<sub>AvrBs3</sub>-Box immer innerhalb von 100 Bp stromaufwärts des TSSs befindet (Kay et al., 2009). In der hier vorliegenden Arbeit resultierte eine Verschiebung der *UPT*<sub>AvrBs3</sub>-Box innerhalb des *Bs3*-Promotors in veränderten TSSs (Römer et al., 2009b). Dabei bewegte sich der Abstand zwischen dem 3'-Ende der *UPT*<sub>AvrBs3</sub>-Box und dem TSS in einer Region zwischen 41 und 46 Bp (Kay et al., 2009; Römer et al., 2009b). In einem *Bs3*-Promotorkonstrukt, in dem drei funktional verschiedene *UPT*-Boxen inseriert wurden, war ebenfalls für jede TAL-Effektor *UPT*-Box Kombination der Abstand zwischen dem TSS und dem 3'-Ende der jeweiligen *UPT*-Box konstant und bewegte sich zwischen 44 und 54 Bp (Römer et al., 2009a). Somit konnte festgestellt werden, dass die *UPT*-Boxen einen bedeutenden Einfluss auf die Position des TSSs haben.

In Promotoren mit *TATA*-Box bindet das *TATA*-Box Bindeprotein (TBP) und bestimmt dadurch den konservierten Abstand von 25-30 Bp zum TSS (Kornberg, 2007). Da in den TAL-Effektor induzierten Promotoren die *UPT*-Boxen den Abstand zum TSS definieren, ist es naheliegend zu vermuten, dass TAL-Effektoren, ähnlich wie das TBP, die sequenzspezifische Komponente in den Präinitiationskomplexen repräsentieren (Abbildung 15). Das 38 kDa TBP bindet an ein 8 Bp langes Sequenzmotiv, die *TATA*-Box (Hernandez, 1993; Kim et al., 1993a; Kim et al., 1993b; Abbildung 15). Da TAL-Effektoren ein vergleichsweise deutlich höheres Molekulargewicht aufweisen (120 – 130 kDa; Knoop et al., 1991; Bonas et al., 1993; Young et al., 1994) könnte dieser Größenunterschied erklären, warum der Abstand zwischen dem 3'-Ende der *UPT*-Boxen und dem TSS mindestens 41 Bp beträgt, während der Abstand zwischen dem *TATA*-Element und dem TSS nur 25-30 Bp beträgt (Kornberg, 2007). In diesem Zusammenhang ist bemerkenswert, dass die unterschiedlich langen TAL-Effektoren AvrBs3 und AvrHah1, die an die *UPT*<sub>AvrBs3</sub>- bzw. *UPT*<sub>AvrHah1</sub>-Box binden am *Bs3*-Promotor identische Transkripte induzieren, obwohl die 3'-Enden ihrer *UPT*-Boxen um 2 Bp differieren (S. Recht und T. Lahaye, unveröffentlicht). Die Hypothese, dass das Molekulargewicht eines TAL-Effektors direkt proportional zu der Größe des bedeckten DNA-Sequenzbereiches ist, konnte unlängst auch in DNaseI-*Footprint* Analysen mit AvrBs3 und AvrBs3 $\Delta$ rep16 gezeigt werden



(Boch et al., 2009; Kay et al., 2009). Interessanterweise ist der Bereich, der zusätzlich zur jeweiligen *UPT*-Box vor Abbau durch DNaseI geschützt wird, konstant und beträgt sowohl am 5'-Ende als auch am 3'-Ende der jeweiligen *UPT*-Box 10 Basenpaare (Boch et al., 2009; Kay et al., 2009). Somit scheint der Bereich, der vor DNaseI-Abbau geschützt wird, durch die Anzahl der *Repeat*-Einheiten und durch den N- und C-terminalen Bereich des TAL-Effektors bestimmt zu werden. Da TAL-Effektoren im N- und C-terminalen Nicht-*Repeat*-Bereich extrem konserviert sind, ist zu vermuten, dass Analysen mit anderen TAL-Effektoren ähnliche Befunde liefern würden. Zusammenfassend kann festgestellt werden, dass die aktuelle Datenlage eine Funktion von TAL-Effektoren als sequenzspezifische Komponente im Präinitiationskomplex glaubhaft erscheinen lässt. Allerdings sind biochemische Studien des Präinitiationskomplexes in Kombination mit TAL-Effektoren notwendig, um diese Hypothese zu beweisen.

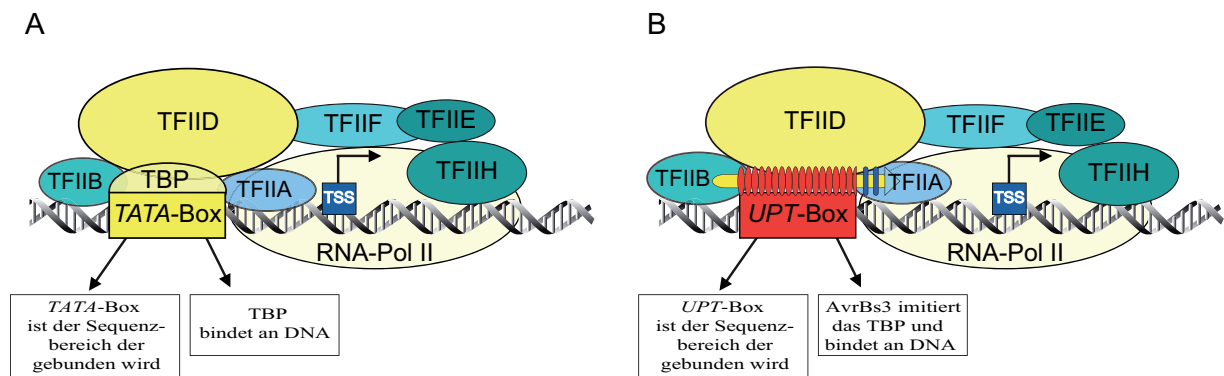


**Abbildung 15: Modell der Bindung von AvrBs3 an die *UPT*-Box**

**A)** Molekulare Wirkungsweise der generellen Transkriptionsfaktoren (GTF) in Promotoren ohne *UPT*-Box. Das *TATA*-Box-bindende Protein (TBP) ist eine Untereinheit des GTF TFIID und bindet an die *TATA*-Box. Das ist die Grundlage für den Zusammenbau des Präinitiationskomplexes. TFIIB stabilisiert die Bindung des TBP an die *TATA*-Box (Buratowski et al., 1989). Im Anschluß bindet TFIIF, TFIIE und TFIIH. **B)** AvrBs3 imitiert das TBP und bindet an einen Sequenzbereich im Promotor, die *UPT*<sub>AvrBs3</sub>-Box. Ein weiterer wichtiger Faktor ist Xa5, die  $\gamma$ -Untereinheit des GTF TFIIA, für die gezeigt wurde, dass sie notwendig für die Funktionsweise der TAL-Effektoren in Reis ist (Gu et al., 2009). Zur Vereinfachung der Abbildung wurde Xa5 nicht als alleinige Untereinheit dargestellt. Durch die Bindung von AvrBs3 kommt es außerdem zu der Verschiebung des Transkriptionsstarts (*transcriptional start site*; TSS). Die Abbildung wurde verändert nach Krishnamurthy und Hampsey (2009).

### 3.9 TAL-Effektoren interagieren vermutlich als Monomere mit der DNA

Arbeiten an AvrBs3 und AvrBs3 $\Delta$ rep16 lieferten Hinweise dafür, dass diese als Di- oder Multimere in den Kern transportiert werden (Gürlebeck et al., 2005). Daraufhin wurde spekuliert, dass TAL-Effektoren als Di- oder Multimere an die DNA binden (Kay, 2008; Hahn, 2009), Grundlage für diese Spekulationen ist die Dimerisierung von AvrBs3 und AvrBs3 $\Delta$ rep16, die in Hefe und *in planta* gezeigt werden konnte (Gürlebeck et al., 2005). Diese Daten zeigen zwar, dass AvrBs3 und AvrBs3 $\Delta$ rep16 Heterodimere bilden, sie ließen jedoch keine Schlussfolgerung zu, ob sie als Di- oder Multimere mit der DNA interagieren (Gürlebeck et al., 2005). Der TAL-Effektor-CODE, dessen Gültigkeit in mehreren unabhängigen Studien belegt wurde (Boch et al., 2009; Moscou und Bogdanove, 2009; Römer et al., 2010), lässt die Hypothese einer Interaktion von TAL-Effektor-Heterodimeren mit der DNA unwahrscheinlich erscheinen. Interessanterweise konnte auch für das TBP gezeigt werden, dass es dimerisiert, allerdings erfolgt die Bindung an die DNA nur durch die monomere Form (Kim et al., 1993a; Kim et al., 1993b; Nikolov et al., 1996). Die Bildung von TBP-Homodimeren wird als Schutzfunktion interpretiert, die unspezifische Bindung des TBP an DNA verhindert. Die Bildung der TBP-Homodimere wurde zuerst in Kristallstrukturen des TBP aus *A. thaliana* beobachtet (Nikolov et al., 1992; Nikolov und Burley, 1994). Möglicherweise ist die Dimerisierung von TAL-Effektoren ebenfalls eine Schutzfunktion, die unspezifische Bindungen an DNA minimiert. Um den Sachverhalt zu klären, wäre es notwendig, die Struktur von TAL-Effektor *UPT*-Box Kokristallen zu klären. Über Kokristallisationsstudien könnte auch geklärt werden, welche Aminosäuren der TAL-Effektoren mit der DNA interagieren. Es wäre möglich, dass die TAL-Effektoren über ihre rechtsgewundene superhelikale Struktur, die in einer 3D-Vorhersage herausgefunden wurde, mit der DNA interagieren (Schornack et al., 2006). Theoretisch müssten die TAL-Effektoren eine Struktur einnehmen, die der DNA-Helix "folgt" bzw. der DNA sehr ähnlich ist, denn TAL-Effektoren mit einer unterschiedlichen Anzahl an *Repeat*-Einheiten folgen alle dem Prinzip des "CODEs". Würden sie eine Struktur einnehmen, die sich stark von der, der DNA unterscheidet, so müssten TAL-Effektoren mit mehr oder weniger *Repeat*-Einheiten ein unterschiedliches Bindungsverhalten aufweisen und der "CODE" wäre nicht mehr universell für alle TAL-Effektoren nutzbar.

### 3.10 Nutzung der TAL-Effektor-Technologie und mögliche Probleme

Die Grundlage für die differentielle Erkennung und Aktivierung von Promotoren ist die sequenzspezifische Bindung von der *Repeat*-Struktur der TAL-Effektoren an korrespondierende Promotorboxen (Boch et al., 2009; Moscou und Bogdanove, 2009). Anhand des “CODEs“ lässt sich erläutern, warum von unterschiedlichen TAL-Effektoren sequenzverschiedene *UPT*-Boxen angesteuert werden, auch wenn die Aktivierung diese Gene nach dem gleichen Mechanismus erfolgt, was in der hier vorliegenden Arbeit am Beispiel von *Bs3*, *Bs3-E*, *Xa27*, *Xa13* (*Os8N3*), *Os11N3* und *OsTFX1* gezeigt werden konnte (Römer et al., 2009a; Römer et al., 2010).

Ein zentraler Aspekt bei der TAL-Effektor-induzierten Genaktivierung, der in der hier vorliegenden Arbeit gezeigt werden konnte ist, dass die Position von *UPT*-Boxen innerhalb von Promotoren variierbar ist und dass verschiedene *UPT*-Boxen in einem Promotor kombiniert werden können (Römer et al., 2009a; Römer et al., 2009b; Römer et al., 2010). Da TAL-Effektoren in der Gattung *Xanthomonas* weit verbreitet sind und viele ökonomisch relevante *Xanthomonas*-Stämme multiple TAL-Effektorproteine enthalten, könnten Promotoren mit multiplen *UPT*-Boxen die Grundlage für die Erzeugung von Breitspektrum- und dauerhafter Resistenz sein. Durch Nutzung von *UPT*-Boxen, die durch Hauptvirulenzfaktoren angesteuert werden (Yang et al., 1996; Yang und White, 2004; Yang et al., 2006; Al-Saadi et al., 2007), sollten die Chancen erhöht werden, evolutionär stabile Resistenzen zu schaffen.

Ein mögliches Problem, das bei der Kombination von verschiedenen *UPT*-Boxen entstehen könnte, ist die transkriptionelle Interferenz. Der Mechanismus der transkriptionellen Interferenz in Eukaryoten wurde vorwiegend in *Drosophila melanogaster* und der Bäckerhefe *Saccharomyces cerevisiae* studiert (Corbin und Maniatis, 1989; Martens et al., 2004). Er wurde aber auch für pflanzliche und menschliche Zellen beschrieben (Padidam und Cao, 2001; Nigumann et al., 2002). Bei der transkriptionellen Interferenz kommt es zur Repression eines Gens durch ein zweites vorgelagertes Bindeelement im Promotor. Ist das vorgelagerte Promotorelement aktiv und kommt es zur Anlagerung der RNA-Polymerase, erfolgt die Synthese von nicht kodierenden RNAs. Durch diese Transkription entsteht eine Promotorkonkurrenz, wobei das zweite Promotorelement nicht für die RNA-Polymerase zugänglich und dessen Transkription somit blockiert ist (Greger et al., 2000; Conte et al., 2002; Shearwin et al., 2005). Um diesen Punkt zu untersuchen, müsste bspw. das Promotorkonstrukt, welches die *UPT*<sub>AvrBs3Δrep16-</sub>, die *UPT*<sub>AvrXa27-</sub>, und die *UPT*<sub>AvrBs3</sub>-Boxen

enthält (siehe 2.5.1), gleichzeitig mit allen drei TAL-Effektoren transient in der Pflanzenzelle exprimiert werden. Anschließend müssten RACE- oder Northern-Blot-Analysen durchgeführt werden, um die Längen der entstandenen Transkripte zu ermitteln, damit eine Aussage möglich ist, ob alle drei Boxen auch gleichzeitig genutzt werden können (Abbildung 16). Für *Bs3* und die Kombination von *UPT*-Boxen konnte schon gezeigt werden, dass alle *UPT*-Boxen, die von ihren TAL-Effektoren angesteuert werden, in der Lage sind ein Transkript zu initiieren, welches in einem funktionalen *Bs3*-Protein resultiert, das eine HR auslöst. Da die Kombination von verschiedenen *UPT*-Boxen möglich ist, könnten durch die Nutzung des "CODEs" *R*-Genpromotoren für TAL-Effektoren erzeugt werden, für die bis jetzt keine natürlichen *R*-Gene bekannt sind bzw. isoliert werden konnten. So sind bspw. für *Xanthomonas axonopodis* pv. *citri* (*Xac*), dem Erreger des ökonomisch relevanten Zitruskrebs keine *R*-Gene jedoch die Sequenzen der TAL-Effektoren bekannt (Khalaf et al., 2008). Mit Hilfe des "CODEs" könnte ein *R*-Genpromotor erstellt werden, welcher die *UPT*-Boxen für zahlreiche TAL-Effektoren aus *Xac* enthält (Abbildung 16). Diesen Promotor fusioniert man anschließend vor die kodierende Sequenz von *Bs3*, um eine Resistenzreaktion auslösen zu können. Alternativ könnte dieser Promotor auch vor ein Effektorgen kloniert werden, das in der entsprechenden Pflanze eine Zelltodreaktion auslöst. Ein Beispiel hierfür wäre das Effektorgen *avrGfl*, welches bei der Expression in Zitrus eine Zelltodreaktion auslöst (Rybak et al., 2009; Abbildung 16). Entscheidend bei so einem Ansatz ist, dass eine kodierende Sequenz an den *R*-Promotor fusioniert wird, die in der jeweiligen Pflanzenspezies in der Lage ist, eine Resistenzreaktion auszulösen. Für *Bs3* konnte bereits gezeigt werden, dass es in *Solanaceen*, *Brassicaceen* und *Fabaceen* eine HR auslöst (P. Römer und T. Lahaye, unveröffentlicht). Wäre es jetzt noch möglich zu beweisen, dass die *Bs3*-vermittelte HR, die durch das Dreifachpromotorkonstrukt (Kombination der  $UPT_{AvrBs3\Delta rep16^-}$ , die  $UPT_{AvrXa27^-}$ , und die  $UPT_{AvrBs3}$ -Boxen) ausgelöst wird, auch das Wachstum des jeweiligen Pathogens einschränkt, dann sind wir auf dem Weg, die bakteriellen TAL-Effektoren biotechnologisch zum Nutzen für die Pflanze zu verwenden und *Xanthomonas*-Stämme mit ihren eigenen Waffen zu bekämpfen.

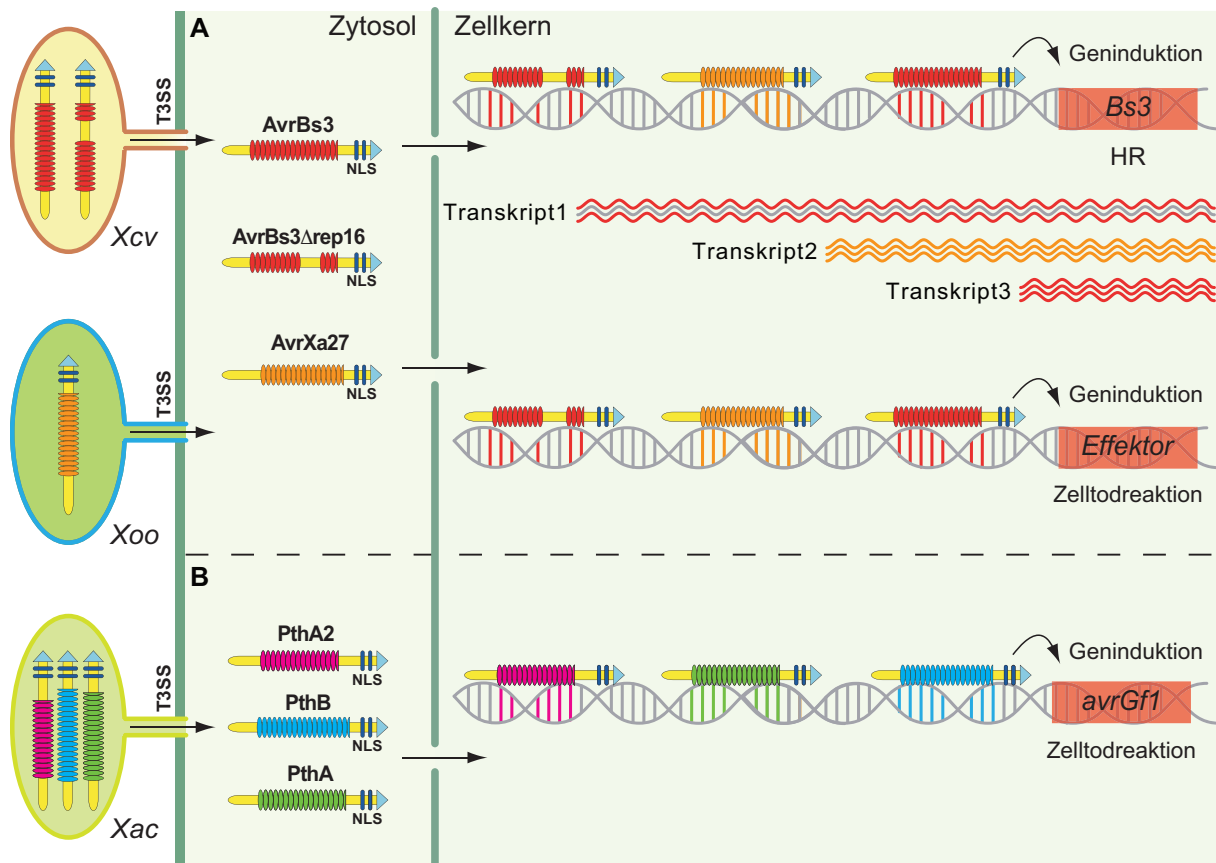


**Abbildung 16: Möglichkeiten der Resistenzgenerierung durch Kombination von UPT-Boxen**

Die verschiedenen *Xanthomonas* spp. *Xcv*, *Xoo* und *Xac* translozieren die TAL-Effektoren *AvrBs3*, *AvrXa27*, *AvrBs3Δrep16*, *PthA*, *PthB* und *PthA2* mit Hilfe des Typ-3-Sekretionssystems (T3SS) in das Zytosol der Pflanzenzelle. Von dort werden die TAL-Effektoren aufgrund ihrer Kernlokalisationssignale (NLS) in den Zellkern transportiert. Dort binden die TAL-Effektoren an ihre korrespondierenden UPT-Boxen. **A)** Die TAL-Effektoren *AvrBs3*, *AvrBs3Δrep16* und *AvrXa27* binden ihre korrespondierenden UPT-Boxen im komplexen Promotor. Dadurch wird die Expression des *R*-Gens *Bs3* induziert und es kommt zur Ausbildung der HR. Durch die verschiedenen Positionen der UPT-Boxen entstehen unterschiedlich lange Transkripte, das hat jedoch keine Auswirkung auf die Funktionalität von *Bs3* und das Auslösen der HR (Römer et al., 2009a). Alternativ zu *Bs3* könnte auch die kodierende Sequenz von Effektoren unter die Kontrolle des komplexen Promotors gestellt werden. Dabei ist es wichtig, dass diese Effektoren in der Lage sind, in der jeweiligen Pflanzenspezies eine Zelltodreaktion zu initiieren. **B)** Für die TAL-Effektoren *PthA2*, *PthB* und *PthA* aus *Xac*, für die kein *R*-Genlokus in Zitrus bekannt ist, können mit Hilfe des TAL-Effektor-CODEs UPT-Boxen erstellt werden. Diese kombiniert man in einen komplexen Promotor, der vor die kodierende Sequenz von dem Effektorgen *avrGf1* fusioniert wird. Die Induktion von *avrGf1* in Zitrus resultiert in einer Zelltodreaktion (Rybak et al., 2009).

## 4 Literaturverzeichnis

- Abramovitch R.B., Anderson J.C. and Martin G.B.** (2006) Bacterial elicitation and evasion of plant innate immunity. *Nat. Rev. Mol. Cell. Biol.* **7**: 601-611
- Al-Saadi A., Reddy J.D., Duan Y.P., Brunings A.M., Yuan Q. and Gabriel D.W.** (2007) All five host-range variants of *Xanthomonas citri* carry one *pthA* homolog with 17.5 repeats that determines pathogenicity on citrus, but none determine host-range variation. *Mol. Plant-Microbe Interact.* **20**: 934-943
- Albrecht M. and Takken F.L.W.** (2006) Update on the domain architectures of NLRs and R proteins. *Biochem. and Bioph. Res. Co.* **339**: 459-462
- Antony G., Yang B. and White F.F.** (2009) The alternate major effector AvrXa7 in bacterial blight of rice evades host resistance by targeting an alternate major host susceptibility gene. *Phytopathology* **99**: S5-S5
- Athinuwat D., Prathuangwong S., Cursino L. and Burr T.** (2009) *Xanthomonas axonopodis* pv. *glycines* soybean cultivar virulence specificity is determined by *avrBs3* homolog *avrXgl*. *Phytopathology* **99**: 996-1004
- Azevedo C., Sadanandom A., Kitagawa K., Freialdenhoven A., Shirasu K. and Schulze-Lefert P.** (2002) The RAR1 interactor SGT1, an essential component of *R* gene-triggered disease resistance. *Science* **295**: 2073-2076
- Bai J., Choi S.-H., Ponciano G., Leung H. and Leach J.E.** (2000) *Xanthomonas oryzae* pv. *oryzae* avirulence genes contribute differently and specifically to pathogen aggressiveness. *Mol. Plant-Microbe Interact.* **13**: 1322-1329
- Ballvora A., Pierre M., Van den Ackerveken G., Schornack S., Rossier O., Ganal M., Lahaye T. and Bonas U.** (2001a) Genetic mapping and functional analysis of the tomato *Bs4* locus, governing recognition of the *Xanthomonas campestris* pv. *vesicatoria* AvrBs4 protein. *Mol. Plant-Microbe Interact.* **14**: 629-638
- Ballvora A., Schornack S., Baker B.J., Ganal M., Bonas U. and Lahaye T.** (2001b) Chromosome landing at the tomato *Bs4* locus. *Mol. Genet. Genomics* **266**: 639-645
- Bartsch M., Gobbato E., Bednarek P., Debey S., Schultze J.L., Bautor J. and Parker J.E.** (2006) Salicylic acid-independent ENHANCED DISEASE SUSCEPTIBILITY1 signaling in *Arabidopsis* immunity and cell death is regulated by the monooxygenase FMO1 and the nudix hydrolase NUDT7. *Plant Cell* **18**: 1038-1051
- Blair M.W., Garris A.J., Iyer A.S., Chapman B., Kresovich S. and McCouch S.R.** (2003) High resolution genetic mapping and candidate gene identification at the *xa5* locus for bacterial blight resistance in rice (*Oryza sativa* L.). *Theor. Appl. Genet.* **107**: 62-73
- Boch J., Scholze H., Schornack S., Landgraf A., Hahn S., Kay S., Lahaye T., Nickstadt A. and Bonas U.** (2009) Breaking the code of DNA binding specificity of TAL-type III effectors. *Science* **326**: 1509-1512
- Bonas U., Conrads-Strauch J. and Balbo I.** (1993) Resistance in tomato to *Xanthomonas campestris* pv. *vesicatoria* is determined by alleles of the pepper-specific avirulence gene *avrBs3*. *Mol. Gen. Genet.* **238**: 261-269
- Bonas U., Stall R.E. and Staskawicz B.** (1989) Genetic and structural characterization of the avirulence gene *avrBs3* from *Xanthomonas campestris* pv. *vesicatoria*. *Mol. Gen. Genet.* **218**: 127-136
- Bradbury J.F.** (1984) Genus II *Xanthomonas* Dowson 1939. *Bergey's Manual of Systematic Bacteriology, Vol I.* In N.R. Krieg, J.G. Holt, eds, Williams and Wilkins, London, pp 199-210.
- Brueggeman R., Rostoks N., Kudrna D., Kilian A., Han F., Chen J., Druka A., Steffenson B. and Kleinhofs A.** (2002) The barley stem rust-resistance gene *Rpg1* is a novel disease-resistance gene with homology to receptor kinases. *Proc. Natl. Acad. Sci. USA* **99**: 9328-9333

- Buratowski S., Hahn S., Guarente L. and Sharp P.A.** (1989) Five intermediate complexes in transcription initiation by RNA polymerase-II. *Cell* **56**: 549-561
- Burch-Smith T.M., Schiff M., Caplan J.L., Tsao J., Czymmek K. and Dinesh-Kumar S.P.** (2007) A novel role for the TIR domain in association with pathogen-derived elicitors. *PLoS Biol.* **5**: e68
- Büttner D. and Bonas U.** (2010) Regulation and secretion of *Xanthomonas* virulence factors. *FEMS Microbiol. Rev.* **34**: 107-133
- Cao Y., Duan L., Li H., Sun X., Zhao Y., Xu C., Li X. and Wang S.** (2007) Functional analysis of *Xa3/Xa26* family members in rice resistance to *Xanthomonas oryzae* pv. *oryzae*. *Theor. Appl. Genet.* **115**: 887-895
- Caplan J., Padmanabhan M. and Dinesh-Kumar S.P.** (2008) Plant NB-LRR immune receptors: from recognition to transcriptional reprogramming. *Cell Host Microbe* **3**: 126-135
- Cashman J.R. and Zhang J.** (2006) Human flavin-containing monooxygenases. *Annu. Rev. Pharmacol. Toxicol.* **46**: 65-100
- Catanzariti A.M., Dodds P.N., Ve T., Kobe B., Ellis J.G. and Staskawicz B.J.** (2010) The AvrM effector from flax rust has a structured C-terminal domain and interacts directly with the M resistance protein. *Mol. Plant-Microbe Interact.* **23**: 49-57
- Century K.S., Holub E.B. and Staskawicz B.J.** (1995) *NDR1*, a locus in *Arabidopsis thaliana* that is required for disease resistance to both a bacterial and a fungal pathogen. *Proc. Natl. Acad. Sci. USA* **92**: 6597-6601
- Century K.S., Shapiro A.D., Repetti P.P., Dahlbeck D., Holub E. and Staskawicz B.J.** (1997) *NDR1*, a pathogen-induced component required for *Arabidopsis* disease resistance. *Science* **278**: 1963-1965
- Chan J.W.Y.F. and Goodwin P.H.** (1999) The molecular genetics of virulence of *Xanthomonas campestris*. *Biotechnol. Adv.* **17**: 489-508
- Chen S., Huang Z., Zeng L., Yang J., Liu Q. and Zhu X.** (2008) High-resolution mapping and gene prediction of *Xanthomonas oryzae* pv. *oryzae* resistance gene *Xa7*. *Mol. Breed.* **22**: 433-441
- Chen X., Shang J., Chen D., Lei C., Zou Y., Zhai W., Liu G., Xu J., Ling Z., Cao G., Ma B., Wang Y., Zhao X., Li S. and Zhu L.** (2006) A B-lectin receptor kinase gene conferring rice blast resistance. *Plant J.* **46**: 794-804
- Cheng Y., Dai X. and Zhao Y.** (2006) Auxin biosynthesis by the YUCCA flavin monooxygenases controls the formation of floral organs and vascular tissues in *Arabidopsis*. *Genes Dev.* **20**: 1790-1799
- Chinchilla D., Bauer Z., Regenass M., Boller T. and Felix G.** (2006) The *Arabidopsis* receptor kinase FLS2 binds flg22 and determines the specificity of flagellin perception. *Plant Cell* **18**: 465-476
- Chinchilla D., Boller T. and Robatzek S.** (2007) Flagellin signalling in plant immunity. *Adv. Exp. Med. Biol.* **598**: 358-371
- Choi H.S., Kim J.K., Cho E.H., Kim Y.C., Kim J.I. and Kim S.W.** (2003) A novel flavin-containing monooxygenase from *Methylophaga* sp strain SK1 and its indigo synthesis in *Escherichia coli*. *Biochem. and Bioph. Res. Co.* **306**: 930-936
- Chu Z., Yuan M., Yao J., Ge X., Yuan B., Xu C., Li X., Fu B., Li Z., Bennetzen J.L., Zhang Q. and Wang S.** (2006) Promoter mutations of an essential gene for pollen development result in disease resistance in rice. *Genes Dev.* **20**: 1250-1255
- Conte C., Dastugue B. and Vaury C.** (2002) Promoter competition as a mechanism of transcriptional interference mediated by retrotransposons. *EMBO J.* **21**: 3908-3916
- Cook A.A. and Guevara Y.G.** (1984) Hypersensitivity in *Capsicum chacoense* to race 1 of the bacterial spot pathogen of pepper. *Plant Dis.* **68**: 329-330
- Cook A.A. and Stall R.E.** (1963) Inheritance of resistance in pepper to bacterial spot. *Phytopathology* **53**: 1060-1062

- Coppinger P., Repetti P.P., Day B., Dahlbeck D., Mehlert A. and Staskawicz B.J.** (2004) Overexpression of the plasma membrane-localized NDR1 protein results in enhanced bacterial disease resistance in *Arabidopsis thaliana*. *Plant J.* **40**: 225-237
- Corbin V. and Maniatis T.** (1989) Role of transcriptional interference in the *Drosophila melanogaster* Adh promoter switch. *Nature* **337**: 279-282
- Cunnac S., Occhialini A., Barberis P., Boucher C. and Genin S.** (2004) Inventory and functional analysis of the large Hrp regulon in *Ralstonia solanacearum*: identification of novel effector proteins translocated to plant host cells through the type III secretion system. *Mol. Microbiol.* **53**: 115-128
- Cutino-Jimenez A.M., Martins-Pinheiro M., Lima W.C., Martin-Tornet A., Morales O.G. and Menck C.F.** (2010) Evolutionary placement of Xanthomonadales based on conserved protein signature sequences. *Mol. Phylogenet. Evol.* **54**: 524-534
- Dangl J.L. and Jones J.D.G.** (2001) Plant pathogens and integrated defence responses to infection. *Nature* **411**: 826-833
- De Feyter R., Yang Y.O. and Gabriel D.W.** (1993) Gene-for-genes interactions between cotton *R*-genes and *Xanthomonas campestris* pv. *malvacearum* *avr* genes. *Mol. Plant-Microbe Interact.* **6**: 225-237
- Deslandes L., Olivier J., Peeters N., Feng D.X., Khounlotham M., Boucher C., Somssich I., Genin S. and Marco Y.** (2003) Physical interaction between RRS1-R, a protein conferring resistance to bacterial wilt, and PopP2, a type III effector targeted to the plant nucleus. *Proc. Natl. Acad. Sci. USA* **100**: 8024-8029
- DeYoung B.J. and Innes R.W.** (2006) Plant NBS-LRR proteins in pathogen sensing and host defense. *Nat. Immunol.* **7**: 1243-1249
- Diener A.C. and Ausubel F.M.** (2005) Resistance to *Fusarium oxysporum* 1, a dominant *Arabidopsis* disease-resistance gene, is not Race specific. *Genetics* **171**: 305-321
- Dixon M.S., Hatzixanthis K., Jones D.A., Harrison K. and Jones J.D.G.** (1998) The tomato *Cf-5* disease resistance gene and six homologs show pronounced allelic variation in leucine-rich repeat copy number. *Plant Cell* **10**: 1915-1925
- Dixon M.S., Jones D.A., Keddie J.S., Thomas C.M., Harrison K. and Jones** (1996) The tomato *Cf-2* disease resistance locus comprises two functional genes encoding leucine-rich repeat proteins. *Cell* **84**: 451-459
- Dodds P.N., Lawrence G.J., Catanzariti A.-M., Teh T., Wang C.-I.A., Ayliffe M.A., Kobe B. and Ellis J.G.** (2006) Direct protein interaction underlies gene-for-gene specificity and coevolution of the flax resistance genes and flax rust avirulence genes. *Proc. Natl. Acad. Sci. USA* **103**: 8888-8893
- Ellis J., Dodds P. and Pryor T.** (2000) Structure, function and evolution of plant disease resistance genes. *Curr. Opin. Plant Biol.* **3**: 278-284
- Exposito-Rodriguez M., Borges A.A., Borges-Perez A., Hernandez M. and Perez J.A.** (2007) Cloning and biochemical characterization of ToFZY, a tomato gene encoding a flavin monooxygenase involved in a tryptophan-dependent auxin biosynthesis pathway. *J. Plant Growth Regul.* **26**: 329-340
- Ezuka A., Horino O., Toriyama K., Shinoda H. and Morinaka T.** (1975) Inheritance of resistance of rice variety Wase Aikoku 3 to *Xanthomonas oryzae*. *Bull. Tokai-kinki Nat. Agric. Exp. Stn.* **28**: 124-130
- Falk A., Feys B.J., Frost L.N., Jones J.D.G., Daniels M.J. and Parker J.E.** (1999) *EDS1*, an essential component of *R* gene-mediated disease resistance in *Arabidopsis* has homology to eukaryotic lipases. *Proc. Natl. Acad. Sci. USA* **96**: 3292-3297
- Flor H.H.** (1942) Inheritance of pathogenicity in *Melampsora lini*. *Phytopathology* **32**: 653-669
- Flor H.H.** (1971) Current status of the gene-for-gene concept. *Annu. Rev. Phytopathol.* **9**: 275-296



- Furutani A., Takaoka M., Sanada H., Noguchi Y., Oku T., Tsuno K., Ochiai H. and Tsuge S.** (2009) Identification of novel type III secretion effectors in *Xanthomonas oryzae* pv. *oryzae*. *Mol. Plant-Microbe Interact.* **22**: 96-106
- Gabriel D.W.** (1997) Targeting of protein signals from *Xanthomonas* to the plant nucleus. *Trends Plant Sci.* **2**: 204-206
- Gabriel D.W. and Rolfe B.G.** (1990) Working models of specific recognition in plant-microbe interactions. *Annu. Rev. Phytopathol.* **28**: 365-391
- Gabriel D.W., Burges A. and Lazo G.R.** (1986) Gene-for-gene interactions of five cloned avirulence genes from *Xanthomonas campestris* pv *malvacearum* with specific resistance genes in cotton. *Proc. Natl. Acad. Sci. USA* **83**: 6415-6419
- Gabriels S.H., Takken F.L., Vossen J.H., de Jong C.F., Liu Q., Turk S.C., Wachowski L.K., Peters J., Witsenboer H.M., de Wit P.J. and Joosten M.H.** (2006) cDNA-AFLP combined with functional analysis reveals novel genes involved in the hypersensitive response. *Mol. Plant-Microbe Interact.* **19**: 567-576
- Gamas P., Niebel F.d.C., Lescure N. and Cullimore J.V.** (1996) Use of a subtractive hybridization approach to identify new *Medicago truncatula* genes induced during root nodule development. *Mol. Plant-Microbe Interact.* **9**: 233-242
- Ge Y.X., Angenent G.C., Dahlhaus E., Franken J., Peters J., Wullems G.J. and Creemers-Molenaar J.** (2001) Partial silencing of the *NEC1* gene results in early opening of anthers in *Petunia hybrida*. *Mol. Genet. Genomics* **265**: 414-423
- Ge Y.X., Angenent G.C., Wittich P.E., Peters J., Franken J., Busscher M., Zhang L.M., Dahlhaus E., Kater M.M., Wullems G.J. and Creemers-Molenaar T.** (2000) *NEC1*, a novel gene, highly expressed in nectary tissue of *Petunia hybrida*. *Plant J.* **24**: 725-734
- Ghosh P.** (2004) Process of protein transport by the type III secretion system. *Microbiol. Mol. Biol. Rev.* **68**: 771-795
- Gómez-Gómez L.** (2004) Plant perception systems for pathogen recognition and defence. *Mol. Immunol.* **41**: 1055-1062
- Gómez-Gómez L. and Boller T.** (2000) FLS2: An LRR receptor-like kinase involved in the perception of the bacterial elicitor flagellin in *Arabidopsis*. *Mol. Cell.* **5**: 1003-1011
- Gómez-Gómez L. and Boller T.** (2002) Flagellin perception: a paradigm for innate immunity. *Trends Plant Sci.* **7**: 251-256
- Greenberg J.T. and Yao N.** (2004) The role and regulation of programmed cell death in plant-pathogen interactions. *Cell. Microbiol.* **6**: 201-211
- Greger I.H., Aranda A. and Proudfoot N.** (2000) Balancing transcriptional interference and initiation on the GAL7 promoter of *Saccharomyces cerevisiae*. *Proc. Natl. Acad. Sci. USA* **97**: 8415-8420
- Gu K., Sangha J.S., Li Y. and Yin Z.** (2008) High-resolution genetic mapping of bacterial blight resistance gene *Xa10*. *Theor. Appl. Genet.* **116**: 155-163
- Gu K., Tian D., Tian, Qui C. and Yin Z.** (2009) Transcription activator-like type III effector AvrXa27 depends on OsTFIIA $\gamma$  for the activation of *Xa27* transcription in rice that triggers disease resistance to *Xanthomonas oryzae* pv. *oryzae*. *Mol. Plant Pathol.* **10**: 829-835
- Gu K., Yang B., Tian D., Wu L., Wang D., Sreekala C., Yang F., Chu Z., Wang G.L., White F.F. and Yin Z.** (2005) *R* gene expression induced by a type-III effector triggers disease resistance in rice. *Nature* **435**: 1122-1125
- Gürlebeck D., Szurek B. and Bonas U.** (2005) Dimerization of the bacterial effector protein AvrBs3 in the plant cell cytoplasm prior to nuclear import. *Plant J.* **42**: 175-187
- Gürlebeck D., Thieme F. and Bonas U.** (2006) Type III effector proteins from the plant pathogen *Xanthomonas* and their role in the interaction with the host plant. *J. Plant Physiol.* **163**: 233-255

- Hahn S.** (2009) Analyse des molekularen Mechanismus der Aktivität des Typ-III-Effektors AvrBs3 aus *Xanthomonas campestris* pv. *vesicatoria*. Dissertation. Naturwissenschaftliche Fakultät I Biowissenschaften. Martin-Luther-Universität Halle-Wittenberg
- Hammond-Kosack K.E., Jones D.A. and Jones J.D.G.** (1994) Identification of two genes required in tomato for full *Cf-9*-dependent resistance to *Cladosporium fulvum*. *Plant Cell* **6**: 361-374
- Hansen B.G., Kliebenstein D.J. and Halkier B.A.** (2007) Identification of a flavin-monooxygenase as the S-oxygenating enzyme in aliphatic glucosinolate biosynthesis in *Arabidopsis*. *Plant J.* **50**: 902-910
- He P., Shan L. and Sheen J.** (2007) Elicitation and suppression of microbe-associated molecular pattern-triggered immunity in plant-microbe interactions. *Cell Microbiol.* **9**: 1385-1396
- Hein I., Pacak M.B., Hrubikova K., Williamson S., Dinesen M., Soenderby I.E., Sundar S., Jarmolowski A., Shirasu K. and Lacomme C.** (2005) Virus-induced gene silencing-based functional characterization of genes associated with powdery mildew resistance in barley. *Plant Physiol.* **138**: 2155-2164
- Herbers K., Conrads-Strauch J. and Bonas U.** (1992) Race-specificity of plant resistance to bacterial spot disease determined by repetitive motifs in a bacterial avirulence protein. *Nature* **356**: 172-174
- Hernandez N.** (1993) TBP, a universal eukaryotic transcription factor. *Genes Dev.* **7**: 1291-1308
- Heuer H., Yin Y.-N., Xue Q.-Y., Smalla K. and Guo J.-H.** (2007) Repeat domain diversity of *avrBs3/pthA*-like genes in *Ralstonia solanacearum* strains and association with host preferences in the field. *Appl. Environ. Microbiol.* **73**: 4379-4384
- Hibberd A.M., Bassett M.J. and Stall R.E.** (1987) Allelism tests of three dominant genes for hypersensitive resistance to bacterial spot of pepper. *Phytopathology* **77**: 1304-1307
- Høiby T., Zhou H., Mitsiou D.J. and Stunnenberg H.G.** (2007) A facelift for the general transcription factor TFIIA. *Biochim. Biophys. Acta* **1769**: 429-436
- Hopkins C.M., White F.F., Choi S.H., Guo A. and Leach J.E.** (1992) Identification of a family of avirulence genes from *Xanthomonas oryzae* pv. *oryzae*. *Mol. Plant-Microbe Interact.* **5**: 451-459
- Iyer A.S. and McCouch S.R.** (2004) The rice bacterial blight resistance gene *xa5* encodes a novel form of disease resistance. *Mol. Plant-Microbe Interact.* **17**: 1348-1354
- Iyer-Pascuzzi A.S., Jiang H., Huang L. and McCouch S.R.** (2008) Genetic and functional characterization of the rice bacterial blight disease resistance gene *xa5*. *Phytopathology* **98**: 289-295
- Jammes F., Lecomte P., Almeida-Engler J., Bitton F., Martin-Magniette M.L., Renou J.P., Abad P. and Favery B.** (2005) Genome-wide expression profiling of the host response to root-knot nematode infection in *Arabidopsis*. *Plant J.* **44**: 447-458
- Jenkins C.L. and Starr M.P.** (1982) The brominated aryl-polyene (xanthomonadin) pigments of *Xanthomonas juglandis* protect against photobiological damage. *Curr. Microbiol.* **7**: 323-326
- Jia Y., McAdams S.A., Bryan G.T., Hershey H.P. and Valent B.** (2000) Direct interaction of resistance gene and avirulence gene products confers rice blast resistance. *EMBO J.* **19**: 4004-4014
- Jiang G.H., Xia Z.H., Zhou Y.L., Wan J., Li D.Y., Chen R.S., Zhai W.X. and Zhu L.H.** (2006) Testifying the rice bacterial blight resistance gene *xa5* by genetic complementation and further analyzing *xa5* (*Xa5*) in comparison with its homolog *TFIIAγ1*. *Mol. Genet. Genomics* **275**: 354-366
- Jirage D., Tootle T.L., Reuber T.L., Frost L.N., Feys B.J., Parker J.E., Ausubel F.M. and Glazebrook J.** (1999) *Arabidopsis thaliana* PAD4 encodes a lipase-like gene that is important for salicylic acid signaling. *Proc. Natl. Acad. Sci. USA* **96**: 13583-13588.

- Johal G.S. and Briggs S.P.** (1992) Reductase activity encoded by the *HMI* disease resistance gene in maize. *Science* **258**: 985-987
- Jones D.A. and Jones J.D.G.** (1997) The role of leucine-rich repeat proteins in plant defences. *Adv. Bot. Res.* **24**: 89-167
- Jones J.B., Lacy G.H., Bouzar H., Stall R.E. and Schaad N.W.** (2004) Reclassification of the xanthomonads associated with bacterial spot disease of tomato and pepper. *Syst. Appl. Microbiol.* **27**: 755-762
- Jones J.B., Stall R.E. and Bouzar H.** (1998) Diversity among xanthomonads pathogenic on pepper and tomato. *Annu. Rev. Phytopathol.* **36**: 41-58
- Jones J.D. and Dangl J.L.** (2006) The plant immune system. *Nature* **444**: 323-329
- Jordan T., Römer P., Meyer A., Szczesny R., Pierre M., Piffanelli P., Bendahmane A., Bonas U. and Lahaye T.** (2006) Physical delimitation of the pepper *Bs3* resistance gene specifying recognition of the AvrBs3 protein from *Xanthomonas campestris* pv. *vesicatoria*. *Theor. Appl. Genet.* **113**: 895-905
- Kajava A.V.** (1998) Structural diversity of leucine-rich repeat proteins. *J. Mol. Biol.* **277**: 519-527
- Kay S.** (2008) Funktionelle Analyse des Typ-III-Effektors AvrBs3 und homologer Proteine aus *Xanthomonas campestris*. Dissertation. Naturwissenschaftliche Fakultät I Biowissenschaften. Martin-Luther-Universität Halle-Wittenberg
- Kay S., Boch J. and Bonas U.** (2005) Characterization of AvrBs3-like effectors from a *Brassicaceae* pathogen reveals virulence and avirulence activities and a protein with a novel repeat architecture. *Mol. Plant-Microbe Interact.* **18**: 838-848
- Kay S., Hahn S., Marois E., Hause G. and Bonas U.** (2007) A bacterial effector acts as a plant transcription factor and induces a cell size regulator. *Science* **318**: 648-651
- Kay S., Hahn S., Marois E., Wieduwild R. and Bonas U.** (2009) Detailed analysis of the DNA recognition motifs of the *Xanthomonas* type III effectors AvrBs3 and AvrBs3 $\Delta$ rep16. *Plant J.* **59**: 859 - 871
- Keen N.T.** (1990) Gene-for-gene complementarity in plant-pathogen interactions. *Annu. Rev. Genet.* **24**: 447-463
- Khalaf A., Moore G.A., Jones J.B. and Gmitter Jr F.G.** (2008) New insights into the resistance of Nagami kumquat to canker disease. *Physiol. Mol. Plant Pathol.* **71**: 240-250
- Kim B.S. and Hartmann R.W.** (1985) Inheritance of a gene (*Bs<sub>3</sub>*) conferring hypersensitive resistance to *Xanthomonas campestris* pv. *vesicatoria* in pepper (*Capsicum annuum*). *Plant Dis.* **69**: 233-235
- Kim J.L., Nikolov D.B. and Burley S.K.** (1993a) Co-crystal structure of TBP recognizing the minor-groove of a TATA element. *Nature* **365**: 520-527
- Kim Y.C., Geiger J.H., Hahn S. and Sigler P.B.** (1993b) Crystal-structure of a yeast TBP TATA-box complex. *Nature* **365**: 512-520
- Knoop V., Staskawicz B. and Bonas U.** (1991) Expression of the avirulence gene *avrBs3* from *Xanthomonas campestris* pv. *vesicatoria* is not under the control of *hrp* genes and is independent of plant factors. *J. Bacteriol.* **173**: 7142-7150
- Koch M., Vorwerk S., Masur C., Sharifi-Sirchi G., Olivieri N. and Schlaich N.L.** (2006) A role for a flavin-containing monooxygenase in resistance against microbial pathogens in *Arabidopsis*. *Plant J.* **47**: 629-639
- Kornberg R.D.** (2007) The molecular basis of eukaryotic transcription. *Proc. Natl. Acad. Sci. USA* **104**: 12955-12961
- Krishnamurthy S. and Hampsey M.** (2009) Eukaryotic transcription initiation. *Curr. Biol.* **19**: R153-R156
- Krueger S.K. and Williams D.E.** (2005) Mammalian flavin-containing monooxygenases: structure/function, genetic polymorphisms and role in drug metabolism. *Pharmacol Ther.* **106**: 357-387

- Lawton M.P., Cashman J.R., Cresteil T., Dolphin C.T., Elfarra A.A., Hines R.N., Hodgson E., Kimura T., Ozols J., Phillips I.R. and et al.** (1994) A nomenclature for the mammalian flavin-containing monooxygenase gene family based on amino acid sequence identities. *Arch. Biochem. Biophys.* **308**: 254-257
- Lee B.M., Park Y.J., Park D.S., Kang H.W., Kim J.G., Song E.S., Park I.C., Yoon U.H., Hahn J.H., Koo B.S., Lee G.B., Kim H., Park H.S., Yoon K.O., Kim J.H., Jung C.H., Koh N.H., Seo J.S. and Go S.J.** (2005) The genome sequence of *Xanthomonas oryzae* pathovar *oryzae* KACC10331, the bacterial blight pathogen of rice. *Nucl. Acids Res.* **33**: 577-586
- Lee S.W., Han S.W., Sriyanum M., Park C.J., Seo Y.S. and Ronald P.C.** (2009) A type I-secreted, sulfated peptide triggers XA21-mediated innate immunity. *Science* **326**: 850-853
- Leister R.T., Dahlbeck D., Day B., Li Y., Chesnokova O. and Staskawicz B.J.** (2005) Molecular genetic evidence for the Role of SGT1 in the intramolecular complementation of Bs2 protein activity in *Nicotiana benthamiana*. *Plant Cell* **17**: 1268-1278
- Leyns F., Declene M., Swings J.G. and Deley J.** (1984) The host range of the genus *Xanthomonas*. *Bot. Rev.* **50**: 308-356
- Li J., Hansen B.G., Ober J.A., Kliebenstein D.J. and Halkier B.A.** (2008) Subclade of flavin-monooxygenases involved in aliphatic glucosinolate biosynthesis. *Plant Physiol.* **148**: 1721-1733
- Li P., Long J.Y., Huang Y.C., Zhang Y. and Wang J.S.** (2004) AvrXa3: A novel member of *avrBs3* gene family from *Xanthomonas oryzae* pv. *oryzae* has a dual function. *Progr. Nat. Sci.* **14**: 774-780
- Lindgren P.B., Peet R.C. and Panopoulos N.J.** (1986) Gene-cluster of *Pseudomonas syringae* pv. *phaseolicola* controls pathogenicity of bean plants and hypersensitivity on nonhost plants. *J. Bacteriol.* **168**: 512-522
- Liu J., Liu X., Dai L. and Wang G.** (2007) Recent progress in elucidating the structure, function and evolution of disease resistance genes in plants. *J. Genet. Genomics* **34**: 765-776
- Liu Y., Schiff M., Serino G., Deng X.-W. and Dinesh-Kumar S.P.** (2002) Role of SCF ubiquitin-ligase and the COP9 signalosome in the *N* gene-mediated resistance response to tobacco mosaic virus. *Plant Cell* **14**: 1483-1496
- Lopes M.S. and Araus J.L.** (2008) Comparative genomic and physiological analysis of nutrient response to  $\text{NH}_4^+$ ,  $\text{NH}_4^+:\text{NO}_3^-$  and  $\text{NO}_3^-$  in barley seedlings. *Physiol. Plant.* **134**: 134-150
- Mackey D., Holt B.F., Wiig A. and Dangl J.L.** (2002) RIN4 interacts with *Pseudomonas syringae* type III effector molecules and is required for RPM1-mediated resistance in *Arabidopsis*. *Cell* **108**: 743-754
- Marois E., Van den Ackerveken G. and Bonas U.** (2002) The *Xanthomonas* type III effector protein AvrBs3 modulates plant gene expression and induces cell hypertrophy in the susceptible host. *Mol. Plant-Microbe Interact.* **15**: 637-646
- Martens J.A., Laprade L. and Winston F.** (2004) Intergenic transcription is required to repress the *Saccharomyces cerevisiae* *SER3* gene. *Nature* **429**: 571-574
- Martin G.B., Brommonschenkel S.H., Chunwongse J., Frary A., Ganai M.W., Spivey R., Wu T.Y., Earle E.D. and Tanksley S.D.** (1993) Map-based cloning of a protein-kinase gene conferring disease resistance in tomato. *Science* **262**: 1432-1436
- McHale L., Tan X., Koehl P. and Michelmore R.** (2006) Plant NBS-LRR proteins: adaptable guards. *Genome Biol.* **7**: 212
- Meeley R.B., Johal G.S., Briggs S.P. and Walton J.D.** (1992) A biochemical phenotype for a disease resistance gene of maize. *Plant Cell* **4**: 71-77

- Mew T.W., Alvarez A.M., Leach J.E. and Swings J.** (1993) Focus on bacterial blight of rice. *Plant Dis.* **77**: 5-12
- Michiels T., Vanooteghem J.C., Derouvroit C.L., China B., Gustin A., Boudry P. and Cornelis G.R.** (1991) Analysis of *virC*, an operon involved in the secretion of Yop Proteins by *Yersinia enterocolitica*. *J. Bacteriol.* **173**: 4994-5009
- Minsavage G., Jones J., Stall R., Miller S. and Ritchie D.** (1999) Hypersensitive resistance in *Capsicum pubescens* PI 235047 to *Xanthomonas campestris* pv. *vesicatoria* (*Xcv*) is elicited by *avrBs3-2*. *Phytopathology* **89**: S53
- Mishina T.E. and Zeier J.** (2006) The *Arabidopsis* flavin-dependent monooxygenase FMO1 is an essential component of biologically induced systemic acquired resistance. *Plant Physiol.* **141**: 1666-1675
- Moffett P., Farnham G., Peart J. and Baulcombe D.C.** (2002) Interaction between domains of a plant NBS-LRR protein in disease resistance-related cell death. *EMBO J.* **21**: 4511-4519
- Moscou M.J. and Bogdanove A.J.** (2009) A simple cipher governs DNA recognition by TAL effectors. *Science* **326**: 1501
- Mukaihara T., Tamura N., Murata Y. and Iwabuchi M.** (2004) Genetic screening of Hrp type III-related pathogenicity genes controlled by the HrpB transcriptional activator in *Ralstonia solanacearum*. *Mol. Microbiol.* **54**: 863-875
- Nigumann P., Redik K., Matlik K. and Speck M.** (2002) Many human genes are transcribed from the antisense promoter of L1 retrotransposon. *Genomics* **79**: 628-634
- Nikolov D.B. and Burley S.K.** (1994) 2.1-Angstrom resolution refined structure of a TATA box-binding protein (TBP). *Nat. Struct. Biol.* **1**: 621-637
- Nikolov D.B., Chen H., Halay E.D., Hoffmann A., Roeder R.G. and Burley S.K.** (1996) Crystal structure of a human TATA box-binding protein/TATA element complex. *Proc. Natl. Acad. Sci. USA* **93**: 4862-4867
- Nikolov D.B., Hu S.H., Lin J., Gasch A., Hoffmann A., Horikoshi M., Chua N.H., Roeder R.G. and Burley S.K.** (1992) Crystal structure of TFIID TATA-box binding protein. *Nature* **360**: 40-46
- Niño-Liu D., Ronald P.C. and Bogdanove A.J.** (2006) *Xanthomonas oryzae* pathovars: model pathogens of a model crop. *Mol. Plant Pathol.* **7**: 303-324
- Noda T. and Hisatoshi K.** (1999) Growth of *Xanthomonas oryzae* pv. *oryzae* in planta and in guttation fluid of rice. *Ann. Phytopathol. Soc. Japan* **65**: 9-14
- Nürnberger T. and Kemmerling B.** (2006) Receptor protein kinases - pattern recognition receptors in plant immunity. *Trends Plant Sci.* **11**: 519-522
- Nürnberger T. and Kemmerling B.** (2009) PAMP-triggered basal immunity in plants. *Plant Innate Immunity* **51**: 1-38
- Ogawa T., Yamamoto T., Khush G.S. and Mew T.W.** (1986) The *Xa-3* gene for resistance to Philippine races of bacterial blight of rice. *Rice Genet. Newslett.* **3**: 77-78
- Ou S.H.** (1985) *Rice diseases*, 2nd edn. Commonwealth Mycological Institute, Kew, England. 380p
- Padidam M. and Cao Y.** (2001) Elimination of transcriptional interference between tandem genes in plant cells. *Biotechniques* **31**: 328-330, 332-324
- Padmanabhan M., Cournoyer P. and Dinesh-Kumar S.P.** (2009) The leucine-rich repeat domain in plant innate immunity: a wealth of possibilities. *Cell Microbiol.* **11**: 191-198
- Palfey B.A. and McDonald C.A.** (2010) Control of catalysis in flavin-dependent monooxygenases. *Arch. Biochem. Biophys.* **493**: 26-36
- Parker J.E.** (2000) Signalling in plant disease resistance. In M. Dickinson, J. Beynon, eds, *Mol. Plant Pathol.*, Vol 4. Academic Press Ltd, Sheffield, pp 144-174
- Parniske M., Hammond-Kosack K.E., Golstein C., Thomas C.M., Jones D.A., Harrison K., Wulff B.B.H. and Jones J.D.G.** (1997) Novel disease resistance specificities

- result from sequence exchange between tandemly repeated genes at the *Cf-4/9* locus of tomato. *Cell* **91**: 821-832
- Peart J.R., Cook G., Feys B.J., Parker J.E. and Baulcombe D.C.** (2002a) An *EDS1* orthologue is required for *N*-mediated resistance against tobacco mosaic virus. *Plant J.* **29**: 569-579
- Peart J.R., Lu R., Sadanandom A., Malcuit I., Moffett P., Brice D.C., Schausser L., Jaggard D.A.W., Xiao S., Coleman M.J., Dow M., Jones J.D.G., Shirasu K. and Baulcombe D.C.** (2002b) Ubiquitin ligase-associated protein SGT1 is required for host and nonhost disease resistance in plants. *Proc. Natl. Acad. Sci. USA* **99**: 10865-10869
- Peart J.R., Mestre P., Lu R., Malcuit I. and Baulcombe D.C.** (2005) NRG1, a CC-NB-LRR protein, together with N, a TIR-NB-LRR protein, mediates resistance against tobacco mosaic virus. *Curr. Biol.* **15**: 968-973
- Pedley K.F. and Martin G.B.** (2003) Molecular basis of Pto-mediated resistance to bacterial speck disease in tomato. *Annu. Rev. Phytopathol.* **41**: 215-243
- Phillips I.R. and Shephard E.A.** (2008) Flavin-containing monooxygenases: mutations, disease and drug response. *Trends Pharmacol. Sci.* **29**: 294-301
- Pierre M., Noël L., Lahaye T., Ballvora A., Veuskens J., Ganal M. and Bonas U.** (2000) High-resolution genetic mapping of the pepper resistance locus *Bs3* governing recognition of the *Xanthomonas campestris* pv. *vesicatoria* AvrBs3 protein. *Theor. Appl. Genet.* **101**: 255-263
- Porter B.W., Chittoor J.M., Yano M., Sasaki T. and White F.F.** (2003) Development and mapping of markers linked to the rice bacterial blight resistance gene *Xa7*. *Crop Sci.* **43**: 1484-1492
- Qu S., Liu G., Zhou B., Bellizzi M., Zeng L., Dai L., Han B. and Wang G.L.** (2006) The broad-spectrum blast resistance gene *Pi9* encodes a nucleotide-binding site-leucine-rich repeat protein and is a member of a multigene family in rice. *Genetics* **172**: 1901-1914
- Rafiqi M., Bernoux M., Ellis J.G. and Dodds P.N.** (2009) In the trenches of plant pathogen recognition: Role of NB-LRR proteins. *Semin. Cell Dev. Biol.* **20**: 1017-1024
- Rairdan G.J., Collier S.M., Sacco M.A., Baldwin T.T., Boettrich T. and Moffett P.** (2008) The coiled-coil and nucleotide binding domains of the potato Rx disease resistance protein function in pathogen recognition and signaling. *Plant Cell* **20**: 739-751
- Rairdan G.J. and Moffett P.** (2006) Distinct domains in the ARC region of the potato resistance protein Rx mediate LRR binding and inhibition of activation. *Plant Cell*
- Rajagopal L., Sundari C.S., Balasubramanian D. and Sonti R.V.** (1997) The bacterial pigment xanthomonadin offers protection against photodamage. *FEBS Lett.* **415**: 125-128
- Roden J.A., Belt B., Ross J.B., Tachibana T., Vargas J. and Mudgett M.B.** (2004) A genetic screen to isolate type III effectors translocated into pepper cells during *Xanthomonas* infection. *Proc. Natl. Acad. Sci. USA* **101**: 16624-16629
- Römer P., Hahn S., Jordan T., Strauß T., Bonas U. and Lahaye T.** (2007) Plant-pathogen recognition mediated by promoter activation of the pepper *Bs3* resistance gene. *Science* **318**: 645-648
- Römer P., Recht S. and Lahaye T.** (2009a) A single plant resistance gene promoter engineered to recognize multiple TAL effectors from disparate pathogens. *Proc. Natl. Acad. Sci. USA* **106**: 20526-20531
- Römer P., Recht S., Strauß T., Elsaesser J., Schornack S., Boch J., Wang S. and Lahaye T.** (2010) Promoter elements of rice susceptibility genes are bound and activated by specific TAL effectors from the bacterial blight pathogen, *Xanthomonas oryzae* pv. *oryzae*. *New Phytol.* DOI: 10.1111/j.1469-8137.2010.03217.x *in press*

- Römer P., Strauß T., Hahn S., Scholze H., Morbitzer R., Grau J., Bonas U. and Lahaye T.** (2009b) Recognition of AvrBs3-like proteins is mediated by specific binding to promoters of matching pepper *Bs3* alleles. *Plant Physiol.* **150**: 1697-1712
- Ronald P.C., Salmeron J.M., Carland F.M. and Staskawicz B.J.** (1992) The cloned avirulence gene *avrPto* induces disease resistance in tomato cultivars containing the *Pto* resistance gene. *J. Bacteriol.* **174**: 1604-1611
- Roumagnac P., Pruvost O., Chiroleu F. and Hughes G.** (2004) Spatial and temporal analyses of bacterial blight of onion caused by *Xanthomonas axonopodis* pv. *allii*. *Phytopathology* **94**: 138-146
- Ryan R.P., Koebnik R., Szurek B., Boureau T., Bernal A., Bogdanove A. and Dow J.M.** (2009) Passing GO (gene ontology) in plant pathogen biology: a report from the *Xanthomonas* genomics conference. *Cell. Microbiol.* **11**: 1689-1696
- Rybak M., Minsavage G.V., Stall R.E. and Jones J.B.** (2009) Identification of *Xanthomonas citri* ssp. *citri* host specificity genes in a heterologous expression host. *Mol. Plant Pathol.* **10**: 249-262
- Sacco M.A. and Moffett P.** (2009) Disease resistance genes: Form and function. In K. Bouarab, N. Brisson, F. Daayf, eds, *Plant-Microbe Interactions*. CABI, Wallingford, UK:, pp 94-141
- Salanoubat M., Genin S., Artiguenave F., Gouzy J., Mangenot S., Arlat M., Billault A., Brottier P., Camus J.C., Cattolico L., Chandler M., Choisine N., Claudel-Renard C., Cunnac S., Demange N., Gaspin C., Lavie M., Moisan A., Robert C., Saurin W., Schiex T., Siguier P., Thebault P., Whalen M., Wincker P., Levy M., Weissenbach J. and Boucher C.A.** (2002) Genome sequence of the plant pathogen *Ralstonia solanacearum*. *Nature* **415**: 497-502
- Schlaich N.L.** (2007) Flavin-containing monooxygenases in plants: looking beyond detox. *Trends Plant Sci.* **12**: 412-418
- Schornack S.** (2006) Struktur, Erkennungsspezifität und Regulationsmechanismus des Resistenzproteins *Bs4* aus Tomate. Dissertation. Naturwissenschaftliche Fakultät I Biowissenschaften. Martin-Luther-Universität Halle-Wittenberg
- Schornack S., Ballvora A., Gürlebeck D., Peart J., Baulcombe D., Baker B., Ganai M., Bonas U. and Lahaye T.** (2004) The tomato resistance protein *Bs4* is a predicted non-nuclear TIR-NB-LRR protein that mediates defense responses to severely truncated derivatives of *AvrBs4* and overexpressed *AvrBs3*. *Plant J.* **37**: 46-60
- Schornack S., Fuchs R., Huitema E., Rothbauer U., Lipka V. and Kamoun S.** (2009) Protein mislocalization in plant cells using a GFP-binding chromobody. *Plant J.* **60**: 744-754
- Schornack S., Meyer A., Römer P., Jordan T. and Lahaye T.** (2006) Gene-for-gene mediated recognition of nuclear-targeted *AvrBs3*-like bacterial effector proteins. *J. Plant Physiol.* **163**: 256-272
- Schornack S., Minsavage G.V., Stall R.E., Jones J.B. and Lahaye T.** (2008) Characterization of *AvrHah1* a novel *AvrBs3*-like effector from *Xanthomonas gardneri* with virulence and avirulence activity. *New Phytol.* **179**: 546-556
- Schornack S., Peter K., Bonas U. and Lahaye T.** (2005) Expression levels of *avrBs3*-like genes affect recognition specificity in tomato *Bs4* but not in pepper *Bs3* mediated perception. *Mol. Plant-Microbe Interact.* **18**: 1215-1225
- Schwessinger B. and Zipfel C.** (2008) News from the frontline: recent insights into PAMP-triggered immunity in plants. *Curr. Opin. Plant Biol.* **11**: 389-395
- Shearwin K.E., Callen B.P. and Egan J.B.** (2005) Transcriptional interference - a crash course. *Trends Genet.* **21**: 339-345
- Shen Q.-H., Zhou F., Bieri S., Haizel T., Shirasu K. and Schulze-Lefert P.** (2003) Recognition specificity and RAR1/SGT1 dependency in barley *Mla* disease resistance alleles to the powdery mildew fungus. *Plant Cell* **15**: 732-744

- Shen Q.H., Saijo Y., Mauch S., Biskup C., Bieri S., Keller B., Seki H., Ulker B., Somssich I.E. and Schulze-Lefert P.** (2007) Nuclear activity of MLA immune receptors links isolate-specific and basal disease-resistance responses. *Science* **315**: 1098-1103
- Sidhu G.S., Khush G.S. and Mew T.W.** (1978) Genetic-analysis of bacterial-blight resistance in 74 cultivars of rice, *Oryza-sativa*-L. *Theor. Appl. Genet.* **53**: 105-111
- Sikorski T.W. and Buratowski S.** (2009) The basal initiation machinery: beyond the general transcription factors. *Curr Opin Cell Biol* **21**: 344-351
- Staal J., Kaliff M., Dewaele E., Persson M. and Dixelius C.** (2008) *RLM3*, a TIR domain encoding gene involved in broad-range immunity of *Arabidopsis* to necrotrophic fungal pathogens. *Plant J.* **55**: 188-200
- Stall R.E., Jones J.B. and Minsavage G.V.** (2009) Durability of resistance in tomato and pepper to xanthomonads causing bacterial spot. *Annu. Rev. Phytopathol.* **47**: 265–284
- Starr M.P. and Stephens W.L.** (1964) Pigmentation and taxonomy of the genus *Xanthomonas*. *J. Bacteriol.* **87**: 293-302
- Stehr M., Diekmann H., Smau L., Seth O., Ghisla S., Singh M. and Macheroux P.** (1998) A hydrophobic sequence motif common to N-hydroxylating enzymes. *Trends Biochem. Sci.* **23**: 56-57
- Sugio A., Yang B., Zhu T. and White F.F.** (2007) Two type III effector genes of *Xanthomonas oryzae* pv. *oryzae* control the induction of the host genes *OsTFIIA $\gamma$ 1* and *OsTFXI* during bacterial blight of rice. *Proc. Natl. Acad. Sci. USA* **104**: 10720-10725
- Sun X., Cao Y., Yang Z., Xu C., Li X., Wang S. and Zhang Q.** (2004) *Xa26*, a gene conferring resistance to *Xanthomonas oryzae* pv. *oryzae* in rice, encodes an LRR receptor kinase-like protein. *Plant J.* **37**: 517-527
- Swarup S., De Feyter R., Brlansky R.H. and Gabriel D.W.** (1991) A pathogenicity locus from *Xanthomonas citri* enables strains from several pathovars of *Xanthomonas campestris* to elicit cankerlike lesions on citrus. *Phytopathology* **81**: 802-809
- Swiderski M.R., Birker D. and Jones J.D.G.** (2009) The TIR domain of TIR-NB-LRR resistance proteins is a signaling domain involved in cell death induction. *Mol. Plant-Microbe Interact.* **22**: 157-165
- Szurek B., Marois E., Bonas U. and Van den Ackerveken G.** (2001) Eukaryotic features of the *Xanthomonas* type III effector AvrBs3: protein domains involved in transcriptional activation and the interaction with nuclear import receptors from pepper. *Plant J.* **26**: 523-534
- Tai T.H., Dahlbeck D., Clark E.T., Gajiwala P., Pasion R., Whalen M.C., Stall R.E. and Staskawicz B.J.** (1999) Expression of the *Bs2* pepper gene confers resistance to bacterial spot disease in tomato. *Proc. Natl. Acad. Sci. USA* **96**: 14153-14158
- Tameling W.I.L. and Joosten M.H.A.J.** (2008) The diverse roles of NB-LRR proteins in plants. *Physiol. Mol. Plant Pathol.* **71**: 126-134
- Thieme F., Koebnik R., Bekel T., Berger C., Boch J., Büttner D., Caldana C., Gaigalat L., Goesmann A., Kay S., Kirchner O., Lanz C., Linke B., McHardy A.C., Meyer F., Mittenhuber G., Nies D.H., Niesbach-Klosgen U., Patschkowski T., Ruckert C., Rupp O., Schneiker S., Schuster S.C., Vorholter F.J., Weber E., Puhler A., Bonas U., Bartels D. and Kaiser O.** (2005) Insights into genome plasticity and pathogenicity of the plant pathogenic bacterium *Xanthomonas campestris* pv. *vesicatoria* revealed by the complete genome sequence. *J. Bacteriol.* **187**: 7254-7266
- Thieme F., Szczesny R., Urban A., Kirchner O., Hause G. and Bonas U.** (2007) New type III effectors from *Xanthomonas campestris* pv. *vesicatoria* trigger plant reactions dependent on a conserved N-myristoylation motif. *Mol. Plant-Microbe Interact.* **20**: 1250–1261
- Tian D. and Yin Z.** (2009) Constitutive heterologous expression of *avrXa27* in rice containing the *R* gene *Xa27* confers enhanced resistance to compatible *Xanthomonas oryzae* strains. *Mol. Plant Pathol.* **10**: 29-39



- Ueda H., Yamaguchi Y. and Sano H.** (2006) Direct interaction between the tobacco mosaic virus helicase domain and the ATP-bound resistance protein, N factor during the hypersensitive response in tobacco plants. *Plant Mol. Biol.* **61**: 31-45
- Van den Ackerveken G., Marois E. and Bonas U.** (1996) Recognition of the bacterial avirulence protein AvrBs3 occurs inside the host plant cell. *Cell* **87**: 1307-1316
- Van der Biezen E.A. and Jones J.D.G.** (1998a) Plant disease-resistance proteins and the gene-for-gene concept. *Trends Biochem. Sci.* **23**: 454-456
- Van der Biezen E.A. and Jones J.D.G.** (1998b) The NB-ARC domain: a novel signalling motif shared by plant resistance gene products and regulators of cell death in animals. *Curr. Biol.* **8**: R226-R227
- Van der Hoorn R.A.L. and Kamoun S.** (2008) From guard to decoy: A new model for perception of plant pathogen effectors. *Plant Cell* **20**: 2009-2017
- van Ooijen G., van den Burg H.A., Cornelissen B.J.C. and Takken F.L.W.** (2007) Structure and function of resistance proteins in solanaceous plants. *Annu. Rev. Phytopathol.* **45**
- Vauterin L., Hoste B., Kersters K. and Swings J.** (1995) Reclassification of *Xanthomonas*. *Int. J. Syst. Bacteriol.* **45**: 472-489
- Vera Cruz C.M., Bai J., Ona I., Leung H., Nelson R.J., Mew T.W. and Leach J.E.** (2000) Predicting durability of a disease resistance gene based on an assessment of the fitness loss and epidemiological consequences of avirulence gene mutation. *Proc. Natl. Acad. Sci. USA* **97**: 13500-13505
- White F.F., Potnis N., Jones J.B. and Koebnik R.** (2009) The Type III effectors of *Xanthomonas*. *Mol. Plant Pathol.* **10**: 749-766
- Wirthmueller L., Zhang Y., Jones J.D. and Parker J.E.** (2007) Nuclear accumulation of the *Arabidopsis* immune receptor RPS4 is necessary for triggering EDS1-dependent defense. *Curr. Biol.* **17**: 2023-2029
- Wu L., Goh M.L., Sreekala C. and Yin Z.** (2008) XA27 depends on an N-terminal signal-anchor-like sequence to localize to the apoplast for resistance to *Xanthomonas oryzae* pv. *oryzae*. *Plant Physiol.* **Vol. 148**: 1497-1509
- Wu X.M., Li Y.R., Zou L.F. and Chen G.Y.** (2007) Gene-for-gene relationships between rice and diverse *avrBs3/pthA* avirulence genes in *Xanthomonas oryzae* pv. *oryzae*. *Plant Pathol.* **56**: 26-34
- Wulff B.B.H., Thomas C.M., Smoker M., Grant M. and Jones J.D.G.** (2001) Domain swapping and gene shuffling identify sequences required for induction of an Avr-dependent hypersensitive response by the tomato Cf-4 and Cf-9 proteins. *Plant Cell* **13**: 255-272
- Xiang Y., Cao Y., Xu C., Li X. and Wang S.** (2006) *Xa3*, conferring resistance for rice bacterial blight and encoding a receptor kinase-like protein, is the same as *Xa26*. *Theor. Appl. Genet.* **113**: 1347-1355
- Xiao S., Ellwood S., Calis O., Patrick E., Li T., Coleman M. and Turner J.G.** (2001) Broad-spectrum mildew resistance in *Arabidopsis thaliana* mediated by *RPW8*. *Science* **291**: 118-120
- Xinghua L., Duanpin Z., Yuefeng X., Qifa Z. and Heping G.** (1996) Mapping a new gene for resistance to bacterial blight using RFLP markers. *Int. Rice Res. Notes* **21**: 30
- Yamamoto Y., Kamiya N., Morinaka Y., Matsuoka M. and Sazuka T.** (2007) Auxin biosynthesis by the YUCCA genes in rice. *Plant Physiol.* **143**: 1362-1371
- Yang B., Sugio A. and White F.F.** (2005) Avoidance of host recognition by alterations in the repetitive and C-terminal regions of AvrXa7, a type III effector of *Xanthomonas oryzae* pv. *oryzae*. *Mol. Plant-Microbe Interact.* **18**: 142-149
- Yang B., Sugio A. and White F.F.** (2006) *Os8N3* is a host disease-susceptibility gene for bacterial blight of rice. *Proc. Natl. Acad. Sci. USA* **103**: 10503-10508

- Yang B. and White F.F.** (2004) Diverse members of the AvrBs3/PthA family of type III effectors are major virulence determinants in bacterial blight disease of rice. *Mol. Plant-Microbe Interact.* **17**: 1192–1200
- Yang B., Zhu W., Johnson L.B. and White F.F.** (2000) The virulence factor AvrXa7 of *Xanthomonas oryzae* pv. *oryzae* is a type III secretion pathway-dependent nuclear-localized double-stranded DNA-binding protein. *Proc. Natl. Acad. Sci. USA* **97**: 9807-9812
- Yang Y.N., Yuan Q.P. and Gabriel D.W.** (1996) Watersoaking function(s) of XcmH1005 are redundantly encoded by members of the *Xanthomonas avr/pth* gene family. *Mol. Plant-Microbe Interact.* **9**: 105-113
- Yoshimura A., Mew T.W., Khush G.S. and Omura T.** (1983) Inheritance of resistance to bacterial blight in rice cultivar Cas209. *Phytopathology* **73**: 1409-1412
- Young S.A., White F.F., Hopkins C.M. and Leach J.E.** (1994) AvrXa10 protein is in the cytoplasm of *Xanthomonas-oryzae* pv. *oryzae*. *Mol. Plant-Microbe Interact.* **7**: 799-804
- Yuan M., Chu Z., Li X., Xu C. and Wang S.** (2009) Pathogen-induced expressional loss of function is the key factor in race-specific bacterial resistance conferred by a recessive *R* gene *xa13* in rice. *Plant Cell Physiol.* **50**: 947-955
- Zhang Y., Dorey S., Swiderski M. and Jones J.D.G.** (2004) Expression of *RPS4* in tobacco induces an AvrRps4-independent HR that requires EDS1, SGT1 and HSP90. *Plant J.* **40**: 213-224
- Zhao D.Z.** (2009) Control of anther cell differentiation: a teamwork of receptor-like kinases. *Sex. Plant Reprod.* **22**: 221-228
- Zhao Y., Christensen S.K., Fankhauser C., Cashman J.R., Cohen J.D., Weigel D. and Chory J.** (2001) A role for flavin monooxygenase-like enzymes in auxin biosynthesis. *Science* **291**: 306-309
- Zhong Y.M., Jiang G.H., Chen X.W., Xia Z.H., Li X.B., Zhu L.H. and Zhai W.X.** (2003) Identification and gene prediction of a 24 kb region containing *xa5*, a recessive bacterial blight resistance gene in rice (*Oryza sativa* L.). *Chin. Sci. Bull.* **48**: 2725-2729
- Zhou J.-M. and Chai J.** (2008) Plant pathogenic bacterial type III effectors subdue host responses. *Curr. Opin. Microbiol.* **11**: 179-185
- Zhu W.G., Yang B., Chittoor J.M., Johnson L.B. and White F.F.** (1998) AvrXa10 contains an acidic transcriptional activation domain in the functionally conserved C terminus. *Mol. Plant-Microbe Interact.* **11**: 824-832
- Ziegler D.M.** (2002) An overview of the mechanism, substrate specificities, and structure of FMOs. *Drug Metab. Rev.* **34**: 503-511
- Zipfel C.** (2009) Early molecular events in PAMP-triggered immunity. *Curr. Opin. Plant Biol.* **12**: 414-420
- Zipfel C. and Felix G.** (2005) Plants and animals: a different taste for microbes? *Curr. Opin. Plant Biol.* **8**: 353-360
- Zipfel C., Kunze G., Chinchilla D., Caniard A., Jones J.D.G., Boller T. and Felix G.** (2006) Perception of the bacterial PAMP EF-Tu by the receptor EFR restricts *Agrobacterium*-mediated transformation. *Cell* **125**: 749-760



Bs3-E 946 -----CAAGTTATCATCCCCTTCTCT  
 PI 235047 959 TAAGTTATCCTCAAACCTT-----CAAGTTATCTTCCCCTTCTCT  
 PI 585270 959 TAAGTTATCCTCAAACCTTTAAGTTATCCTCAAACCTTCAAGTTATCTTCCCCTTCTCT

Bs3-E 968 TTTCTCCTCTTGTTCTTGTCAACCGCTAAATCTATCAAAACACAAGTAGTCCTAGTTGCA  
 PI 235047 1000 TTTCTCCTCTTGTTCTTGTCAACCACTAAATCTATCAAAACACAAGTAGTCCTAGTTGCA  
 PI 585270 1019 TTTCTCCTCTTGTTCTTGTCAACCACTAAATCTATCAAAACACAAGTAGTCCTAGTTGCA

Bs3-E 1028 CATATATTTTCATGATGAATCAGAATTGCTTTAATTCTTGTTACCTCTAACTGTTGATGC  
 PI 235047 1060 CATATATTTTCATGACGAATCAGAATTGCTTTAATTCTTGTTACCTCTAACTGTTGATGC  
 PI 585270 1079 CATATATTTTCATGACGAATCAGAATTGCTTTAATTCTTGTTACCTCTAACTGTTGATGC

Bs3-E 1088 ACTTGAACCAAAAAAATCCTCTTGTGCTGCTAAATGCATACAAGTAAATGGTCCTCTTAT  
 PI 235047 1120 ACTTGAACCAAAAAAATCCTCTTGTGCTGCTAAATGCATACTTAGTAAATGGTCCTCTTAT  
 PI 585270 1139 ACTTGAACCAAAAAAATCCTCTTGTGCTGCTAAATGCATACTTAGTAAATGGTCCTCTTAT

Bs3-E 1148 TGTTGGAGCTGGCCCTTCAGGCTTGGCTACTGCTGCCGTCTTAAGCAATACAGTGTTC  
 PI 235047 1180 TGTTGGAGCTGGCCCTTCAGGCTTGGCTACTGCTGCTGTCTTAAGCAATACAGTGTTC  
 PI 585270 1199 TGTTGGAGCTGGCCCTTCAGGCTTGGCTACTGCTGCTGTCTTAAGCAATACAGTGTTC

Bs3-E 1208 GTATGTAATCATTGAACGCGCGGACTGCATTGCTTCTCTGTGGCAACACAAGACCTACGA  
 PI 235047 1240 GTATGTAATCATTGAACGCGCGGACTGCATTGCTTCTCTGTGGCACACAAAACCTACGA  
 PI 585270 1259 GTATGTAATCATTGAACGCGCGGACTGCATTGCTTCTCTGTGGCACACAAAACCTACGA

Bs3-E 1268 TCGGCTTAGGCTTAACGTGCCACGACAATACTGCGAATTGCCTGGCTTGCCATTTCCACC  
 PI 235047 1300 TCGACTTAGGCTTAACGTGCCACGACGATACTGTGAATTGCCTGGCTTGCCATTTCCACC  
 PI 585270 1319 TCGACTTAGGCTTAACGTGCCACGACGATACTGTGAATTGCCTGGCTTGCCATTTCCACC

Bs3-E 1328 AGACTTTCCAGAGTATCCAACCAAAAACCAATTCATCAGCTACCTCGTATCTTATGCAA  
 PI 235047 1360 AGACTTTCCAGAGTATCCAACGAAAAACCAATTCATCAGCTACCTCGAATCTTATGCAA  
 PI 585270 1379 AGACTTTCCAGAGTATCCAACGAAAAACCAATTCATCAGCTACCTCGAATCTTATGCAA

Bs3-E 1388 GCATTTTCGAGATCAAACCACAACCTCAACGAGTCAGTAAACTTAGCTGGATATGATGAGAC  
 PI 235047 1420 GCATTTTCGAGATCAAACCACGACTCAACGAGTCAGTAAACTTAGCTGGATATGATGAGAC  
 PI 585270 1439 GCATTTTCGAGATCAAACCACGACTCAACGAGTCAGTAAACTTAGCTGGATATGATGAGAC

Bs3-E 1448 ATGTGGTTTATGGAAGGTGAAAACAGTTTCTGAAATCAATGGTTCAACCTCTGAATACAT  
 PI 235047 1480 ATATGGTTTATGGAAGGTGAAAACAGTTTCTGAAATCAATGGTTCAACCTCTGAATACAT  
 PI 585270 1499 ATATGGTTTATGGAAGGTGAAAACAGTTTCTGAAATCAATGGTTCAACCTCTGAATACAT

Bs3-E 1508 GTGTAAGTGGCTTATTGTGGCCACAGGAGAGAATGCTGAGATGATAGTGCCCGAATTCGA  
 PI 235047 1540 GTGTAAGTGGCTTGTGTGGCCACAGGAGAGAATGCTGAGATGATAGTGCCCGAATTCGA  
 PI 585270 1559 GTGTAAGTGGCTTGTGTGGCCACAGGAGAGAATGCTGAGATGATAGTGCCCGAATTCGA

Bs3-E 1568 AGGATTGCAAGATTTTGGTGGCCAGGTTATTCATGCTTGTGAGTACAAGACTGGGGAATA  
 PI 235047 1600 AGGATTGCAAGATTTTGGTGGCCAGGTTATTCATGCTTGTGAGTACAAGACTGGGGAATA  
 PI 585270 1619 AGGATTGCAAGATTTTGGTGGCCAGGTTATTCATGCTTGTGAGTACAAGACTGGGGAATA

Bs3-E 1628 CTATACTGGAGAAAATGTGCTGGCGGTTGGCTGTGGCAATTCCGGGATCGATATCTCACT  
 PI 235047 1660 CTATACTGGAGAAAATGTGCTGGTGGTTGGCTGTGGCAATTCCGGGATCGATATCTCACT  
 PI 585270 1679 CTATACTGGAGAAAATGTGCTGGTGGTTGGCTGTGGCAATTCCGGGATCGATATCTCACT

Bs3-E 1688 TGATCTTTCCCAACATAATGCAAATCCATTCATGGTAGTTTCAAGCTCGGTAAGTTTTAT  
 PI 235047 1720 TGATCTTTCCCAACATAATGCAAATCCATTCATGGTAGTTTCAAGCTCGGTAAGTTTTAT  
 PI 585270 1739 TGATCTTTCCCAACATAATGCAAATCCATTCATGGTAGTTTCAAGCTCGGTAAGTTTTAT

Bs3-E 1748 ATTCATAAGTATTATTTTTCAAGTAACACTAGAAAGTGATCTTGTATCTTTCATTTGCT  
 PI 235047 1780 ATTCATAAGTATTATTTTTCAAGTAACACTAGAAAGTGATCTTGTATCTTTCATTTGCT  
 PI 585270 1799 ATTCATAAGTATTATTTTTCAAGTAACACTAGAAAGTGATCTTGTATCTTTCATTTGCT

Bs3-E 1808 CGCATGAATATATTATATTCACACATGAATGATATCATCTAGTTTTGTTAATCTTTCAGG  
 PI 235047 1840 CGCATGAATATATTATATTCACACATGAATGATATCATCTAGTTTTGTTAATCTTTCAGG  
 PI 585270 1859 CGCATGAATATATTATATTCACACATGAATGATATCATCTAGTTTTGTTAATCTTTCAGG

Bs3-E	1868	TACAGGGTCGTAATTTCCCTGAGGAAATAAACATAGTTCCAGCAATCAAGAAATTTACTC
PI 235047	1900	TACAGGGTCGTAATTTCCCTGAGGAAATAAAGGATAGCTCCAGCAATCAAGAAATTTACTC
PI 585270	1919	TACAGGGTCGTAATTTCCCTGAGGAAATAAAGGATAGCTCCAGCAATCAAGAAATTTACTC
Bs3-E	1928	AAGGAAAAGTAGAATTTGTTAATGGACAAATTCTAGAGATCGACTCTGTTATCTTGGCAA
PI 235047	1960	AAAGAAAAGTAGAATTTGTTAATGGACAAATTCTTGGAGATTGACTCTGTAATCTTGGCAA
PI 585270	1979	AAAGAAAAGTAGAATTTGTTAATGGACAAATTCTTGGAGATTGACTCTGTAATCTTGGCAA
Bs3-E	1988	CTGGTTATACCAGCAATGTAACCTTCTTGGTTAATGGTAAGGAAATACACAAGTTTTATTT
PI 235047	2020	CTGGGTATACCAGCAATGTAACCTTCTTGGTTAATGGTAAGGAAATACACAAGTTTTATTT
PI 585270	2039	CTGGGTATACCAGCAATGTAACCTTCTTGGTTAATGGTAAGGAAATACACAAGTTTTATTT
Bs3-E	2048	CTATGCCTAATTAATTTGGTGTTTAATCATAAATTATATATAGTACTAAGTATGATAAAA
PI 235047	2080	CTATGCCTAATTAATTTGGAGTTTAAATCATAAATTATATATAGTACTAATGTATGATAAAA
PI 585270	2099	CTATGCCTAATTAATTTGGAGTTTAAATCATAAATTATATATAGTACTAATGTATGATAAAA
Bs3-E	2108	GCTCCTTCAACTATAAAGGATGATTTAGTCAAATGAACTCTTAATGAATGTAGTAATTAT
PI 235047	2140	GCTCCTTCAACTATAAAGGATGATTTAATTCAAATGAACTCTTAATGAATGTAGTAATTAT
PI 585270	2159	GCTCCTTCAACTATAAAGGATGATTTAATTCAAATGAACTCTTAATGAATGTAGTAATTAT
Bs3-E	2168	TTATGGATTCTTGTTACATTCATGTAAGTTGGTATCTCATTATCCTGTGGATTCTTTCTC
PI 235047	2200	TTATGGATTCTTGTTACATTCATGTAAGTTGGTATCTCATTATCCTGTGGATTCTTTCTC
PI 585270	2219	TTATGGATTCTTGTTACATTCATGTAAGTTGGTATCTCATTATCCTGTGGATTCTTTCTC
Bs3-E	2228	TTGAGTTATTAATTAGTTAGAATTCACTATAACCGTCTTTTTTCTTTTACCCTTTCCCTC
PI 235047	2260	TTTGAGTTATTAATTTGGTTAGAATTCACTATAACCGTCTTTTTTCTTTTACCCTTTCCCTC
PI 585270	2279	TTTGAGTTATTAATTTGGTTAGAATTCACTATAACCGTCTTTTTTCTTTTACCCTTTCCCTC
Bs3-E	2287	ATACCTTTTTGTTCTTTTGATAACTCGAACTCACAATCTTAAGATTGGGAATAAGGGGCT
PI 235047	2320	ATACCTTTTTGTTCTTTCTGATAACTCAAACTCACAATCTTAAGATTGGGAATAAGGGGCT
PI 585270	2339	ATACCTTTTTGTTCTTTCTGATAACTCAAACTCACAATCTTAAGATTGGGAATAAGGGGCT
Bs3-E	2347	CTTTACCATCTGAGCAACTTTCTCTCGTCTATAATAGCCCTCTTCGAAATTTGGTCTAA
PI 235047	2380	CTTTACCATCTCGAGCAACTTTCTCTCGTCTATAATAGCCCTCTTCGAAATTTGGTCTAA
PI 585270	2399	CTTTACCATCTCGAGCAACTTTCTCTCGTCTATAATAGCCCTCTTCGAAATTTGGTCTAA
Bs3-E	2407	TGAGAATTTTACTGATACAGGAGAGTGAATTTTTTTTCAAGGGAGGGGATGTCCAAAAAGCC
PI 235047	2440	TGAGAATTTTACTGATACAGGAGAGTGAATTTTTTTTCAAGGGAGGGGATGTCCAAAAAGCC
PI 585270	2459	TGAGAATTTTACTGATACAGGAGAGTGAATTTTTTTTCAAGGGAGGGGATGTCCAAAAAGCC
Bs3-E	2467	CATTCCCAAATGGTTGGAAGGGGGAGGATGGTCTCTATGCAGTTGGATTACAGGAATAG
PI 235047	2500	CATTTCCCAAATGGTTGGAAGGGGAGAGGATGGTCTCTATGCAGTTGGATTACAGGAATAG
PI 585270	2519	CATTTCCCAAATGGTTGGAAGGGGAGAGGATGGTCTCTATGCAGTTGGATTACAGGAATAG
Bs3-E	2527	GACTGTTTGGTGCTTCTATAGATGCCACTAATGTTGCACAAGATATTGCCAAAATTTGGA
PI 235047	2560	GACTGTTTGGTGCTTCTATAGATGCCACTAATGTTGCACAAGATATTGCCAAAATTTGGA
PI 585270	2579	GACTGTTTGGTGCTTCTATAGATGCCACTAATGTTGCACAAGATATTGCCAAAATTTGGA
Bs3-E	2587	AAGAACAAATGTAG
PI 235047	2620	AAGAACAAATGTAG
PI 585270	2639	AAGAACAAATGTAG

**Abbildung 17: Sequenzvergleich der Bs3-Homologen von *C. pubescens* und *C. annuum***

Dargestellt ist der Sequenzvergleich der Promotoren und der kodierenden Sequenz der *Bs3-E*-Allele. Das ATG Startkodon ist blau unterlegt. Die 19-bp Duplikation ist grün unterlegt und der Bereich, der dupliziert ist, wurde gelb markiert. Der rot gekennzeichnete Bereich stellt die *UPT*<sub>AvrBs3Δrep16</sub>-Box dar. Weisse Buchstaben auf schwarzen Hintergrund symbolisieren gleiche Nukleotide, wohingegen schwarze Buchstaben auf weissen Hintergrund und weisse Buchstaben auf grauem Hintergrund die Sequenzunterschiede anzeigen. Der Sequenzvergleich wurde mit dem Programm ClustalW Version 2.0.12 (<http://www.ebi.ac.uk/clustalw/>) und den Standardeinstellungen durchgeführt. Visualisierung des Alignments erfolgte mit dem Programm boxshade 3.21 ([http://www.ch.embnet.org/software/BOX\\_form.html](http://www.ch.embnet.org/software/BOX_form.html)).

PI 585270	1	MTNQNCFNCSPLTVDALEPKKSSCAAACILVNGPLIVGAGPSGLATAAVLKQYSVPYVI
PI 235047	1	MTNQNCFNCSPLTVDALEPKKSSCAAACILVNGPLIVGAGPSGLATAAVLKQYSVPYVI
Bs3-E	1	MMNQNCFNCSPLTVDALEPKKSSCAAACIQVNGPLIVGAGPSGLATAAVLKQYSVPYVI
Bs3	1	MMNQNCFNCSPLTVDALEPKKSSCAAACIQVNGPLIVGAGPSGLATAAVLKQYSVPYVI
PI 585270	61	IERADCIASLW <del>HH</del> KTYDRLRLNVPRRYCELPGLPFPDFPEYPTKNQFISYLE <del>E</del> SYAKHFE
PI 235047	61	IERADCIASLW <del>HH</del> KTYDRLRLNVPRRYCELPGLPFPDFPEYPTKNQFISYLE <del>E</del> SYAKHFE
Bs3-E	61	IERADCIASLW <del>Q</del> HKTYDRLRLNVPROYCELPGLPFPDFPEYPTKNQFISYLVSYAKHFE
Bs3	61	IERADCIASLW <del>Q</del> HKTYDRLRLNVPROYCELPGLPFPDFPEYPTKNQFISYLVSYAKHFE
PI 585270	121	IKPRLNESVNLAGYDETYGLWKVKTVSEINGSTSEYMCKWLVVATGENAEMIVPEFEGLO
PI 235047	121	IKPRLNESVNLAGYDETYGLWKVKTVSEINGSTSEYMCKWLVVATGENAEMIVPEFEGLO
Bs3-E	121	IKPQLNESVNLAGYDETCGLWKVKTVSEINGSTSEYMCKWLVVATGENAEMIVPEFEGLO
Bs3	121	IKPQLNESVNLAGYDETCGLWKVKTVSEINGSTSEYMCKWLVVATGENAEMIVPEFEGLO
PI 585270	181	D <del>F</del> GGQVIHACEYKTGEYYTGENVLIVV <del>G</del> CGNSGIDISLDLSQHNANPFMVVRSVQGRNFP
PI 235047	181	D <del>F</del> GGQVIHACEYKTGEYYTGENVLIVV <del>G</del> CGNSGIDISLDLSQHNANPFMVVRSVQGRNFP
Bs3-E	181	D <del>F</del> GGQVIHACEYKTGEYYTGENVLAV <del>G</del> CGNSGIDISLDLSQHNANPFMVVRSVQGRNFP
Bs3	181	D <del>F</del> GGQVIHACEYKTGEYYTGENVLAV <del>G</del> CGNSGIDISLDLSQHNANPFMVVRSVQGRNFP
PI 585270	241	EEIKI <del>I</del> APAIKKFTQ <del>R</del> KVEFVNGQILEIDSVILATGYTSNVTSWLMESEFFSREGY <del>P</del> PKSPF
PI 235047	241	EEIKI <del>I</del> APAIKKFTQ <del>R</del> KVEFVNGQILEIDSVILATGYTSNVTSWLMESEFFSREGY <del>P</del> PKSPF
Bs3-E	241	EEINIVPAIKKFTQ <del>G</del> KVEFVNGQILEIDSVILATGYTSNVTSWLMESEFFSREG <del>C</del> PKSPF
Bs3	241	EEINIVPAIKKFTQ <del>G</del> KVEFVNGQILEIDSVILATGYTSNVTSWLMESE <del>L</del> FSREG <del>C</del> PKSPF
PI 585270	301	PNGWKGEDGLYAVGFTGIGLFGASIDATNVAQDI <del>A</del> KIWKEQM
PI 235047	301	PNGWKGEDGLYAVGFTGIGLFGASIDATNVAQDI <del>A</del> KIWKEQM
Bs3-E	301	PNGWKGEDGLYAVGFTGIGLFGASIDATNVAQDI <del>A</del> KIWKEQM
Bs3	301	PNGWKGEDGLYAVGFTGIGLFGASIDATNVAQDI <del>A</del> KIWKEQM

**Abbildung 18: Proteinsequenzvergleich der *Bs3*-Allele aus *C. pubescens* und *C. annuum***

Dargestellt ist der Sequenzvergleich der Proteinsequenz der *Bs3*-Allele. Weisse Buchstaben auf schwarzen Hinter-grund symbolisieren gleiche AS, wohingegen schwarze Buchstaben auf weissen Hintergrund die Sequenzunterschiede anzeigen. Die konservierten Motiv der FMOs sind als rote Buchstaben auf schwarzen Untergrund dargestellt. Das Sequenzalignent wurde mit dem Programm ClustalW Version 2.0.12 (<http://www.ebi.ac.uk/clustalw/>) und den Standardeinstellungen durchgeführt. Visualisierung des Aligments erfolgte mit dem Programm boxshade 3.21 ([http://www.ch.embnet.org/software/BOX\\_form.html](http://www.ch.embnet.org/software/BOX_form.html)).

**Tabelle 4: Analyse der F<sub>2</sub>-*C. pubesence*-Pflanzen, die für den Kopplungstest verwendet wurden**

Pflanze	AvrBs4	PR-Bs3	Pflanze	AvrBs4	PR-Bs3
PI 235047	HR	R	PI 235047	HR	R
PI 585270	keine HR	S	PI 585270	keine HR	S
157-1	keine HR	S	166-3	keine HR	R
157-2	keine HR	H	166-4	keine HR	R
157-3	keine HR	H	167-1	HR	R
157-4	keine HR	H	167-2	HR	H
161-1	HR	S	167-3	HR	H
161-3	keine HR	S	168-1	HR	R
161-4	keine HR	S	168-2	keine HR	R
162-1	HR	R	168-3	HR	R
162-2	HR	R	144-1	HR	H
165-1	HR	S	144-2	HR	H
165-2	HR	R	144-3	HR	H
165-3	HR	R	156-1	HR	R
165-4	HR	S	156-2	HR	R
165-5	HR	S	156-3	keine HR	R
166-1	keine HR	R	156-4	keine HR	R
166-2	keine HR	R	156-5	HR	R

Die Zahlen bezeichnen die einzelnen F<sub>2</sub>-Pflanzen aus einer Kreuzung der AvrBs4-suszeptiblen und -resistenten *C. pubesence*-Linien (PI 235047 x PI585270) an.

HR: Pflanzen, die nach der Inokulation mit *Xcv*, die AvrBs4 translozieren eine HR ausbildeten;

keine HR: Pflanzen, die nach Inokulation mit *Xcv*, die AvrBs4 translozieren keine HR ausgebildet haben;

R: PCR-Fragment in der Größe des resistenten Elter (PI 235047),

S: PCR-Fragment in der Größe des suszeptiblen Elter (PI 585270),

H: PCR-Fragmente des resistenten und des suszeptiblen Elter,

Grau: Pflanzen, bei denen der Inokulationsphänotyp nicht mit dem Markerphänotyp übereinstimmt

**Tabelle 5: Bestimmte Nukleotide im oberen Strang der DNA werden präferentiell von bestimmten RVDs gebunden**

TAL-Effektor/Promotor	RVDs												andere									
	HD			HG			NG			NI				NN			NS					
	A	C	G	A	C	G	A	C	G	A	C	G		A	C	G	A	C	G	T		
AvrXa27 (17) <i>Xa27</i>	2						3	1					4			2		3		1		
AvrBs3 (18) <i>Bs3</i>	2	5							1				3									
AvrBs3Δrep16 (14) <i>Bs3-E</i>	1	4											5									
AvrBs3 (18) <i>UPA20</i>	1	5	1										3									
AvrHahI (14) <i>Bs3</i>	1	4											2			2						IG→T
AvrBs3Δrep109 (15) <i>Bs3</i>	1	3								1	1		3									
PthXo7 (22) <i>OsTFIIAγ</i>		5			1					2			4				2			1		
PthXo1 (24) <i>Os8N3</i>		5							1	4			4	4	3			2				
PthXo6 (23) <i>OsTFXI</i>		4			1				2	1			1	5	1	3		2		1	2	
Tal9A (20) <i>OsHEN1</i>		8											5	3		1	1					HI→C; ND→C
Tal1C (16) <i>OsHEN1</i>		8							1	1			4				1	1				
Tal2d (16) <i>Os04g49194</i>		4							3	1			2	1		1	1	2				NK→G
AvrXa7 (26) <i>OsIIN3</i>	1	5							1	1	2		2	3		2	2	1		1		
Tal3b (18) <i>Os05g27590</i>		5								4				4	1	2				1		NK→G
Zusammen	7	67	1	2		8	4	17	2	42	5	2	46	6	11	13	6	2	13	6	2	

Aufgelistet sind TAL-Effektoren aus *Xanthomonas* ssp in Kombination mit ihren korrespondierenden Promotoren. Die Zahlen geben an wie oft ein bestimmtes Nukleotid im oberen Strang der DNA von bestimmten RVDs gebunden wird. Die Zahlen in Klammern bezeichnen die Anzahl der Repeat-Einheiten des jeweiligen TAL-Effektors. Nukleotide im oberen Strang der DNA, die bevorzugt von einem bestimmten RVD gebunden werden, sind grau hinterlegt.



## Danksagung

Hiermit bedanke ich mich bei allen, die zum Gelingen dieser Arbeit beigetragen haben.

An erster Stelle richtet sich mein Dank an Frau Professor Dr. Ulla Bonas für die Aufnahme in Ihre Arbeitsgruppe und die Möglichkeit an diesem vielseitigen und interessanten Thema arbeiten zu dürfen. Ich bedanke mich bei Ihr für die Betreuung und die Begutachtung der Arbeit, sowie Ihrem großen Interesse am Fortschritt der Experimente.

Mein ganz besonderer Dank gilt Dr. Thomas Lahaye. Ich danke Dir für die äußerst erfolgreiche Zeit in Deinem Labor und für die Unterstützung bei der Lösung der zahlreichen theoretischen und praktischen Fragen, die im Laufe der Arbeit entstanden sind. Ich danke Dir auch für das entgegengebrachte Vertrauen, die zahlreichen Diskussionsrunden und die „Ideen vom Chef“.

Tina J., Annett und Sebastian danke ich für die gute Laboratmosphäre, die „Nachbarschaftshilfen“ im Laboralltag und die hilfreichen Kommentare beim Korrekturlesen. Desweiteren danke ich allen Mitgliedern des Labors 212, besonders Tom, Tina S., Jana, Sabine, Robert und Conni für die gute Arbeitsatmosphäre. Bei Simone Hahn („Frau Dr. Hahn“) möchte ich mich für die bedeutenden Beiträge zu den Publikationen bedanken.

„Meinen“ Praktikanten und HiWis Monique Egler, Heidi Scholze, Tom Schreiber, Sabine Recht und besonders Tina Strauß möchte ich für die Unterstützung im Laboralltag und die hervorragende Hilfe bei der Bewältigung umfangreicher Experimente danken.

Carola möchte ich für die vielen Sequenzen und so manchen hilfreichen Rat im Laboralltag danken. Marina danke ich für ständig neues Medium und immer gespülte Röhrchen. Bianca gilt ein besonderer Dank für die Anzucht und die Pflege, der von mir bearbeiteten Pflanzen.

Bei der gesamten Arbeitsgruppe bedanke ich mich für die Unterstützung und die kreative Arbeitsatmosphäre. Vielen Dank!

Bei Dr. Gerd Hause möchte ich mich für die wunderbaren Mikroskopbilder bedanken und bei allen Ko-Autoren bedanke ich mich für ihre Beiträge zu den Publikationen.

Meinen Eltern danke ich ganz herzlich dafür, dass sie mich immer unterstützt haben und mir diesen Weg ermöglicht haben.

Von Herzen bedanke ich mich bei Bini für Ihre Liebe und Ihr Verständnis, vor allem in der Endphase der Arbeit.

## Lebenslauf

### Persönliche Daten:

Name: Patrick Römer  
Anschrift: Dorfstraße 53 in 06369 Riesdorf  
Geburtsdatum: 18.04.1979  
Geburtsort: Lutherstadt Wittenberg  
Familienstand: ledig  
Staatsangehörigkeit: deutsch

### Ausbildung:

1985-1989 Grundschule in Radegast  
1989-1991 Oberschule in Radegast  
1991-1997 Ludwigsgymnasium in Köthen  
Abschluss Abitur  
1997-1998 Wehrdienst beim 1. Sanitätsregiment 1 in Hildesheim  
1998-2004 Biologiestudium an der Martin-Luther-Universität  
Halle-Wittenberg  
2003-2004 Diplomarbeit am Institut für Genetik der Martin-Luther-Universität Halle-Wittenberg in der Arbeitsgruppe von Frau Prof. Dr. Ulla Bonas unter der Betreuung von Dr. Thomas Lahaye  
Thema: „Physikalische Kartierung und funktionelle Analysen des Paprika *Bs3*-Resistenzgens“  
  
Abschluss: Diplom-Biologe  
  
2005-2010 Promotionsarbeit am Institut für Biologie Bereich Genetik der Martin-Luther-Universität Halle-Wittenberg in der Arbeitsgruppe von Frau Prof. Dr. Ulla Bonas unter der Betreuung von Dr. Thomas Lahaye  
Thema: „Isolierung des Paprika *Bs3*-Resistenzgens und Interaktionsanalyse zwischen TAL-Effektoren und pflanzlichen Promotoren“

## Veröffentlichungen

**Jordan, T., Römer, P., Meyer, A., Szczesny, R., Pierre, M., Piffanelli, P., Bendahmane, A., Bonas, U. and Lahaye, T. (2006).**

Physical delimitation of the pepper *Bs3* resistance gene specifying recognition of the AvrBs3 protein from *Xanthomonas campestris* pv. *vesicatoria* Theor. Appl. Genet. **113**: 895-905

**Römer, P., Hahn, S., Jordan, T., Strauß, T., Bonas, U. and Lahaye, T. (2007)**

Plant pathogen recognition mediated by promoter activation of the pepper *Bs3* resistance gene Science **318**: 645-648

**Römer, P., Strauß, T., Hahn, S., Scholze, H., Morbitzer, R., Grau, J., Bonas, U. and Lahaye, T. (2009)** Recognition of AvrBs3-like proteins is mediated by specific binding to promoters of matching pepper *Bs3* alleles Plant Physiology **150**: 1697-1712

**Römer, P., Recht, S. and Lahaye, T. (2009)**

A single plant resistance gene promoter engineered to recognize multiple TAL effectors from disparate pathogens PNAS **106**: 20526-20531

**Römer, P., Jordan, T. and Lahaye, T. (2010)**

Identification and application of a DNA-based marker that is diagnostic for the pepper (*Capsicum annuum*) bacterial spot resistance gene *Bs3* Plant Breeding (DOI: 10.1111/j.1439-0523.2009.01750.x *in press*)

**Römer, P., Recht, S., Strauß, T., Elsaesser, J., Schornack, S., Boch, J., Wang, S. and Lahaye, T. (2010)** Promoter elements of rice susceptibility genes are bound and activated by specific TAL effectors from the bacterial blight pathogen, *Xanthomonas oryzae* pv. *oryzae* New Phytologist (DOI: 10.1111/j.1469-8137.2010.03217.x *in press*)

**Übersichtsartikel:**

**Schornack, S., Meyer, A., Römer, P., Jordan, T. and Lahaye, T. (2006).**

Gene-for-gene-mediated recognition of nuclear-targeted AvrBs3-like bacterial effector proteins. *Journal of Plant Physiology* **163**: 256-272

**Patent:**

Titel des Patents	"Bs3 Resistance Genes and Methods of Use"
Int. Application No	PCT/US2008/077639
Int. Filing Date	25.09.2008
Inventors	Thomas Lahaye, Ulla Bonas, Patrick Römer

## Erklärung

Hiermit erkläre ich, dass ich die vorliegende wissenschaftliche Arbeit selbstständig und ohne fremde Hilfe verfasst habe. Ich erkläre weiterhin, dass andere als die von mir angegebenen Quellen und Hilfsmittel nicht benutzt und die den benutzten Werken wörtlich oder inhaltlich entnommenen Stellen als solche kenntlich gemacht wurden. Mit dieser Arbeit bewerbe ich mich erstmals um die Erlangung des Doktorgrades.

Halle, 31. Mai 2010

Patrick Römer